Rapid Synthesis, Characterization, and Catalytic Function of Rhodium(III) and Iridium(III) Chloro-bridged Dimers

Loren Brown

Dissertation submitted to the faculty of Virginia Polytechnic Institute and State University in partial fulfillment of the requirements for the degree of

Doctor of Philosophy

In

Chemistry

Joseph S. Merola

Paul A. Deck

Feng Lin

Gordon T. Yee

May 7, 2019

Blacksburg, VA

Keywords: iridium; rhodium; lactone; oxidative lactonization, transfer dehydrogenation, microwave synthesis, ligand effects

Rapid Synthesis, Characterization, and Catalytic Function of Rhodium(III) and Iridium(III) Chloro-bridged Dimers

Loren Brown

ABSTRACT

Rh(III) and Ir(III) dimeric complexes with tunable cyclopentadienyl (Cp) rings have proven versatile for both catalysis and as synthetic precursors. An efficient microwave method to synthesize Rh(III) and Ir(III) dimeric complexes $[(\eta^5\text{-ring})MCl]_2(\mu^2\text{-Cl})_2$, (where $(\eta^5\text{-ring})MCl$ = $(\eta^5\text{-Me}_4C_5R)Rh(III)Cl$ or $(\eta^5\text{-Me}_4C_5R)Ir(III)Cl$) was developed. A modular design for the substituted cyclopentadienes HC_5Me_4R was based on Grignard reactions of 2,3,4,5-tetramethylcyclopent-2-en-1-one (R = alkyl, 12 examples; R = aryl, 3 examples) or by S_NAr reactions of potassium tetramethylcyclopentadienide with perfluoroarenes (R = perfluoroaryl, 3 examples). Reaction of the Me_4CpHR ligands with $[M(COD)](\mu^2\text{-Cl})_2$ (M = Rh, Ir; COD = 1,5-cyclooctadiene) produced the dimeric complexes $[Cp^{*R}MCl]_2(\mu^2\text{-Cl})_2$ in moderate to excellent yield. The resulting dimers were characterized by nuclear magnetic resonance (NMR) spectroscopy, single-crystal X-ray diffraction (XRD), high-resolution mass spectrometry (HRMS), elemental analysis, and examined as catalysts for oxidative lactonization of 1,4- and 1,5-diols.

Oxidative lactonization of 1,4-butanediol to afford γ-butyrolactone proceeded selectively and efficiently using $[(\eta^5\text{-Me}_4C_5R)IrCl]_2(\mu^2\text{-Cl})_2$ as the catalyst. Several R substituents were tested to assess electronic substituent effects. The most active complex contained an electron donating group, R = $CHMe_2$ and successfully catalyzed the formation of diols to lactones across a range of 1,4- and 1,5-diols, generally in high yield. Computational analysis of the rate-determining β-hydrogen elimination reactions provided an atomistic account of observed trends in reaction yield and selectivity as a function of substrate structure, while accounting neatly for the observed

selective formation of lactones (vs. succinaldehyde) in the transfer dehydrogenation of 1,4-butyrolactone.

Rapid Synthesis, Characterization, and Catalytic Function of Rhodium(III) and Iridium(III) Chloro-bridged Dimers

Loren Brown

GENERAL ABSTRACT

Rhodium(III) and iridium(III) complexes are useful synthetic precursors, catalysts, and biologically active compounds. This dissertation explores a rapid synthesis of these metal complexes and their subsequent catalytic applications with 1,4- and 1,5-diols. The oxidative lactonization of diols with rhodium and iridium complexes is an attractive one-pot synthesis, opening a variety of lactones to be produced. Structural studies involving novel fluorinated rhodium and iridium chloro-bridged dimers are discussed in detail.

Table of Contents

Abbreviations

ADP = Anisotropic displacement parameters

Acac = Acetylacetonate

Bn = Benzyl

COD = 1,5-Cyclooctadiene

Cp* = Pentamethylcyclopentadienyl

Cy = Cyclohexyl

Cyp = Cyclopentyl

DCM = Dichloromethane

EDG = Electron donating group

EWG = Electron withdrawing group

Hex = Hexanes

Isopropyl = iPr

RBF = Round bottom flask

Chapter 1 Introduction

1.1 Transfer hydrogenation

The utility of hydrogenation in synthesis is well-known among chemists. Applications of hydrogenation range widely across many functional groups, as a variety of unsaturated systems can undergo addition of hydrogen (**Figure 1**). C=C double bonds have been the most widely studied, but the reduction of C=O and C=N bonds are also of interest. This introduction will focus on transformations of C=O double bonds.

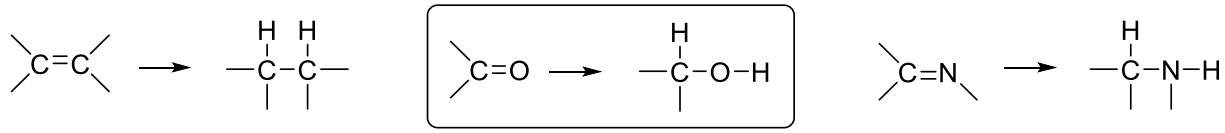

Figure 1. Hydrogenation reactions.

There are two main strategies to achieve hydrogenation of aldehydes or ketones to afford primary or secondary alcohols, respectively. The term "hydrogenation" traditionally implies the use of H_2 gas, often under pressure, as the source of the hydrogen atoms. Recently, however, a method known as *transfer hydrogenation* (TH) has emerged.[1] This approach utilizes an alternative hydrogen source, which is often a secondary alcohol.

While there are relatively few practical advantages of TH over conventional catalytic hydrogenation, the development of TH and the elucidation of the TH mechanism have opened up interesting new synthetic opportunities for the reverse, or *dehydrogenation*, reaction. Dehydrogenation of alcohols implies the removal of molecular hydrogen to form the C=O bond.[2–4] However, conventional hydrogenation catalysts do not effect this transformation except under harsh reaction conditions. On the other hand, the TH process has been shown to be freely reversible using the same types of catalysts – the reaction can be run either in the forward (hydrogenation /

reduction) or reverse (dehydrogenation / oxidation) direction. This introduction will focus on dehydrogenation of alcohols using late transition metal catalysts.

One of the most interesting features of transfer dehydrogenation (TDH) is its application to diols. When a diol like 1,4-butanediol (1,4-BD) is dehydrogenated using an appropriate transition metal catalyst, instead of each terminal carbon atom undergoing a single oxidation, one carbon atom is oxidized twice with ring-closure to form a lactone. This process is known as *oxidative lactonization* (**Figure 2**).

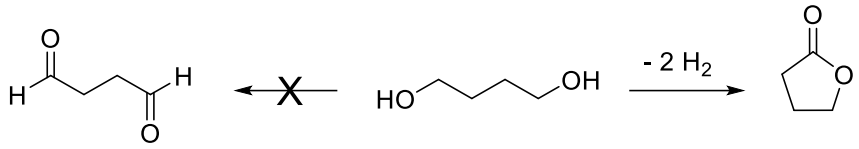

Figure 2. Oxidative lactonization of 1,4-butanediol.

This introduction describes the development of late transition metal catalysts for these important reactions. The last portion of this introduction will describe our project design, which encompasses further development of rhodium(III) and iridium(III) catalysts for oxidative lactonization and C-H activation.

1.2 Importance of lactones

Because oxidative lactonization is a key focus of this research, this section summarizes the significance of lactones as a class of organic compounds. Lactones are valuable intermediates in the synthesis of natural products, pharmaceuticals, and polyesters.[5,6,15–18,7–14] One of the most common uses for lactones is in ring-opening polymerization (ROP). ROP is driven by the release of ring-strain to form linear aliphatic polyesters.[5] The most familiar example is ROP of caprolactone (**Figure 3**) to afford poly(caprolactone). This polymer is biodegradable and has been explored for use in drug delivery and in biocompatible adhesives.[11] Modifying the structure of polyesters influences their physical properties for specific applications.[5] Therefore, exploring the

lactonization of diols with varied structures and substitution patterns provides an opportunity to expand the substrate scope for ROP.

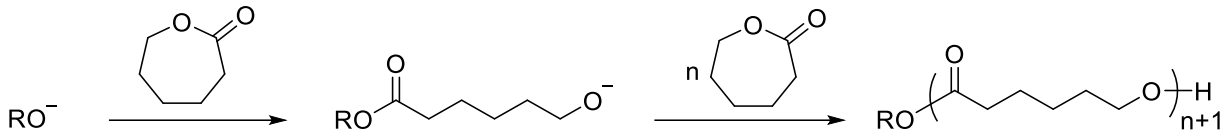

Figure 3. ROP of caprolactone.

1.3 Oxidative lactonization of diols

There are many pathways for the synthesis of lactones; however, a direct route from diols presents an attractive alternative. An example of this route is provided a generalized *stoichiometric* pathway in **Figure 4**. The oxidation steps are beta-hydride elimination reactions of metal alkoxides. This process is the *reverse* of a traditional catalytic hydrogenation of an aldehyde. A significant challenge in this field would be to achieve this transformation in a catalytic fashion; that is, how to turn over the metal hydride back to the corresponding chloride or alkoxide. The two most obvious possibilities are shown. The metal oxidation state remains fixed throughout the process. An ideal method would dehydrogenate an alcohol to the corresponding aldehyde, which is a desirable process and is discussed in more detail later.

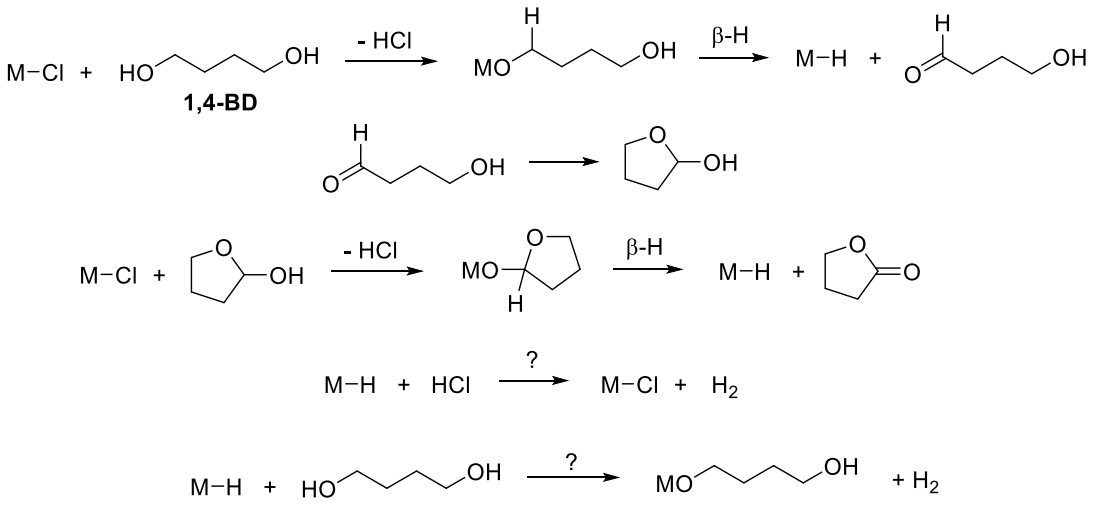

Figure 4. Conceptual scheme for the lactonization of 1,4-butanediol.

In the absence of special additives (hydride acceptors) to induce catalyst turnover, high temperatures are commonly required for the transformation shown in **Figure 4**. Evidently, the two turnover steps are just too slow or unfavorable. However, a few pioneering studies demonstrated "proof of concept" using late-transition metal catalysts.

Zhao et al. developed the acceptorless catalyst $(Me_3P)_2RuCl_2(en)$, to convert 1,4-butanediol (BD) into γ-butyrolactone in 99% yield at a very high temperature (205 ˚C).[19] Zhao only explored the conversion of BD. Likewise, Touchy et al. used Pt-doped SnO_2 to produce lactones in an acceptorless reaction.[15] Touchy's catalytic system boasted of low catalyst loadings (1 mol% Pt) and excellent yields (11 examples). The reaction was carried out neat (no solvent) at 180 °C. Despite good conversions, high temperatures and long reaction times were required - conditions not compatible with thermally sensitive functionalities.

Another approach to turning over the metal hydride (**Figure 4**) is to use a simple stoichiometric oxidant, and dioxygen might seem to be an obvious choice. While not all complexes will tolerate oxygen, those that avoid sensitive ligands such as phosphines are often compatible. Nishimura et al. found that $Pd(OAc)_2$ catalyzed the conversion of diols (four examples) into the corresponding lactones (**Table 1**).[20] The reaction conditions included pyridine, 3Å molecular sieves, and toluene as the solvent, at 80 °C. These authors also found good results converting mono-alcohols to the corresponding aldehydes. The reaction requires continuous bubbling of air or oxygen, and the authors proposed that the catalyst turns over by O_2-oxidation of a metal-hydride intermediate to form hydrogen peroxide. Lactonization of 2,2-dimethylpentanediol was not selective.

Table 1. Pd(II)-catalyzed oxidation of diols by molecular oxygen.

Entry	Diol	Product	Yield (%)
1	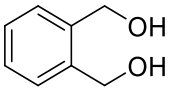	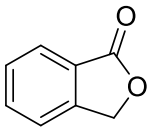	85
2	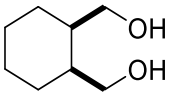	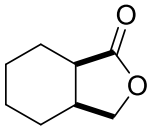	80
3	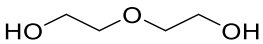	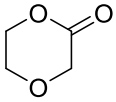	95
4	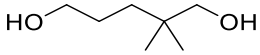	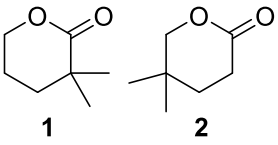 **1** **2**	91 (**1**/**2** = 53/47)

Findings such as these have led to the discovery and development of more efficient hydride acceptors, notably ketones. Lin et al. explored chalcone and acetone, using ($(Ph_3P)_3RuH_4$) and ($(^iPr_3P)_2IrH_5$) to lactonize diols in benzene.[13] This catalytic system achieved yields of 61% – 96%, with the iridium catalyst outperforming its ruthenium counterpart.

Endo et al. converted substituted 1,4- and 1,5-diols into lactones using a combination of a cobalt additive and 2,6-dimethoxybenzoquinone (terminal oxidant) in chlorobenzene at 80 ˚C (**Figure 5**).[21] Lactones containing a second (fused) ring formed more efficiently than simple 1,4-diols like 1,4-BD. Endo also studied the lactonization of 3-substituted 1,5-diols (**Table 2**). His results include the use of diethanolamine derivatives (3-aza-1,5-pentanediols). His system tolerated tertiary amines, but no yield of lactone was observed for a secondary amine.[21] A "complicated mixture" was obtained instead. Finally, 1,6-, 1,7-, and 1,8-diols were converted into their respective lactones, with yields of 86% – 89% (**Table 3**).

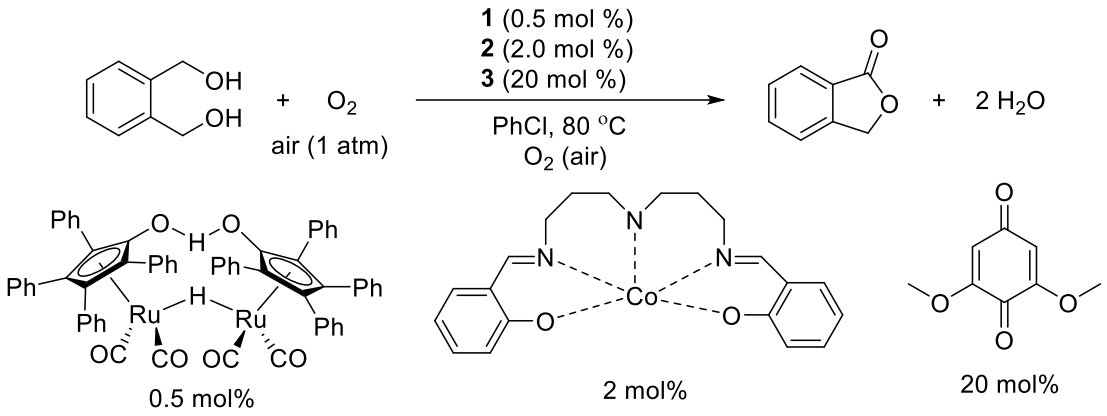

Figure 5. Lactonization of 1,2-benzenedimethanol with a bimetallic catalyst system.

Table 2. Lactonization of 1,5-diols.

Entry	Diol	Product	Conv. [%]	Yield [%]
1	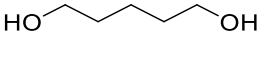	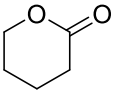	97	95
2	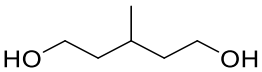	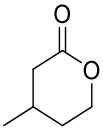	97	92
3	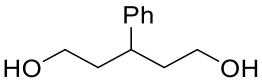	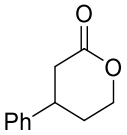	>99	90
4	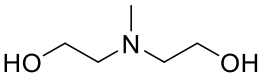	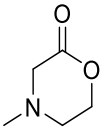	>99	82
5	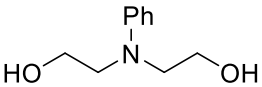	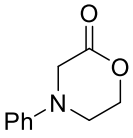	>99	85
6	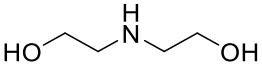	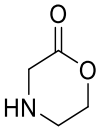	>99	n.d.

Table 3. Lactonization of 1,3-, 1,6-, 1,7-, and 1,8-diols.

Entry	Diol	Product	Conv. [%]	Yield [%]
1	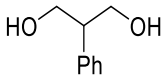	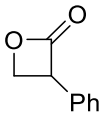	>99	0
2	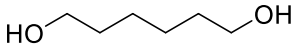	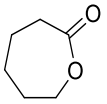	>99	86
3		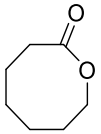	98	89
4	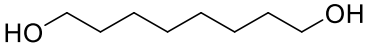	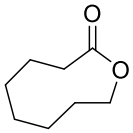	97	89

Utilizing different hydrogen acceptors, Shvo et al. employed a ruthenium carbonyl, $Ru_3(CO)_{12}$, at 145 ˚C (**Figure 6**) to catalyze oxidative lactonization of several aliphatic diols from ethylene glycol to 1,6-hexanediol (1,6-HD) and 1,10-decanediol.[22] Historically, this ruthenium-based system was the first to demonstrate successful formation of lactones; however, limitations were observed as 1,4-BD was the only diol to exclusively form butyrolactone, while other diols formed undesired polymeric side products.

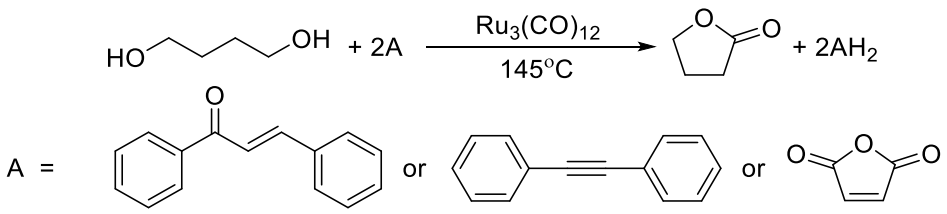

Figure 6. Shvo's ruthenium-based catalyst for oxidative lactonization.

The simplest ketone to use as a hydrogen acceptor would be acetone. Murahashi found that 3 equiv of acetone resulted in the improvement of the conversion of diols to 88% or greater for most 1,4- and 1,5-diols using $RuH_2(PPh_3)_4$ (**eq 1**).[23,24] Murahashi further showed that an increase in the quantity of acetone improved overall yields of lactones from various substituted 1,4-BDs and 1,5-

PDs. The amount of acetone that could be added was somewhat limited because the normal boiling point of acetone is 56 °C and Murahashi's reaction conditions were based on earlier work with an acceptorless catalyst (180 °C).[23] Conversions of the various diols were good (> 85%).

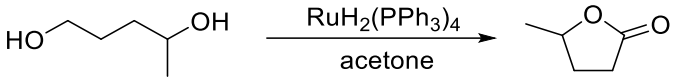

(1)

Lactones of varying ring sizes have played important roles in ROP to synthesize various polyesters. Of the most commonly utilized lactones, caprolactone is used as an intermediate along with ammonia to form caprolactam, the monomer for nylon-6, of which approximately 4 million tons is produced per year.[25] Caprolactone can be synthesized with a 1 mol% catalytic mixture of $[(\text{cymene})\text{RuCl}]_2(\mu^2\text{-Cl})_2$ and 1,1'-bis(diphenylphosphino)ferrocene (DPPF) via reflux of 1,6-hexanediol in methyl isobutyl ketone (MIBK) for 0.5 h (**eq 2**).[25]

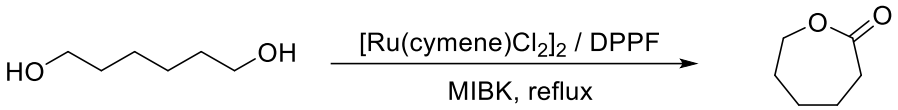

(2)

As a continuation of his previous work with the lactonization of 1,6-hexanediol, Buntara et al. explored the activity of six catalysts (**eq 3** & **Table 4**), all of which showed poor conversion for the transformation of 1,6-HD into caprolactone.[26] However, Buntara showed that a catalytic mixture of $[(p\text{-cymene})\text{RuCl}]_2(\mu^2\text{-Cl})_2$/DPPF with K_2CO_3 converted 1,6-HD into caprolactone with a 100% yield, following a screening of several ligands. Solvent conditions were optimized by replacing acetone with MIBK, resulting in improved conversion from 54% to 87%. Though 1,6-hexanediol conversion was the main goal, Buntara's research converted 1,4-BD and 1,5-PD in 80% and 82% yields, respectively. Based on the yields obtained, there is still room for improvement in the conversion of 1,4-BD and 1,5-PD into their respective lactones.

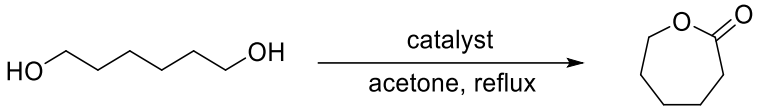

(3)

Table 4. Catalyst screening for the oxidation of 1,6-hexanediol to caprolactone.

Entry	Catalyst	Conversion [%]	Selectivity [%]
1	-	-	-
2	$[Cp^*IrCl_2]_2$	44	33
3	$(Ph_3P)_3RuCl_2$	31	81
4	Ru/C	-	-
5	Ru/TiO_2	3	90
6	Ru(*p*-cymene)$Cl_2]_2$/DPPP	54	87
7	$RuCl_3$/DPPP	3	90
8	Ru $(acac)_3$	-	-

Ishii et al. investigated the Thorpe-Ingold effect on lactonization (

Table 5) using a range of ruthenium complexes of the general type $RuCl_2L_2$ (L = phosphine).[27]

Table 5. Stereoselectivity of various 1,4-diols converted into their respective lactones.

Entry	Diol	Product	Yield. [%]	Selectivity (**2** : **3**)
1	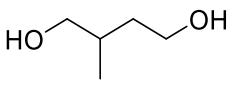	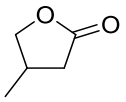 **2** 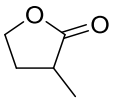 **3**	91	67 / 33
2	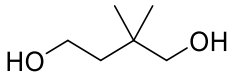	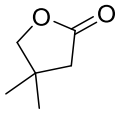 **2** 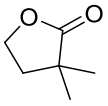 **3**	98	89 / 11
3	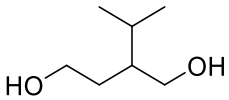	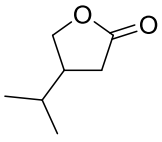 **2** 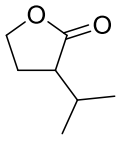 **3**	91	73 / 27
4	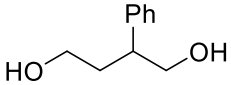	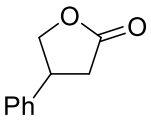 **2** 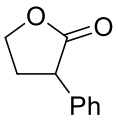 **3**	98	77 / 23

Ishii's screening of catalysts and substrates was thorough and, in some cases, very high yields and selectivities were obtained. Overall, using triphenylphosphine as the ligand generally resulted in higher yields than linked diphosphines.

As previously described, exploration of ruthenium catalysts for the lactonization of diols has been extensive. There has been much less research conducted with Group 9 complexes. Musa et al. demonstrated that an iridium PCP pincer complex is an effective catalyst for the oxidation of alcohols.[28] However, his research was limited only to 1,4-BD. His catalyst, in combination with a Cs_2CO_3 additive, produced γ-butyrolactone. Significant progress was not seen until the early 2000s, when Fujita opened the door to exploration iridium(III) complexes.

We wanted to explore the effects of varying the R substituent in Me_4C_5R ligands because we saw an opportunity to vary electronic effects and steric effects systematically.[29,30] Fluorinated substituents, in particular, are known to exhibit significant electronic effects on reactions catalyzed by Group 9 metals. Recently, rhodium(III) pentasubstituted cyclopentadienyl complexes have been utilized for C-H activation.[31,32,41–50,33–40] However, modified variants of η^5-Me_4C_5R groups have not been investigated in the oxidative lactonization of diols.

The dehydrogenation of alcohols has been explored in numerous catalytic systems utilizing rhodium(III) and iridium(III) complexes.[51–54] Fujita et al. investigated $[(\eta^5\text{-}Me_5C_5)MCl]_2(\mu^2\text{-}Cl)_2$ (M = Rh, Ir) dimers for the oxidation of secondary alcohols under mild conditions to provide a safer alternative to toxic chromium reagents.[51] Though most hydrogen transfer oxidation studies have involved secondary alcohols, Fujita also examined the conversion of primary alcohols to aldehydes (**eq 4**). $[(\eta^5\text{-}Me_5C_5)IrCl]_2(\mu^2\text{-}Cl)_2$ was found to have greater activity than the rhodium analog. In a study of substituted benzyl alcohols (**Table 6**), yields improved with electron donating groups (EDG) in the para position (entries 2 and 3), and decreased with electron withdrawing

groups (EWG) (entries 7 and 8) in the para positions. Conversion of the alcohol also decreased when the EDG was in the ortho position. The oxidation of secondary alcohols was found to have similar results (**Table 7**).

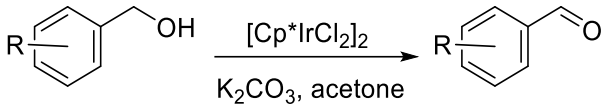

(4)

Table 6. Oxidation of benzyl alcohols ($RC_6H_4CH_2OH$) to benzaldehydes catalyzed by 2.0 mol% $[Cp^*IrCl]_2(\mu^2\text{-}Cl)_2$ and K_2CO_3 (0.10 mmol) in acetone (30 mL) at room temperature. Product yields were determined by gas chromatography; isolated yields are in parentheses.

Entry	R	Conv. of alcohol (%)	Yield of aldehyde (%)
1	H	87	87(74)
2	*p*-Me	100	93(82)
3	*p*-OMe	100	99(90)
4	*o*-OMe	70	67(63)
5	*m*-OMe	85	85(77)
6	*p*-OH	77	60
7	*p*-Cl	72	70(61)
8	*p*-NO_2	32	20

Table 7. Oxidation of secondary alcohols (2.0 mmol) to ketones catalyzed by 0.5 mol% $[Cp^*IrCl]_2(\mu^2\text{-}Cl)_2$ and K_2CO_3 (0.20 mmol) in acetone (2 mL) at room temperature. Product yields were determined by gas chromatography (GC). Isolated yields in parentheses.

Entry	Alcohol	Conv. Of alcohol (%)	Yield of ketone (%)
1	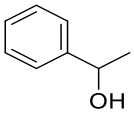	100	100(94)
2	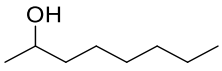	89	88(77)
3	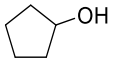	100	100
4	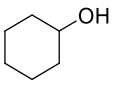	79	79

The mechanism of this reaction involves the formation of a metal alkoxide (**1**, **Figure 7**) by substitution of a halide with an alcohol. A base, often K_2CO_3, consumes the HX byproduct. Following the release of the aldehyde or ketone via β-hydride elimination (**2**, **Figure 7**), a metal hydride is formed. The next step is key in rationalizing the success that Lin, Shvo, Murahashi, and others attained by using acetone and other ketones as hydrogen acceptors. The metal hydride undergoes migratory insertion of the ketone to form a metal isopropoxide (**3**, **Figure 7**). Finally, alkoxide exchange turns the cycle over.[51] Lactonization of a diol requires a "second pass" through the same catalytic cycle, starting instead with the lactol (hemiacetal) as shown in **Figure 4**.

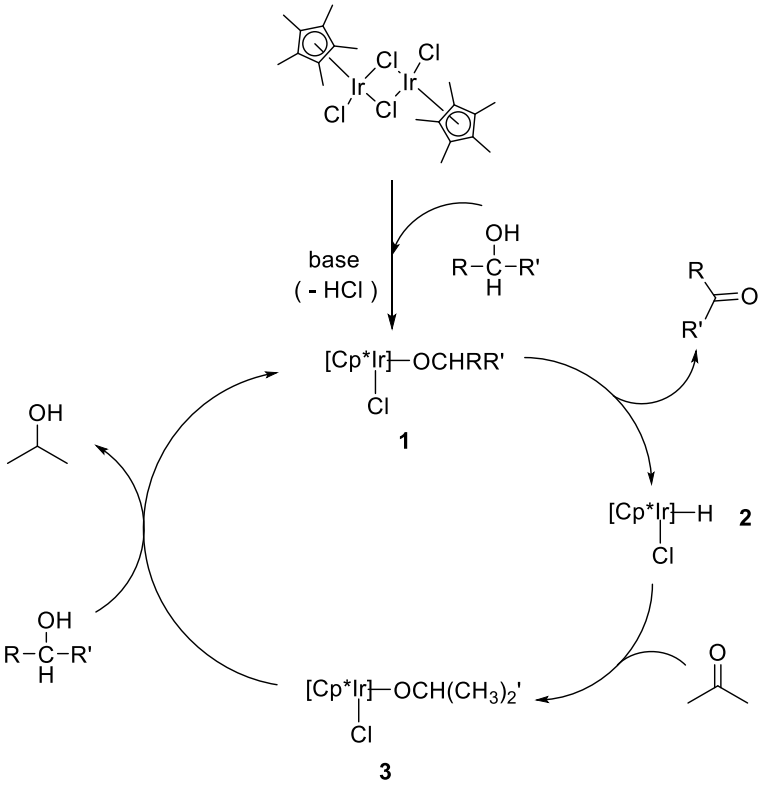

Figure 7. Proposed mechanism for the oxidation of primary and secondary alcohols.

In addition to their application as catalysts outright, iridium and rhodium pentamethylcyclopentadienyl dimers are also employed as synthetic precursors to a much broader

range of half-sandwich complexes.[55,56,65,57–64] The facile synthesis of these compounds allows half-sandwich complexes to be easily tailored for biological or catalytic applications.

Fujita et al. is well known for his research in iridium catalysis involving oxidation of alcohols. He showed that a substituted (η^5-Me_5C_5)Ir(bpy) complex (**Figure 8**) catalyzed the transformation of diols, in refluxing water, achieving yields between 52% and 97% and moderate selectivity for unsymmetrical diols (22 examples).[67] The main achievement of this work was the water-solubility of the catalyst. However, the reaction did require a relatively high temperature (100 °C).

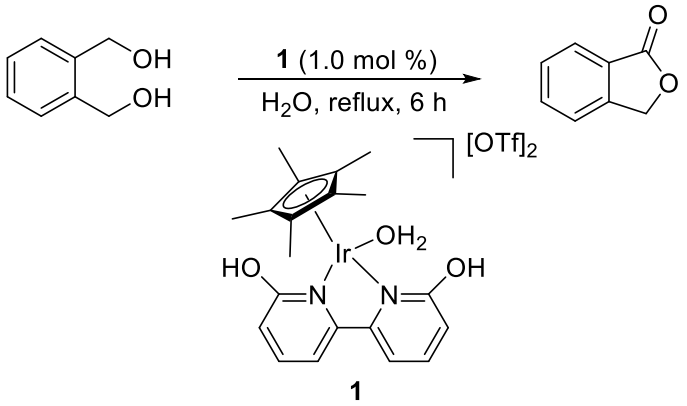

Figure 8. Dehydrogenative lactonization of 1,2-benzenedimethanol in water catalyzed by (**1**).

Suzuki et al. examined the use of an (η^5-Me_5C_5)Ir($OCH_2C(C_6H_5)_2NH_2$) complex for the oxidative lactonization of 1,4- and 1,5- diols (**eq 5**) with greater than 95% yield in most cases (**Table 8**).[68] All diols were successfully converted into their corresponding lactones. The less hindered hydroxyl group of unsymmetrical diols were oxidized to produce the lactones in entries 9 and 10.[68]

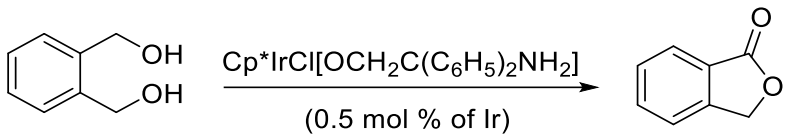

(5)

Table 8. Oxidative lactonization of diols (eq 5, diol/Ir = 200:1, in acetone).

Entry	diol	time, h	product	% yield
1	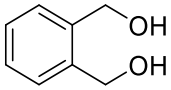	4	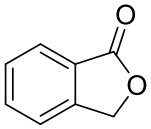	>99
2	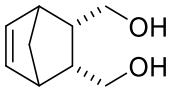	48	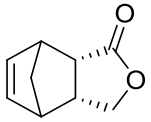	97
3	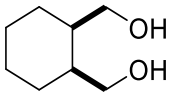	36	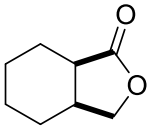	97
4	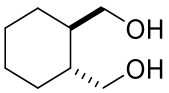	36	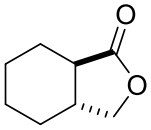	98
5 6	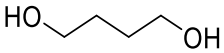	20 48	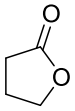	96 89
7	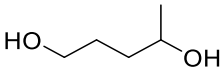	36	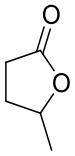	88
8	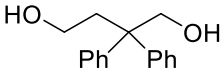	20	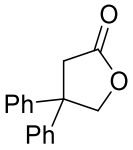	98
9	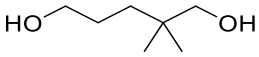	26	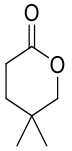	>99
10	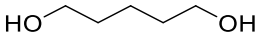	24	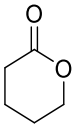	95
11	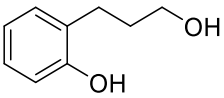	5	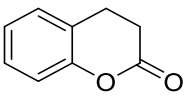	95

Although each method described thus far is suitable for the conversion of diols into lactones, every method could be improved upon and explored further. To date, there has been only modest success in achieving good selectivity with unsymmetrical aliphatic diols. In addition, many of the

reaction systems still require high temperatures to effect fast conversion. Ideally, the solvent would be acetone, which would then act as both the solvent and a hydrogen acceptor which is transformed into isopropanol via transfer hydrogenation. Acetone is also less toxic than other solvents like toluene or chlorobenzene. Additionally, employing a substituted cyclopentadienyl ring will tailor reaction selectivity, as it will affect substrate interaction at the metal. Finally, ideal experimental conditions require low catalyst loadings, providing an inexpensive catalytic system for the oxidative cyclization of diols.

1.4 Project design - oxidative lactonization of diols

Rhodium and iridium were chosen as the metal centers due to their known abilities to act as transfer hydrogenation catalysts.[51,52,54,68–74] Pentasubstituted cyclopentadienyl ligands were chosen as they are more electron rich than their cyclopentadiene counterparts, and are not easily displaced.[75] Alteration of the substituents on the pi ligand allows for examination of steric and electronic effects in many catalytic applications.[75–78] The introduction henceforth describes the synthesis of iridium(III) and rhodium(III) dimeric cyclopentadienyl complexes, and their subsequent catalytic transformation of diols to lactones.

1.5 Importance of rhodium(III) and iridium(III) complexes

Rhodium(III) and iridium(III) dimers $[Cp^*MCl]_2(\mu^2\text{-}Cl)_2$ (M = Rh, Ir) are conventionally obtained by refluxing $MCl_3 \cdot xH_2O$ and pentamethylcyclopentadiene in aqueous alcohol for 24-96 hours.[43,79] In addition to long reaction times, many of the previously reported $[Cp^{*R}MCl]_2(\mu^2\text{-}Cl)_2$ (M = Rh, Ir) cyclopentadiene derivatives were synthesized in poor yield. Morris et al., Sadler et al., and Dooley et al. have demonstrated that the synthesis of modified Cp* iridium(III) dimeric complexes proceeds with low yields, 40 - 57%, 39%, and 16% respectively.[57,80,81] In comparison, Piou et al. synthesized modified rhodium(III) dimeric complexes in yields ranging from 39 – 80%,

and require abnormally long reaction times of 96 hours in most cases.[43] Consequently, the synthesis of dimeric rhodium(III) and iridium(III) derivatized-cyclopentadienyl complexes is in need of improvement. Strides have been taken recently with Mantell et al. by using an alternative solvent than methanol or ethanol.[82] Mantell discovered Rh(I)-carbonyl side products were being formed using these traditional solvents, varying the yield of the desired $[Cp^{*3iPr}MCl]_2(\mu^2\text{-}Cl)_2$. As a result, Mantell developed a synthetic scheme that utilizes isopropanol and a much shorter reaction time of 16 hours to obtain the desired rhodium dimers.

An alternative to the traditional synthesis of $[Cp^{*R}MCl]_2(\mu^2\text{-}Cl)_2$ (M = Rh, Ir) involves oxidation of the M(I) cyclooctadiene (COD) dimer with concentrated HCl. As COD is easily displaced, dimeric cyclooctadiene compounds are excellent precursors to M(III) cyclopentadienyl dimeric complexes that are more challenging to synthesize. Therefore, the reaction of $[M(COD)]_2(\mu^2\text{-}Cl)_2$ with the desired HMe4CpR (**Figure 9**) will yield the corresponding pentasubstituted cyclopentadienyl dimeric complex. Using this method, El Amouri et al. showed $[Cp^*IrCl]_2(\mu^2\text{-}Cl)_2$ can be synthesized in a 96% yield after benchtop reflux for 2.5 hours compared to 85% after a 48-hour reflux. Similarly, the synthesis of $[Cp^*RhCl]_2(\mu^2\text{-}Cl)_2$ was achieved in 91-93% yield.[83]

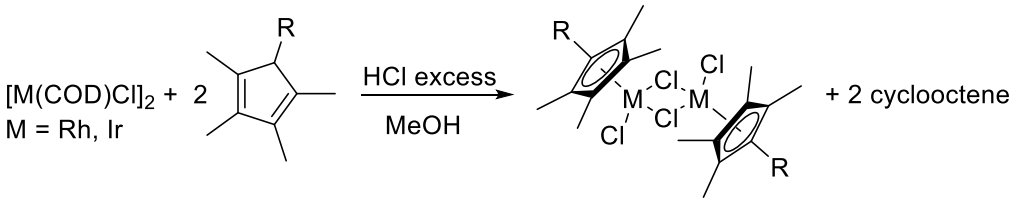

Figure 9. General scheme for the synthesis of $[Cp^{*R}MCl_2]_2(\mu^2\text{-}Cl)_2$ from $[M(COD)]_2(\mu^2\text{-}Cl)_2$ (M = Rh, Ir).

By using a microwave reactor, improved yields and shorter reaction times in the synthesis of pentasubstituted cyclopentadienyl dimers can be achieved. Baghurst et al. was the first to

demonstrate a successful synthesis of metal olefin dimers in ≤ 1 minute with comparable or better yields than previously reported.[84]

Morris et al. investigated the use of modified iridium(III) chelating amino acid complexes as asymmetric transfer hydrogenation (ATH) catalysts.[57] Morris showed the identity of the R-substituent on the cyclopentadiene affected both conversion and enantiomeric excess (ee) in the reduction of ketones. The ketones, pinacolone and acetophenone, were found to have increased ee with a less rigid R substituent following the trend $Me_4C_5Ph < Me_4C_5Bn < Me_4C_5iPr$.

Rhodium(III) and iridium(III) half-sandwich complexes have recently been used in chemotherapeutic and anti-microbial applications.[55,56,58,60,63,85–88] Because the catalytic chemistry in the Merola group is coupled strongly with the discovery of new antimicrobials, the cyclopentadienyl scope was expanded. Karpin et al. examined iridium and rhodium amino acid complexes as anti-microbial agents with minimum inhibitory concentrations (MIC) as low as 8 μg/mL.[55] Moreover, DuChane et al. examined the reaction of $[Cp^*MCl]_2(\mu^2\text{-}Cl)_2$ (M = Rh, Ir) with various acetylacetonates (acacs).[58] DuChane showed that these piano stool compounds exhibit modest activity as antimicrobial agents, with an MIC as low as 2.30 μM.[58]

Similarly, Liu et al. examined the use of half-sandwich iridium complexes bearing N,N chelating moieties. Liu showed that submicromolar activity can be obtained with increasing lipophilicity of HMe_4C_5R ligands, Me_4C_5Ph and Me_4C_5biPh. The increase in phenyl substituents enhanced cell accumulation uptake, allowing the complexes to be comparable to cis-platin as anti-cancer agents for human ovarian cancer cells.[80]

1.6 Dissertation overview

Chapter 1 outlines the synthetic utility of transfer hydrogenation with alcohols and highlights the importance of lactones as synthetic precursors. Oxidative lactonization is a useful transfer

dehydrogenation transformation of diols to afford lactones. The application of late transition metals has been highlighted and can be improved upon. Catalytic properties of rhodium(III) and iridium(III) chloro-bridged dimers make them excellent candidates for TDH catalysts. Lastly, previous reported literature states the difficulty in synthesizing rhodium and iridium dimers in good yields. Therefore, microwave synthesis allows for an adaptation to normal procedures in order to better produce these dimeric species in excellent yield.

A rapid microwave-assisted synthesis was developed and is described in Chapter 2. The full characterization of each dimer was conducted using ^{1}H, ^{13}C NMR, HRMS, and x-ray crystallography.

In Chapter 3, the oxidative lactonization of 15 diols was studied with a variety of Ir(III) chloro-bridged dimers. Electronic effects played a role in the successful lactonization of 1,4-BD, with more EDG R substituents outperforming their EWG counterparts.

Chapter 4 details the novel synthesis of 5 EWG rhodium(III) and iridium(III) chloro-bridged dimers. The complexes synthesized are the first to be studied for unique H-F coupling observed between an ortho-F and hydrogens on an adjacent methyl group. Unfortunately, C-H activation studies with these complexes did not produce improved yields of known reactions, nor work with any similar proposed substrates.

Chapter 5 provides the supplemental information for Chapters 2 – 4, including the general procedures, experimental procedures, and product characterization for all products reported.

References

(1) Wang, D.; Astruc, D. *Chem. Rev.* **2015**, *115* (13), 6621–6686.

(2) Fu, P. P.; Harvey, R. G. *Chem. Rev.* **1978**, *78* (4), 317–361.

(3) Xu, R.; Chakraborty, S.; Yuan, H.; Jones, W. D. *ACS Catal.* **2015**, *5* (11), 6350–6354.

(4) Sawatlon, B.; Surawatanawong, P. *Dalt. Trans.* **2016**, *45* (38), 14965–14978.

(5) Williams, C. K. *Chem. Soc. Rev.* **2007**, *36* (10), 1573–1580.

(6) Pommier, A.; Pons, J. M.; Kocienski, P. J. *J. Org. Chem.* **1995**, *60* (22), 7334–7339.

(7) Nishiura, M.; Hou, Z.; Koizumi, T. A.; Imamoto, T.; Wakatsuki, Y. *Macromolecules* **1999**, *32* (25), 8245–8251.

(8) Lowe, C.; Vederas, J. C. *Org. Prep. Proced. Int.* **1995**, *27* (3), 305–346.

(9) Chen, T.; Qin, Z.; Qi, Y.; Deng, T.; Ge, X.; Wang, J.; Hou, X. *Polym. Chem.* **2011**, *2* (5), 1190–1194.

(10) Albertsson, A. C.; Varma, I. K. *Biomacromolecules* **2003**, *4* (6), 1466–1486.

(11) Hsiao, H. C.; Datta, A.; Chen, Y. F.; Chang, W.; Lee, T. Y.; Lin, C. H.; Huang, J. H. *J. Organomet. Chem.* **2016**, *804*, 35–41.

(12) Ito, M.; Osaku, A.; Shiibashi, A.; Ikariya, T. *Org. Lett.* **2007**, *9* (9), 1821–1824.

(13) Lin, Y.; Zhu, X.; Zhou, Y. *J. Organomet. Chem.* **1992**, *429* (2), 269–274.

(14) Mitsudome, T.; Noujima, A.; Mizugaki, T.; Jitsukawa, K.; Kaneda, K. *Green Chem.* **2009**, *11* (6), 793–797.

(15) Touchy, A. S.; Shimizu, K. I. *RSC Adv.* **2015**, *5* (37), 29072–29075.

(16) Xie, X.; Stahl, S. S. *J. Am. Chem. Soc.* **2015**, *137* (11), 3767–3770.

(17) Nair, L. S.; Laurencin, C. T. *Prog. Polym. Sci.* **2007**, *32* (8–9), 762–798.

(18) Lou, X.; Detrembleur, C.; Jérôme, R. *Macromol. Rapid Commun.* **2003**, *24* (2), 161–172.

(19) Zhao, J.; Hartwig, J. F. *Organometallics* **2005**, *24* (10), 2441–2446.

(20) Nishimura, T.; Onoue, T.; Ohe, K.; Uemura, S. *J. Org. Chem.* **1999**, *64* (18), 6750–6755.

(21) Endo, Y.; Bäckvall, J. E. *Chem. - A Eur. J.* **2011**, *17* (45), 12596–12601.

(22) Shvo, Y.; Blum, Y.; Reshef, D.; Menzin, M. *J. Organomet. Chem.* **1982**, *226* (1), C21–C24.

(23) Murahashi, S. I.; Ito, K. ichiro; Naota, T.; Maeda, Y. *Tetrahedron Lett.* **1981**, *22* (52), 5327–5330.

(24) Murahashi, S. I.; Naota, T.; Ito, K.; Maeda, Y.; Taki, H. *J. Org. Chem.* **1987**, *52* (19), 4319–4327.

(25) Buntara, T.; Noel, S.; Phua, P. H.; Melián-Cabrera, I.; De Vries, J. G.; Heeres, H. J. *Angew. Chemie - Int. Ed.* **2011**, *50* (31), 7083–7087.

(26) Nicklaus, C. M.; Phua, P. H.; Buntara, T.; Noel, S.; Heeres, H. J.; de Vries, J. G. *Adv. Synth. Catal.* **2013**, *355* (14–15), 2839–2844.

(27) Ishii, Y.; Osakada, K.; Ikariya, T.; Saburi, M.; Yoshikawa, S. *Tetrahedron Lett.* **1983**, *24* (26), 2677–2680.

(28) Musa, S.; Shaposhnikov, I.; Cohen, S.; Gelman, D. *Angew. Chemie - Int. Ed.* **2011**, *50* (15), 3533–3537.

(29) Cuenca, T.; Royo, P. *Coord. Chem. Rev.* **1999**, *193–195*, 447–498.

(30) Brinkman, J. A.; Nguyen, T. T.; Sowa, J. R. *Org. Lett.* **2000**, *2* (7), 981–983.

(31) *Rhodium Catalysis in Organic Synthesis*; Tanaka, K., Ed.; Wiley-VCH Verlag GmbH & Co. KGaA: Weinheim, Germany, 2019.

(32) Shibata, Y.; Tanaka, K. *Angew. Chemie - Int. Ed.* **2011**, *50* (46), 10917–10921.

(33) Hoshino, Y.; Shibata, Y.; Tanaka, K. *Adv. Synth. Catal.* **2014**, *356* (7), 1577–1585.

(34) Fukui, M.; Hoshino, Y.; Satoh, T.; Miura, M.; Tanaka, K. *ChemInform* **2014**, *45* (42), no-no.

(35) Takahama, Y.; Shibata, Y.; Tanaka, K. *Chem. - A Eur. J.* **2015**, *21* (25), 9053–9056.

(36) Fukui, M.; Shibata, Y.; Hoshino, Y.; Sugiyama, H.; Teraoka, K.; Uekusa, H.; Noguchi, K.; Tanaka, K. *Chem. - An Asian J.* **2016**, *11* (16), 2260–2264.

(37) Honjo, Y.; Shibata, Y.; Kudo, E.; Namba, T.; Masutomi, K.; Tanaka, K. *Chem. - A Eur. J.* **2018**, *24* (2), 317–321.

(38) Yamada, T.; Shibata, Y.; Tanaka, K. *Asian J. Org. Chem.* **2018**, *7* (7), 1396–1402.

(39) Terasawa, J.; Shibata, Y.; Kimura, Y.; Tanaka, K. *Chem. - An Asian J.* **2018**, *13* (5), 505–509.

(40) Huh, S.; Hong, S. Y.; Chang, S. *Org. Lett.* **2019**, *21* (8), 2808-2812.

(41) Piou, T.; Rovis, T. *J. Am. Chem. Soc.* **2014**, *136* (32), 11292–11295.

(42) Piou, T.; Romanov-Michailidis, F.; Ashley, M. A.; Romanova-Michaelides, M.; Rovis, T. *J. Am. Chem. Soc.* **2018**, *140* (30), 9587–9593.

(43) Piou, T.; Romanov-Michailidis, F.; Romanova-Michaelides, M.; Jackson, K. E.; Semakul, N.; Taggart, T. D.; Newell, B. S.; Rithner, C. D.; Paton, R. S.; Rovis, T. *J. Am. Chem. Soc.* **2017**, *139* (3), 1296–1310.

(44) Piou, T.; Rovis, T. *Nature* **2015**, *527* (7576), 86–90.

(45) Romanov-Michailidis, F.; Phipps, E. J. T.; Rovis, T. In *Rhodium Catalysis in Organic Synthesis*; Wiley-VCH Verlag GmbH & Co. KGaA: Weinheim, Germany, 2019; pp 593–628.

(46) Semakul, N.; Jackson, K. E.; Paton, R. S.; Rovis, T. *Chem. Sci.* **2017**, *8* (2), 1015–1020.

(47) Hyster, T. K.; Dalton, D. M.; Rovis, T. *Chem. Sci.* **2015**, *6* (1), 254–258.

(48) Davis, T. A.; Wang, C.; Rovis, T. *Synlett* **2015**, *26* (11), 1520–1524.

(49) Neely, J. M.; Rovis, T. *J. Am. Chem. Soc.* **2014**, *136* (7), 2735–2738.

(50) Hyster, T. K.; Rovis, T. *Chem. Commun.* **2011**, *47* (43), 11846–11848.

(51) Fujita, K. I.; Furukawa, S.; Yamaguchi, R. *J. Organometalic Chem.* **2002**, *649* (2), 289–292.

(52) Fujita, K. I.; Yamamoto, K.; Yamaguchi, R. *Org. Lett.* **2002**, *4* (16), 2691–2694.

(53) Suzuki, T.; Morita, K.; Tsuchida, M.; Hiroi, K. *J. Org. Chem.* **2003**, *68* (4), 1601–1602.

(54) Suzuki, T.; Ghozati, K.; Katoh, T.; Sasai, H. *Org. Lett.* **2009**, *11* (19), 4286–4288.

(55) Karpin, G. W.; Merola, J. S.; Falkinham, J. O. *Antimicrob. Agents Chemother.* **2013**, *57* (7), 3434–3436.

(56) Karpin, G. W.; Morris, D. M.; Ngo, M. T.; Merola, J. S.; Falkinham, J. O. *Medchemcomm* **2015**, *6* (8), 1471–1478.

(57) Morris, D. M.; McGeagh, M.; De Peña, D.; Merola, J. S. *Polyhedron* **2014**, *84* (0), 120–135.

(58) Duchane, C. M.; Brown, L. C.; Dozier, V. S.; Merola, J. S. *Organometallics* **2018**, *37* (4), 530–538.

(59) Shimogawa, R.; Takao, T.; Suzuki, H. *Chem. Lett.* **2016**, *46* (2), 197–199.

(60) Petrini, A.; Pettinari, R.; Marchetti, F.; Pettinari, C.; Therrien, B.; Galindo, A.; Scopelliti, R.; Riedel, T.; Dyson, P. J. *Inorg. Chem.* **2017**, *56* (21), 13600–13612.

(61) Liu, J.; Wu, X.; Iggo, J. A.; Xiao, J. *Coord. Chem. Rev.* **2008**, *252* (5–7), 782–809.

(62) Štarha, P.; Trávníček, Z.; Crlíková, H.; Vančo, J.; Kašpárková, J.; Dvořák, Z. *Organometallics* **2018**, *37* (16), 2749–2759.

(63) Payne, R.; Govender, P.; Therrien, B.; Clavel, C. M.; Dyson, P. J.; Smith, G. S. *J.*

Organomet. Chem. **2013**, *729*, 20–27.

(64) Yao, Z. J.; Lin, N.; Qiao, X. C.; Zhu, J. W.; Deng, W. *Organometallics* **2018**, *37* (21), 3883–3892.

(65) Yang, Y.; Guo, L.; Tian, Z.; Ge, X.; Gong, Y.; Zheng, H.; Shi, S.; Liu, Z. *Organometallics* **2019**, acs.organomet.9b00080.

(66) Takashima, Y.; Osaki, M.; Harada, A. *J. Am. Chem. Soc.* **2004**, *126* (42), 13588–13589.

(67) Fujita, K. I.; Ito, W.; Yamaguchi, R. *ChemCatChem* **2014**, *6* (1), 109–112.

(68) Suzuki, T.; Morita, K.; Tsuchida, M.; Hiroi, K. *Org. Lett.* **2002**, *4* (14), 2361–2363.

(69) Fujita, K. ichi; Enoki, Y.; Yamaguchi, R. *Tetrahedron* **2008**, *64* (8), 1943–1954.

(70) Fujita, K. I.; Li, Z.; Ozeki, N.; Yamaguchi, R. *Tetrahedron Lett.* **2003**, *44* (13), 2687–2690.

(71) Fujita, K. I.; Takahashi, Y.; Owaki, M.; Yamamoto, K.; Yamaguchi, R. *Org. Lett.* **2004**, *6* (16), 2785–2788.

(72) Kawahara, R.; Fujita, K. I.; Yamaguchi, R. *Adv. Synth. Catal.* **2011**, *353* (7), 1161–1168.

(73) Fujita, K. I.; Fujii, T.; Yamaguchi, R. *Org. Lett.* **2004**, *6* (20), 3525–3528.

(74) Suzuki, T.; Yamada, T.; Watanabe, K.; Katoh, T. *Bioorganic Med. Chem. Lett.* **2005**, *15* (10), 2583–2585.

(75) Jutzi, P. *J. Organomet. Chem.* **1990**, *400* (1–2), 1–17.

(76) Coville, N. J.; du Plooy, K. E.; Pickl, W. *Coord. Chem. Rev.* **1992**, *116* (C), 1–267.

(77) Morris, D. M.; McGeagh, M.; De Peña, D.; Merola, J. S. *Polyhedron* **2014**, *84*, 120–135.

(78) Pinkas, J.; Lamač, M. *Coord. Chem. Rev.* **2015**, *296*, 45–90.

(79) White, C.; Yates, A.; Maitlis, P. M.; Heinekey, D. M. In *Inorganic Syntheses*; John Wiley & Sons, Inc., 2007; Vol. 29, pp 228–234.

(80) Liu, Z.; Habtemariam, A.; Pizarro, A. M.; Fletcher, S. A.; Kisova, A.; Vrana, O.; Salassa, L.; Bruijnincx, P. C. A.; Clarkson, G. J.; Brabec, V.; Sadler, P. J. *J. Med. Chem.* **2011**, *54* (8), 3011–3026.

(81) Dooley, T.; Fairhurst, G.; Chalk, C. D.; Tabatabaian, K.; White, C. *Transit. Met. Chem.* **1978**, *3* (1), 299–302.

(82) Mantell, M. A.; Kampf, J. W.; Sanford, M. *Organometallics* **2018**, *37* (19), 3240–3242.

(83) El Amouri, H.; Gruselle, M.; Jaouén, G. *Synth. React. Inorg. Met. Chem.* **2007**, *24* (3), 395–400.

(84) Baghurst, D. R.; Mingos, D. M. P. *J. Organomet. Chem.* **1990**, *384* (3), C57–C60.

(85) Liu, Z.; Habtemariam, A.; Pizarro, A. M.; Clarkson, G. J.; Sadler, P. J. *Organometallics* **2011**, *30* (17), 4702–4710.

(86) Millett, A. J.; Habtemariam, A.; Romero-Canelón, I.; Clarkson, G. J.; Sadler, P. J. *Organometallics* **2015**, *34* (11), 2683–2694.

(87) Burgoyne, A. R.; Makhubela, B. C. E.; Meyer, M.; Smith, G. S. *Eur. J. Inorg. Chem.* **2015**, *2015* (8), 1433–1444.

(88) Lucas, S. J.; Lord, R. M.; Basri, A. M.; Allison, S. J.; Phillips, R. M.; Blacker, A. J.; McGowan, P. C. *Dalt. Trans.* **2016**, *45* (16), 6812–6815.

Chapter 2 Rapid Access to Derivatized, Dimeric, Ring-Substituted Dichloro(cyclopentadienyl)-rhodium(III) and Iridium(III) Complexes

2.1 Contributions

The work described in this chapter was conducted in collaboration with Emily Ressegue. The author is responsible for the synthesis and characterization of all Rh(III) and Ir(III) complexes. Synthesis of modified cyclopentadienyl ligands were conducted by Emily Ressegue and characterized by the author. The final manuscript was prepared in collaboration with Dr. Joseph S. Merola and is available online. [Brown, L. C., Ressegue, E. & Merola, J. S. Rapid Access to Derivatized, Dimeric, Ring-Substituted Dichloro(cyclopentadienyl)rhodium(III) and Iridium(III) Complexes. *Organometallics* **35,** 4014–4022 (2016).]

2.2 Abstract

The present work describes the design and synthesis of a series of rhodium and iridium dimers $[(\eta^5\text{-ring})MCl]_2(\mu^2\text{-Cl})_2$ (where $(\eta^5\text{-ring})MCl$ = $(\eta^5\text{-Me}_4C_5R)Rh(III)Cl$ or $(\eta^5\text{-Me}_4C_5R)Ir(III)Cl$) using a new and efficient 1 h procedure. Rhodium and iridium dimeric complexes were synthesized via a microwave reaction. The modified HMe_4C_5R (R = isopropyl, n-butyl, isobutyl, sec-butyl, n-pentyl, n-hexyl, n-heptyl, n-octyl, phenyl, benzyl, phenethyl, cyclohexyl, and cyclopentyl) type ligands were synthesized by reaction of 2,3,4,5-tetramethylcyclopent-2-en-1-one with the respective Grignard reagent (RMgX), followed by elimination of water under acidic conditions to produce the tetramethyl(alkyl or aryl)cyclopentadienes in moderate to excellent yields (40−98%). Reaction of the HMe_4C_5R ligands with $[M(COD)](\mu^2\text{-Cl})_2$ (M = Rh, Ir; COD = 1,5-cyclooctadiene) gave the dimeric complexes $[(\eta^5\text{-Me}_4C_5R)MCl]_2(\mu^2\text{-Cl})_2$ in yields ranging from 47% to 96%. The derivatized dimers were tested for antimicrobial activity, showing activity against Mycobacterium smegmatis and improved activity with derivatized R groups against Staphylococcus aureus and

MRSA 43300. The characterization of these complexes was completed by NMR spectroscopy, single-crystal X-ray diffraction, high-resolution mass spectrometry, and elemental analysis.

2.3 Introduction

The importance of cyclopentadienyl ligands to the development of organometallic chemistry cannot be overstated.[1–7] Metal complex chemistry of cyclopentadienyl systems was further elaborated with the use of pentamethylcyclopentadienyl ligands that blocked unwanted reactions of the metal center with cyclopentadiene C-H bonds.[8–10] Our group has focused on the synthesis of η^5-Me_4C_5R type complexes of rhodium and iridium with an eye toward developing both catalytic and biological chemistry of these metals.[11–13] Rhodium and iridium dimers of the type $[(\eta^5\text{-}Me_5C_5)MCl]_2(\mu^2\text{-}Cl)_2$ (M = Rh, Ir) are employed in various catalytic systems[14–27] and are useful synthetic precursors in half-sandwich chemistry.[28]

Rhodium and iridium dimers have many uses in catalytic applications, as do the subsequent half-sandwich complexes synthesized from their respective dimers.[11,29–31] The literature features an abundance of half-sandwich (piano stool) complexes with various chelating agents including acacs,[32] amino alcohols,[30,33,34] amino acids,[12] ethylenediamines,[13] C,N chelating ligands,[35] hydroxyquinolines,[36,37] and bipyridyls.[38] The facile synthesis of these compounds allows half-sandwich complexes to be easily tailored for catalytic or biological applications. Recently, η^4-Me_5C_5H complexes have been shown to be effective catalysts for H_2 evolution and an essential intermediate in the catalytic reduction of NAD.[39,40] This development opens the door for modified complexes as they can help influence H migration onto the η^5-ring via select R groups that can direct that migration. Various substituents on substituted cyclopentadienes may facilitate and/or direct substrates into best alignment with the metal center. As a result, this may lead to unique complexes with catalytic properties yet to be explored. In addition to catalysis, chain length of η^5-

Me_4C_5R rhodium and iridium dimeric complexes has been shown to affect biological activity.[12,41,42] Therefore, expanding the library of varying chain lengths is of particular interest. However, synthesis of most derivatized η^5-Me_4C_5R rhodium and iridium dimeric complexes proceed with low yields.[11,38,43–45] As a result, we have investigated a more efficient procedure than the conventional method, which aims to exploit the benefits of a microwave reactor.

Microwave reactors have been shown to expedite the synthesis of organic and organometallic reactions, providing an alternative to time consuming conventional techniques.[46–50] Traditionally, the synthesis of rhodium and iridium dimers require alcoholic solvents and these solvents are excellent hydrogen bonding solvents for microwave irradiation. In addition, the increased temperature and pressure provided by a closed system used in the microwave reactors are advantageous synthetic conditions that are absent in benchtop reflux.

Modified η^5-Me_4C_5R rhodium and iridium dimers have been explored, but not to the depth that would be required to understand how "R" affects sandwich and half-sandwich compound chemistry. Moreover, most of the dimers previously reported were synthesized in low yield. The work reported herein describes the successful use of a microwave reactor to synthesize iridium and rhodium dimeric cyclopentadienyl complexes with yields ranging from 47 – 96% This alternate approach was developed based on modifications to previously reported methodology in order to provide an efficient and cost effective pathway to further rhodium and iridium dimers. This article describes the highly efficient, microwave reactor assisted synthesis of a series of η^5-ring (η^5-Me_4C_5R) complexes in only 1 hour.

2.4 Results and Discussion

2.4.1 General comments and naming scheme

The numbering scheme used throughout this paper to discuss the various ligands and corresponding complexes may be found in **Chart 1**.

2.4.2 Cyclopentadienyl ligand synthesis

One approach to synthesizing HMe_4C_5R dienes is via lithiation of 2-bromo-2-butene followed by reaction with the appropriate ester or lactone.[10,51] This synthesis requires multiple steps and is an unfavorable method for producing a series of HMe_4C_5R ligands. Therefore, we decided a more rational approach to synthesizing a series of HMe_4C_5R ligands is via Grignard reactions with 2,3,4,5-tetramethylcyclopent-2-enone. While this has been used previously to make pentamethylcyclopentadiene[52] and a few other unsymmetrically substituted pentaalkylcyclopentadienyl compounds,[53,54] we extend this method to utilize a wide variety of Grignard reagents that are commercially available to develop an extensive library of unsymmetrical Cp*-type ligands and Rh and Ir dimers as precursors to half-sandwich compounds.

The modified HMe_4C_5R variants were synthesized via reaction 2,3,4,5-tetramethylcyclopent-2-enone and 1.25 equiv. of a Grignard reagent and in anhydrous THF. The resulting reaction produced an alcohol intermediate; subsequently, elimination of water under acidic conditions gave the corresponding diene (**Scheme 1**).

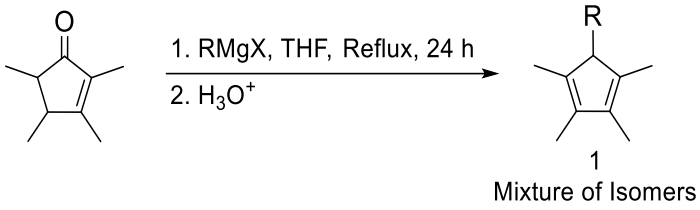

Scheme 1. General scheme for the synthesis of HMe_4C_5R dienes.

Purification of the HMe_4C_5R dienes was carried out by column chromatography on silica gel using hexanes as the eluent. The solvent was removed under reduced pressure to obtain the ligand as a yellow oil. The ^1H NMR spectra of the cyclopentadienes are quite complex since the reaction does not form a single isomer. Multiple double bond positions around the asymmetrically substituted ring are produced including having a double bond exo to the ring (**Figures S1 – S6**). Fortunately, all isomers can react under the synthesis conditions to form the desired cyclopentadienyl metal complexes.

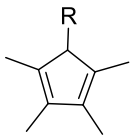

1

1a = R = CH_2CH_3	1b = R = $(CH_2)_2CH_3$
1c = R = $CH(CH_3)_2$	1d = R = $(CH_2)_3CH_3$
1e = R = $CH_2CH(CH_3)_2$	1f = R = $CH(CH_3)(CH_2CH_3)$
1g = R = $(CH_2)_4CH_3$	1h = R = $(CH_2)_5CH_3$
1i = R = $(CH_2)_6CH_3$	1j = R = $(CH_2)_7CH_3$
1k = R = Ph	1l = R = CH_2Ph
1m = R = $(CH_2)_2Ph$	1n = R = Cyh
1o = R = Cyp	

Chart 1. A list of various HMe_4C_5R dienes synthesized.

2.4.3 Microwave synthesis vs conventional synthesis

Rhodium(III) and iridium(III) dimers $[(\eta^5\text{-}Me_4C_5R)MCl]_2(\mu^2\text{-}Cl)_2$ (M = Rh, Ir) are conventionally obtained from refluxing $MCl_3 \cdot xH_2O$ and pentamethylcyclopentadiene in aqueous alcohol for 36-48 hours.[55] In addition to long reaction times, conventional syntheses of $[(\eta^5\text{-}Me_4C_5R)MCl]_2(\mu^2\text{-}Cl)_2$ (M = Rh, Ir) pentasubstituted cyclopentadiene derivatives yield less than 50% in some cases.[11,38,43–45] An alternative to the conventional synthesis of $[(\eta^5\text{-}Me_4C_5R)MCl]_2(\mu^2\text{-}Cl)_2$ involves oxidation of the rhodium(I) and iridium(I) cyclooctadiene, COD, dimers with concentrated HCl.[56] As COD is displaced with stronger coordinating ligands, dimeric cyclooctadiene compounds are excellent precursors to cyclopentadienyl dimers that are more

challenging to synthesize. Therefore, the synthesis of modified pentasubstituted cyclopentadienyl iridium and rhodium dimeric species was carried out using an adaptation of a previously reported literature procedure (**Scheme 2**) in combination with a microwave reactor.[56]

The reaction of $[M(COD)]_2(\mu^2\text{-}Cl)_2$ with 3.5-5 equivalents of the HMe_4C_5R in the presence of HCl led to formation of the corresponding $[(\eta^5\text{-}Me_4C_5R)MCl]_2(\mu^2\text{-}Cl)_2$. For rhodium, the yellow suspension of $[Rh(COD)]_2(\mu^2\text{-}Cl)_2$ and diene was microwaved for one hour to yield a red precipitate or a red solution. Similarly, for iridium, the orange suspension formed an orange precipitate or an orange solution after being microwaved for 1 hour. In both syntheses, the solvent was removed under reduced pressure and the crude product was recrystallized from DCM and hexanes to yield the desired product as a red powder (Rh) or an orange powder (Ir). Upon removal of the sample from the microwave, we noticed a small amount of byproduct, which was decanted from the methanolic solution of the dimer prior to the workup. Further investigation of this byproduct led us to identify excess diene, as expected, as well as cyclooctene by NMR spectroscopy (**Figure S67**). This finding contrasts that of an earlier publication suggesting cyclooctane is the fate of the reduced diene.[56]

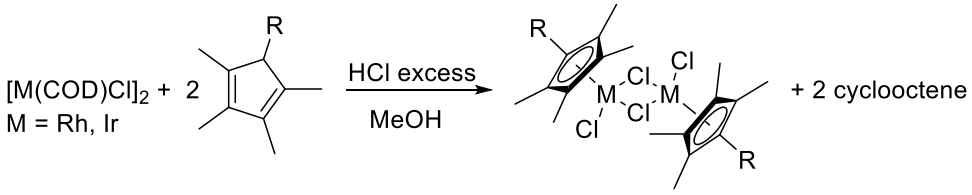

Scheme 2. General scheme for the synthesis of $[(\eta^5\text{-}Me_4C_5R)MCl]_2(\mu^2\text{-}Cl)_2$ from $[M(COD)]_2(\mu^2\text{-}Cl)_2$ (M = Rh, Ir).

The iridium dimers were obtained in yields ranging from 47 – 96% (**Table 1**) whereas the rhodium dimers were obtained in yields ranging from 50 – 89% (**Table 2**). A few reactions of rhodium complexes did not go to completion, giving instead a mixture of desired product and

starting material. This phenomenon was not observed for reactions of iridium complexes, which suggests that $[Rh(COD)]_2(\mu^2\text{-}Cl)_2$ does not oxidize as readily as $[Ir(COD)]_2(\mu^2\text{-}Cl)_2$. This leads us to the conclusion that the rate of oxidation of $[Rh(COD)]_2(\mu^2\text{-}Cl)_2$ is slower than the rate of complex formation. The yields reported are for the conditions listed in the experimental. In general, reaction performed on larger scales led to higher percentage yields.

Microwave-facilitated reaction of modified dienes with $[M(COD)]_2(\mu^2\text{-}Cl)_2$ showed a significantly improved yield for most complexes in comparison to that obtained by conventional heating methods. The ^{1}H NMR pattern of the Me_4C_5R complexes are very straightforward since there is no longer an isomer issue. Modified dimers exhibit two singlets from the chemically non-equivalent methyl groups of the $\eta^5\text{-}Me_4C_5R$ ring upon introduction of the R group, dissimilar to the typical $[(\eta^5\text{-}Me_5C_5)MCl]_2(\mu^2\text{-}Cl)_2$, which exhibits a singlet for all methyl groups. In the case of *sec*-butyl, more peaks are seen due to the presence of a chiral center on the ligand. All complexes synthesized exhibited a typical piano stool arrangement with chloro bridges between the metal centers and a terminal chloride bound to the metal, similarly to other reported iridium and rhodium dimers.[11,38,44,57–60]

Table 1. Comparison of iridium dimers synthesized conventionally and with a microwave reactor.

Iridium Dimer	Conventional (%)[a]	Microwave (%)[b,c]	Overall (%)[e]
2a	45, (16)[44]	50	46
2b	17	61	57
2c	56	70	64
2d	20	55	51
2e	NR[d]	76	70
2f	NR[d]	96	88
2g	16	86	79
2h	9	57	52
2i	4	47	43
2j	(58)[61]	83	77
2k	(39)[62]	69	64
2l	42	87	80
2m	23	84	78
2n	49	48	45
2o	NR[d]	60	55

[a] The reaction was carried out using $IrCl_3 \cdot xH_2O$ and the corresponding ligand refluxed in MeOH for 48 h under N_2. [b] The reaction was carried out in a microwave pressure tube for 1 h. [c] Isolated yield. [d] No reaction. [e] Based on a 92% yield for $[Ir(COD)]_2(\mu^2\text{-}Cl)_2$. [f] Yields in parentheses are reported literature values.

The conventional syntheses for rhodium dimers with long chains and saturated rings yielded numerous undesired and unidentifiable side products. Consequently, these reactions gave low yields as the product could not be isolated from impurities, despite great efforts. As a result, only rhodium dimers with short chains or conjugated rings were successfully synthesized and purified via the conventional method. Modified cyclopentadienyl dimers synthesized via the alternative route between $[Rh(COD)]_2(\mu^2\text{-}Cl)_2$ and the appropriate HMe_4C_5R proceeded without any complications or difficulties in purifying the final product. The difficulties encountered when following the conventional synthesis emphasize not only the importance of the alternative method

in synthesizing difficult dimers, but also the efficiency and cost effectiveness of this synthetic pathway.

Table 2. Comparison of various rhodium dimers synthesized conventionally and with a microwave reactor.

Rhodium Dimer	Conventional (%)[a]	Microwave (%)[b,c]	Overall Yield (%)[e]
3a	(95)[44]	79	74
3b	47	80	75
3c	(72)[63], (77)[64]	50	47
3d	3	63	59
3e	-	89	83
3f	-	54[d]	51
3g	-	77	72
3h	-	73	68
3i	-	52	49
3j	-	52	49
3k	(71)[65], (78)[60]	75	70
3l	35	89	83
3m	66, (45)[45]	77	72
3n	-	64[d]	60
3o	-	54[d]	51

[a] The reaction was carried out using $RhCl_3 \cdot xH_2O$ and the corresponding ligand refluxed in MeOH for 48 h under N_2. [b] The reaction was carried out in a microwave pressure tube for 1 h. [c] Isolated yield. [d] Reacted yield. [e] Based on a 94% yield for $[Rh(COD)]_2(\mu^2\text{-}Cl)_2$. [f] Yields in parentheses are reported literature values.

2.4.4 Characterization

The $[(\eta^5\text{-ring})MCl]_2(\mu^2\text{-}Cl)_2$ complexes described in this paper have been structurally characterized using HRMS, ^1H NMR, ^{13}C NMR, XRD, and elemental analysis. A notable trend was observed with the methylene adjacent to the η^5-ring among Me_4C_5R chains ranging from *n*-propyl to *n*-octyl. The ^1H NMR spectrum of each methylene did not show a well resolved triplet as expected, which implies slightly hindered rotation of the alkyl chain. A variable temperature NMR study was conducted to investigate this hypothesis using complex **2b** on a 500 MHz NMR

(**Figure S68**). At 70˚C (a), there was little difference between the spectrum at room temperature (b). When the temperature was lowered to -10˚C (c), the methylene began to resolve into a more triplet like shape than observed at higher temperatures. This result corroborates our hypothesis that the methylene adjacent to the η^5-ring of longer chain complexes experience hindered rotation.

2.4.5 Molecular structures

The crystal structures of complexes **2a**, **2d**, **2e**, **2f**, **2g**, **2m**, **2o**, **3a**, **3b**, **3d**, **3e**, **3g**, **3h**, **3l**, **3m**, **3n**, and **3o**, were determined by single crystal X-ray diffraction. X-ray crystallographic data are listed in supporting information (**Tables S1–S4**) and the .cif files for all structures are also available. The $[(\eta^5\text{-ring})MCl]_2(\mu^2\text{-Cl})_2$ complexes exhibit a pseudo-tetrahedral, piano-stool geometry around the metal center with the η^5-ring occupying the "seat" position and three chloride ligands (two bridging and one terminal) making up the "legs" of the stool. Examination of the various metal complexes reveals little to no difference between the M-C(centroid), M-Cl, and the M-Cl(bridging) bond distances. Greater variability is observed with bond angles for both iridium and rhodium complexes. Rhodium complexes had larger X_1-M-X_2, X_1-M-Cl, and X_2-M-Cl bond angles, whereas iridium complexes had a larger M-Cl-M bond angle.

A thermal ellipsoid plot of **3m**, the [bis((tetramethyl)phenethylcyclopentadienyl)dirhodium tetrachloride) compound is provided in **Figure 1** as an exemplar. For **3m**, the asymmetric unit is ½ of the dinuclear complex with the full complex generated by the inversion operation. In **Figure 1**, the generated atoms are labeled with (i) to show they are produced by the inversion operation. Thermal ellipsoid plots and full listings of angles and bonds for 18 structures can be found in the supplementary information. In addition, cif files are provided in the supporting information.

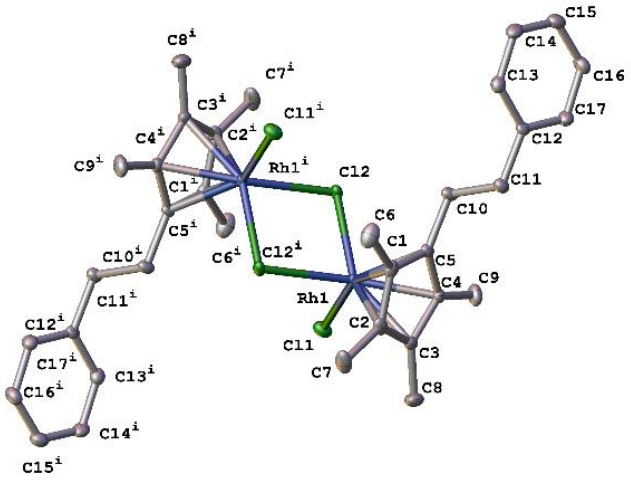

Figure 1. Thermal ellipsoid plot of the rhodium dimer, **3m**. Ellipsoids shown at 50% probability.

It is worth noting that complexes **3a**, **3h**, and **3n** exhibited disorder within their structures that were easily handled with two-site models. While most compounds crystallized without lattice solvent, complexes **3b**, **2g**, **3g**, and **3n** had solvent present within the crystal lattice. Complex **3b** crystallizes both without solvent as well as a structure with dichloromethane in the lattice. Comparison of the two shows the structures have varied chain behavior with the propyl chain projecting out from the ring in the case of the dichloromethane solvate while the solventless structure finds those chains folding back over the Cp ring (**Figure S71** & **Figure S72**). In addition, the structure with dichloromethane exhibited a shorter Rh-Rh distance between metal centers (**Table S3**). There are short C-H-Cl interactions between the H on dichloromethane and Cl on Rh as well that could account for the differing bond distances.

At this time, this is the first complete study of modified η^5-ring dimers with group 9 metals. Each of these modified complexes showed that rhodium and iridium behave similarly in solid state. These results suggest that various substituents on the η^5-ring do not show a significant change in structure.

2.4.6 Antimicrobial results

The bulk of work examining activity of metal complexes for medicinal purposes has been directed toward anti-cancer activity.[35,41,62,66] We have become more interested in the activity against resistant bacterial strains such as tuberculosis and MRSA.[12,13] While our previous work was with piano-stool complexes of amino acids and ethylenediamines, we find that the dimers reported here also show high anti-microbial activity. The complexes reported herein were tested against various strains of microbes, showing that long chains showing improved activity against *S. aureus, E. coli, M. smegmatis, and MRSA.* (**Tables 3 & Table 4**) Rhodium appears to have greater antimicrobial activity than its iridium counterpart. Complexes **2i** and **3i** exhibited improved activity across all microbes, with the exception of *M. Smegmatis*. These results of improved potency with increasing chain length are consistent with similar findings by Lucas *et al.*[41] for anti-cancer activity. An in-depth structure activity relationship study is underway with $[(\eta^5\text{-ring})MCl]_2(\mu^2\text{-}Cl)_2$ complexes as well as their corresponding half-sandwich compounds with a variety of ligands.

Table 3. Antimicrobial activity of derivatized iridium complexes.

Bacteria Line	MIC[a] (μM)			
	IrCp*[b]	**2g**	**2i**	**2o**
S. *aureus*	628	93	44	184
E. *coli*	628	550	173	553
M. *smegmatis*	10	18	17	18
MRSA 43300	628	70	44	184

[a] Minimal inhibitory concentration. [b] $[(Cp^*)IrCl]_2(\mu^2\text{-}Cl)_2$. [c] Results are the averages of triplicates.

Table 4. Antimicrobial activity of derivatized rhodium complexes.

Bacteria Line	MIC[a] (μM)			
	RhCp*[b]	**3g**	**3i**	**3o**
S. *aureus*	400	228	133	340
E. *coli*	400	680	320	688
M. *smegmatis*	4	5	4.2	6
MRSA 43300	400	143	107	344

[a] Minimal inhibitory concentration. [b] $[(Cp^*)RhCl]_2(\mu^2\text{-}Cl)_2$. [c] Results are the averages of triplicates.

2.5 Conclusions

Several iridium and rhodium dimeric complexes of the form $[(\eta^5\text{-ring})MCl]_2(\mu^2\text{-}Cl)_2$ were synthesized and characterized. The use of a microwave reactor reduced the conventional reaction time from 48 hours to 1 hour. Previously, 9 of the modified dimers have been described using the conventional method. In this paper, we report comparable, if not improved yields via microwave route. The other 21 modified dimers reported here allow for a complete comparison of the substituent effect on modified cyclopentadienes with various R groups between iridium and rhodium.

In summary, this work has shown that modular design is greatly facilitated by the use of a microwave reactor. This new route lessens the number and amounts of reagents used, involves less chromatography, and reduces the amount of rhodium and iridium metal lost during reactions. The range of new substituted Cp^{*R} dimers allow for examining the potential structure/activity relationships not only in the biological arena but in the catalytic arena as well.[43,64] Rhodium and iridium derivatized dimeric species are being explored further in catalysis with preliminary results showing both iridium and rhodium dimers catalyze diols into their corresponding lactones without a need for additional ligand substituion.[34] More details on the effect of substitution of the Cp ring will be forthcoming.

2.6 Experimental Section

All materials for synthesis, purification, and characterization were used as received unless otherwise stated. Snap ring tops and 10 mL pressure tubes were purchased from CEM Corporation. $RhCl_3 \cdot xH_2O$ and $IrCl_3 \cdot xH_2O$ were purchased from Pressure Chemical, Pittsburgh, PA 15201. Heptylmagnesium chloride, and 2,3,4,5-tetramethylcyclopent-2-en-1-one were purchased from Alfa Aesar, Ward Hill, MA 01835. Reagent grade solvents, ethyl-tetramethylcyclopentadiene (**1a**), tetramethyl(*n*-propyl)cyclopentadiene (**1b**), benzylmagnesium chloride, cyclohexylmagnesium chloride, cyclopentylmagnesium bromide, phenylmagnesium bromide, phenethylmagnesium chloride, isopropylmagnesium bromide, butylmagnesium chloride, isobutylmagnesium chloride, *sec*-butylmagnesium chloride, pentylmagnesium bromide, hexylmagnesium bromide, and octylmagnesium bromide were purchased from Sigma Aldrich, St. Louis, MO 63013. Deuterated solvents for NMR spectroscopy were obtained from Cambridge Isotope Laboratories. Elemental analyses were performed by Atlantic Microlabs, Norcross, GA. ^{1}H NMR and ^{13}C NMR spectra were collected on a Varian MR-400 NMR spectrometer. ^{13}C NMR were correspondingly recorded at 101 MHz. HRMS were collected on an Agilent 6220 Accurate Mass TOF LC-MS using electrospray ionization (ESI+).

2.6.1 Synthesis of HMe_4C_5R dienes

Unless otherwise stated, all reactions were conducted under an N_2 atmosphere.

2.6.2 General procedure of HMe_4C_5R dienes

A solution of the respective Grignard reagent (18.1 mmol) in THF was added to a stirred solution of 2,3,4,5-tetramethyl-2-cyclopentenone (2.00 g, 15.2 mmol) in anhydrous THF (20 mL). The mixture was refluxed for 24 h, then cooled to 0 °C and quenched with HCl. This solution was warmed to room temperature and agitated for 2 h. The mixture was diluted with diethyl ether (30

mL), washed with water (3 x 30 mL), and the organic layer dried over $MgSO_4$. The products were concentrated under reduced pressure, and purified by column chromatography (Silica gel, hexanes) to afford the product and isomers as a yellow oil. The ^1H NMR spectra of the dienes are complex due to the signal overlap of the isomers. Both ^1H and ^{13}C NMR spectra of dienes 1i, 1m and 1n are reproduced in the Supporting Information (**Figures S1-S6**) to illustrate that complexity. We relied on HRMS and success in further reactions as proof of synthesis. Dienes **1c - 1h** and **1j – 1o** have previously been reported.[11,38,67–73]

Synthesis of 5-isopropyl-2,3,4,5-tetramethylcyclopenta-1,3-diene (1c) Yield: 1.04 g (44%).

Synthesis of 5-butyl-1,2,3,4-tetramethylcyclopenta-1,3-diene (1d) Yield: 2.53 g (98%).

Synthesis of 5-isobutyl-1,2,3,4-tetramethylcyclopenta-1,3-diene (1e) Yield: 2.49 g (96%). HRMS/APCI+ (m/z): Calc. for $C_{13}H_{23}$ 179.1800; Found 179.1798

Synthesis of 5-(*sec*-butyl)-1,2,3,4-tetramethylcyclopenta-1,3-diene (1f) Yield: 1.02 g (40%). HRMS/APCI+ (m/z): Calc. for $C_{13}H_{23}$ 179.1800; Found 179.1794

Synthesis of 1,2,3,4-tetramethyl-5-pentylcyclopenta-1,3-diene (1g) Yield: 1.76 g (63%). HRMS/ESI+ (m/z): Calc. for $C_{14}H_{23}$ 191.1800; Found 191.1792

Synthesis of 5-hexyl-1,2,3,4-tetramethylcyclopenta-1,3-diene (1h) Yield: 0.651 g (52%).

Synthesis of 5-heptyl-1,2,3,4-tetramethylcyclopenta-1,3-diene (1i) Yield: 2.53 g (79%). HRMS/APCI+ (m/z): Calc. for $C_{16}H_{29}$ 221.2269; Found 221.2264

Synthesis of 1,2,3,4-tetramethyl-5-octylcyclopenta-1,3-diene (1j) Yield: 2.61g (77%).

Synthesis of (2,3,4,5-tetramethylcyclopenta-2,4-dien-1-yl)benzene (1k) Yield: 2.78 g (97%).

Synthesis of ((2,3,4,5-tetramethylcyclopenta-2,4-dien-1-yl)methyl)benzene (1l) Yield: 2.58 g (84%).

Synthesis of (2-(2,3,4,5-tetramethylcyclopenta-2,4-dien-1-yl)ethyl)benzene (1m) Yield: 2.51 g (77%). HRMS/APCI+ (m/z): Calc. for $C_{17}H_{23}$ 227.1800; Found 227.1799

Synthesis of (2,3,4,5-tetramethylcyclopenta-2,4-dien-1-yl)cyclohexane (1n) Yield: 2.18 g (74%).

Synthesis of 2,3,4,5-tetramethyl[1,1'-bi(cyclopentane)]-2,4-diene (1o) Yield: 1.57 g (57%). HRMS/APCI+ (m/z): Calc. for $C_{14}H_{21}$ 191.1800; Found 191.1794

2.6.3 General procedure for the synthesis of $[(\eta^5\text{-}Me_4C_5R)IrCl]_2(\mu^2\text{-}Cl)_2$

A microwave pressure tube was fitted with the appropriate amounts of the respective $[Ir(COD)]_2(\mu^2\text{-}Cl)_2$, HMe_4C_5R, in 4 mL of methanol with 0.5 mL of concentrated HCl. The reaction mixture was heated to 115 °C at 50 watts and 150 psi and held for 1 hour, yielding an orange solution. The solvent was evaporated under reduced pressure and the resulting powder recrystallized from DCM and cold hexanes, collected via filtration, and washed with cold hexanes. Complexes **2a**, **2b**, **2c**, **2k**, **2l**, **2m**, and **2n** have previously been reported and were identified via spectral comparison.[11,38,44,74,75]

Synthesis of $[Cp^{*ethyl}IrCl]_2(\mu^2\text{-}Cl)_2$ (2a). Following the general procedure, $[Ir(COD)]_2(\mu^2\text{-}Cl)_2$ (0.100 g, 0.149 mmol), **1a** (0.045 g, 0.298 mmol), and 0.5 mL of HCl were reacted in methanol (4 mL) to give **2a** (0.061 g, 50% yield). ^{1}H NMR (400 MHz, $CDCl_3$) δ 2.16 – 2.10 (q, 4H, $^2J_{HH}$ = 7.7 Hz, 2 CH_2), 1.58 (s, 12 H, 4 CpCH_3), 1.56 (s, 12H, 4 CpCH_3), 1.07-1.03 (t, 6 H, $^2J_{HH}$ = 7.7 Hz, 2 CH_3). ^{13}C{^{1}H} NMR (101 MHz, $CDCl_3$) δ 89.06 (Cp*C*), 86.49 (Cp*C*), 86.18 (Cp*C*), 17.56 (*C*H_2), 11.63 (*C*H_3), 9.30 (Cp*C*H_3), 9.13 (Cp*C*H_3). Anal. Calc. for $C_{22}H_{34}Cl_4Ir_2$, C, 32.04; H, 4.16; Found, C, 31.88; H, 3.96

Synthesis of $[Cp^{*n\text{-}propyl}IrCl]_2(\mu^2\text{-}Cl)_2$ (2b). Following the general procedure, $[Ir(COD)]_2(\mu^2\text{-}Cl)_2$ (0.100 g, 0.149 mmol), **1b** (0.0851 g, 0.521 mmol), and 0.5 mL of HCl were reacted in methanol

(4 mL) to give **2b** (0.078 g, 61% yield). ^{1}H NMR (400 MHz, $CDCl_3$) δ 2.13 – 2.09 (m, 4H, 2 C*H*$_2$CH$_2$CH$_3$), 1.59 (s, 12 H, 4 CpC*H*$_3$), 1.57 (s, 12H, 4 CpC*H*$_3$), 1.49-1.40 (m, 4H, 2 CH$_2$C*H*$_2$CH$_3$), 0.94-0.90 (app. t, 6 H, 2 C*H*$_3$). ^{13}C{^{1}H} NMR (101 MHz, $CDCl_3$) δ 87.96 (Cp*C*), 86.52 (Cp*C*), 86.52 (Cp*C*), 26.16 (*C*H$_2$CH$_2$CH$_3$), 21.00 (CH$_2$*C*H$_2$CH$_3$), 14.36 (*C*H$_3$), 9.55 (Cp*C*H$_3$), 9.47 (Cp*C*H$_3$). HRMS/ESI+ (m/z): C_{24} H_{38}[^{193}Ir]$_2Cl_3$ 817.1298; Found 817.1331

Synthesis of [Cp*^{isopropyl}IrCl]$_2$(μ^2-Cl)$_2$ (2c). Following the general procedure, [Ir(COD)]$_2$(μ^2-Cl)$_2$ (0.100 g, 0.149 mmol), **1c** (0.0851 g, 0.521 mmol), and 0.5 mL of HCl were reacted in methanol (4 mL) to give **2c** (0.089 g, 70% yield). ^{1}H NMR (400 MHz, $CDCl_3$) δ 2.54 – 2.43 (m, 2H, 2 C*H*), 1.68 (s, 12 H, 4 CpC*H*$_3$), 1.60 (s, 12H, 4 CpC*H*$_3$), 1.29-1.27 (d, 12 H, $^{2}J_{HH}$ = 7.1 Hz, 4 C*H*$_3$). ^{13}C{^{1}H} NMR (101 MHz, $CDCl_3$) δ 90.38 (Cp*C*), 86.47 (Cp*C*), 86.21 (Cp*C*), 25.39 (*C*H(CH$_3$)$_2$), 20.78 (CH(*C*H$_3$)$_2$), 10.40 (Cp*C*H$_3$), 9.68 Cp*C*H$_3$) HRMS/ESI+ (m/z): C_{24} H_{38}[^{193}Ir]$_2Cl_3$ 817.1298; Found 817.1326 Anal. Calc. for $C_{24}H_{38}Cl_4Ir_2$, C, 33.80; H, 4.49; Found, C, 34.01; H, 4.48

Synthesis of [Cp*$^{n\text{-}butyl}$IrCl]$_2$(μ^2-Cl)$_2$ (2d). Following the general procedure, [Ir(COD)]$_2$(μ^2-Cl)$_2$ (0.300 g, 0.447 mmol), **1d** (0.159 g, 0.893 mmol), and 0.5 mL of HCl were reacted in methanol (4 mL) to give **2d** (0.109 g, 55% yield). ^{1}H NMR (400 MHz, $CDCl_3$) δ 2.15 – 2.11 (m, 4H, 2 C*H*$_2$(CH$_2$)$_2$CH$_3$), 1.60 (s, 12H, 4 CpC*H*$_3$), 1.58 (s, 12H, 4 CpC*H*$_3$), 1.41-1.28 (m, 8H, 2 CH$_2$(C*H*$_2$)$_2$CH$_3$), 0.91-0.88 (app. t, 6H, 2 C*H*$_3$). ^{13}C{^{1}H} NMR (101 MHz, $CDCl_3$) δ 88.26 (Cp*C*), 86.57 (Cp*C*), 86.55 (Cp*C*), 29.97 (CH$_2$*C*H$_2$CH$_2$CH$_3$), 24.05 (*C*H$_2$CH$_2$CH$_2$CH$_3$), 23.00 (CH$_2$CH$_2$*C*H$_2$CH$_3$), 14.04 (*C*H$_3$), 9.55 (Cp*C*H$_3$), 9.51 (Cp*C*H$_3$). HRMS/ESI+ (m/z): $C_{26}H_{42}$[^{193}Ir]$_2Cl_3$ 845.1611; Found 845.1617 Anal. Calc. for $C_{26}H_{42}Cl_4Ir_2$, C, 35.45; H, 4.81; Found, C, 35.61; H, 4.80

Synthesis of [Cp*^{isobutyl}IrCl]$_2$(μ^2-Cl)$_2$ (2e). Following the general procedure, [Ir(COD)]$_2$(μ^2-Cl)$_2$ (0.200 g, 0.298 mmol), **1e** (0.186 g, 1.04 mmol), and 0.5 mL of HCl were reacted in methanol (4

mL) to give **2e** (0.199 g, 76% yield). ^{1}H NMR (400 MHz, $CDCl_3$) δ 2.06 – 2.04 (d, 4H, $^{2}J_{HH}$ = 7.5 Hz, 2 CH_2), 1.77-1.66 (m, 2H, 2 C*H*), 1.61 (s, 12H, 4 CpCH_3), 1.60 (s, 12H, 4 CpCH_3), 0.90-0.89 (d, 12H, $^{2}J_{HH}$ = 6.7 Hz, 4 CH_3). ^{13}C{^{1}H} NMR (101 MHz, $CDCl_3$) δ 87.48 (Cp*C*), 87.00 (Cp*C*), 86.59 (Cp*C*), 33.13 (*C*H_2CH(CH_3)$_2$), 27.91 (CH_2*C*H(CH_3)$_2$), 22.83 (CH_2CH(*C*H_3)$_2$), 10.08 (Cp*C*H_3), 9.55 (Cp*C*H_3). HRMS/ESI+ (m/z): $C_{26}H_{42}[^{193}Ir]_2Cl_3$ 845.1611; Found 845.1602 Anal. Calc. for $C_{26}H_{42}Cl_4Ir_2$, C, 35.45; H, 4.81; Found, C, 35.66; H, 4.70

Synthesis of [Cp*$^{sec\text{-}butyl}$IrCl]$_2$(μ^2-Cl)$_2$ (2f). Following the general procedure, [Ir(COD)]$_2$(μ^2-Cl)$_2$ (0.500 g, 0.744 mmol), **1f** (0.465 g, 2.61 mmol), and 0.5 mL of HCl were reacted in methanol (4 mL) to give **2f** (0.6276 g, 96% yield). ^{1}H NMR (400 MHz, $CDCl_3$) δ 2.23 – 2.18 (m, 2H, C*H*), 1.68 (s, 6H, 2 CpCH_3), 1.66 – 1.67 (m, 2H, CH*H*), 1.66 (s, 6H, 2 CpCH_3), 1.62 (s, 6H, 2 CpCH_3), 1.58 (s, 6H, 2 CpCH_3), 1.53 – 1.43 (m, 2H, C*H*H), 1.33 – 1.31 (d, 6H, $^{2}J_{HH}$ = 7.2 Hz, CH_3CH), 0.90 – 0.86 (t, 6 H, $^{2}J_{HH}$ = 7.4 Hz, CH_2CH_3). ^{13}C{^{1}H} NMR (101 MHz, $CDCl_3$) δ 91.03 (Cp*C*), 90.44 (Cp*C*), 87.08 (Cp*C*), 86.29 (Cp*C*), 85.01 (Cp*C*), 32.04 (*C*H), 27.71 (*C*H_2), 18.47 (*C*H_3CH), 12.84 (*C*H_3CH_2), 10.77 (Cp*C*H_3), 10.40 (Cp*C*H_3), 9.82 (Cp*C*H_3), 9.61 (Cp*C*H_3). HRMS/ESI+ (m/z): $C_{26}H_{42}[^{193}Ir]_2Cl_3$ 845.1611; Found 845.1695 Anal. Calc. for $C_{26}H_{42}Cl_4Ir_2$, C, 35.45; H, 4.81; Found, C, 35.19; H, 4.71

Synthesis of [Cp*$^{n\text{-}pentyl}$IrCl]$_2$(μ^2-Cl)$_2$ (2g). Following the general procedure, [Ir(COD)]$_2$(μ^2-Cl)$_2$ (0.100 g, 0.149 mmol), **1g** (0.100 g, 0.521 mmol), and 0.5 mL of HCl were reacted in methanol (4 mL) to give **2g** (0.116 g, 86% yield). ^{1}H NMR (400 MHz, $CDCl_3$) δ 2.14 – 2.11 (m, 4H, 2 CH_2(CH_2)$_3CH_3$), 1.61 (s, 12H, 4 CpCH_3), 1.59 (s, 12H, 4 CpCH_3), 1.43-1.34 (m, 4H, 2 CH_2CH_2(*C*H_2)$_2CH_3$), 1.34-1.24 (m, 8H, 2 CH_2CH_2(*CH*$_2$)$_2CH_3$), 0.88-0.85 (app. t, 6H, 2 CH_3). ^{13}C{^{1}H} NMR (101 MHz, $CDCl_3$) δ 88.23 (Cp*C*), 86.49 (Cp*C*), 86.46 (Cp*C*), 31.90 (*C*H_2), 27.43 (*C*H_2), 24.16 (*C*H_2), 22.48 (*C*H_2), 13.95 (*C*H_3), 9.51 (Cp*C*H_3), 9.48 (Cp*C*H_3). HRMS/ESI+ (m/z):

$C_{28}H_{46}[^{193}Ir]_2Cl_3$ 873.1924; Found 873.1965 Anal. Calc. for $C_{28}H_{46}Cl_4Ir_2$, C, 37.00; H, 5.10; Found, C, 37.60; H, 5.08

Synthesis of [Cp*$^{n\text{-hexyl}}$IrCl]$_2$(μ^2-Cl)$_2$ (2h). Following the general procedure, [Ir(COD)]$_2$(μ^2-Cl)$_2$ (0.300 g, 0.447 mmol), **1h** (0.230 g, 1.12 mmol), and 0.5 mL of HCl were reacted in methanol (4 mL) to give **2h** (1.56 g, 52% yield).^{1}H NMR (400 MHz, $CDCl_3$) δ 2.14 – 2.10 (m, 4H, 2 C*H*$_2$(CH$_2$)$_4$CH$_3$), 1.61 (s, 12 H, 4 CpC*H*$_3$), 1.59 (s, 12H, 4 CpC*H*$_3$), 1.42-1.23 (m, 16H, 2 CH$_2$(C*H*$_2$)$_4$CH$_3$), 0.88-0.84 (app. t, 6H, 2 C*H*$_3$). ^{13}C{^{1}H} NMR (101 MHz, $CDCl_3$) δ 88.34 (Cp*C*), 86.60 (Cp*C*), 86.56 (Cp*C*), 31.65 (*C*H$_2$), 29.53 (*C*H$_2$), 27.76 (*C*H$_2$), 24.26 (*C*H$_2$), 22.62 (*C*H$_2$), 14.16 (*C*H$_3$), 9.54 (Cp*C*H$_3$), 9.51 (Cp*C*H$_3$). HRMS/ESI+ (m/z): $C_{30}H_{50}[^{193}Ir]_2Cl_3$ 901.2237; Found 901.2145 Anal. Calc. for $C_{30}H_{50}Cl_4Ir_2$, C, 38.46; H, 5.38; Found, C, 38.46; H, 5.38

Synthesis of [Cp*$^{n\text{-heptyl}}$IrCl]$_2$(μ^2-Cl)$_2$ (2i). Following the general procedure, [Ir(COD)]$_2$(μ^2-Cl)$_2$ (0.250 g, 0.372 mmol), **1i** (0.287 g, 1.30 mmol), and 0.5 mL of HCl were reacted in methanol (4 mL) to give **2i** (0.168, 47% yield). ^{1}H NMR (400 MHz, $CDCl_3$) δ 2.14 – 2.10 (m, 4H, 2 C*H*$_2$(CH$_2$)$_5$CH$_3$), 1.60 (s, 12H, 4 CpC*H*$_3$), 1.59 (s, 12H, 4 CpC*H*$_3$), 1.41-1.34 (m, 4H, 2 CH$_2$C*H*$_2$(CH$_2$)$_4$CH$_3$), 1.31-1.21 (m, 16H, CH$_2$CH$_2$(C*H*$_2$)$_4$CH$_3$), 0.88-0.84 (app. t, 6H, 2 C*H*$_3$). ^{13}C{^{1}H} NMR (101 MHz, $CDCl_3$) δ 88.32 (Cp*C*), 86.59 (Cp*C*), 86.53 (Cp*C*), 31.82 (*C*H$_2$), 29.84 (*C*H$_2$), 29.18 (*C*H$_2$), 27.81 (*C*H$_2$), 24.27 (*C*H$_2$), 22.75 (*C*H$_2$), 14.23 (*C*H$_3$), 9.57 (Cp*C*H$_3$), 9.52 (Cp*C*H$_3$). HRMS/ESI+ (m/z): $C_{32}H_{54}[^{193}Ir]_2Cl_3$ 929.2550; Found 929.2531 Anal. Calc. for $C_{32}H_{54}Cl_4Ir_2$, C, 39.83; H, 5.64; Found, C, 39.89; H, 5.60

Synthesis of [Cp*$^{n\text{-octyl}}$IrCl]$_2$(μ^2-Cl)$_2$ (2j). Following the general procedure, [Ir(COD)]$_2$(μ^2-Cl)$_2$ (0.200 g, 0.298 mmol), **1j** (0.349 g, 1.49 mmol), and 0.5 mL of HCl were reacted in methanol (4 mL) to give **2j** (0.246 g, 83% yield). ^{1}H NMR (400 MHz, $CDCl_3$) δ 2.14 – 2.10 (app. t, 4H, 2 C*H*$_2$(CH$_2$)$_6$CH$_3$), 1.61 (s, 12 H, 4 CpC*H*$_3$), 1.59 (s, 12H, 4 CpC*H*$_3$), 1.44-1.34 (m, 4H, 2

$CH_2CH_2(CH_2)_5CH_3$), 1.33-1.19 (m, 20H, 2 $CH_2CH_2(CH_2)_5CH_3$), 0.88-0.85 (app. t, 6H, 2 CH_3). $^{13}C\{^1H\}$ NMR (101 MHz, $CDCl_3$) δ 88.33 (Cp*C*), 86.60 (Cp*C*), 86.54 (Cp*C*), 31.95 (CH_2), 29.88 (CH_2), 29.47 (CH_2), 29.27 (CH_2), 27.81 (CH_2), 24.28 (CH_2), 22.78 (CH_2), 14.23 (CH_3), 9.58 (CpCH_3), 9.54 (CpCH_3). HRMS/ESI+ (m/z): $C_{34}H_{58}[^{193}Ir]_2Cl_3$ 957.2863; Found 957.2828 Anal. Calc. for $C_{34}H_{58}Cl_4Ir_2$, C, 41.12; H, 5.89; Found, C, 41.28; H, 5.74

Synthesis of [Cp*^{phenyl}IrCl]$_2$(μ^2-Cl)$_2$ (2k). Following the general procedure, [Ir(COD)]$_2$(μ^2-Cl)$_2$ (0.250 g, 0.372 mmol), **1k** (0.295 g, 1.49 mmol), and 0.5 mL of HCl were reacted in methanol (4 mL) to give **2k** (0.237 g, 69% yield). ^1H NMR (400 MHz, $CDCl_3$) δ 7.58 – 7.55 (m, 4H, Ar*H*), 7.37 – 7.34 (m, 6H, Ar*H*), 1.72 (s, 12 H, 4 CpCH_3), 1.63 (s, 12H, 4 CpCH_3). $^{13}C\{^1H\}$ NMR (101 MHz, CDCl3) δ 130.34 (Ar*C*), 129.94 (Ar*C*), 128.79 (Ar*C*), 128.58 (Ar*C*), 93.64 (Cp*C*), 85.61 (Cp*C*), 82.10 (Cp*C*), 10.50 (CpCH_3), 9.77 (CpCH_3). HRMS/ESI+ (m/z): Calc. for $C_{30}H_{34}[^{193}Ir]_2Cl_3$ 885.0985; Found 885.1018 Anal. Calc. for $C_{30}H_{34}Ir_2Cl_4$, C, 39.13; H, 3.72; Found, C, 38.89; H, 3.51

Synthesis of [Cp*^{benzyl}IrCl]$_2$(μ^2-Cl)$_2$ (2l). Following the general procedure, [Ir(COD)]$_2$(μ^2-Cl)$_2$ (0.100 g, 0.149 mmol), **1l** (0.111 g, 0.521 mmol), and 0.5 mL of HCl were reacted in methanol (4 mL) to give **2l** (0.123 g, 87% yield). ^1H NMR (400 MHz, $CDCl_3$) δ 7.30 – 7.27 (m, 2H, Ar*H*), 7.26 – 7.25 (m, 2H, Ar*H*), 7.23 – 7.18 (m, 2H, Ar*H*), 7.11 – 7.09 (m, 4H, Ar*H*), 3.57 (s, 4 H, 2 CH_2), 1.65 (s, 12 H, 4 CpCH_3), 1.63 (s, 12H, 4 CpCH_3). $^{13}C\{^1H\}$ NMR (101 MHz, $CDCl_3$) δ 136.97 (Ar*C*), 128.88 (Ar*C*), 128.38 (Ar*C*), 126.90 (Ar*C*), 87.68 (Cp*C*), 86.90 (Cp*C*), 85.93 (Cp*C*), 30.58 (CH_2), 9.97 (CpCH_3), 9.53 (CpCH_3). HRMS/ESI+ (m/z): Calc. for $C_{32}H_{38}[^{193}Ir]_2Cl_3$ 913.1298; Found 913.1347 Anal. Calc. for $C_{32}H_{38}Ir_2Cl_4$, C, 40.51; H, 4.04; Found, C, 40.40; H, 3.98

Synthesis of [Cp*^{phenethyl}IrCl]$_2$(μ^2-Cl)$_2$ (2m). Following the general procedure, [Ir(COD)]$_2$(μ^2-Cl)$_2$ (0.200 g, 0.298 mmol), **1m** (0.336 g, 1.49 mmol), and 0.5 mL of HCl were reacted in methanol

(4 mL) to give **2m** (0.245 g, 84% yield). ^{1}H NMR (400 MHz, $CDCl_3$) δ 7.25 – 7.16 (m, 6H, Ar*H*), 7.04 – 7.02 (m, 4H, Ar*H*), 2.77 – 2.73 (t, 4H, $^{2}J_{HH}$ = 7.3 Hz, 2 PhCH_2CH_2), 2.48 – 2.45 (t, 4H, $^{2}J_{HH}$ = 7.3 Hz, 2 PhCH_2CH_2), 1.55 (s, 12 H, 4 CpCH_3), 1.36 (s, 12H, 4 CpCH_3). ^{13}C{^{1}H} NMR (101 MHz, $CDCl_3$) δ 140.14 (Ar*C*), 128.64 (Ar*C*), 128.46 (Ar*C*), 126.35 (Ar*C*), 87.22 (Cp*C*), 86.30 (Cp*C*), 86.29 (Cp*C*), 33.60 (Ph*C*H_2CH_2), 26.60 (PhCH_2*C*H_2), 9.27 (Cp*C*H_3), 9.09 (Cp*C*H_3). HRMS/ESI+ (m/z): Calc. for $C_{34}H_{42}[^{193}Ir]_2Cl_3$ 941.1611; Found 941.1616 Anal. Calc. for $C_{34}H_{42}Ir_2Cl_4$, C, 41.80; H, 4.33; Found, C, 41.92; H, 4.22

Synthesis of [Cp*^{cyclohexyl}IrCl]$_2$(μ^2-Cl)$_2$ (2n). Following the general procedure, [Ir(COD)]$_2$(μ^2-Cl)$_2$ (0.200 g, 0.298 mmol), **1n** (0.152 g, 0.744 mmol), and 0.5 mL of HCl were reacted in methanol (4 mL) to give **2n** (0.079 g, 48% yield). ^{1}H NMR (400 MHz, $CDCl_3$) δ 2.08 – 2.01 (m, 2H, 2 C*H*), 1.93 – 1.89 (m, 4H, 2 CH_2), 1.78 – 1.74 (m, 4H, 2 CH_2), 1.67 (s, 12 H, 4 CpCH_3), 1.59 (s, 12H, 4 CpCH_3), 1.43 – 1.22 (m, 10H, CH_2), 1.18 – 1.09 (m, 2H, CH_2). ^{13}C{^{1}H} NMR (101 MHz, $CDCl_3$) δ 90.77 (Cp*C*), 85.99 (Cp*C*), 84.81 (Cp*C*), 35.75 (*C*H), 30.88 (*C*H_2), 27.10 (*C*H_2), 26.20 (*C*H_2), 10.70 (Cp*C*H_3), 9.74 (Cp*C*H_3). HRMS/ESI+ (m/z): Calc. for $C_{30}H_{46}[^{193}Ir]_2Cl_3$ 897.1924; Found 897.1946 Anal. Calc. for $C_{30}H_{46}Ir_2Cl_4$, C, 38.62; H, 4.97; Found, C, 38.77; H, 4.92

Synthesis of [Cp*^{cyclopentyl}IrCl]$_2$(μ^2-Cl)$_2$ (2o). Following the general procedure, [Ir(COD)]$_2$(μ^2-Cl)$_2$ (0.250 g, 0.372 mmol), **1o** (0.248 g, 1.30 mmol), and 0.5 mL of HCl were reacted in methanol (4 mL) to give **2o** (0.213 g, 59% yield). ^{1}H NMR (400 MHz, $CDCl_3$) δ 2.63 – 2.54 (m, 2H, 2 C*H*), 2.09 – 2.02 (m, 4H, 2 CH_2), 1.74 – 1.71 (m, 2H, CH_2), 1. 68 (s, 12 H, 4 CpCH_3), 1.67 – 1.60 (m, 10H, CH_2), 1.59 (s, 12H, 4 CpCH_3). ^{13}C{^{1}H} NMR (101 MHz, $CDCl_3$) δ 89.60 (Cp*C*), 86.07 (Cp*C*), 85.92 (Cp*C*), 36.05 (*C*H), 31.34 (*C*H_2), 26.67 (*C*H_2), 10.46 (Cp*C*H_3), 9.72 (Cp*C*H_3). HRMS/ESI+ (m/z): Calc. for $C_{28}H_{42}[^{193}Ir]_2Cl_3$ 869.1611; Found 869.1567

2.6.4 General procedure for the synthesis of $[(\eta^5\text{-}Me_4C_5R)RhCl]_2(\mu^2\text{-}Cl)_2$

A microwave pressure tube was fitted with the appropriate amounts of the respective $[Rh(COD)]_2(\mu^2\text{-}Cl)_2$, HMe_4C_5R, in 4 mL of methanol with 0.5 mL of concentrated HCl. The reaction mixture was heated to 115 °C at 50 watts and 150 psi and held for 1 hour, yielding a red solution. The solvent was evaporated under reduced pressure, and the resulting powder recrystallized from DCM and cold hexanes, collected via filtration, and washed with cold hexanes. Complexes **3a**, **3c**, **3k**, **3m**, and **3n** have previously been reported and were identified by HRMS as well as by comparison of NMR spectra with those reported in the literature.[43–45,63,65]

Synthesis of $[Cp^{*ethyl}RhCl]_2(\mu^2\text{-}Cl)_2$ (3a). Following the general procedure, $[Rh(COD)]_2(\mu^2\text{-}Cl)_2$ (0.250 g, 0.507 mmol), **1a** (0.244 g, 1.62 mmol), and 0.5 mL of HCl were reacted in methanol (4 mL) to give **3a** (0.259 g, 79% yield). ^{1}H NMR (400 MHz, $CDCl_3$) δ 2.27 – 2.23 (q, 4H, $^2J_{HH}$ = 7.7 Hz, 2 CH_2), 1.61 (s, 12 H, 4 CpCH_3), 1.60 (s, 12H, 4 CpCH_3), 1.01-0.97 (t, 6 H, $^2J_{HH}$ = 7.7 Hz, 2 CH_3). ^{13}C{^{1}H} NMR (101 MHz, $CDCl_3$) δ 97.41-97.31 (d, J_{CRh} = 9.3 Hz, Cp*C*), 94.76-94.66 (d, J_{CRh} = 9.2 Hz, Cp*C*), 94.00-93.91 (d, J_{CRh} = 9.1 Hz, Cp*C*), 17.61 (*C*H_2), 11.55 (*C*H_3), 9.51 (Cp*C*H_3), 9.30 (Cp*C*H_3). HRMS/ESI+ (m/z): Calc. for $C_{22}H_{34}Cl_3Rh_2$ 608.9836; Found 608.9761

Synthesis of $[Cp^{*n\text{-}propyl}RhCl]_2(\mu^2\text{-}Cl)_2$ (3b). Following the general procedure, $[Rh(COD)]_2(\mu^2\text{-}Cl)_2$ (0.150 g, 0.304 mmol) of, **1b** (0.200 g, 1.22 mmol), and 0.5 mL of HCl were reacted in methanol (4 mL) to give **3b** (0.164 g, 80% yield). ^{1}H NMR (400 MHz, $CDCl_3$) δ 2.27 – 2.23 (m, 4H, 2 CH_2CH$_2$CH$_3$), 1.64 (s, 12H, 4 CpCH_3), 1.62 (s, 12H, 4 CpCH_3), 1.45-1.36 (m, 4H, 2 CH$_2$CH_2CH$_3$), 0.94-0.91 (app. t, 6H, 2 CH_3). ^{13}C{^{1}H} NMR (101 MHz, $CDCl_3$) δ 96.19-96.10 (d, J_{CRh} = 9.4 Hz, Cp*C*), 94.73-94.64 (d, J_{CRh} = 9.2 Hz, Cp*C*), 94.36-94.27 (d, J_{CRh} = 9.3 Hz, Cp*C*), 26.06 (*C*H$_2$CH$_2$CH$_3$), 20.91 (CH$_2$*C*H$_2$CH$_3$), 14.33 (*C*H$_3$), 9.61 (Cp*C*H$_3$), 9.55 (Cp*C*H$_3$).

HRMS/ESI+ (m/z): Calc. for $C_{24}H_{38}Cl_3Rh_2$ 637.0149; Found 637.0173 Anal. Calc. for $C_{24}H_{38}Cl_4Rh_2$, C, 42.76; H, 5.68; Found, C, 42.47; H, 5.68

Synthesis of [Cp*^{isopropyl}RhCl]$_2$(μ^2-Cl)$_2$ (3c). Following the general procedure, [Rh(COD)]$_2$(μ^2-Cl)$_2$ (0.100 g, 0.203 mmol), **1c** (0.112 g, 0.710 mmol), and 0.5 mL of HCl were reacted in methanol (4 mL) to give **3c** (0.067 g, 50% yield). ^{1}H NMR (400 MHz, $CDCl_3$) δ 2.66 – 2.55 (m, 2H, 2 C*H*), 1.72 (s, 12 H, 4 CpC*H*$_3$), 1.60 (s, 12H, 4 CpC*H*$_3$), 1.31-1.29 (d, 12H, $^2J_{HH}$ = 7.1 Hz, 4 C*H*$_3$). ^{13}C{^{1}H} NMR (101 MHz, $CDCl_3$) δ 97.71-97.62 (d, J_{CRh} = 9.1 Hz, Cp*C*), 95.44-95.34 (d, J_{CRh} = 10.0 Hz, Cp*C*), 94.22-94.13 (d, J_{CRh} = 9.2 Hz, Cp*C*), 25.09 (*C*H(CH$_3$)$_2$), 20.79 (CH(*C*H$_3$)$_2$), 10.51 (Cp*C*H$_3$), 9.62 (Cp*C*H$_3$). HRMS/ESI+ (m/z): Calc. for $C_{24}H_{38}Cl_3Rh_2$ 637.0149; Found 637.014

Synthesis of [Cp*$^{n\text{-}butyl}$RhCl]$_2$(μ^2-Cl)$_2$ (3d). Following the general procedure, [Rh(COD)]$_2$(μ^2-Cl)$_2$ (0.200 g, 0.406 mmol), **1d** (0.289 g, 1.62 mmol), and 0.5 mL of concentrated HCl were reacted in methanol (4 mL) to give **3d** (0.180 g, 63%). ^{1}H NMR (400 MHz, $CDCl_3$) δ 2.27 – 2.24 (m, 4H, 2 C*H*$_2$(CH$_2$)$_2$CH$_3$), 1.63 (s, 12H, 4 CpC*H*$_3$), 1.61 (s, 12H, 4 CpC*H*$_3$), 1.38-1.27 (m, 8H, 2 CH$_2$(C*H*$_2$)$_2$CH$_3$), 0.90-0.87 (app. t, 6H, 2 C*H*$_3$). ^{13}C{^{1}H} NMR (101 MHz, $CDCl_3$) δ 96.33-96.24 (d, J_{CRh} = 9.6 Hz, Cp*C*), 94.64-94.55 (d, J_{CRh} = 9.2 Hz, Cp*C*), 94.26-94.17 (d, J_{CRh} = 9.2 Hz, Cp*C*), 29.76, 23.85, 22.90, 13.96 (*C*H$_3$), 9.54 (Cp*C*H$_3$), 9.54 (Cp*C*H$_3$). HRMS/ESI+ (m/z): Calc. for $C_{26}H_{42}Cl_3Rh_2$ 665.0462; Found 665.0447 Anal. Calc. for $C_{26}H_{42}Cl_4Rh_2$, C, 44.47; H, 6.03; Found, C, 44.55; H, 5.96

Synthesis of [Cp*^{isobutyl}RhCl]$_2$(μ^2-Cl)$_2$ (3e). Following the general procedure, [Rh(COD)]$_2$(μ^2-Cl)$_2$ (0.200 g, 0.406 mmol), **1e** (0.362 g, 2.03 mmol), and 0.5 mL of HCl were reacted in methanol (4 mL) to give **3e** (0.252 g, 89% yield). ^{1}H NMR (400 MHz, $CDCl_3$) δ 2.19 – 2.17 (d, 4H, $^2J_{HH}$ = 7.5 Hz, 2 C*H*$_2$), 1.73-1.64 (m, 2H, 2 C*H*), 1.63 (s, 12H, 4 CpC*H*$_3$), 1.62 (s, 12H, 4 CpC*H*$_3$), 0.88-0.87 (d, 12 H, $^2J_{HH}$ = 6.7 Hz, 4 C*H*$_3$). ^{13}C{^{1}H} NMR (101 MHz, $CDCl_3$) δ 95.58-95.49 (d, J_{CRh} =

9.4 Hz, Cp*C*), 94.74-94.66 (d, J_{CRh} = 9.2 Hz, Cp*C*), 94.70-94.61 (d, J_{CRh} = 9.2 Hz, Cp*C*), 32.93 ($CH_2CH(CH_3)_2$), 27.98 ($CH_2CH(CH_3)_2$), 23.84 ($CH_2CH(CH_3)_2$), 10.09 (CpCH_3), 9.58 (CpCH_3). HRMS/ESI+ (m/z): $C_{26}H_{42}Cl_3Rh_2$ 665.0462; Found 665.0459 Anal. Calc. for $C_{26}H_{42}Cl_4Rh_2$, C, 44.47; H, 6.03; Found, C, 44.18; H, 5.96

Synthesis of [Cp*$^{sec\text{-butyl}}$RhCl]$_2$(μ^2-Cl)$_2$ (3f). Following the general procedure, [Rh(COD)]$_2$(μ^2-Cl)$_2$, **1f** (0.289 g, 1.62 mmol), and 0.5 mL of HCl were reacted in methanol (4 mL). Upon cooling, an orange-yellow powder (0.123 g) formed in a red solution. The powder was isolated and the red solution evaporated under reduced pressure. The resulting red powder was recrystallized from DCM and cold hexanes and collected by filtration. The red powder was washed with cold hexanes to give **3f** in a reacted yield of 0.0589 g (54%). ^{1}H NMR (400 MHz, $CDCl_3$) δ 2.37 – 2.28 (m, 2H, 2 C*H*), 1.72 (s, 6H, 2 CpCH_3), 1.69 (s, 6H, 2 CpCH_3), 1.67 – 1.64 (m, 2H, CH*H*), 1.61 (s, 6H, 2 CpCH_3), 1.60 (s, 6H, 2 CpCH_3), 1.51 – 1.42 (m, 2H, C*H*H), 1.39 – 1.37 (d, 6H, $^2J_{HH}$ = 7.1 Hz, CH_3CH), 0.90 – 0.86 (t, 6H, $^2J_{HH}$ = 7.4 Hz, CH_2CH_3). ^{13}C{^{1}H} NMR (101 MHz, $CDCl_3$) δ 98.37-98.29 (d, J_{CRh} = 8.8 Hz, Cp*C*), 97.61-97.53 (d, J_{CRh} = 8.9 Hz, Cp*C*), 95.35-95.25 (d, J_{CRh} = 10.1 Hz, Cp*C*), 95.29-95.20 (d, J_{CRh} = 9.0 Hz, Cp*C*), 92.83-92.73 (d, J_{CRh} = 9.4 Hz, Cp*C*), 31.65 (*C*H), 27.79 (CH_2), 18.41 (CH_3CH), 12.65 (CH_3CH_2), 10.89 (CpCH_3), 10.45 (CpCH_3), 9.83 (CpCH_3), 9.44 (CpCH_3). HRMS/ESI+ (m/z): $C_{26}H_{42}Cl_3Rh_2$ 665.0462; Found 665.0472

Synthesis of [Cp*$^{n\text{-pentyl}}$RhCl]$_2$(μ^2-Cl)$_2$ (3g). Following the general procedure, [Rh(COD)]$_2$(μ^2-Cl)$_2$ (0.200 g, 0.406 mmol), **1g** (0.312 g, 1.62 mmol), and 0.5 mL of HCl were reacted in methanol (4 mL) to give **3g (**0.227 g, 77%). ^{1}H NMR (400 MHz, $CDCl_3$) δ 2.27 – 2.23 (m, 4H, 2 C$H_2(CH_2)_3CH_3$), 1.63 (s, 12H, 4 CpCH_3), 1.62 (s, 12H, 4 CpCH_3), 1.38-1.24 (m, 12H, $CH_2(CH_2)_3CH_3$), 0.87-0.84 (app. t, 6H, 2 CH_3). ^{13}C{^{1}H} NMR (101 MHz, $CDCl_3$) δ 96.44-96.34 (d, J_{CRh} = 9.3 Hz, Cp*C*), 94.69-94.60 (d, J_{CRh} = 9.1 Hz, Cp*C*), 94.29-94.19 (d, J_{CRh} = 9.2 Hz, Cp*C*),

31.88 (*C*H_2), 27.33 (*C*H_2), 24.10 (*C*H_2), 22.50 (*C*H_2), 13.96 (*C*H_3), 9.58 (Cp*C*H_3), 9.56 (Cp*C*H_3). HRMS/ESI+ (m/z): Calc. for $C_{28}H_{46}Cl_3Rh_2$ 693.0775; Found 693.0788 Anal. Calc. for $C_{28}H_{46}Cl_4Rh_2$, C, 46.05; H, 6.35; Found, C, 45.77; H, 6.16

Synthesis of [Cp*$^{n\text{-hexyl}}$RhCl]$_2$(μ^2-Cl)$_2$ (3h). Following the general procedure, [Rh(COD)]$_2$(μ^2-Cl)$_2$ (0.200 g, 0.304 mmol), **1h** (0.344 g, 1.62 mmol), and 0.5 mL of HCl were reacted in methanol (4 mL) to give **3h** (0.224 g, 73% yield). ^{1}H NMR (400 MHz, $CDCl_3$) δ 2.26 – 2.23 (m, 4H, 2 C*H*$_2$(CH$_2$)$_4$CH$_3$), 1.63 (s, 12H, 4 CpC*H*$_3$), 1.61 (s, 12H, 4 CpC*H*$_3$), 1.37-1.24 (m, 16H, 2 CH$_2$(C*H*$_2$)$_4$CH$_3$), 0.87-0.84 (app. t, 6H, 2 C*H*$_3$). ^{13}C{^{1}H} NMR (101 MHz, $CDCl_3$) δ 96.41-96.31 (d, J_{CRh} = 9.4 Hz, Cp*C*), 94.68-94.59 (d, J_{CRh} = 9.1 Hz, Cp*C*), 94.26-94.17 (d, J_{CRh} = 9.3 Hz, Cp*C*), 31.61 (*C*H_2), 29.46 (*C*H_2), 27.62 (*C*H_2), 24.14 (*C*H_2), 22.58 (*C*H_2), 14.13 (*C*H_3), 9.57 (Cp*C*H_3), 9.55 (Cp*C*H_3). HRMS/ESI+ (m/z): Calc. for $C_{30}H_{50}Cl_3Rh_2$ 721.1088; Found 721.1106

Synthesis of [Cp*$^{n\text{-heptyl}}$RhCl]$_2$(μ^2-Cl)$_2$ (3i). Following the general procedure, [Rh(COD)]$_2$(μ^2-Cl)$_2$ (0.150 g, 0.304 mmol), **1i** (0.344 g, 1.62 mmol), and 0.5 mL of HCl were reacted in methanol (4 mL) to give **3i** (0.125g, 52% yield). ^{1}H NMR (400 MHz, $CDCl_3$) δ 2.26 – 2.22 (m, 4H, 2 C*H*$_2$(CH$_2$)$_5$CH$_3$), 1.63 (s, 12H, 4 CpC*H*$_3$), 1.61 (s, 12H, 4 CpC*H*$_3$), 1.33-1.22 (m, 20H, CH$_2$(C*H*$_2$)$_5$CH$_3$), 0.87-0.83 (app. t, 6H, 2 C*H*$_3$). ^{13}C{^{1}H} NMR (101 MHz, $CDCl_3$) δ 96.41-96.32 (d, J_{CRh} = 9.5 Hz, Cp*C*), 94.69-94.60 (d, J_{CRh} = 9.2 Hz, Cp*C*), 94.26-94.17 (d, J_{CRh} = 9.2 Hz, Cp*C*), 31.77 (*C*H_2), 29.76 (*C*H_2), 29.13 (*C*H_2), 27.66 (*C*H_2), 24.13 (*C*H_2), 22.17 (*C*H_2), 14.20 (*C*H_3), 9.57 (Cp*C*H_3), 9.55 (Cp*C*H_3). HRMS/ESI+ (m/z): Calc. for $C_{32}H_{54}Cl_3Rh_2$ 749.1401; Found 749.1413 Anal. Calc. for $C_{32}H_{54}Cl_4Rh_2$, C, 48.88; H, 6.92; Found, C, 49.11; H, 6.87

Synthesis of [Cp*$^{n\text{-octyl}}$RhCl]$_2$(μ^2-Cl)$_2$ (3j). Following the general procedure, [Rh(COD)]$_2$(μ^2-Cl)$_2$ (0.200 g, 0.304 mmol), **1j** (0.344 g, 1.62 mmol), and 0.5 mL of HCl were reacted in methanol (4 mL) to give **3j** (0.173 g, 52% yield). ^{1}H NMR (400 MHz, $CDCl_3$) δ 2.26 – 2.22 (app. t, 4H, 2

C*H*$_2$(CH$_2$)$_6$CH$_3$), 1.63 (s, 12H, 4 CpC*H*$_3$), 1.61 (s, 12H, 4 CpC*H*$_3$), 1.29-1.23 (m, 24H, CH$_2$(C*H*$_2$)$_6$CH$_3$), 0.87-0.84 (app. t, 6 H, 2 C*H*$_3$). ^{13}C{^{1}H} NMR (101 MHz, CDCl$_3$) δ 96.41-96.32 (d, J_{CRh} = 9.5 Hz), 94.69-94.60 (d, J_{CRh} = 9.2 Hz, Cp*C*), 94.26-94.17 (d, J_{CRh} = 9.2 Hz, Cp*C*), 32.23 (*C*H$_2$), 30.12 (*C*H$_2$), 29.74 (*C*H$_2$), 29.53 (*C*H$_2$), 27.98 (*C*H$_2$), 24.46 (*C*H$_2$), 23.07 (*C*H$_2$), 14.53 (*C*H$_3$), 9.89 (Cp*C*H$_3$), 9.87 (Cp*C*H$_3$). HRMS/ESI+ (m/z): Calc. for C$_{34}$H$_{58}$Cl$_3$Rh$_2$ 777.1717; Found 777.1701 Anal. Calc. for C$_{34}$H$_{58}$Cl$_4$Rh$_2$, C, 50.14; H, 7.18; Found, C, 50.43; H, 7.09

Synthesis of [Cp*^{phenyl}RhCl]$_2$(μ^2-Cl)$_2$ (3k). Following the general procedure, [Rh(COD)]$_2$(μ^2-Cl)$_2$ (0.200 g, 0.406 mmol), **1k** (0.322 g, 1.62 mmol), and 0.5 mL of HCl were reacted in methanol (4 mL) to give **3k** (0.225 g, 75%). ^{1}H NMR (400 MHz, CDCl$_3$) δ 7.66 – 7.64 (m, 4H, Ar*H*), 7.39 – 7.36 (m, 6H, Ar*H*), 1.71 (s, 12 H, 4 CpC*H*$_3$), 1.68 (s, 12H, 4 CpC*H*$_3$). ^{13}C{^{1}H} NMR (101 MHz, CDCl$_3$) δ 130.36 (Ar*C*), 129.02 (Ar*C*), 128.74 (Ar*C*), 128.41 (Ar*C*), 100.47-100.39 (d, J_{CRh} = 8.6 Hz, Cp*C*), 93.67-93.58 (d, J_{CRh} = 9.0 Hz, Cp*C*), 90.70-90.60 (d, J_{CRh} = 10.2 Hz, Cp*C*), 10.75 (Cp*C*H$_3$), 9.75 (Cp*C*H$_3$). HRMS/ESI+ (m/z): Calc. for C$_{30}$H$_{34}$Cl$_3$Rh$_2$ 704.9836; Found 704.9854

Synthesis of [Cp*^{benzyl}RhCl]$_2$(μ^2-Cl)$_2$ (3l). Following the general procedure, [Rh(COD)]$_2$(μ^2-Cl)$_2$ (0.200 g, 0.406 mmol), **1l** (0.344 g, 1.62 mmol), and 0.5 mL of HCl were reacted in methanol (4 mL) to give **3l** (0.276 g, 89% yield). ^{1}H NMR (400 MHz, CDCl$_3$) δ 7.28 – 7.25 (m, 2H, Ar*H*), 7.24 – 7.18 (m, 4H, Ar*H*), 7.08-7.06 (m, 4 H, Ar*H*), 3.71 (s, 4 H, 2 C*H*$_2$), 1.67 (s, 12 H, 4 CpC*H*$_3$), 1.65 (s, 12H, 4 CpC*H*$_3$). ^{13}C{^{1}H} NMR (101 MHz, CDCl$_3$) δ 136.17 (Ar*C*), 128.81 (Ar*C*), 128.26 (Ar*C*), 126.86 (Ar*C*), 95.09-95.00 (d, J_{CRh} = 9.1 Hz, Cp*C*), 94.94-94.85 (d, J_{CRh} = 9.0 Hz, Cp*C*), 93.98-93.88 (d, J_{CRh} = 9.5 Hz, Cp*C*), 30.14 (*C*H$_2$), 9.87 (Cp*C*H$_3$), 9.44 (Cp*C*H$_3$). HRMS/ESI+ (m/z): Calc. for C$_{32}$H$_{38}$Cl$_3$Rh$_2$ 733.0149; Found 733.0158 Anal. Calc. for C$_{32}$H$_{38}$Cl$_4$Rh$_2$, C, 49.90; H, 4.97; Found, C, 50.49; H, 5.19

Synthesis of [Cp*^{phenethyl}RhCl]$_2$(μ^2-Cl)$_2$ (3m). Following the general procedure, [Rh(COD)]$_2$(μ^2-Cl)$_2$ (0.150 g, 0.304 mmol), **1m** (0.274 g, 1.22 mmol), and 0.5 mL of HCl were reacted in methanol (4 mL) to give **3m** (0.186 g, 77% yield). ^{1}H NMR (400 MHz, $CDCl_3$) δ 7.23 – 7.14 (m, 6H, Ar*H*), 6.99 – 6.97 (m, 4H, Ar*H*), 2.72-2.69 (t, 4 H, $^2J_{HH}$ = 7.3 Hz, 2 PhC*H*$_2$CH$_2$), 2.61-2.57 (t, 4 H, $^2J_{HH}$ = 7.3 Hz, 2 PhCH$_2$C*H*$_2$), 1.57 (s, 12 H, 4 CpC*H*$_3$), 1.36 (s, 12H, 4 CpC*H*$_3$). ^{13}C{^{1}H} NMR (101 MHz, $CDCl_3$) δ 139.75 (Ar*C*), 128.60 (Ar*C*), 128.50 (Ar*C*), 126.47 (Ar*C*), 94.82-94.73 (d, J_{CRh} = 9.1 Hz, Cp*C*), 94.61-94.52 (d, J_{CRh} = 9.5 Hz, Cp*C*), 94.44-94.35 (d, J_{CRh} = 9.2 Hz, Cp*C*), 33.37 (Ph*C*H$_2$CH$_2$), 26.45 (PhCH$_2$*C*H$_2$), 9.32 (Cp*C*H$_3$), 9.12 (Cp*C*H$_3$). HRMS/ESI+ (m/z): Calc. for $C_{34}H_{38}Cl_3Rh_2$ 761.0462; Found 761.0466 Anal. Calc. for $C_{34}H_{42}Cl_4Rh_2$, C, 51.15; H, 5.30; Found, C, 50.89; H, 5.18

Synthesis of [Cp*^{cyclohexyl}RhCl]$_2$(μ^2-Cl)$_2$ (3n). Following the general procedure, [Rh(COD)]$_2$(μ^2-Cl)$_2$ (0.200 g, 0.406 mmol), **1n** (0.332 g, 1.62 mmol), and 0.5 mL of HCl were reacted in methanol (4 mL). Upon cooling, an orange-yellow powder (0.091 g) formed in a red solution. The powder was isolated and the red solution evaporated under reduced pressure. The resulting red powder was recrystallized from DCM and cold hexanes and collected by filtration. The red powder was washed with cold hexanes to give **3n** in a reacted yield of 0.106 g (64%). ^{1}H NMR (400 MHz, $CDCl_3$) δ 2.20 – 2.12 (m, 2H, 2 C*H*), 2.01 – 1.98 (m, 4H, 2 C*H*$_2$), 1.79 – 1.75 (m, 4H, 2 C*H*$_2$), 1.71 (s, 12 H, 4 CpC*H*$_3$), 1.59 (s, 12H, 4 CpC*H*$_3$), 1.44 – 1.25 (m, 10H, C*H*$_2$), 1.19 – 1.08 (m, 2H, C*H*$_2$). ^{13}C{^{1}H} NMR (101 MHz, $CDCl_3$) δ 97.95-97.86 (d, J_{CRh} = 8.9 Hz, Cp*C*), 94.08-93.99 (d, J_{CRh} = 9.1 Hz, Cp*C*), 93.83-93.74 (d, J_{CRh} = 9.1 Hz, Cp*C*), 35.39 (*C*H), 30.76 (*C*H$_2$), 26.83 (*C*H$_2$), 26.12 (*C*H$_2$), 10.78 (Cp*C*H$_3$), 9.66 (Cp*C*H$_3$). HRMS/ESI+ (m/z): Calc. for $C_{30}H_{46}Cl_3Rh_2$ 717.0775; Found 717.0782 Anal. Calc. for $C_{30}H_{46}Cl_4Rh_2$, C, 47.77; H, 6.15; Found, C, 47.27; H, 5.88

Synthesis of [Cp*^{cyclopentyl}RhCl]$_2$(μ^2-Cl)$_2$ (3o). Following the general procedure, [Rh(COD)]$_2$(μ^2-Cl)$_2$ (0.150 g, 0.304 mmol), **1o** (0.232 g, 1.22 mmol), and 0.5 mL of HCl were reacted in methanol (4 mL). Upon cooling, an orange-yellow powder (0.031 g) formed in a red solution. The powder was isolated and the red solution evaporated under reduced pressure. The resulting red powder was recrystallized from DCM and cold hexanes and collected by filtration. The red powder was washed with cold hexanes to give **3o** in a reacted yield of 0.095 g (54%).^{1}H NMR (400 MHz, $CDCl_3$) δ 2.71 – 2.62 (m, 2H, 2 C*H*), 2.13 – 2.06 (m, 4H, 2 CH_2), 1. 72 (s, 12H, 4 CpCH_3), 1.69 – 1.62 (m, 12H, CH_2), 1.60 (s, 12H, 4 CpCH_3). ^{13}C{^{1}H} NMR (101 MHz, $CDCl_3$) δ 97.15-97.05 (d, J_{CRh} = 9. 0 Hz, Cp*C*), 94.56-94.47 (d, J_{CRh} = 9.0 Hz, Cp*C*), 93.97-93.88 (d, J_{CRh} = 9.3 Hz, Cp*C*), 35.63 (*C*H), 31.60 (*C*H$_2$), 26.69 (*C*H$_2$), 10.56 (Cp*C*H$_3$), 9.63 (Cp*C*H$_3$). HRMS/ESI+ (m/z): Calc. for $C_{28}H_{42}Cl_3Rh_2$ 689.0462; Found 689.0503

Biological Testing

MICs were measured by broth microdilution of fresh overnight cultures according to the Clinical and Laboratory Standards Institute (CCLI) guidelines with cation-adjusted Mueller–Hinton broth and an inoculum of 105 CFU mL^{-1}. [76] Stocks of the compounds were dissolved in Mueller–Hinton broth. The MIC (μgmL^{-1}) was defined as the lowest concentration of compound completely inhibiting the appearance of turbidity by eye and confirmed by absorbance 540 nm. The MBC (μgmL^{-1}) was defined as the lowest concentration of compound reducing the colony count by 99.9% of the colony count in the initial, compound-free, inoculated well after 24 hr incubation. All results represent the average of three independent measurements. Both MIC and MBC experiments were also performed using brain heart infusion broth (BHIB), resulting in similar data for both MIC and MBC.

References

1. Cuenca, T. & Royo, P. Transition metal complexes with functionalized silyl-substituted cyclopentadienyl and related ligands: Synthesis and reactivity. *Coord. Chem. Rev.* **193–195,** 447–498 (1999).

2. Thornberry, M. P., Slebodnick, C., Deck, P. A. & Fronczek, F. R. Synthesis and structure of piano stool complexes derived from the tetrakis(pentafluorophenyl)cyclopentadienyl ligand. *Organometallics* **20,** 920–926 (2001).

3. Thornberry, M. P., Slebodnick, C., Deck, P. A. & Fronczek, F. R. Structural and electronic effects of pentafluorophenyl substituents on cyclopentadienyl complexes of Fe, Co, Mn, and Re. *Organometallics* **19,** 5352–5369 (2000).

4. Deck, P. A., Jackson, W. F. & Fronczek, F. R. Synthesis of pentafluorophenyl-substituted cyclopentadienes and their use as transition-metal ligands. *Organometallics* **15,** 5287–5291 (1996).

5. Wilkinson, G. The iron sandwich. A recollection of the first four months. *J. Organomet. Chem.* **100,** 273–278 (1975).

6. Werner, H. At Least 60 Years of Ferrocene: The Discovery and Rediscovery of the Sandwich Complexes. *Angew. Chemie Int. Ed.* **51,** 6052–6058 (2012).

7. Slocum, D. W. & Ernst, C. R. Electronic Effects in Metallocenes and Certain Related Systems. in *Advances in Organometallic Chemistry* **10,** 79–114 (1972).

8. Wolczanski, P. T. & Bercaw, J. E. Alkyl and hydride derivatives of (pentamethylcyclopentadienyl)zirconium(IV). *Organometallics* **1,** 793–799 (1982).

9. Brintzinger, H. & Bercaw, J. E. Bis(pentamethylcyclopentadienyl)titanium(II). Isolation and reactions with hydrogen, nitrogen, and carbon monoxide. *J. Am. Chem. Soc.* **93,** 2045–2046 (1971).

10. Threlkel, R. S. & Bercaw, J. E. A convenient synthesis of Alkyltetramethylcyclopentadienes and Phenyltetramethylcyclopentadiene. *J. Organomet. Chem.* **136,** 1–5 (1977).

11. Morris, D. M., McGeagh, M., De Peña, D. & Merola, J. S. Extending the range of pentasubstituted cyclopentadienyl compounds: The synthesis of a series of tetramethyl(alkyl or aryl)cyclopentadienes (Cp∗R), their iridium complexes and their catalytic activity for asymmetric transfer hydrogenation. *Polyhedron* **84,** 120–135 (2014).

12. Karpin, G. W., Merola, J. S. & Falkinham, J. O. Transition metal-α-amino acid complexes with antibiotic activity against Mycobacterium spp. *Antimicrob. Agents Chemother.* **57,** 3434–3436 (2013).

13. Karpin, G. W., Morris, D. M., Ngo, M. T., Merola, J. S. & Falkinham, J. O. Transition metal diamine complexes with antimicrobial activity against Staphylococcus aureus and methicillin-resistant S. aureus (MRSA). *Medchemcomm* **6,** 1471–1478 (2015).

14. Chen, S., Lu, G. & Cai, C. A base-controlled chemoselective transfer hydrogenation of α,β-unsaturated ketones catalyzed by $[IrCp^*Cl_2]_2$ with 2-propanol. *RSC Adv.* **5,** 13208–13211 (2015).

15. Gunay, A. *et al.* Oxidation catalysis in air with Cp*Ir: Influence of added ligands and reaction conditions on catalytic activity and stability. *Catal. Sci. Technol.* **5,** 1198–1205 (2015).

16. Xia, Y., Liu, Z., Feng, S., Zhang, Y. & Wang, J. Ir(III)-catalyzed aromatic C-H bond functionalization via metal carbene migratory insertion. *J. Org. Chem.* **80,** 223–236 (2015).

17. Kim, K. & Hong, S. H. Iridium-Catalyzed Single-Step N -Substituted Lactam Synthesis from Lactones and Amines. *J. Org. Chem.* **80,** 4152–4156 (2015).

18. Matsu-Ura, T., Sakaguchi, S., Obora, Y. & Ishii, Y. Guerbet reaction of primary alcohols leading to β-alkylated dimer alcohols catalyzed by iridium complexes. *J. Org. Chem.* **71,** 8306–8308 (2006).

19. Fujita, K. I., Takahashi, Y., Owaki, M., Yamamoto, K. & Yamaguchi, R. Synthesis of five-, six-, and seven-membered ring lactams by Cp*Rh complex-catalyzed oxidative N-heterocyclization of amino alcohols. *Org. Lett.* **6,** 2785–2788 (2004).

20. Fujita, K., Furukawa, S. & Yamaguchi, R. Oxidation of primary and secondary alcohols catalyzed by a pentamethylcyclopentadienyliridium complex. *J. Organomet. Chem.* **649,** 289–292 (2002).

21. Fujita, K., Li, Z., Ozeki, N. & Yamaguchi, R. N-Alkylation of amines with alcohols catalyzed by a Cp*Ir complex. *Tetrahedron Lett.* **44,** 2687–2690 (2003).

22. Kawahara, R., Fujita, K. I. & Yamaguchi, R. N-alkylation of amines with alcohols catalyzed by a water-soluble Cp*iridium complex: An efficient method for the synthesis of amines in aqueous media. *Adv. Synth. Catal.* **353,** 1161–1168 (2011).

23. Saidi, O. *et al.* Iridium-catalyzed formylation of amines with paraformaldehyde. *Tetrahedron Lett.* **51,** 5804–5806 (2010).

24. Kumaran, E. & Leong, W. K. $[Cp^*RhCl_2]_2$ -Catalyzed Alkyne Hydroamination to 1,2-Dihydroquinolines. *Organometallics* **34,** 1779–1782 (2015).

25. Iuchi, Y., Obora, Y. & Ishii, Y. Iridium-catalyzed α-alkylation of acetates with primary alcohols and diols. *J. Am. Chem. Soc.* **132,** 2536–2537 (2010).

26. Izumi, A., Obora, Y., Sakaguchi, S. & Ishii, Y. Oxidative dimerization of primary alcohols to esters catalyzed by iridium complexes. *Tetrahedron Lett.* **47,** 9199–9201 (2006).

27. Koda, K., Matsu-ura, T., Obora, Y. & Ishii, Y. Guerbet Reaction of Ethanol to n -Butanol Catalyzed by Iridium Complexes. *Chem. Lett.* **38,** 838–839 (2009).

28. Liu, J., Wu, X., Iggo, J. A. & Xiao, J. Half-sandwich iridium complexes—Synthesis and applications in catalysis. *Coord. Chem. Rev.* **252,** 782–809 (2008).

29. Suzuki, T., Matsuo, T., Watanabe, K. & Katoh, T. Iridium-catalyzed oxidative dimerization of primary alcohols to esters using 2-butanone as an oxidant. *Synlett* 1453–1455 (2005).

30. Suzuki, T., Ghozati, K., Katoh, T. & Sasai, H. Ir-catalyzed oxidative desymmetrization of meso-diols. *Org. Lett.* **11,** 4286–4288 (2009).

31. Suzuki, T., Morita, K., Tsuchida, M. & Hiroi, K. Iridium-catalyzed oppenauer oxidations of primary alcohols using acetone or 2-butanone as oxidant. *J. Org. Chem.* **68,** 1601–1602 (2003).

32. Collins, J. E. *et al.* Synthesis, Characterization, and Molecular Structure of Bis(tetraphenylcyclopentdienyl)rhodium(II). *Organometallics* **14,** 1232–1238 (1995).

33. Suzuki, T., Yamada, T., Watanabe, K. & Katoh, T. Iridium-catalyzed oxidative lactonization and intramolecular Tishchenko reaction of δ-ketoaldehydes for the synthesis of isocoumarins and 3,4-dihydroisocoumarins. *Bioorganic Med. Chem. Lett.* **15,** 2583–2585 (2005).

34. Suzuki, T., Morita, K., Tsuchida, M. & Hiroi, K. Mild and chemoselective synthesis of lactones from diols using a novel metal-ligand bifunctional catalyst. *Org. Lett.* **4,** 2361–2363 (2002).

35. Millett, A. J., Habtemariam, A., Romero-Canelón, I., Clarkson, G. J. & Sadler, P. J. Contrasting Anticancer Activity of Half-Sandwich Iridium(III) Complexes Bearing Functionally Diverse 2-Phenylpyridine Ligands. *Organometallics* **34,** 2683–2694 (2015).

36. Śliwińska, U., Pruchnik, F. P., Ułaszewski, S., Latocha, M. & Nawrocka-Musiał, D. Properties of η^5-pentamethylcyclopentadienyl rhodium(III) and iridium(III) complexes with quinolin-8-ol and their cytostatic activity. *Polyhedron* **29,** 1653–1659 (2010).

37. Thai, T.-T., Therrien, B. & Süss-Fink, G. Pentamethylcyclopentadienyl rhodium and iridium complexes containing oxinato ligands. *Inorg. Chem. Commun.* **12,** 806–807 (2009).

38. Liu, Z. *et al.* Organometallic half-sandwich iridium anticancer complexes. *J Med Chem* **54,** 3011–3026 (2011).

39. Quintana, L. M. A. *et al.* Proton–hydride tautomerism in hydrogen evolution catalysis. *Proc. Natl. Acad. Sci.* **113,** 6409–6414 (2016).

40. Pitman, C. L., Finster, O. N. L. & Miller, A. J. M. Cyclopentadiene-mediated hydride transfer from rhodium complexes. *Chem. Commun.* **52,** 9105–9108 (2016).

41. Lucas, S. J. *et al.* Increasing anti-cancer activity with longer tether lengths of group 9 Cp* complexes. *Dalt. Trans.* **45,** 6812–6815 (2016).

42. Karpin, G. W., Morris, D. M., Ngo, M. T., Merola, J. S. & Falkinham, J. O. Transition Metal Ethylenediamine Complexes with Antimicrobial Activity Against Staphylococcus aureus and Methicillin-Resistant S. aureus (MRSA). *Med. Chem. Commun.* **6,** 1471 - 1478 (2015).

43. Piou, T. & Rovis, T. Rhodium-catalysed syn-carboamination of alkenes via a transient directing group. *Nature* **527,** 86–90 (2015).

44. Dooley, T., Fairhurst, G., Chalk, C. D., Tabatabaian, K. & White, C. Ethyltetramethylcyclopentadienyl complexes of cobalt, rhodium, iridium and ruthenium. *Transit. Met. Chem.* **3,** 299–302 (1978).

45. Gusev, O. V, Sergeev, S., Saez, I. M. & Maitlis, P. M. Ring-Methyl Activation in Pentamethylcyclopentadienyl Complexes. 3. Synthesis and Reactions of (η^4-

Tetramethylfulvene)(η^5-cyclopentadienyl)rhodium and iridium. *Organometallics* **13,** 2059–2065 (1994).

46. Baghurst, D. R., Michael, D., Mingos, P. & Watson, M. J. Application of microwave dielectric loss heating effects for the rapid and convenient synthesis of organometallic compounds. *J. Organomet. Chem.* **368,** C43–C45 (1989).

47. Baghurst, D. R., Cooper, S. R., Greene, D. L., Mingos, D. M. P. & Reynolds, S. M. Application of microwave dielectric loss heating effects for the rapid and convenient synthesis of coordination compounds. *Polyhedron* **9,** 893–895 (1990).

48. Strauss, C. & Trainor, R. Invited review. Developments in microwave-assisted organic chemistry, Aust. *Aust. J. Chem.* **48,** 1665–1692 (1995).

49. Larhed, M. & Hallberg, A. Microwave-assisted high-speed chemistry: A new technique in drug discovery. *Drug Discov. Today* **6,** 406–416 (2001).

50. Gedye, R. *et al.* The use of microwave ovens for rapid organic synthesis. *Tetrahedron Lett.* **27,** 279–282 (1986).

51. Blacker, J., Treacher, K. & Screen, T. Unsaturated carbocyclic compounds linked to solid supports as ligands for transition metal-catalyzed hydrogenation and metathesis reactions. *PCT Int. Appl.* 23pp. (2009).

52. Fendrick, C. M. *et al.* Large-Scale Synthesis of 1,2,3,4,5-Pentamethylcyclopentadiene. in *Inorganic Syntheses* 193–198 (John Wiley & Sons, Inc., 1992).

53. Evans, W. J., Forrestal, K. J. & Ziller, J. W. Isopropyltetramethylcyclopentadienyl samarium chemistry: structural studies of divalent $(C_5Me_4iPr)_2Sm(THF)$ and mixed valent $[(C_5Me_4iPr)_2Sm]_2(\mu\text{-}Cl)$. *Polyhedron* **17,** 4015–4021 (1998).

54. Liu, Z. *et al.* Organometallic half-sandwich iridium anticancer complexes. *J. Med. Chem.* **54,** 3011–3026 (2011).

55. White, C., Yates, A. & Maitlis, P. M. (η^5-pentamethylcyclopentadienyl)Rhodium and Iridium Compounds. *Inorg. Synth.* **29,** 228 (1992).

56. El Amouri, H., Gruselle, M. & Jaouén, G. bis[Dichloro(η-pentamethylcyclopentadienyl)rhodium(III) and iridium(III)] from bis[Chloro(1, 5-cyclooctadiene)rhodium(I) and -iridium(I)] Oxidation, and Formation of 1, 5-Cyclooctadiene(η-pentamethylcyclopentadienyl)rhodium(I). *Synth. React. Inorg. Met. Chem.* **24,** 395–400 (1994).

57. Abramov, P. A., Sokolov, M. N., Virovets, A. V. & Fedin, V. P. Crystal structure of $[(C_5Me_4Et)_3Rh_3(\mu^3\text{-}Se)_2](PF_6)_2CH_3CN$ and $[(C_5Me_4Et)_2Rh_2(\mu^2\text{-}Cl)_3]PF_6$. *J. Struct. Chem.* **50,** 162–165 (2009).

58. Churchill, M. R. & Julis, S. A. Crystal structure and molecular geometry of homogeneous hydrogenation catalyst $[\eta^5\text{-}C_5Me_5IrCl]_2(\mu\text{-}H)(\mu\text{-}Cl)$ and of its precursor $[\eta^5\text{-}C_5Me_5IrCl]_2(\mu\text{-}Cl)_2$. A Direct comparison of Ir(μ-H)(μ-Cl)Ir and $Ir(\mu\text{-}Cl)_2Ir$ and bridging systems. *Inorg. Chem.* **16,** 1488–1494 (1977).

59. Churchill, M. R., Julis, S. A. & Rotella, F. J. Comparative geometry of $Rh(\mu\text{-}Cl)_2Rh$ and Rh(μ-H)(μ-Cl)Rh bridges. Crystal structure of $[\eta^5\text{-}C_5Me_5RhCl]_2(\mu\text{-}Cl)_2$ and its relation to $[\eta^5\text{-}C_5Me_5RhCl]_2(\mu\text{-}H)(\mu\text{-}Cl)$. *Inorg. Chem.* **16,** 1137–1141 (1977).

60. Miyano, Y., Nakai, H., Hayashi, Y. & Isobe, K. Synthesis and structural characterization of a photoresponsive organodirhodium complex with active S-S bonds: $[(Cp^{Ph}Rh)_2(\mu\text{-}CH_2)_2(\mu\text{-}O_2SSO_2)]$ (CpPh = η^5-C_5Me_4Ph). *J. Organomet. Chem.* **692,** 122–128 (2007).

61. Morris, D. M. Design and Modficiation of Half-Sandwich Ir(III), Rh(III), and Ru(II) Amino Acid Complexes for Application in Asymmetric Transfer Hydrogenation Reactions. *Chemistry* **Ph.D.,** (Virginia Polytechnic Institute and State University, 2015).

62. Liu, Z., Habtemariam, A., Pizarro, A. M., Clarkson, G. J. & Sadler, P. J. Organometallic Iridium(III) Cyclopentadienyl Anticancer Complexes Containing C,N-Chelating Ligands. *Organometallics* **30,** 4702–4710 (2011).

63. Jardim, G. A. M., Da Silva, E. N. & Bower, J. F. Overcoming naphthoquinone deactivation: Rhodium-catalyzed C-5 selective C-H iodination as a gateway to functionalized derivatives. *Chem. Sci.* **7,** 3780–3784 (2016).

64. Piou, T. & Rovis, T. Rh(III)-catalyzed cyclopropanation initiated by C-H activation: Ligand development enables a diastereoselective [2 + 1] annulation of N-enoxyphthalimides and alkenes. *J. Am. Chem. Soc.* **136,** 11292–11295 (2014).

65. Cadenbach, T., Gemel, C., Schmid, R. & Fischer, R. A. Mechanistic insights into an unprecedented C-C bond activation on a Rh/Ga bimetallic complex: A combined experimental/computational approach. *J. Am. Chem. Soc.* **127,** 17068–17078 (2005).

66. Guo, Z. & Sadler, P. J. Metals in Medicine. *Angew. Chemie Int. Ed.* **38,** 1512–1531 (1999).

67. Suzuki, Y., Yasumoto, T., Mashima, K. & Okuda, J. Hafnocene catalysts for selective propylene oligomerization: Efficient synthesis of 4-methyl-1-pentene by β-methyl transfer. *J. Am. Chem. Soc.* **128,** 13017–13025 (2006).

68. Seidel, R. W. *et al.* catena-Poly[[(tetrahydrofuran-κO)potassium]-μ-(η^5:η^5)-2,3,4,5-tetramethyl-1-η-pentylcyclopentadienyl]. *Acta Crystallogr. Sect. C Cryst. Struct. Commun.* **69,** 573–576 (2013).

69. Uemura, M. & Fujita, M. Transition metal compound, polymerization-initiator system comprising the same, and process for producing polymer. (2007).

70. Ngubane, S., Hakansson, M., Jagner, S., Moss, J. R. & Sivaramakrishna, A. Synthesis, structure and some reactions of (C5Me4hex)2Ru2(CO)4. *J. Organomet. Chem.* **693,** 343–348 (2008).

71. Flores, J. C., Wood, J. S., Chien, J. C. W. & Rausch, M. D. [1-(2-Phenylethyl)-2,3,4,5-tetramethylcyclopentadienyl] titanium Compounds. Synthesis and Their Use for the Syndiospecific Polymerization of Styrene. *Organometallics* **15,** 4944–4950 (1996).

72. McArdle, P., Ryder, A. G. & Cunningham, D. Synthesis of Novel Chiral Cyclopentadienes: Synthesis of Chiral Iron Complexes and the Crystal Structures of [(η^5-(1S)-1-(6-methoxynaphthalenyl)-1-(tetramethyl-cyclopentadienyl)ethane)$Fe(CO)_2SnCl_3$] and [(η^5-$C_5(Me)_4C(H)(CH_3)(C_2H_5)$)Fe(CO)-($\eta^4$-diphenylbutadiene)]$^+$[$BF_4$]$^-$. *Organometallics* **16,** 2638–2645 (1997).

73. Ma, Z., Wang, N., Guo, K., Zheng, X. & Lin, J. Reactions of substituted tetramethylcyclopentadienes with molybdenum hexacarbonyl. *Inorganica Chim. Acta* **399,** 126–130 (2013).

74. Merola, J. S., Morris, D. & De Weerd, N. Di-µ2-chlorido-bis-[chlorido(η^5-2,3,4,5-tetramethyl-1-propylcyclopentadienyl)iridium(III)]. *Acta Crystallogr Sect E Struct Rep Online* **69,** m176 (2013).

75. Miguel-Garcia, J. A., Adams, H., Beiley, N. A. & Maitlis, P. M. Ring-methyl activation in pentamethylcyclopentadienyliridium complexes; synthesis of [($C_5Me_4CH_2E$)IrLn] (E = $SiMe_3$, $PhCH_2$, CH_2=$CHCH_2$, PPh_2, and $Pt(PEt_3)_2Cl$), and synthesis and X-ray structure of [(1,3-$C_5Me_3(CH_2SiMe_3)_2$)Ir(CO)Me(Cl)]. *J. Organomet. Chem.* **413,** 427–444 (1991).

76. Maisuria, B. B. *et al.* Comparing micellar, hemolytic, and antibacterial properties of di- and tricarboxyl dendritic amphiphiles. *Bioorganic Med. Chem.* **19,** 2918–2926 (2011).

Chapter 3 Substrate Scope, Selectivity, and Mechanism in Ir(III)-Catalyzed Oxidative Lactonization of Diols

3.1 Contributions

The work described in this chapter was conducted in collaboration with William Owen, Dr. Robert Chapleski, and Dr. Diego Troya. The author is responsible for the catalytic studies of all Ir(III) complexes and substrates. Synthesis of substrates were conducted by William Owen and characterized by the author. All theoretical calculations were carried out by Robert Chapleski and Dr. Diego Troya. The final manuscript was prepared in collaboration with Dr. Joseph S. Merola, Dr. Paul Deck, and Dr. Diego Troya and has been submitted to...

3.2 Abstract

Oxidative lactonization of 1,4-butanediol to afford γ-butyrolactone proceeds selectively and efficiently using $[(\eta^5\text{-}RMe_4C_5)IrCl]_2(\mu^2\text{-}Cl)_2$ as the catalyst (acetone solution, 50 °C, 24 h) with R = C_6F_5, Ph, CH_2CHMe_2, Me, or $CHMe_2$, in order of increasing respective yield. The complex with R = $CHMe_2$ catalyzes the oxidative lactonization of a range of 1,4- and 1,5- diols, generally in high yield (15 examples). Computational analysis of the putative rate-determining β-hydrogen elimination reactions provides new mechanistic insight, rationalizing the selective formation of γ-butyrolactone (e.g., instead of succinaldehyde) from 1,4-butanediol based on electronic effects. The calculations additionally reveal that a combination of steric and stereoelectronic effects control selectivity in asymmetrically substituted diols.

3.3 Introduction

Lactones are valuable intermediates in the synthesis of natural products, pharmaceuticals, and polyesters.[1-14] Among various synthetic approaches,[1–6] only oxidative lactonization (eq 1) offers one-pot simplicity starting from a diol.[7–13]

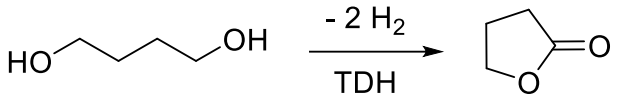

(1)

Oxidative lactonization is closely related to transfer dehydrogenation (TDH).[14–19] In catalytic TDH (eq 2-5, [M] = metal complex, R = alkyl or aryl), coordination of the alcohol (eq 2) followed by β-hydrogen elimination (eq 3) affords the corresponding aldehyde.[20–29] Catalytic turnover requires a terminal oxidant (e.g., acetone), which inserts into the hydride (eq 4) and exchanges with the substrate (eq 5), forming 2-propanol as the by-product. In principle, eq 3-5 are freely reversible reactions, whereas eq 2 is typically driven by an added base. Fujita and co-workers first demonstrated the use of $[(\eta^5\text{-}Me_5C_5)IrCl]_2(\mu^2\text{-}Cl)_2$, for TDH of primary and secondary alcohols under mild conditions, using acetone as the oxidant and reaction solvent.[15]

$$RCH_2OH + [M]X \rightarrow RCH_2O[M] + HX \quad (2)$$

$$RCH_2O[M] \rightarrow RCHO + [M]H \quad (3)$$

$$[M]H + Me_2CO \rightarrow [M]OCHMe_2 \quad (4)$$

$$[M]OCHMe_2 + RCH_2OH \rightarrow RCH_2O[M] + Me_2CHOH \quad (5)$$

Oxidative lactonization of the type explored herein comprises two TDH processes in succession (**Figure 1**).[30,31] Suzuki and co-workers demonstrated catalytic oxidative lactonization using the Ir(III) complex $(\eta^5\text{-}Me_5C_5)Ir(OCH_2C(C_6H_5)_2NH)$ in acetone solvent.[32] Their system requires an expensive ligand but affords high yields for a variety of 1,4- and 1,5-diols (ca. 11 examples). Fujita and co-workers further modified the Ir(III) half-sandwich design using a hydroxylated bipyridine ligand and showed that oxidative lactonization was feasible in aqueous solution.[33] The relatively hydrophobic $[(\eta^5\text{-}Me_5C_5)IrCl]_2(\mu^2\text{-}Cl)_2$ did not show aqueous catalytic activity. Dehydrogenations that remove H_2 directly can also lead to lactonization of diols, but more

forcing conditions are typically required, likely because of the additional metal-centered redox steps required to achieve catalytic turnover.[11,13,26,30,31,34–37]

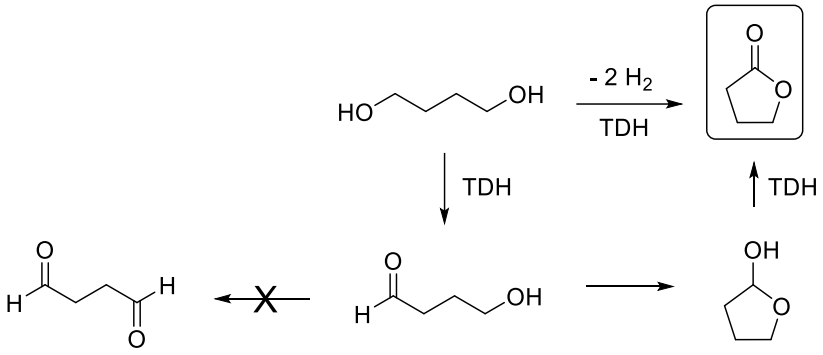

Figure 1. Oxidative lactonization of 1,4-butanediol.

Based in part on Fujita's TDH findings, we now show that the Ir(III) complex $[(\eta^5\text{-}RMe_4C_5)IrCl]_2(\mu^2\text{-}Cl)_2$ (R = $CHMe_2$) catalyses oxidative lactonization of 1,4- and 1,5-diols (15 examples). We have also been studying cyclopentadienyl (Cp) substituent effects in Ir(III) complexes,[38,39] and herein we compare five derivatives of the type $[(\eta^5\text{-}RMe_4C_5)IrCl]_2(\mu^2\text{-}Cl)_2$ (R = C_6F_5, Ph, Me, $CHMe_2$, and CH_2CHMe_2) as catalysts for oxidative lactonization using 1,4-butanediol as the test substrate.

While thinking about mechanisms of oxidative lactonization, we noted that a particularly striking feature of the chemistry shown in **Figure 1** is the *selectivity* for the formation of butyrolactone over succinaldehyde. If we suppose that all of the "simple" mechanistic steps (ligand exchanges and the ring-closure of the intermediate hydroxyaldehyde) are fast and reversible, then the product distribution should depend only on the relative rates of the different β-hydrogen elimination reactions (**Figure 2**). We have explored these details using quantum-chemical calculations, and we also report an atomistic mechanism confirming that β-hydrogen elimination from the intermediate lactol (k_2, **Figure 2**) is much faster than β-hydrogen elimination from a normal alkoxide (k_1 or k_1'), to the extent that the lactone should indeed form selectively. We are

not aware of previous studies, whether computational or experimental, of the origins of selectivity in these reactions using Ir(III) catalysts.

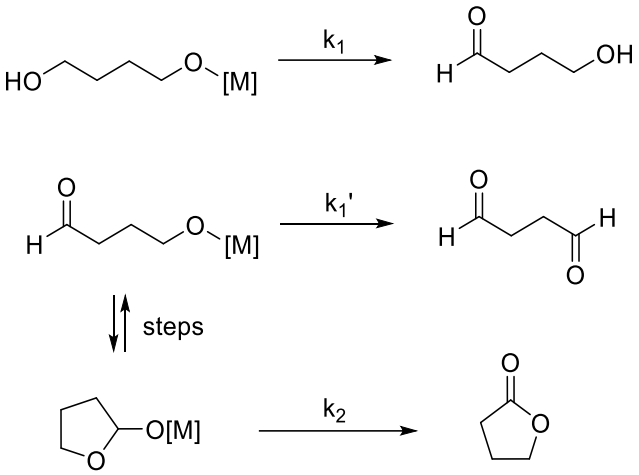

Figure 2. Conceptual kinetic scheme for oxidative lactonization of 1,4-butanediol. Selective lactonization requires $k_2 >> k_1'$.

3.4 Results and discussion

For our study of Ir(III)-catalyzed oxidative lactonization, we selected the five complexes shown in **Chart 1**. These dimeric complexes were conveniently prepared from the corresponding substituted cyclopentadienes and $[Ir(COD)]_2(\mu^2\text{-}Cl)_2$ (COD = 1,5-cyclooctadiene) in methanol solvent using a general microwave-based method that we described previously.[39]

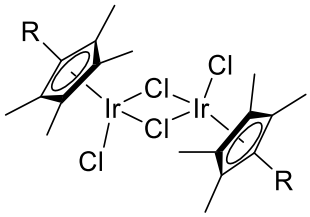

1a: R = Me
1b: R = $CHMe_2$
1c: R = Ph
1d: R = CH_2CHMe_2
1e: R = C_6F_5

Chart 1. Ir(III) catalysts for oxidative lactonization of diols.

We first conducted a round of experiments (**Table 1**) using 1,4-butanediol as the substrate to establish the optimum reaction conditions and catalyst to carry forward into further studies.

Conversion of substrate and yield of butyrolactone were established using NMR (see Supporting Information). All of the reactions were run for the same time (24 h), at the same temperature (50 °C), and at the same concentrations of substrate (1 M), base (0.1 M), and catalyst (0.01 M).

Several noteworthy trends emerge from the data in **Table 1**. First, stronger bases lead to lower conversion and yield (entries 4-5), possibly due to poisoning of the Lewis-acidic Ir(III) center or by promoting side-reactions with the acetone solvent. Sodium bicarbonate as the base seemed best. Second, ligand substituent trends (entries 7-10) suggest that a moderately bulky, electron-releasing substituent is optimal for this system. Catalysts **1a** (R = Me) and **1b** (R = $CHMe_2$) gave comparable results. The less electron-rich complex **1e** (R = C_6F_5) gave the lowest yield. We speculate that the active catalytic species is monomeric and that the more electron-deficient dimeric complexes may not be cleaved as readily under the reaction conditions. Further studies to understand these empirical trends are underway.

Table 1. Oxidative lactonization catalyzed by Ir(III) complexes (Chart 1) using diol (1.0 mmol), base (0.10 mmol), and catalyst (0.010 mmol) in acetone (1.0 mL) at 50 ˚C for 24 h. Conversion and yield were determined by ^{1}H NMR.

Entry	Catalyst	Base	Conversion %	Yield %
1	**1a**	K_2CO_3	65	27
2	**1a**	Na_2CO_3	82	64
3	**1a**	Cs_2CO_3	63	14
4	**1a**	LiOH	58	<1
5	**1a**	Me_3COK	76	7
6	**1a**	Et_3N	52	34
7	**1a**	$NaHCO_3$	87	80
8	**1b**	**$NaHCO_3$**	**89**	**84**
9	**1c**	$NaHCO_3$	83	73
10	**1d**	$NaHCO_3$	90	74
11	**1e**	$NaHCO_3$	66	43

Using conditions optimized in the 1,4-butanediol screen (catalyst **1b**, R = $CHMe_2$; base = $NaHCO_3$), we next explored the substrate scope of lactonization. The data in **Table 2** show that both 1,4- and 1,5-diols are converted smoothly to the corresponding lactones. Simple symmetrical diols (**Table 2**, entries 1, 7, 10, 12, 14, and 15) all give good yields of lactones. Substrates bearing substituents on the gamma carbon do not seem to have any significant effect on yield (with the curious exception of 3-phenyl-1,4-pentanediol, entry 14). Methyl or phenyl groups on the carbon atom undergoing oxidation (**Table 2**, entries 2, 5, 8, and 13) strongly divert the reaction toward ω-hydroxyketones as major products. Electronic-structure calculations (see below) reveal an electronic effect that promotes TDH from secondary vs. primary alcohols. ω-Hydroxyketones can undergo further TDH in the open-chain form, but not in the corresponding lactol because there is no β-hydrogen to eliminate. In acetone solution, ring-chain equilibrium constants are close to 1.[40,41] Related work using supported gold nanoparticles as the catalyst converted 88% of the starting 1,4-pentanediol to 44% of γ-valerolactone as well as some 4-ketopentanal and 5-hydroxy-2-pentanone.[8] We do not observe more than small traces of 4-ketopentanal or 5-ketohexanal by

NMR. Finally, unsymmetrical β-substituted substrates (**Table 2**, entries 3, 4, 6, 9, and 11) show an opposite effect: The less hindered alcohol is preferentially oxidized. This effect is amplified in the case of unsymmetrically beta-disubstituted diols (entries 4 and 11). The density functional theory (DFT) calculations shown below also rationalize this trend.

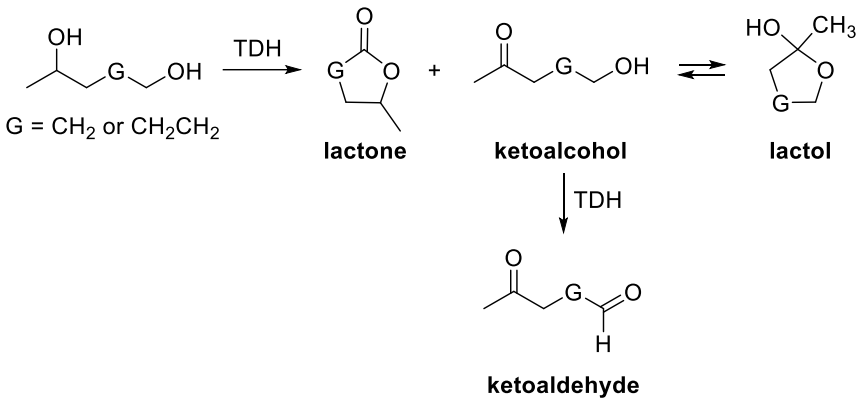

Figure 3. Conceptual scheme for the formation of byproducts during TDH of 1,4-pentanediol and 1,5-hexanediol.

Table 2. Substrate scope of oxidative lactonization. Reactions used diol (1.0 mmol), $NaHCO_3$ (0.1 mmol), and catalyst **1b** (0.010 mmol) in acetone (1.0 mL) at 50 ˚C for 24 h. Conversions and yields were determined by ^1H NMR.

Entry	Diol	Lactone	Conversion %	Yield %
1	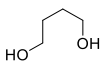		89	84
2	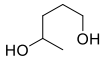	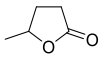	94	28[a]
3	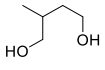	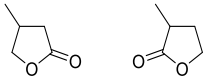	94	62/32
4	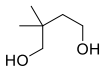	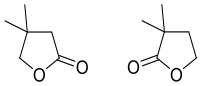	94	82/11
5	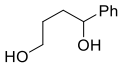	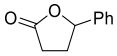	90	23[b]
6	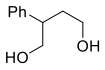	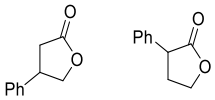	70	44/19
7	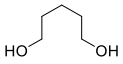		97	96
8	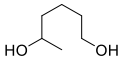		95	29[c]
9	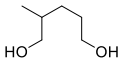	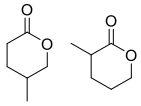	95	58/30
10	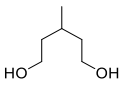		>99	96
11	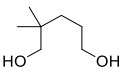	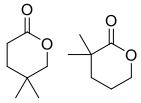	95	80/13
12	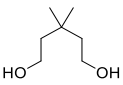	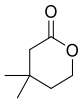	>99	98
13	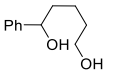		94	20[d]
14	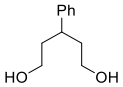	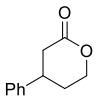	69	65
15	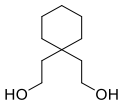	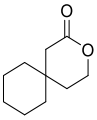	>99	99

[a]5-hydroxy-2-pentanone was formed as a byproduct (62% by NMR). [b]4-hydroxy-1-phenylbutanone was formed as a byproduct (67% by NMR). [c]6-hydroxy-2-hexanone was formed as a byproduct (64% by NMR). [d]5-hydroxy-1-phenylpentanone was formed as a byproduct (62% by NMR).

In concert with our computational studies (Section 2.1 below), we wanted to confirm, as the centerpiece of our overall mechanistic proposal, that initial TDH (k_1 in Figure 2) is rate-limiting. We conducted a kinetic isotope effect (KIE) study using 1,1-dideuterio-1,4-butanediol. The product ratio, determined by ^{1}H-NMR spectrometry, shows a significant primary KIE (k_H/k_D ~ 2.7) indicating C—H bond rupture in the rate-limiting step.[42–46] This finding securely corroborates our proposal that β-H elimination at iridium is rate-limiting. Failure to observe more than the smallest traces of any aldehyde species in the NMR spectra of our product mixtures strongly suggests, from an experimental standpoint, that $k_2 >> k_1'$.

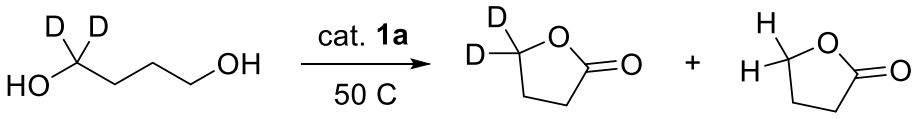

3.4.1 Computational mechanistic studies

As mentioned above, the formation of lactones instead of dicarbonyl compounds suggests significant selectivity among the various β-hydrogen-elimination reactions that might occur. However, no fundamental understanding of this selectivity is provided in any prior work of which we are aware. Starting with a diol, the initial TDH process forms a hydroxyaldehyde (**Figure 2**). The hydroxyaldehyde could simply coordinate again to Ir(III) through the remaining OH functionality and undergo a second β-hydrogen elimination to form a dialdehyde (k_1' in **Figure 2**). Alternatively, the hydroxyaldehyde can cyclize to the lactol (chain-ring isomerism), coordinate to Ir(III) through the OH functionality, and proceed through β-hydrogen elimination to the lactone.

If we assume that β-hydrogen eliminations are relatively slow, and that ligand (halide and alkoxide) substitutions at Ir(III) as well as ring-chain hydroxyaldehyde-lactol interconversion are fast and freely reversible steps, then the question of selectivity for formation of the lactone essentially comes down to whether the Ir(III)-lactoxide complex undergoes β-hydrogen

elimination (k_2 in **Figure 2**) faster than the corresponding Ir(III) complex of a typical primary alkoxide (k_1 or k_1'). While formation of the lactone certainly suggests that $k_2 >> k_1$ or k_1'), we sought to confirm our mechanistic proposal with a detailed computational investigation of the reaction mechanism using detailed electronic-structure (DFT) calculations.

Figure 4 (upper, red trace) shows the results of these calculations for the β-hydrogen elimination of 1,4-butanediol. This pathway begins with the Ir(III) alkoxide formed by substitution at the monomeric iridium catalyst [(η^5-Me_5C_5)$IrCl_2$ by the diol (with removal of HCl), followed by the putative (rate-limiting) transition state (**TS1**), leading to a shallow minimum corresponding to the η^2-coordinated 4-hydroxybutanal product, which evolves to the more stable η^1 product through a barrier that is not rate-limiting.

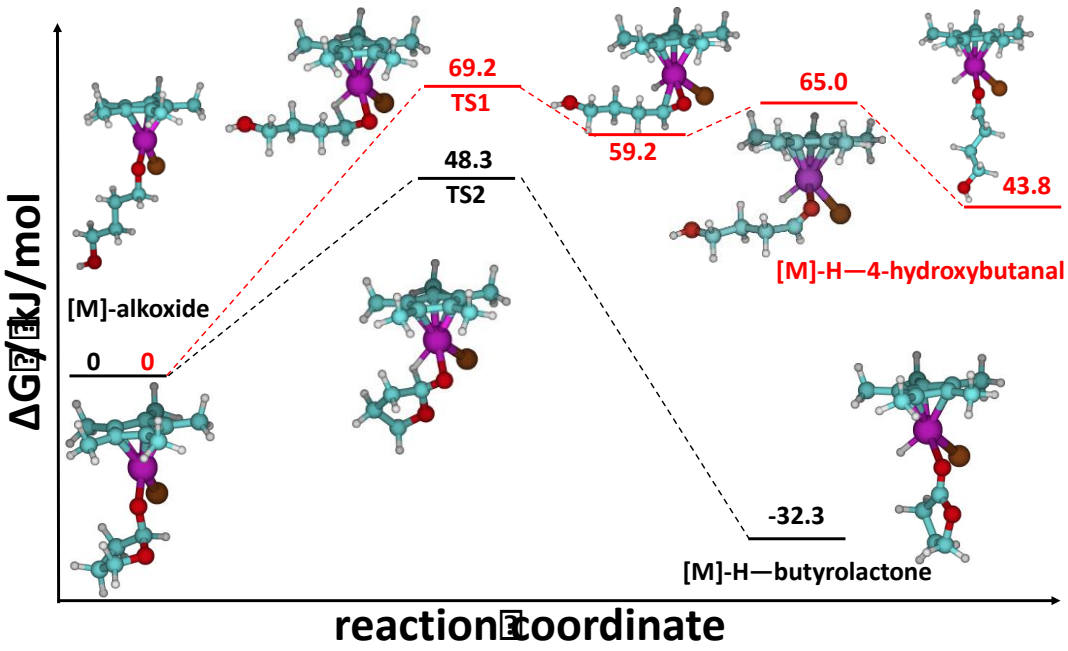

Figure 4. Reaction pathways for β-hydrogen elimination of 1,4-butanediol (red trace) and for the lactol resulting from ring closure of 4-hydroxybutanal (black trace) as catalyzed by [(η^5-Me_5C_5)$IrCl]_2(\mu^2$-$Cl)_2$. For each pathway, the alkoxide bound to the catalyst following ligand substitution is taken as the zero of energy so that barriers of the two β-hydrogen elimination reactions may be compared directly. Insets show structures of stationary points. Color scheme for insets: Ir: magenta, C: cyan, H: gray, O: red, Cl: brown. Energies were calculated using M06-L/def2TZVP//def2SVP; please refer to Experimental Section for further details.

Dissociation of the 4-hydroxybutanal product and ring closure affords the lactol, which may re-coordinate through the exocyclic lactol oxygen atom. We assume these steps are fast. **Figure 4** (lower, black trace) shows the analogous β-hydrogen elimination pathway for the iridium lactoxide. This pathway is similar to that leading to 4-hydroxybutanal but proceeding through transition state **TS2**, again to a coordinated product, which may also readily desorb from the catalyst.

Importantly, the calculations indicate a significant decrease in the reaction barrier for the lactoxide species compared to the normal alkoxide. Using the data shown in **Figure 4**, we can directly compare the rate of β-hydrogen elimination from the normal alkoxide (k_1 in **Figure 2**) with that of the lactol (k_2) to find a $k_{lactol}/k_{butanediol}$ rate constant ratio of 4590 @ 298.15 K. Calculations with other functionals (Table S1) corroborate the significantly lower barrier for β-hydrogen elimination from the lactol compared to the normal alkoxide.

To determine the underlying reasons for such a vast rate-constant difference, we considered both electronic and geometric effects. Geometrically, ring strain in the iridium lactoxide might be relieved upon formation of the sp^2 carbon in the coordinated lactone, enhancing the rate. Electronically, the same resonance effects that chemically stabilize esters relative to aldehydes might also stabilize the incipient sp^2 carbon atoms in the β-H-elimination transition states (**Figure 5**).

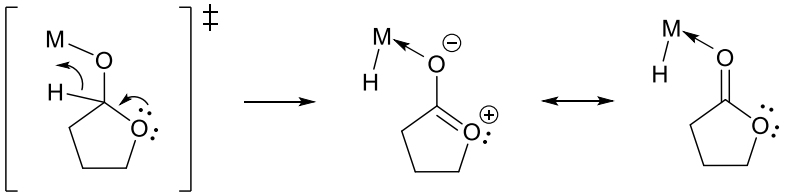

Figure 5. Resonance effect proposed to rationalize the relative facility of lactol oxidation.

In an attempt to separate the contribution of these geometric and electronic effects, we compared β-hydrogen elimination from the ethoxide complex $(Me_5C_5)Ir(Cl)OCH_2CH_3$ with β-hydrogen elimination from the corresponding hemiacetal complex, $(Me_5C_5)Ir(Cl)OCH(OCH_2CH_3)CH_3$. Both of these substrates are acyclic, but their electronic structures model the normal diols (ethanol) and the lactols (hemiacetal), thereby enabling investigation of electronic resonance effects in isolation. Results are diagrammed in **Figure 6**. The energetics and stationary-point structures of the two β-hydrogen eliminations are compared in **Figure S30**. The calculations reveal that the rate of ester formation from the hemiacetal is 7450 times the rate of ethanal formation at 298.15 K. We therefore believe that the differences in the electronic structure of the substrate play a primary role in the selectivity toward lactonization reported in this work. This finding is also consistent with recent experimental findings in an acceptorless dehydrogenation system which showed that the formation of ester is very fast in comparison to the aldehyde.[47]

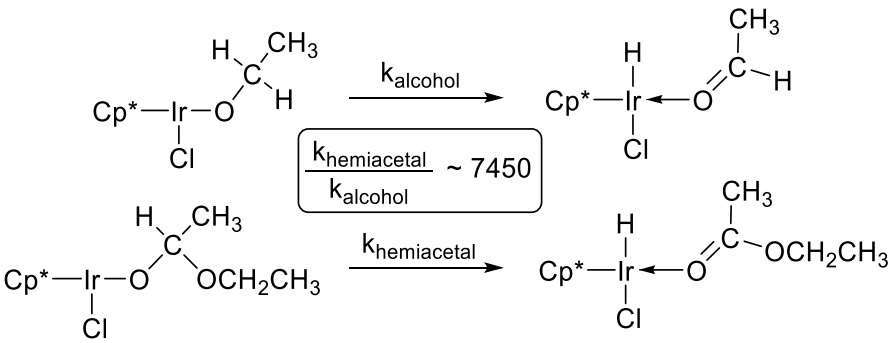

Figure 6. Comparison of β-hydride elimination from a primary alcohol and a hemiacetal using DFT calculations at 298.15 K.

To delve deeper into additional electronic contributions to the transition state stabilization suggested by **Figures 5** and **6**, we also investigated the role played by the degree of substitution in the carbon atom from which hydrogen elimination takes place, as more substituted carbons

generally present lower barriers for hydrogen atom transfer.[48] **Figure 7** and **Figure S31** show a comparison of the reaction paths for β-hydrogen elimination from ethanol and isopropyl alcohol by (η^5-Me_5C_5)$IrCl_2$. While hydrogen elimination from the more substituted carbon atom proceeds over a lower-energy transition state, the barrier decrease from ethanol to isopropyl alcohol (2.1 kJ/mol) is not nearly as large as when resonance effects are present (as illustrated by the 22.1 kJ/mol decrease in barrier from ethanol to a hemiacetal in **Figure S30**). Nevertheless, this result probably explains why entries 2, 5, 8, and 13 in **Table 2** gave ω-hydroxyketones as major products.

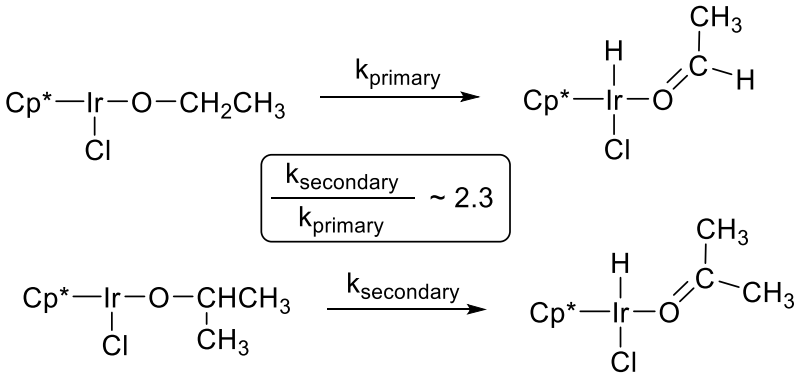

Figure 7. Comparison of β-hydride elimination from primary and secondary Ir(III) alkoxides using DFT calculations at 298.15 K. The rate ratio is consistent with observed ketoalcohol: lactone product ratios of roughly 2:1 with 1,4-pentanediol or 1,5-hexanediol as substrates (**Table 2**, entries 2, 5, 8, and 13).

Furthermore, we also considered the effect of substitution at the carbon atom *adjacent* to the site of β-hydride elimination. Our preliminary expectation was that an increase in the substrate's electron density would help stabilize the transition state and therefore increase the rate. However, our empirical findings (**Table 2**, entries 3, 4, 6, 9, and 11) were exactly opposite: methyl substitution in this adjacent position impedes the TDH process. We probed the origin of this ostensibly counterintuitive result with DFT calculations. The calculations corroborate the experimental finding that methyl substitution in the C atom adjacent to the β-hydride elimination

indeed decelerates reaction. Further, the calculations advance two different stereoelectronic explanations for the results. First, as shown in **Figure 8**, reaction at the most substituted $CH_3C(R_1)(R_2)CH_2OH$ alcohol model ($R_1 = R_2 = CH_3$) is impaired by the significant steric strain between R_1 and the C_5Me_5 ligand, which misaligns the substrate with respect to the Ir(III) center for β-hydride elimination. In **Figure 8** the non-bonding H-to-Cl distance (blue double-headed arrow) is compressed by about 0.3 Å compared to the less-substituted substrates. Accordingly, entries 4 and 11 in Table 2 show the highest selectivity for TDH of the less substituted substrate terminus. Second, when R_1 = H, steric strain is relieved, but the remaining R_2 group is positioned antiperiplanar to the departing hydride. Cieplak showed that when a C–H bond is antiperiplanar to a breaking or forming C···H bond, the transition state is stabilized to a larger extent than when a C–C bond is antiperiplanar to the breaking bond. This effect is due to the superior electron-donating ability of C–H bonds compared to C–C bonds.[49] Our calculations and measurements are in full agreement with this stereoelectronic argument because we calculate (**Figure 8**) a higher β-hydride elimination rate for the substrates that place a C-H bond antiperiplanar to the breaking C-H bond (R_2 = H) than when a C-C bond is ($R_2 = CH_3$). While the difference in transition state energies with antiperiplanar C–H or C–C bonds is moderate, it is certainly sufficient to lead to selectivity toward the *less* substituted alcohol in the asymmetrically substituted diols of entries 3 and 9 in **Table 2**.

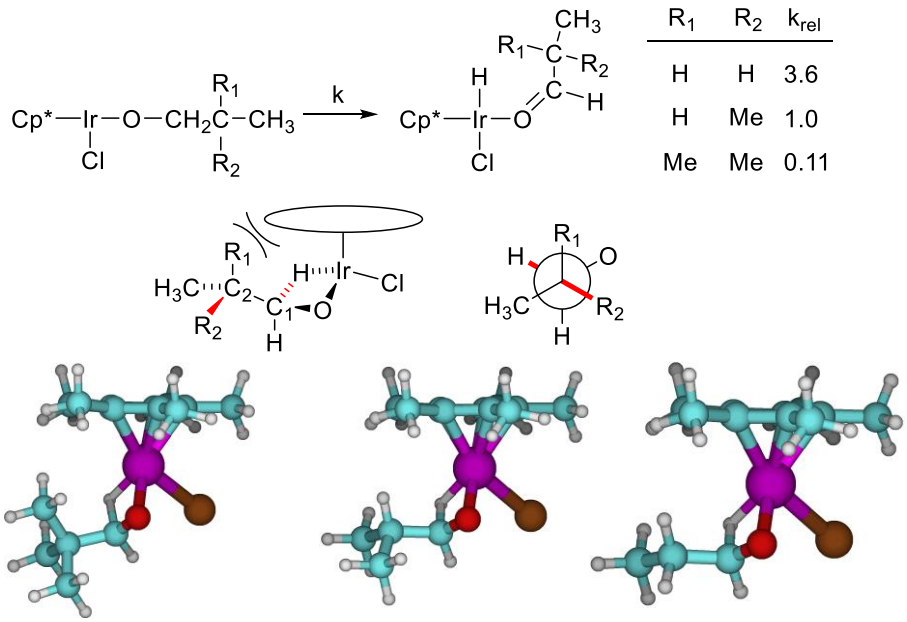

Figure 8. Effect of methyl substitution at the carbon adjacent to the site of hydride abstraction in TDH reactions of Ir(III) alkoxides (relative rates and transition-state structures calculated by DFT at 298.15 K). Conformational models reveal unfavorable steric strain when $R_1 = R_2 = CH_3$; the H-to-Cl distance (blue arrow) is compressed by about 0.3 Å to relieve repulsions between the substrate ($R_1 = CH_3$) and the CH_3 groups of the ancillary C_5Me_5 ligand. *Antiperiplanar* interactions of the $C_1\cdots H$ and $C_2–CH_3$ (red bonds) rationalize slightly more facile TDH when $R_1 = R_2 = H$ vs. $R_1 = H$ and $R_2 = CH_3$. The substrate with $R_1 = R_2 = H$ (1-propanol) adopts the conformation that avoids the CH_3–O *gauche* interaction.

Finally, the potential-energy diagrams in Fig. 4 indicate that β-hydride elimination from a lactol is thermodynamically more favorable than from an alcohol, in addition to proceeding over a lower barrier. In effect, the lactol reaction is exoergic, but the alcohol reaction exhibits a positive reaction Gibbs energy. To clarify the driving force for the entire catalytic process, we show in Fig. S31 the Gibbs energy of sequential steps leading from 1,4-butanediol to butyrolactone using acetone as the oxidant. The overall 1,4-butanediol + 2 acetone → butyrolactone + 2 2-propanol reaction is exoergic, and acts as the driving force for the catalytic process. Interestingly, the first TDH step (1,4-butanediol + acetone → 4-hydroxybutanal + 2-propanol) is slightly uphill. However

the second TDH process from the ensuing lactol (after cyclization of 4-hydroxybutanal) is sufficiently exoergic to drive all preceding reaction steps. The presence of acetone (the terminal oxidant) in large excess (as the reaction solvent) also serves to advance the catalytic process toward products.

3.5 Conclusions

In summary, our computational results reveal the microscopic origin of the experimentally observed selectivity in the formation of lactones vs. dialdehydes from 1,4-diols with Ir(III) complexes. For example, our study of ethanol TDH suggests that the sequence shown in eq 6-8 should be selective for formation of ethyl acetate over ethanal, which runs contrary to Fujita's well-established aldehyde synthesis by TDH of primary alcohols.[15] We surmise that under those reaction conditions, formation of the hemiacetal (eq 7) could be less favorable than ring-closure of a hydroxyaldehyde to form the corresponding lactol. However, we also note that linear esters have been observed in other studies.[11,13,34,50–53] Moreover, observation of 5-hydroxy-2-pentanone *but not 4-ketopentanal* in the oxidative lactonization of 1,4-pentanediol suggests that the ketoalcohol may be trapped in its lactol form. On the other hand, previous studies have showed that ring-chain tautomer ratios involving 5-membered-ring lactols are about 1:1.[41,54] Therefore, a careful examination of the underlying assumptions, especially regarding which of the various exchange reactions are "fast," and a systematic study of reactant concentration effects, may be needed to gain deeper fundamental understanding of this system.

$$CH_3CH_2OH \rightarrow CH_3CHO \quad (6)$$

$$CH_3CHO + CH_3CH_2OH \leftrightharpoons CH_3CH(OH)OCH_2CH_3 \quad (7)$$

$$CH_3CH(OH)OCH_2CH_3 \rightarrow CH_3C(O)OCH_2CH_3 \quad (8)$$

We also learn that subtle stereoelectronic effects are at play in the β-hydride step of TDH reactions. First, we see that repulsion between the ancillary C_5Me_5 ligand of the catalyst and heavily substituted substrates impedes proper binding of the substrate, decreasing the rate. Furthermore, we reveal that the same effect that induces asymmetry in hydrogenation of cyclic ketones[49] is responsible for a larger reaction rate in substrates that place a C–H bond antiperiplanar to the breaking C···H compared to substrates that locate an antiperiplanar C–C bond instead.

3.6 Experimental section

Please see Supporting Information for detailed descriptions of all experimental materials and methods.

3.6.1 General procedure for oxidative lactonization

In a sealed 1-dram vial, a mixture of catalyst (0.010 mmol), diol (1.0 mmol), base (0.10 mmol), and acetone (1.0 mL) was stirred at 50 ˚C for 24 h. Catalysts, diols, and bases used in specific experiments are summarized in **Tables 1** and **2**. After evaporation of the acetone solvent, the crude product mixture was analyzed by ^{1}H NMR spectrometry using anisole as an internal standard to determine conversion and yield. Recycle delay of 5 s was used to ensure accurate integration; longer delays did not change integration values.

3.6.2 Computational methods

Electronic structure calculations were completed using the M06-L[55] density functional as implemented in the Gaussian09 suite of software.[56] M06-L was chosen for its computational efficiency and its focus on transition-metal chemistry. Indeed, M06-L has been successfully employed in prior studies of Ir(III) complexes that undergo β-hydrogen elimination.[57–61] Sample calculations were performed with 5 other functionals to verify the trends obtained with M06-L. Geometries of stationary points were optimized with the def2SVP basis set. A superfine integration

grid was required to ensure smooth convergence to optimum geometries. The nature of stationary points was verified using vibrational frequency calculations. Single-point electronic energies were calculated in acetone using the PCM solvation model[62] for optimized geometries using the larger def2TZVP basis set. Free energies reported in this work reflect these single-point energies modified by free-energy corrections at 298.15 K and 1 atm, calculated at the level of geometry optimization. The calculations used the anti conformers of all alkoxide species for convenience.

References

(1) Swart, P. D. R.; Rautenbach, K.; Raubenheimer, J. E. *SAJCH South African J. Child Heal.* **2014**, *8* (1), 23–27.

(2) Dohi, T.; Takenaga, N.; Goto, A.; Maruyama, A.; Kita, Y. *Org. Lett.* **2007**, *9* (16), 3129–3132.

(3) Bonollo, S.; Ahmady, A. Z.; Petrucci, C.; Marrocchi, A.; Pizzo, F.; Vaccaro, L. *Org. Lett.* **2014**, *16* (21), 5721–5723.

(4) Shu, C.; Liu, M. Q.; Sun, Y. Z.; Ye, L. W. *Org. Lett.* **2012**, *14* (18), 4958–4961.

(5) Leisch, H.; Morley, K.; Lau, P. C. K. *Chem. Rev.* **2011**, *111* (7), 4165–4222.

(6) Huang, L.; Jiang, H.; Qi, C.; Liu, X. *J. Am. Chem. Soc.* **2010**, *132* (50), 17652–17654.

(7) Endo, Y.; Bäckvall, J. E. *Chem. - A Eur. J.* **2011**, *17* (45), 12596–12601.

(8) Mitsudome, T.; Noujima, A.; Mizugaki, T.; Jitsukawa, K.; Kaneda, K. *Green Chem.* **2009**, *11* (6), 793–797.

(9) Ito, M.; Osaku, A.; Shiibashi, A.; Ikariya, T. *Org. Lett.* **2007**, *9* (9), 1821–1824.

(10) Nishimura, T.; Onoue, T.; Ohe, K.; Uemura, S. *J. Org. Chem.* **1999**, *64* (18), 6750–6755.

(11) Murahashi, S. I.; Ito, K. ichiro; Naota, T.; Maeda, Y. *Tetrahedron Lett.* **1981**, *22* (52), 5327–5330.

(12) Nicklaus, C. M.; Phua, P. H.; Buntara, T.; Noel, S.; Heeres, H. J.; De Vries, J. G. *Adv. Synth. Catal.* **2013**, *355* (14–15), 2839–2844.

(13) Murahashi, S. I.; Naota, T.; Ito, K.; Maeda, Y.; Taki, H. *J. Org. Chem.* **1987**, *52* (19), 4319–4327.

(14) Fujita, K. I.; Yamamoto, K.; Yamaguchi, R. *Org. Lett.* **2002**, *4* (16), 2691–2694.

(15) Fujita, K. I.; Furukawa, S.; Yamaguchi, R. *J. Organometalic Chem.* **2002**, *649* (2), 289–292.

(16) Suzuki, T.; Morita, K.; Tsuchida, M.; Hiroi, K. *J. Org. Chem.* **2003**, *68* (4), 1601–1602.

(17) Suzuki, T.; Ghozati, K.; Katoh, T.; Sasai, H. *Org. Lett.* **2009**, *11* (19), 4286–4288.

(18) Suzuki, T. *Chem. Rev.* **2011**, *111* (3), 1825–1845.

(19) Sølvhøj, A.; Madsen, R. *Organometallics* **2011**, *30* (21), 6044–6048.

(20) Obora, Y. *ACS Catal.* **2014**, *4* (11), 3972–3981.

(21) Gunay, A.; Mantell, M. A.; Field, K. D.; Wu, W.; Chin, M.; Emmert, M. H. *Catal. Sci. Technol.* **2015**, *5* (2), 1198–1205.

(22) Yamaguchi, R.; Kobayashi, D.; Shimizu, M.; Fujita, K. ichi. *J. Organomet. Chem.* **2017**, *843*, 14–19.

(23) Fujita, K. I.; Tamura, R.; Tanaka, Y.; Yoshida, M.; Onoda, M.; Yamaguchi, R. *ACS Catal.* **2017**, *7* (10), 7226–7230.

(24) Zeng, G.; Sakaki, S.; Fujita, K.; Sano, H.; Yamaguchi, R. *ACS Catal.* **2014**, *4* (3), 1010–1020.

(25) González Miera, G.; Martínez-Castro, E.; Martín-Matute, B. *Organometallics* **2018**, *37* (5), 636–644.

(26) Cherepakhin, V.; Williams, T. J. *ACS Catal.* **2018**, *8* (5), 3754–3763.

(27) Nakano, D.; Itoh, C.; Ishii, F.; Kawanishi, H.; Takaoka, M.; Kiso, Y.; Tsuruoka, N.; Tanaka, T.; Matsumura, Y. *Biol. Pharm. Bull.* **2003**, *26* (12), 1701–1705.

(28) Zhao, W.; Ma, W.; Xiao, T.; Li, F. *ChemistrySelect* **2017**, *2* (13), 3608–3612.

(29) Liu, P.; Liang, R.; Lu, L.; Yu, Z.; Li, F. *J. Org. Chem.* **2017**, *82* (4), 1943–1950.

(30) Zhao, J.; Hartwig, J. F. *Organometallics* **2005**, *24* (10), 2441–2446.

(31) Touchy, A. S.; Shimizu, K. I. *RSC Adv.* **2015**, *5* (37), 29072–29075.

(32) Suzuki, T.; Morita, K.; Tsuchida, M.; Hiroi, K. *Org. Lett.* **2002**, *4* (14), 2361–2363.

(33) Fujita, K. I.; Ito, W.; Yamaguchi, R. *ChemCatChem* **2014**, *6* (1), 109–112.

(34) Shvo, Y.; Blum, Y.; Reshef, D.; Menzin, M. *J. Organomet. Chem.* **1982**, *226* (1), C21–C24.

(35) Ishii, Y.; Osakada, K.; Ikariya, T.; Saburi, M.; Yoshikawa, S. *Tetrahedron Lett.* **1983**, *24* (26), 2677–2680.

(36) Ishii, Y.; Osakada, K.; Ikariya, T.; Saburi, M.; Yoshikawa, S. *J. Org. Chem.* **1986**, *51* (11), 2034–2039.

(37) Lin, Y.; Zhu, X.; Zhou, Y. *J. Organomet. Chem.* **1992**, *429* (2), 269–274.

(38) Morris, D. M.; McGeagh, M.; De Peña, D.; Merola, J. S. *Polyhedron* **2014**, *84* (0), 120–135.

(39) Brown, L. C.; Ressegue, E.; Merola, J. S. *Organometallics* **2016**, *35* (24), 4014–4022.

(40) Whiting, J. E.; Edward, J. T. *Ring–Chain Tautomerism of Hydroxyketones*; 1971; Vol. 49.

(41) Hurd, C. D.; Saunders, W. H. *J. Am. Chem. Soc.* **1952**, *74* (21), 5324–5329.

(42) Ten Brink, G. J.; Arends, I. W. C. E.; Sheldon, R. A. *Adv. Synth. Catal.* **2002**, *344* (3–4), 355–369.

(43) Johnson, J. B.; Bäckvall, J. E. *J. Org. Chem.* **2003**, *68* (20), 7681–7684.

(44) Mueller, J. A.; Goller, C. P.; Sigman, M. S. *J. Am. Chem. Soc.* **2004**, *126* (31), 9724–9734.

(45) Pearson, D. M.; Waymouth, R. M. *Organometallics* **2009**, *28* (13), 3896–3900.

(46) Tseng, K. N. T.; Kampf, J. W.; Szymczak, N. K. *ACS Catal.* **2015**, *5* (9), 5468–5485.

(47) Nguyen, D. H.; Trivelli, X.; Capet, F.; Swesi, Y.; Favre-Réguillon, A.; Vanoye, L.; Dumeignil, F.; Gauvin, R. M. *ACS Catal.* **2018**, *8* (5), 4719–4734.

(48) Troya, D. *J. Phys. Chem. A* **2007**, *111* (42), 10745–10753.

(49) Cieplak, A. S. *J. Am. Chem. Soc.* **1981**, *103* (15), 4540–4552.

(50) Suzuki, T.; Matsuo, T.; Watanabe, K.; Katoh, T. *Synlett* **2005**, No. 9, 1453–1455.

(51) Zhang, J.; Balaraman, E.; Leitus, G.; Milstein, D. *Organometallics* **2011**, *30* (21), 5716–5724.

(52) Moromi, S. K.; Hakim Siddiki, S. M. A.; Ali, M. A.; Kon, K.; Shimizu, K. I. *Catal. Sci. Technol.* **2014**, *4* (10), 3631–3635.

(53) Izumi, A.; Obora, Y.; Sakaguchi, S.; Ishii, Y. *Tetrahedron Lett.* **2006**, *47* (52), 9199–9201.

(54) Safonova, T. S.; Sheinker, J. N.; Nemerjuck, M. P.; Peresleni, E. M.; Syrova, G. P. *Tetrahedron* **1971**, *27* (22), 5453–5458.

(55) Zhao, Y.; Truhlar, D. G. *J. Chem. Phys.* **2006**, *125* (19), 194101.

(56) Gaussian 09, Revision D.01, Frisch, M. J.; Trucks, G. W.; Schlegel, H. B.; Scuseria, G. E.; Robb, M. A.; Cheeseman, J. R.; Scalmani, G.; Barone, V.; Menucci, G. A.; Petersson, G. A.; Nakatsuji, H.; Caricato, A.; Li, X.; Hratchian, H.; P.; Izmaylov, A. F.; Bloino, J.; Zheng, G.; Sonnenberg, J. L.; Hada, M.; Ehara, M.; Toyota, K.; Fukuda, R.; Hasegawa, J.; Ishida, M.; Nakajima, T.; Honda, Y.; Kitao, O.; Nakai, H.; Vreven, T.; Montgomery, J. A., Jr.; Peralta, J. E.; Ogliaro, F.; Bearpark, M.; Heyd, J. J.; Brothers, E.; Kudin, K. N.; Staroverov, V. N. . Kobayashi; R.; Normand, J.; Raghavachari, K.; Rendell, A.; Burant, J. C.; Iyengar; S. S.; Tomasi, J.; Cossi, M.; Rega, N.; Millam, J. M.; Klene, M.; Knox, J. E.; Cross, J. B.; Bakken, V.; Adamo, C.; Jaramillo, J.; Gomperts, R.; Stratmann, R. E.; Yazyev, O.; Austin, A. J.; Cammi, R.; Pomelli, C.; Ochterski, J. W.; Martin, R. L.; Morokuma, K.; Zakrzewski, V. G.; Voth, G. A.; Salvador, P.; Dannenberg, J. J.; Dapprich, S.; Daniels, A.; D.; Farkas, O.; Foresman, J. B.; Ortiz, J. V.; Cioslowski, J.; Fox, D. J. Gaussian, Inc., Wallingford CT, 2016.

(57) Uhe, A.; Hölscher, M.; Leitner, W. *Chem. - A Eur. J.* **2013**, *19* (3), 1020–1027.

(58) Li, J.; Li, J.; Zhang, D.; Liu, C. *ACS Catal.* **2016**, *6* (7), 4746–4754.

(59) Sieffert, N.; Réocreux, R.; Lorusso, P.; Cole-Hamilton, D. J.; Bühl, M. *Chem. - A Eur. J.* **2014**, *20* (14), 4141–4155.

(60) Gao, Y.; Guan, C.; Zhou, M.; Kumar, A.; Emge, T. J.; Wright, A. M.; Goldberg, K. I.; Krogh-Jespersen, K.; Goldman, A. S. *J. Am. Chem. Soc.* **2017**, *139* (18), 6338–6350.

(61) Zhang, D. D.; Chen, X. K.; Liu, H. L.; Huang, X. R. *New J. Chem.* **2014**, *38* (8), 3862–3873.

(62) Barone, V.; Cossi, M. *J. Phys. Chem. A* **1998**, *102* (11), 1995–2001.

Chapter 4 Structural and Electronic Effects of Fluorinated Aryl Groups on Pentasubstituted Cyclopentadienyl Complexes of Rh(III) and Ir(III)

4.1 Contributions

The work described in this chapter had its origins in the work of Dr. Matthew Thornberry, Dr. Mason R. Haneline, Michael E. Lane, and Jennifer L. Edwards (nee Montgomery), former students in Paul Deck's research group. Contributions were also provided by Kenneth Knott (variable-temperature ^{19}F NMR spectrometry), and Dr. Carla Slebodnick (assistance with X-ray crystallography). The author is responsible for the synthesis and characterization of all fluorinated cyclopentadienes and the corresponding Rh(III) and Ir(III) complexes. The final manuscript was prepared in collaboration with Dr. Joseph Merola and Dr. Paul Deck and is in preparation to be submitted to the *Journal of Organometallic Chemistry*.

4.2 Abstract

Nucleophilic substitution reactions of potassium tetramethylcyclopentadienide with perfluoroarenes (RF, R = C_6F_5, C_5F_4N, and C_7F_7) afford mixtures of monoarylated and diarylated tetramethylcyclopentadienes (HMe_4C_5R and 2,5-$R_2Me_4C_5$, respectively). The diarylated diene 2,5-$R_2Me_4C_5$ showed conformational fluxionality: The C_5-C_{ipso} rotational barrier with R = C_6F_5 was estimated at 12 kcal/mol using dynamic NMR spectrometry. Dienes HMe_4C_5R react with $[M(COD)](\mu^2\text{-}Cl)_2$ (COD = 1,5-cyclooctadiene) or $MCl_3\cdot 3H_2O$ (M = Rh, Ir) to afford $[(\eta^5\text{-}Me_4C_5R)MCl]_2(\mu^2\text{-}Cl)_2$ in yields ranging from 25% to 82%. All six complexes were structurally characterized.

4.3 Introduction

While it is well-established that the electronic effects of cyclopentadienyl (Cp) ligands can be manipulated through ring substitution, efforts to understand the effects of electron-withdrawing

ring substituents have attracted more recent attention.[1–3] Many catalytic systems also demand significant steric bulk from the Cp ligand, and several recent reports have emphasized derivatives of the form C_5Me_4R and $C_5Me_3R_2$ as means of manipulating the electronic effects of the well-known Cp* (Me_5Cp) ligand.[1,2,11–13,3–10] Herein we focus on application of this strategy to the chemistry of Rh(III) and Ir(III). In particular, complexes of the form $[(C_5Me_3R_2)MCl]_2(\mu^2\text{-}Cl)_2$ and $[(C_5Me_4R)RhCl]_2(\mu^2\text{-}Cl)_2$ (M = Rh, Ir) have been found to catalyze a wide-range of C-H activation processes.[1,3,12,14–20] For example, complexes with R = CH_3 (i.e., using Cp* as the ligand) efficiently catalyze oxidative annulation of acetanilides, but only at relatively high temperatures.[21] However, with R = CO_2Et, useful catalytic activity was realized at room temperature.[10,22] At a more atomistic level, complexes with electron-withdrawing R substituents were shown to enhance alkene migratory insertions leading to [4+1] cyclization whereas electron donating groups (R = bulky alkyl) yielded [4+2] annulation products instead.[23] Advantages of electron-withdrawing substituents are not limited to the Cp* family of ligands. CF_3 substitution was found to improve hydroboration regio- and stereoselectivity using η^5-indenylrhodium catalysts.[24–28]

A common synthetic starting point for many compounds within the $(C_5Me_4R)Rh(III)$ and $(C_5Me_4R)Ir(III)$ family is the dimeric species $[(C_5Me_4R)MCl]_2(\mu^2\text{-}Cl)_2$ (M = Rh, Ir; R = substituent). Methods for the synthesis of this important system continue to evolve.[4,5] Herein we describe the synthesis of three cyclopentadienes of the type HC_5Me_4R (R = C_6F_5, C_5F_4N, and C_7F_7) by nucleophilic substitution reactions of C_5Me_4K with perfluoroarenes (RF). We show that these cyclopentadienes are viable precursors to $[(C_5Me_4R)MCl]_2(\mu^2\text{-}Cl)_2$ (M = Rh, Ir). One of the reported dienes (R = C_6F_5) was prepared using addition of perfluorophenyllithium to 2,3,4,5-tetramethylcyclopentadien-2-en-1-one and converted to the corresponding dimeric $RhCl_2$

derivative in a solvothermal reaction with $RhCl_3 \cdot 3H_2O$.[17] The method offered herein is more general for the wider family of fluoroaromatic substituents.

4.4 Results and Discussion

4.4.1 Cyclopentadiene synthesis.

We have described previously that cyclopentadienyl anions are effective reagents for nucleophilic substitution reactions of perfluoroarenes.[7] When alkylated cyclopentadienyl anions are used, their increased nucleophilicity tends to result in lower selectivity for monoarylation.[29] In accord with these findings, potassium tetramethylcyclopentadienide (KMe_4Cp) reacts with perfluoroarenes (**Scheme 1**) to afford mixtures of monoarylated and diarylated tetramethylcyclopentadienes.[30] Compounds **1a** – **1c** and **2a** – **2c** were easily separated by silica gel chromatography, but the tautomeric mixture of monoarylated dienes (e.g., **1a** and **iso-1a**) were not separated. Another means of separating **2** from the reaction mixture is to remove the THF solvent prior to aqueous workup, and then wash the resulting residue with hexane; diene **2** is soluble in hexane, but **1** is not soluble in hexane as its sodium salt. The latter method, which is better for larger-scale preparations, requires thorough removal of the THF but leads, after workup, to reasonably pure **1** as a distillable oil.

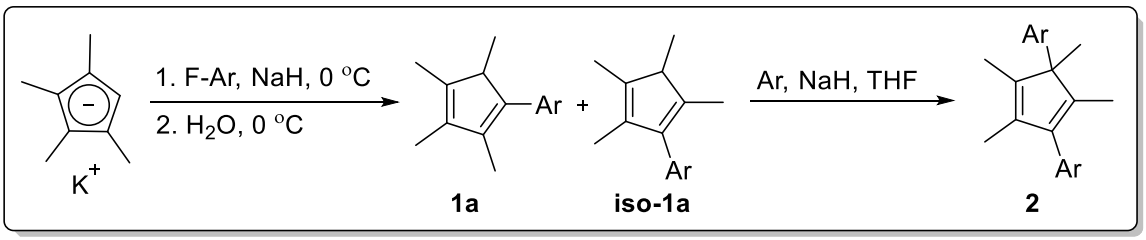

Scheme 1. General scheme for the synthesis of fluorinated monoaryl cyclopentadienes (Ar = C_6F_5 (**1a**), $C_6F_4CF_3$ (**1b**), C_5F_4N (**1c**)) and diaryl cyclopentadienes (Ar = C_6F_5 (**2a**), $C_6F_4CF_3$ (**2b**), C_5F_4N (**2c**)).

4.4.2 Cyclopentadiene characterization

As each diene (**1**) was isolated as a mixture of tautomers, we used ^{1}H NMR spectrometry to characterize each mixture. The most characteristic signal is the methine quartet, which appears at about 3.3 ppm in the major isomer and about 2.8 ppm in the minor isomer (with small variations in these chemical shifts as the substituent changes). This result allowed us to assign the structures of **1** and **iso-1**, since the downfield methine signal corresponds to the isomer having the proximal electron-withdrawing perfluoroaryl group. The minor species **iso-1** is typically about 10% of the mixture. Corresponding doublets are observed upfield (0.95 ppm and 1.15 ppm, respectively for coupled methyl groups. A doublet from H-F coupling of adjacent methyl group and an ortho fluorine around 1.92 ppm. The corresponding ^{19}F NMR spectra show typical chemical shifts and couplings for C_6F_5, $C_6F_4CF_3$, and C_5F_4N groups. One interesting feature in the spectrum at room temperature is dynamic rotation about the Ar-C_5 bond. As an example, in the spectrum of **1a** (R = C_6F_5), this rotation manifests as a very broad singlet for the two exchanging *ortho* fluorine atoms. In contrast, the vicinal methyl groups in the minor isomer (**iso-1a**) prevent rotation, and the two chemically inequivalent *ortho* fluorine signals are well resolved. Because these compounds are, unfortunately, not especially pure, we decided not to pursue modeling of the dynamic behavior of these monoarylated dienes. The NMR spectra of the diarylated dienes **2** confirm the assigned structure, but only partly. The ^{1}H NMR spectrum shows four distinct CH_3 signals (one of which exhibits long-range H—F coupling that is described below), and the ^{19}F NMR spectrum shows that both of the C_6F_5 groups are in slow torsional exchange at room temperature (although the 5-C_6F_5 group exhibits some exchange broadening that is also describe in more detail below). These data did not allow us to unambiguously assign the regiochemistry of the two C_6F_5 groups, but fortunately we were able to obtain their crystal structures and so we decided not to pursue

additional NMR measurements that we would have needed to establish the structure of these dienes (**2**).

4.4.3 Diarylated cyclopentadiene crystal structures.

Each of the diarylcyclopentadienes (**2**) was crystallized from hexanes at -18 ˚C and structurally characterized using X-ray diffraction. Thermal ellipsoid plots, crystal data, and selected bond lengths and angles are provided in the SI. These structures all confirm the assignment of the distal (2,5) regiochemistry of the two aryl groups. Not surprisingly the three structures also are substantially the same with respect to their essential features (i.e., bond lengths and angles of the cyclopentadiene moiety). We note that diene **2a** exhibited an unusual form of twinning in its crystalline form. Fine details of that procedure are provided in the SI. One feature of these structures bears further attention. The perfluoroaryl group at the C_5 position is oriented such that one of the *ortho* fluorines is in much closer spatial proximity to the C_5 methyl group than the other. This feature becomes significant in our interpretation of the dynamic NMR behavior of diene **2a**.

4.4.4 Conformational dynamic behavior of diarylcyclopentadiene **2a**.

Figure 1 displays an ^{1}H NMR spectrum of **2a** recorded at ambient temperature (about 25 °C) that features an interesting coupled signal at 1.6 ppm. This signal is assigned to the methyl group on the 5-carbon; the other CH_3 protons are allylic and therefore appear downfield (1.65 – 1.73 ppm). Noting the close proximity of the 5-CH_3 to one fluorine atom on the 5-C_6F_5 group, we considered the possibility of coupling between them. Because of the unusual lineshape of the 5-CH_3 signal, as well as the signal-broadening observed in the ^{19}F NMR spectra of these dienes (**2a**), we conducted a variable-temperature study of diene **2a** (**Figure 2**) coupled with computational (spin-mechanics) modeling (see below) with the primary aim of establishing the coupling scheme and the secondary goal of determining the torsional barrier at the C_5—C_6F_5 bond. At temperatures

of 15 °C and below, the 5-CH_3 group appears as a doublet with an apparent coupling constant of 7.5 Hz. We acknowledge here that all of the signals in these spectra are somewhat broad, which tends to mask small coupling constants. Lacking that further information, we assigned one of the $^5J_{HF}$ values to 7.5 Hz, and the other to 0 Hz. At 45 °C and above, the 5-CH_3 signal appears as a triplet with half the coupling constant (3.8 Hz), because the two H-F couplings (7.5 Hz and 0 Hz) are time-averaged in the fast-exchange limit. In the intermediate temperature regime, the spectra required computational modeling. We used a spin model with two ^{19}F nuclei (the two *ortho* fluorines that are undergoing degenerate two-site exchange) and three equivalent ^1H nuclei (the 5-CH_3 group). All other possible coupling interactions to the 5-CH_3 group were disregarded. For each temperature, the ^1H NMR spectrum was calculated using gNMR software (Peter Budzelaar, University of Manitoba), varying the two-site exchange rates within the software (the first-order rate constant is parametric) until the model lineshape matched visually with the experimental lineshape. These rate constants were subjected to an Arrhenius analysis giving a serviceable line (**Figure S27**) with a slope corresponding to an activation barrier of 12 kcal/mol for the two-site exchange. Details of the Arrhenius analysis are deposited in the supporting information. Corresponding variable-temperature ^{19}F NMR spectra were also collected (**Error! Reference source not found.**), which shows continued broadening of the exchanging *ortho* fluorines until coalescence is reached at about 85 °C. Because the ^{19}F spectra are complicated with significant vicinal couplings, we decided not to model that data.

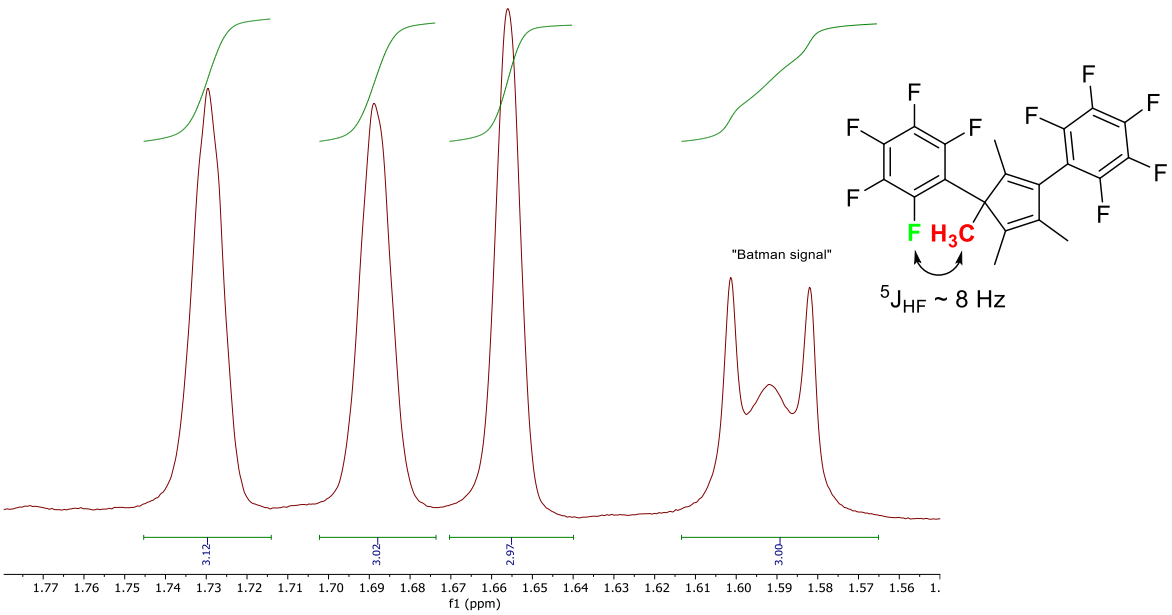

Figure 1. ^{1}H NMR spectrum of **2a** (400 MHz, toluene-d_8) showing a unique methyl signal exhibiting additional coupling assigned to $^{5}J_{HF}$. Dynamic rotation of the C_5—C_6F_5 bond results in time-averaged coupling. Modeling of the coupling is described in the text.

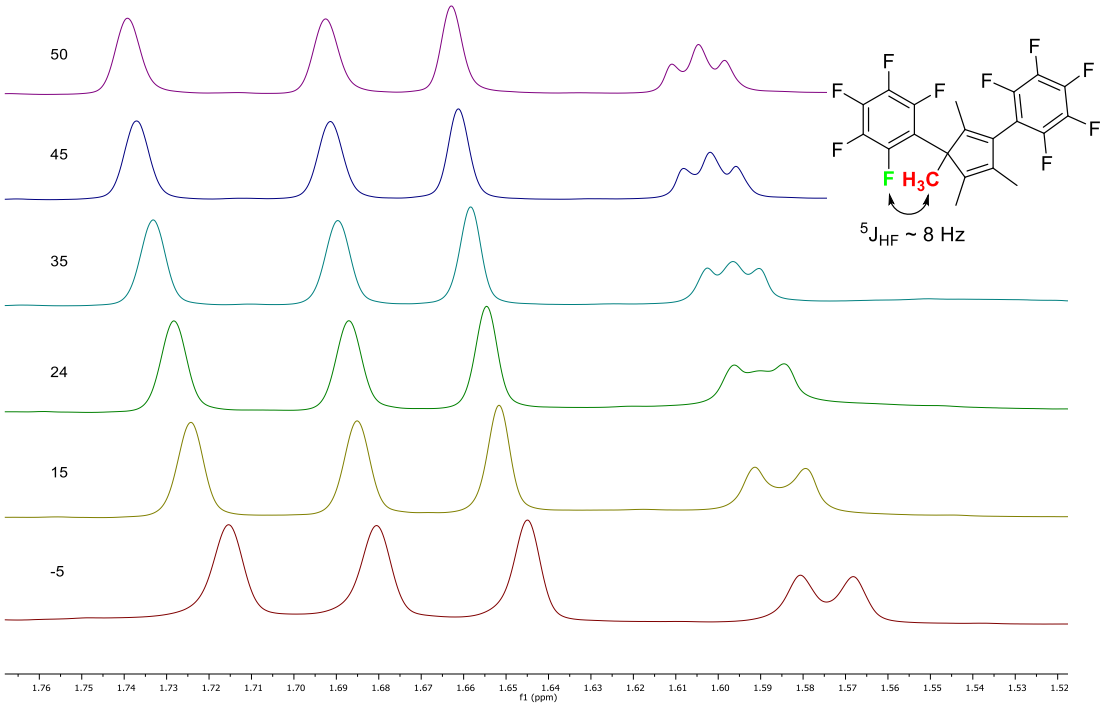

Figure 2. Variable temperature ^{1}H NMR spectra of **2a** (400 MHz, $CDCl_3$).

We are not entirely sure why, in this model, coupling of the 5-CH_3 group to the two *ortho* fluorine atoms differs so significantly. However, the crystallographic data suggest that *through-space* coupling could be invoked, as it has by others.[31–35] In the solid-state structure, one of the *ortho* fluorine atoms is in close proximity to the methyl group (C—F distance of about 2.73 A for **2a**). We surmise that through-space coupling of the 5-CH_3 to this *ortho* fluorine accounts for our NMR observations.

4.4.5 Synthesis of rhodium(III) and iridium(III) chloro-bridged dimers.

Iridium dimeric complexes (**4**) were conveniently prepared from the corresponding substituted fluorinated cyclopentadienes and $[Ir(COD)]_2(\mu^2\text{-}Cl)_2$ (COD = 1,5-cyclooctadiene) in methanol solvent using a general microwave synthesis that we described previously (**Figure 3**).[4] The iridium dimers were obtained in yields ranging from 49% - 82%. We had more difficulty preparing the corresponding rhodium complexes. This method proved to be less effective for rhodium. We were able to prepare **3a** using our microwave method (31% yield), but for complexes **3b** and **3c** we instead used method previously reported by others and obtained yields of 25% and 38% respectively.[17]

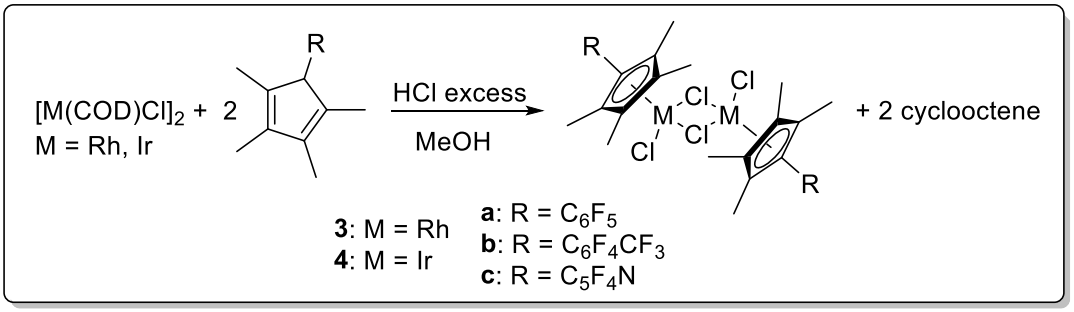

Figure 3. Ir(III) and Rh(III) chloro-bridged dimers synthesized via an established literature procedure.[4]

4.4.6 NMR characterization of chloro-bridged dimers **3** and **4**.

The ^{1}H NMR spectra of the dimers (**3** and **4**) show the expected two signals for the CH_3 groups proximal (vicinal) and distal to the aryl group, as a result of time-averaged C_2h symmetry for the dimer overall. One of the CH_3 signals exhibits an interesting long-range coupling, which we assign to coupling of the proximal CH_3 and the *ortho* fluorine atom(s) on the basis of a heteronuclear decoupling experiment (**Figure 4**). Interestingly this coupling appears in the spectrum as a doublet ($^{5}J_{HF}$ = 1.2 Hz), which suggests unequal coupling to the two *ortho* fluorine atoms. Lacking additional information (i.e., from high-level ab-initio models), we cannot rationalize this difference, but since the two *ortho* fluorines are chemically equivalent (and not in dynamic exchange), they could couple differently. The corresponding ^{1}H-decoupled ^{19}F spectrum was too noisy and complex for us to assign the ^{1}H coupling (which would be septet coupling) to any particular signal among the five ^{19}F signals. We note also that the coupling observed here, which must be a *through-bond* coupling, is much smaller in magnitude (1.2 Hz) than the coupling we observed in diene **2a** (7.5 Hz), which we ascribed to *through-space* H—F coupling.

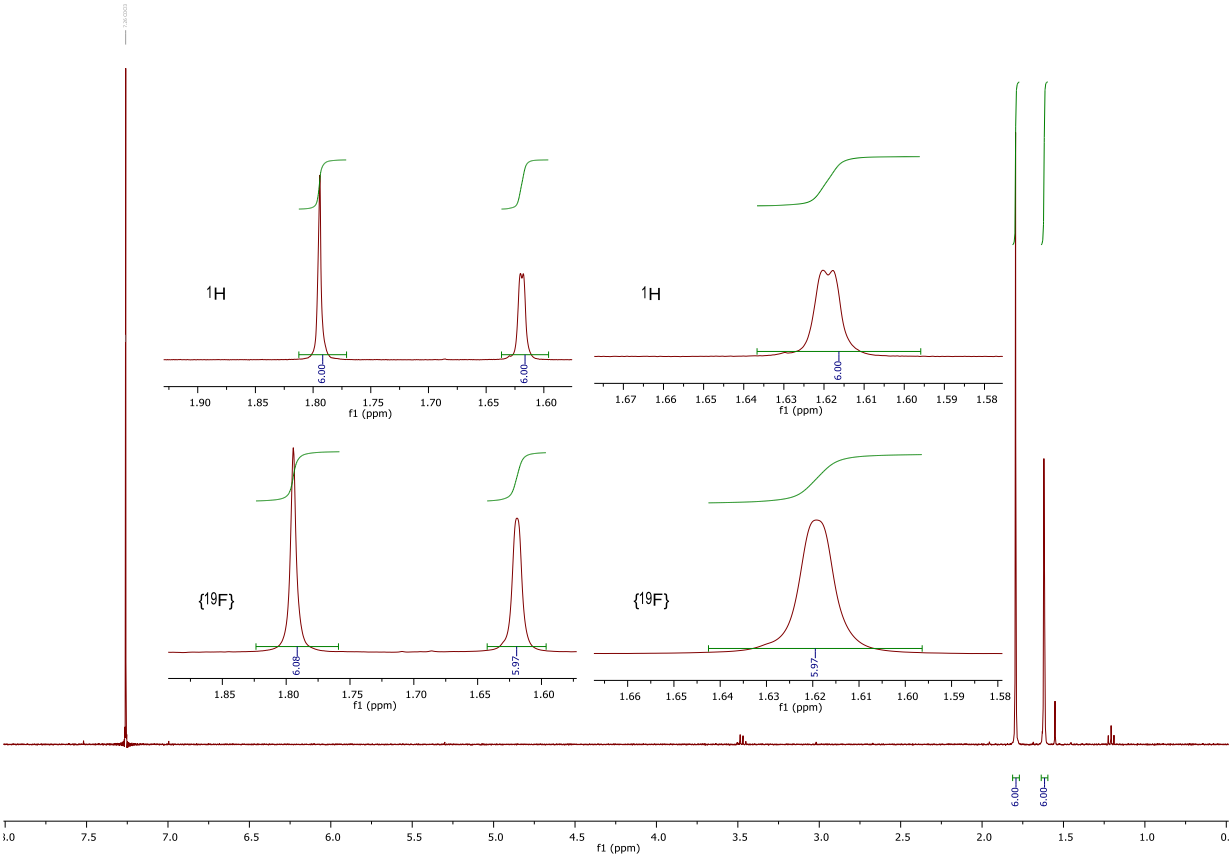

Figure 4. ^{1}H NMR (top) and $^{1}H\{^{19}F\}$ (bottom) spectra (400 MHz, $CDCl_3$) of iridium dimer **4a** revealing the origin of the observed doublet at 1.62 ppm in coupling to an aromatic fluorine.

4.4.7 Rhodium(III) and iridium(III) chloro-bridged dimer crystal structures.

Crystallization of the chloro-bridged dimers by slow diffusion of pentane into dichloromethane afforded samples for X-ray diffraction. All dimers exhibited a typical pseudo-tetrahedral structure. The structure of complex **3a** was previously reported by Piou et al. and corresponds well to our structure (which is trivially different in that their substance was characterized as a chloroform solvate).[17] There is little variation among the six structures except that rhodium displays larger X_1-Rh-X_2, X_1-Rh-Cl, and X_2-Rh-Cl (where X_1 = first bridging Cl and X_2 = second bridging Cl) bond angles than its iridium counterpart (**Tables S3 and S4**).

4.5 Conclusions

Cyclopentadienes of general structure $HMe_4C_5(Ar)$ (Ar = C_6F_5, $C_6F_4CF_3$, and C_5F_4N) are readily prepared from KMe_4Cp and the corresponding perfluoroarenes, together with the readily separated diarylated cyclopentadienes $Me_4C_5(Ar)_2$ as minor byproducts. Reactions of the monoarylated cyclopentadienes with an appropriate rhodium- or iridium-containing precursor afford chloro-bridged dimers $[(\eta^5\text{-}Me_4C_5R)MCl]_2(\mu^2\text{-}Cl)_2$. NMR studies reveal details of the dynamic behavior (torsional C_5—C_6F_5 rotations) and various couplings of ring CH_3 and aromatic fluorine atoms. Work is underway in our laboratories to compare the electronic effects of the three distinct perfluoroaryl substituents described herein and to explore the utility of these complexes as catalysts for transfer dehydrogenation and C-H activation reactions.

4.6 Experimental

Please see Supporting Information for detailed descriptions of all experimental materials and methods.

4.6.1 General procedure for the synthesis of HMe_4C_5R and $Me_4C_5R_2$ dienes

Under nitrogen, $KCpMe_4$ was slowly added to a solution of a perfluoroarene in THF and the mixture was stirred at 25 °C for 16 h. The solvent was removed under reduced pressure, and the residue was slurried in hexanes. DI water was added and the layers were separated. The organic layer was dried over $MgSO_4$, filtered, and evaporated. The residue was separated via column chromatography (silica gel / hexanes) with the monoarylated product eluting first and the diarylated product eluting last. The initial fraction containing the monoarylated product was evaporated under reduced pressure to yield the monoarylated diene.

4.6.2 General procedure for the synthesis of $[(\eta^5\text{-}Me_4C_5R)MCl]_2(\mu^2\text{-}Cl)_2$ (M = Rh, Ir)

Unless otherwise stated, a microwave pressure tube was fitted with the appropriate amounts of the respective $[M(COD)]_2(\mu^2\text{-}Cl)_2$, HMe_4C_5R, in 4 mL of methanol with 0.5 mL of concentrated HCl. The reaction mixture was heated to 115 °C at 50 W and 150 psi and held for 1 h, yielding an orange or red solution. The solvent was evaporated under reduced pressure, and the resulting powder recrystallized from DCM and cold hexanes, collected via filtration, and washed with cold hexanes. Complexes were prepared according to an established literature procedure.[4]

References

1. Piou, T. & Rovis, T. Electronic and Steric Tuning of a Prototypical Piano Stool Complex: Rh(III) Catalysis for C-H Functionalization. *Acc. Chem. Res.* **51,** 170–180 (2018).
2. Conway, J. H. & Rovis, T. Regiodivergent Iridium(III)-Catalyzed Diamination of Alkenyl Amides with Secondary Amines: Complementary Access to γ- Or δ-Lactams. *J. Am. Chem. Soc.* **140,** 135–138 (2018).
3. Romanov-Michailidis, F., Ravetz, B. D., Paley, D. W. & Rovis, T. Ir(III)-Catalyzed Carbocarbation of Alkynes through Undirected Double C-H Bond Activation of Anisoles. *J. Am. Chem. Soc.* **140,** 5370–5374 (2018).
4. Brown, L. C., Ressegue, E. & Merola, J. S. Rapid Access to Derivatized, Dimeric, Ring-Substituted Dichloro(cyclopentadienyl)rhodium(III) and Iridium(III) Complexes. *Organometallics* **35,** 4014–4022 (2016).
5. Mantell, M. A., Kampf, J. W. & Sanford, M. Improved Synthesis of $[Cp^{R}RhCl_2]_2$ Complexes . *Organometallics* **37,** 3240–3242 (2018).
6. Yamada, T., Shibata, Y. & Tanaka, K. Functionalized Cyclopentadienyl Ligands and Their Substituent Effects on a Rhodium(III)-Catalyzed Oxidative [4+2] Annulation of Indole- and Pyrrole-1-Carboxamides with Alkynes. *Asian J. Org. Chem.* **7,** 1396–1402 (2018).
7. Deck, P. A. Perfluoroaryl-substituted cyclopentadienyl complexes of transition metals. *Coord. Chem. Rev.* **250,** 1032–1055 (2006).
8. Davis, T. A., Wang, C. & Rovis, T. Rhodium(III)-Catalyzed C-H Activation: An Oxidative Intramolecular Heck-Type Reaction Directed by a Carboxylate. *Synlett* **26,** 1520–1524 (2015).

9. Fukui, M. *et al.* Rhodium(III)-Catalyzed Tandem [2+2+2] Annulation–Lactamization of Anilides with Two Alkynoates via Cleavage of Two Adjacent C−H or C−H/C−O bonds. *Chem. - An Asian J.* **11,** 2260–2264 (2016).

10. Hoshino, Y., Shibata, Y. & Tanaka, K. Oxidative annulation of anilides with internal alkynes using an (Electron-Deficient η^5-cyclopentadienyl)rhodium(III) catalyst under ambient conditions. *Adv. Synth. Catal.* **356,** 1577–1585 (2014).

11. Takahama, Y., Shibata, Y. & Tanaka, K. Oxidative olefination of anilides with unactivated alkenes catalyzed by an (electron-deficient η^5-cyclopentadienyl)rhodium(III) complex under ambient conditions. *Chem. - A Eur. J.* **21,** 9053–9056 (2015).

12. Semakul, N., Jackson, K. E., Paton, R. S. & Rovis, T. Heptamethylindenyl (Ind*) enables diastereoselective benzamidation of cyclopropenes via Rh(III)-catalyzed C-H activation. *Chem. Sci.* **8,** 1015–1020 (2017).

13. Shibata, Y. & Tanaka, K. Catalytic [2+2+1] cross-cyclotrimerization of silylacetylenes and two alkynyl esters to produce substituted silylfulvenes. *Angew. Chemie - Int. Ed.* **50,** 10917–10921 (2011).

14. Romanov-Michailidis, F., Sedillo, K. F., Neely, J. M. & Rovis, T. Expedient Access to 2,3-Dihydropyridines from Unsaturated Oximes by Rh(III)-Catalyzed C-H Activation. *J. Am. Chem. Soc.* **137,** 8892–8895 (2015).

15. Neely, J. M. & Rovis, T. Rh(III)-catalyzed decarboxylative coupling of acrylic acids with unsaturated oxime esters: Carboxylic acids serve as traceless activators. *J. Am. Chem. Soc.* **136,** 2735–2738 (2014).

16. Hyster, T. K., Dalton, D. M. & Rovis, T. Ligand design for Rh(iii)-catalyzed C-H activation: An unsymmetrical cyclopentadienyl group enables a regioselective synthesis of

dihydroisoquinolones. *Chem. Sci.* **6,** 254–258 (2015).

17. Piou, T. *et al.* Correlating reactivity and selectivity to cyclopentadienyl ligand properties in Rh(III)-catalyzed C-H activation reactions: An experimental and computational study. *J. Am. Chem. Soc.* **139,** 1296–1310 (2017).
18. Piou, T., Romanov-Michailidis, F., Ashley, M. A., Romanova-Michaelides, M. & Rovis, T. Stereodivergent Rhodium(III)-Catalyzed cis-Cyclopropanation Enabled by Multivariate Optimization. *J. Am. Chem. Soc.* **140,** 9587–9593 (2018).
19. Piou, T. & Rovis, T. Rh(III)-catalyzed cyclopropanation initiated by C-H activation: Ligand development enables a diastereoselective [2 + 1] annulation of N-enoxyphthalimides and alkenes. *J. Am. Chem. Soc.* **136,** 11292–11295 (2014).
20. Piou, T. & Rovis, T. Rhodium-catalysed syn-carboamination of alkenes via a transient directing group. *Nature* **527,** 86–90 (2015).
21. Guimond, N., Gorelsky, S. I. & Fagnou, K. Rhodium(III)-catalyzed heterocycle synthesis using an internal oxidant: Improved reactivity and mechanistic studies. *J. Am. Chem. Soc.* **133,** 6449–6457 (2011).
22. Fukui, M., Hoshino, Y., Satoh, T., Miura, M. & Tanaka, K. ChemInform Abstract: The Oxidative Annulation of Tertiary Benzyl Alcohols with Internal Alkynes Using an (Electron-Deficient η^5-Cyclopentadienyl)Rhodium(III) Catalyst under Ambient Conditions. . *ChemInform* **45,** no-no (2014).
23. Romanov-Michailidis, F., Phipps, E. J. T. & Rovis, T. Sterically and Electronically Tuned Cp Ligands for Rhodium(III)-Catalyzed Carbon-Hydrogen Bond Functionalization. in *Rhodium Catalysis in Organic Synthesis* 593–628 (Wiley-VCH Verlag GmbH & Co. KGaA, 2019). doi:10.1002/9783527811908.ch20

24. Brinkman, J. A., Nguyen, T. T. & Sowa, J. R. Trifluoromethyl-Substituted Indenyl Rhodium and Iridium Complexes Are Highly Selective Catalysts for Directed Hydroboration Reactions. *Org. Lett.* **2,** 981–983 (2000).

25. Fang, M. *et al.* Cobalt complexes containing pendant amines in the second coordination sphere as electrocatalysts for H2 production. *Organometallics* **33,** 5820–5833 (2014).

26. Darmon, J. M. *et al.* Iron complexes for the electrocatalytic oxidation of hydrogen: Tuning primary and secondary coordination spheres. *ACS Catal.* **4,** 1246–1260 (2014).

27. Liu, T. *et al.* Iron Complexes Bearing Diphosphine Ligands with Positioned Pendant Amines as Electrocatalysts for the Oxidation of H_2. *Organometallics* **34,** 2747–2764 (2015).

28. Kumar, N. *et al.* Outer Coordination Sphere Proton Relay Base and Proximity Effects on Hydrogen Oxidation with Iron Electrocatalysts. *Organometallics* (2019).

29. Deck, P. A., Kroll, C. E., Gary Hollis, W. & Fronczek, F. R. Conformational control of intramolecular arene stacking in ferrocene complexes bearing tert-butyl and pentafluorophenyl substituents. *J. Organomet. Chem.* **637–639,** 107–115 (2001).

30. Thornberry, M. P., Slebodnick, C., Deck, P. A. & Fronczek, F. R. Structural and electronic effects of pentafluorophenyl substituents on cyclopentadienyl complexes of Fe, Co, Mn, and Re. *Organometallics* **19,** 5352–5369 (2000).

31. Kui, S. C. F., Zhu, N. & Chan, M. C. W. Observation of intramolecular C-H···F-C contacts in non-metallocene polyolefin catalysts: Model for weak attractive interactions between polymer chain and noninnocent ligand. *Angew. Chemie - Int. Ed.* **42,** 1628–1632 (2003).

32. Chan, M. C. W. *et al.* Neutron and X-ray diffraction and spectroscopic investigations of

intramolecular [C-H···F-C] contacts in post-metallocene polyolefin catalysts: Modeling weak attractive polymer-ligand interactions. *Chem. - A Eur. J.* **12,** 2607–2619 (2006).

33. So, L. C. *et al.* Scalar Coupling Across [C-H···F-C] Interactions in (σ-Aryl)-Chelating Post-Metallocenes. *Chem. - A Eur. J.* **18,** 565–573 (2012).

34. Liu, C.-C. *et al.* Highly Fluorinated (σ-Aryl)-Chelating Titanium(IV) Post-Metallocene: Characterization and Scalar [C–H···F–C] Coupling. *Organometallics* **31,** 5274–5281 (2012).

35. Iwashita, A., Chan, M. C. W., Makio, H. & Fujita, T. Attractive interactions in olefin polymerization mediated by post-metallocene catalysts with fluorine-containing ancillary ligands. *Catal. Sci. Technol.* **4,** 599–610 (2014).

Chapter 5 Supporting Information

5.1 General methods

Unless otherwise noted, all reactions in Chapters 2-4 were conducted using standard Schlenk techniques and flame-dried glassware. All reagents purchased in Chapters 2-4 were used as received. Antimicrobial studies were performed using an established literature procedure.[1]

5.2 Instrumentation

^{1}H, ^{13}C, ^{19}F NMR spectra were obtained using an Agilent DD2 400 MHZ spectrometer. All chemical shifts are reported in parts per million (ppm) using CDCl3 (7.26 ppm – ^{1}H and 77.16 ppm – ^{13}C) as a standard, unless otherwise stated. Spectral data are reported using the following notation: chemical shift, multiplicity (s – singlet, d – doublet, t – triplet, q – quartet, m – multiplet, dd – doublet of doublets, dt – doublet of triplets, br – broad), coupling constant (*J* – Hz), and integration value. High resolution mass spectra (HRMS) were acquired using an Agilent LC-ESI-TOF electrospray ionization technique (+ESI), unless otherwise stated.

5.3 Synthetic procedures and characterization of products from Chapter 2

5.3.1 General procedure for the conventional synthesis of $[(\eta^5\text{-}Me_4C_5R)RhCl]_2(\mu^2\text{-}Cl)_2$

$RhCl_3 \cdot 3H_2O$ (500 mg, 1.90 mmol, 1.0 equiv) was combined with $\eta^5\text{-}Me_4C_5R$ (1.1 – 1.5 equiv) dissolved in 30 mL of MeOH in a round bottom flask under nitrogen. The resulting solution was stirred and refluxed for 48 hours. The reaction mixture was evaporated to dryness under reduced pressure. The red residue was recrystallized by dissolving the complex in a minimal amount of DCM, followed by slow addition of pentane or hexanes to produce a red powder. The complexes were filtered and rinsed with pentane or hexanes then dried under high vacuum overnight.

5.3.2 General procedure for the conventional synthesis of $[(\eta^5\text{-}Me_4C_5R)IrCl]_2(\mu^2\text{-}Cl)_2$

$IrCl_3 \cdot 3H_2O$ (500 mg, 1.42 mmol, 1.0 equiv) was combined with $\eta^5\text{-}Me_4C_5R$ (1.1 – 1.5 equiv) dissolved in 30 mL of MeOH in a round bottom flask under nitrogen. The resulting solution was stirred and refluxed for 48 hours. The reaction mixture was evaporated to dryness under reduced pressure. The orange residue was recrystallized by dissolving the complex in a minimal amount of DCM, followed by slow addition of pentane or hexanes to produce an orange powder. The complexes were filtered and rinsed with pentane or hexanes then dried under high vacuum overnight.

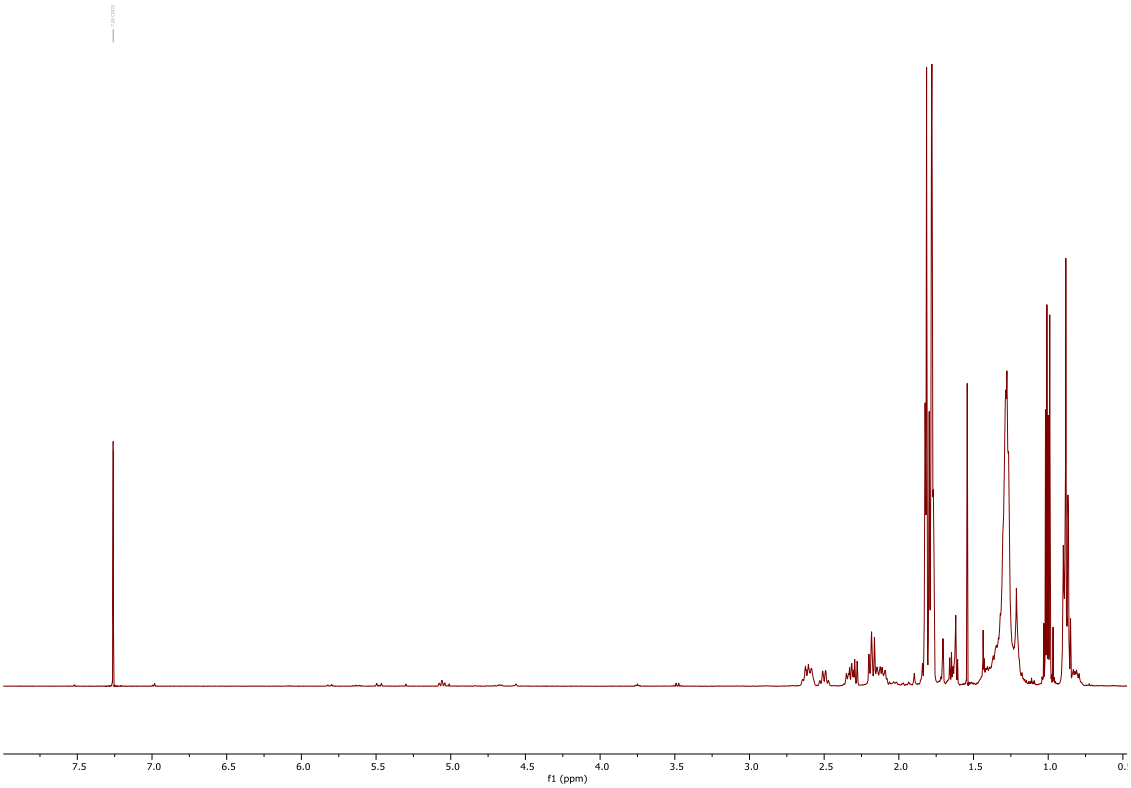

Figure S1. ^{1}H NMR spectrum of **1i** in $CDCl_3$ at 400 MHz.

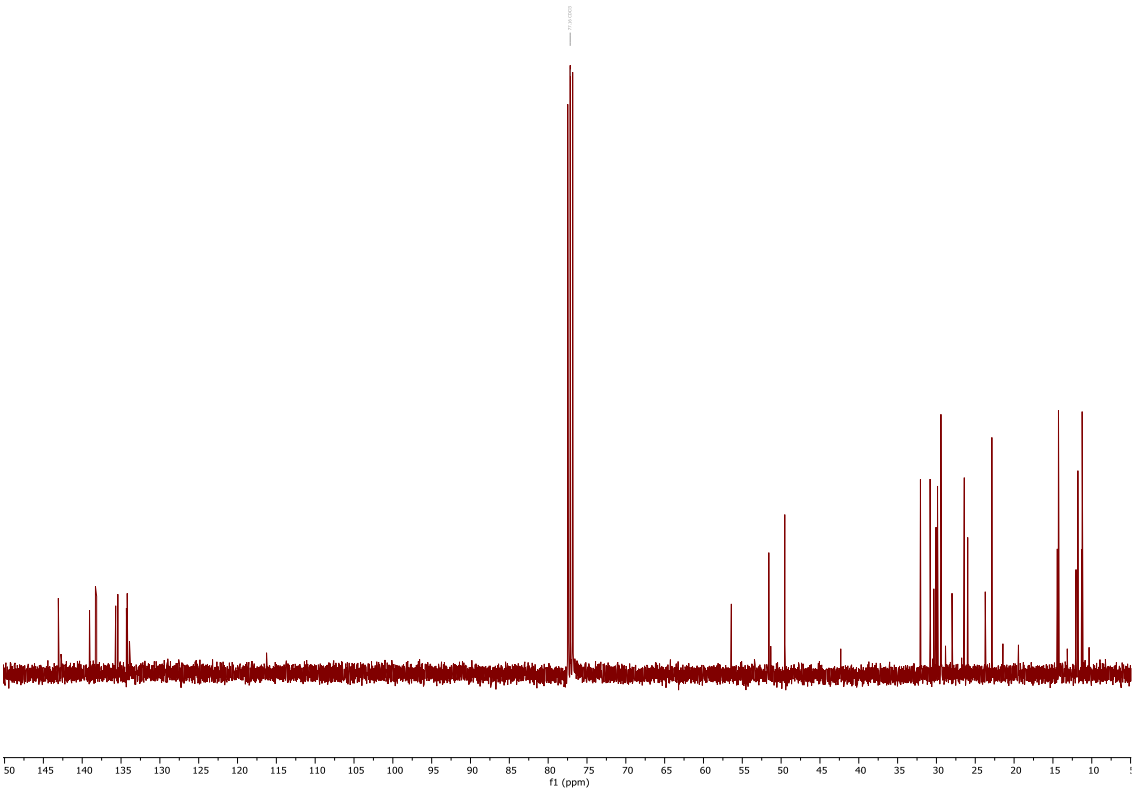

Figure S2. $^{13}C\{^{1}H\}$ NMR spectrum of **1i** in $CDCl_3$ at 101 MHz.

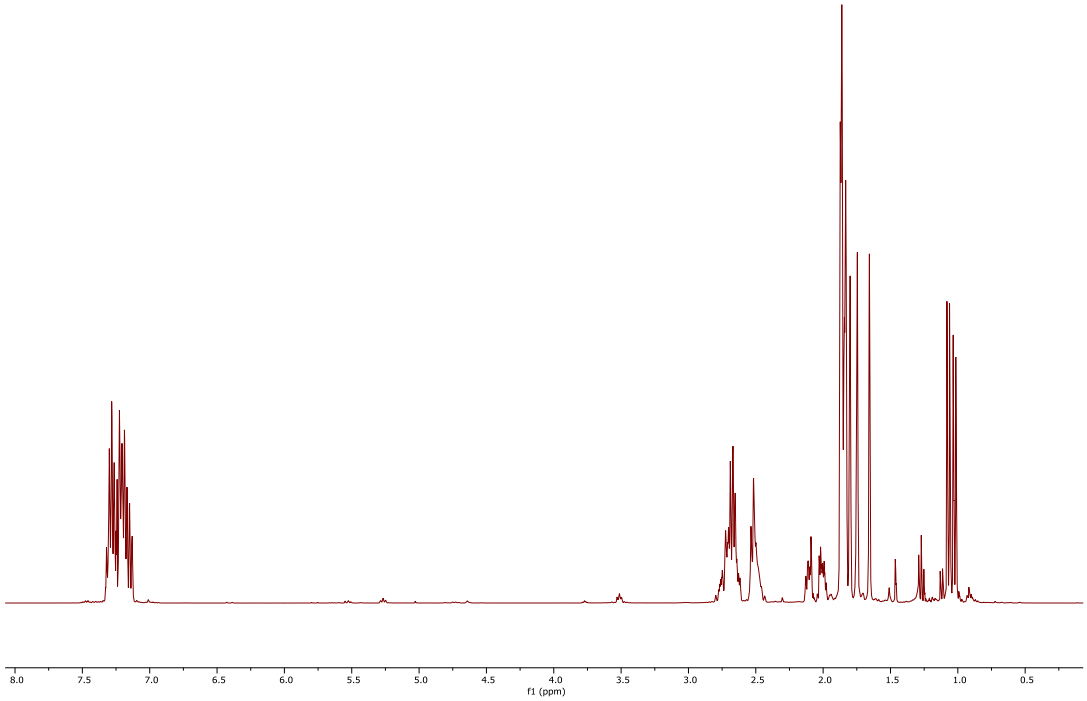

Figure S3. ^{1}H NMR spectrum of **1m** in $CDCl_3$ at 400 MHz.

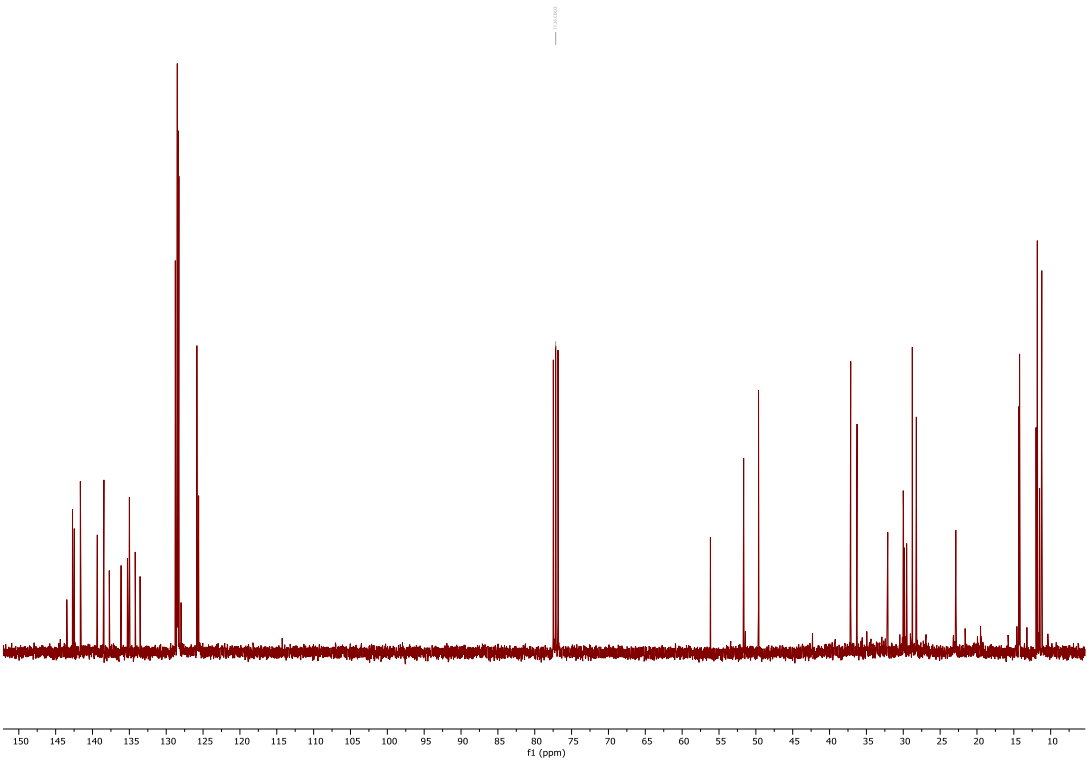

Figure S4. $^{13}C\{^{1}H\}$ NMR spectrum of **1m** in $CDCl_3$ at 101 MHz.

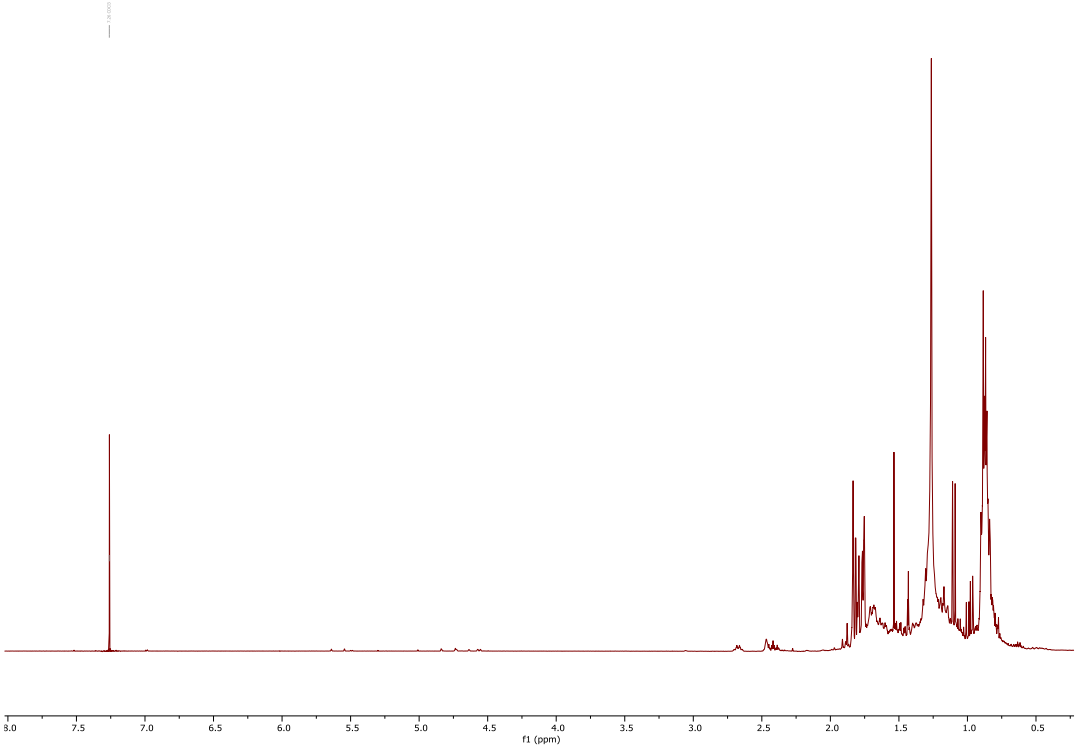

Figure S5. ^{1}H NMR spectrum of **1n** in $CDCl_3$ at 400 MHz.

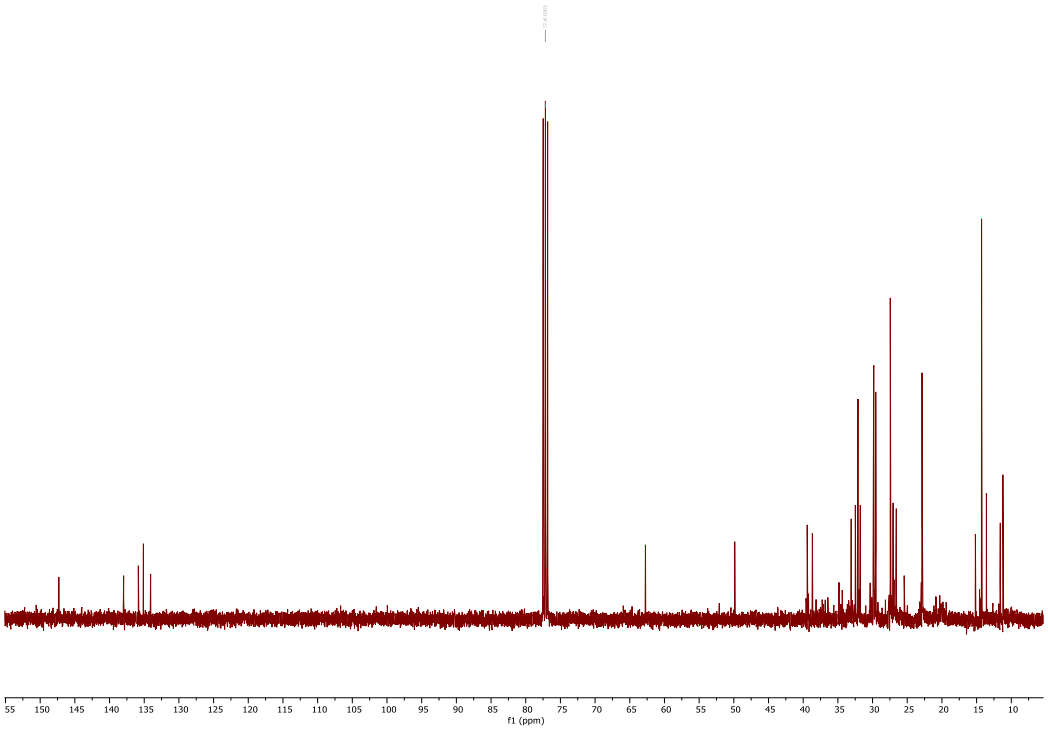

Figure S6. $^{13}C\{^{1}H\}$ NMR spectrum of **1n** in $CDCl_3$ at 101 MHz.

$[Cp^{*ethyl}IrCl]_2(\mu^2\text{-}Cl)_2$ (**2a**)

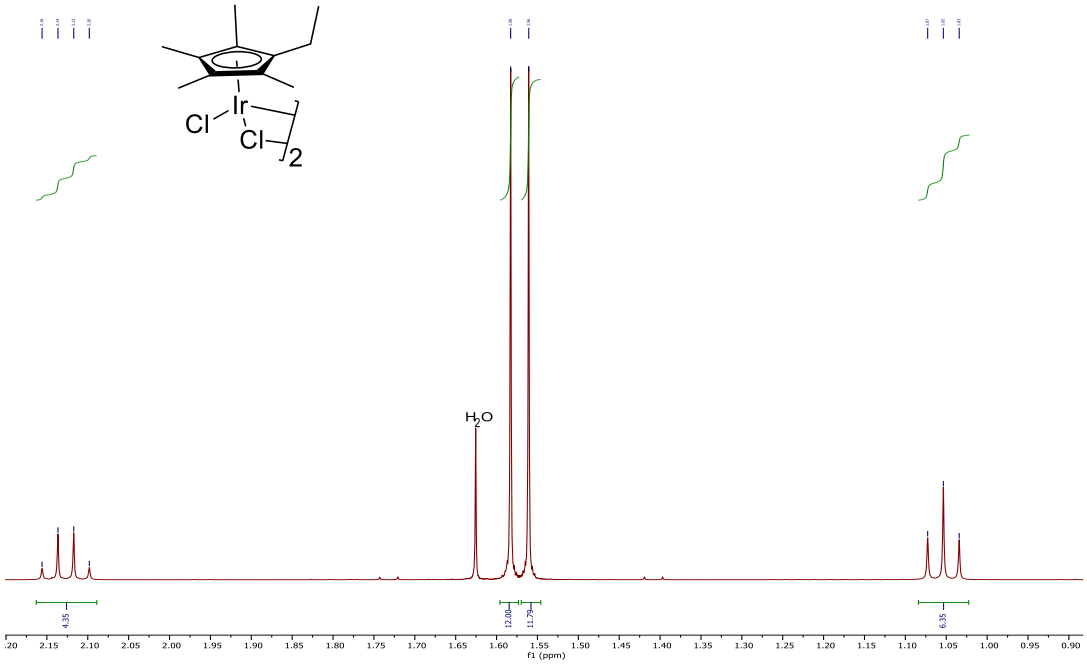

Figure S7. ^{1}H NMR spectrum of **2a** in $CDCl_3$ at 400 MHz.

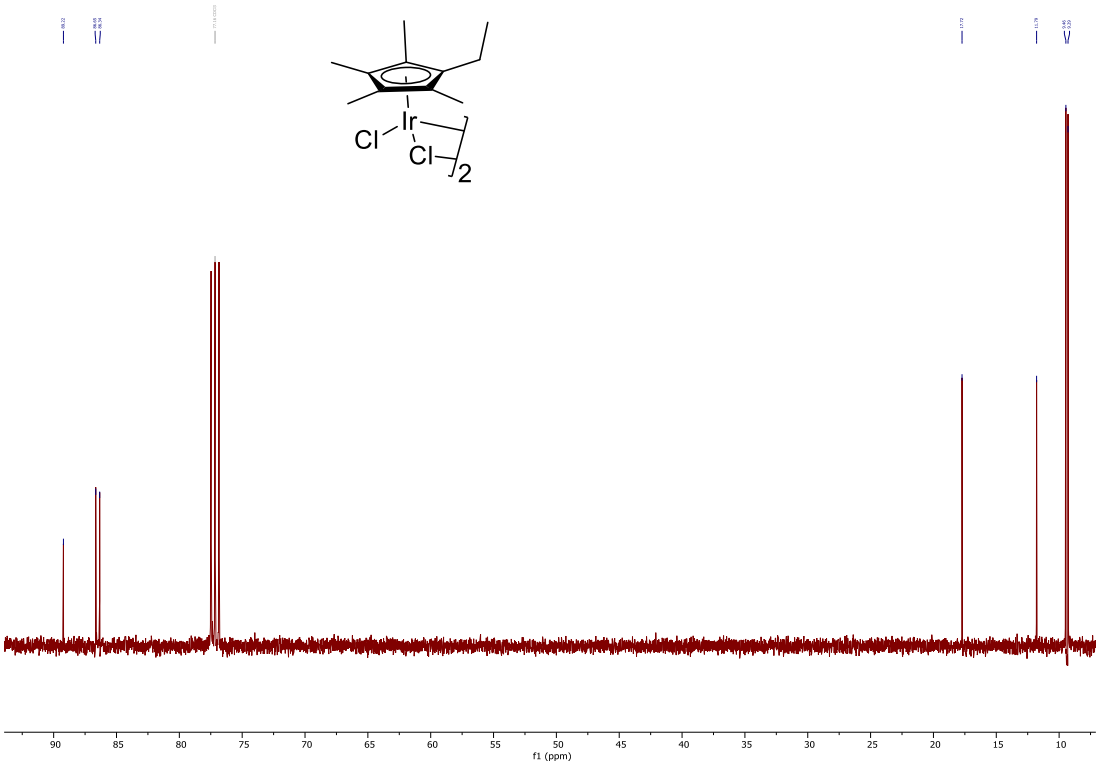

Figure S8. $^{13}C\{^{1}H\}$ NMR spectrum of **2a** in $CDCl_3$ at 101 MHz.

[Cp*$^{n\text{-propyl}}$IrCl]$_2$(μ^2-Cl)$_2$ (**2b**)

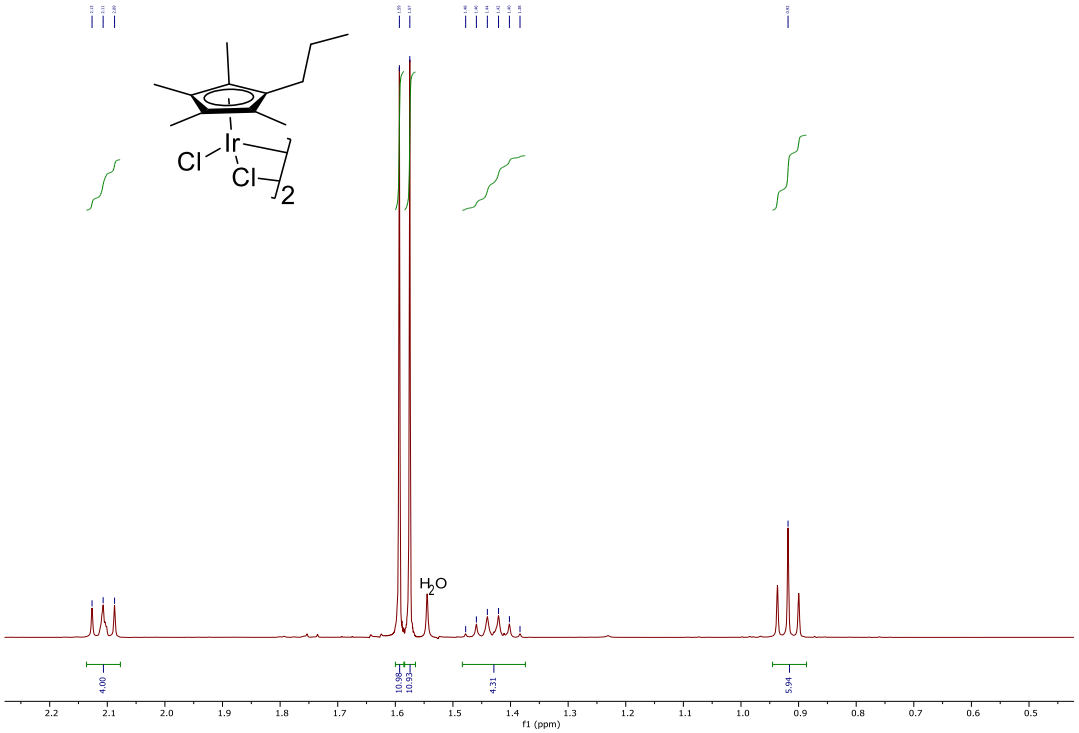

Figure S9. ^{1}H NMR spectrum of **2b** in $CDCl_3$ at 400 MHz.

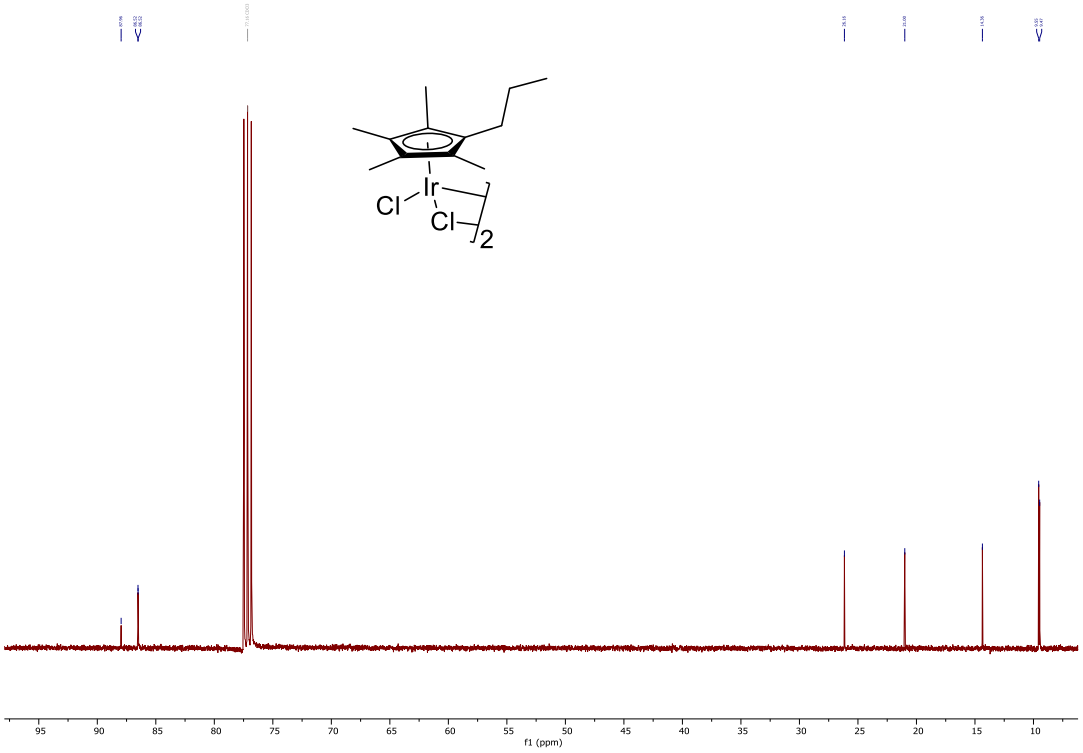

Figure S10. $^{13}C\{^1H\}$ NMR spectrum of **2b** in $CDCl_3$ at 101 MHz.

$[Cp^{*isopropyl}IrCl]_2(\mu^2\text{-}Cl)_2$ (**2c**)

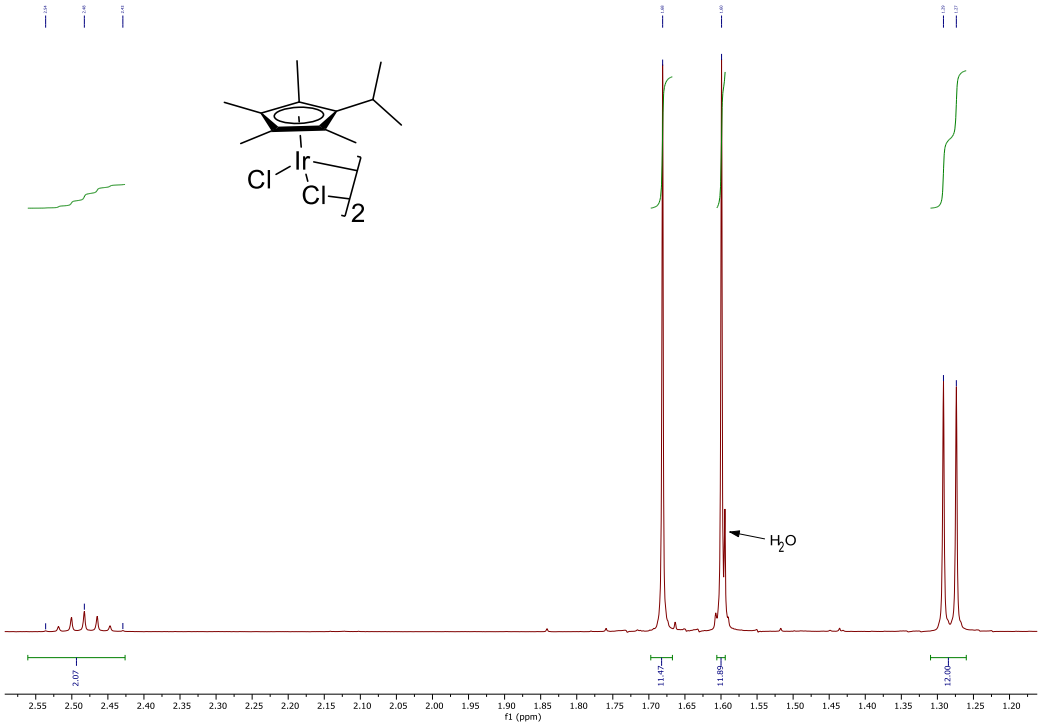

Figure S11. ^{1}H NMR spectrum of **2c** in $CDCl_3$ at 400 MHz.

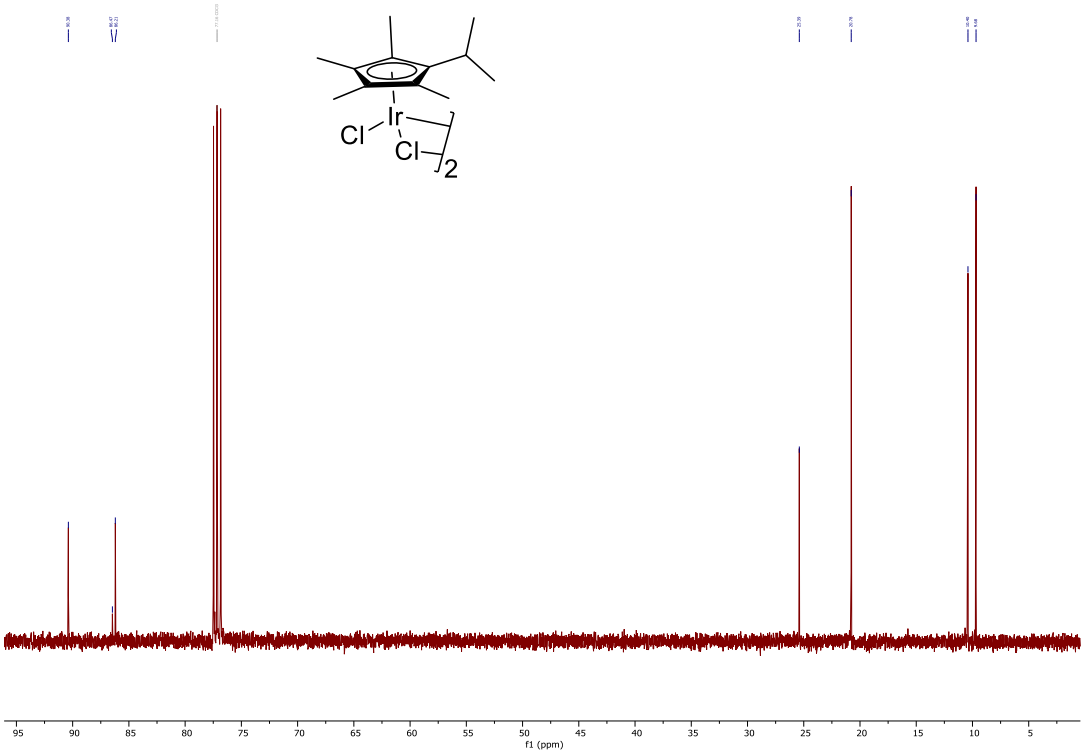

Figure S12. $^{13}C\{^{1}H\}$ NMR spectrum of **2c** in $CDCl_3$ at 101 MHz.

[Cp*$^{n\text{-butyl}}$IrCl]$_2$(μ^2-Cl)$_2$ (**2d**)

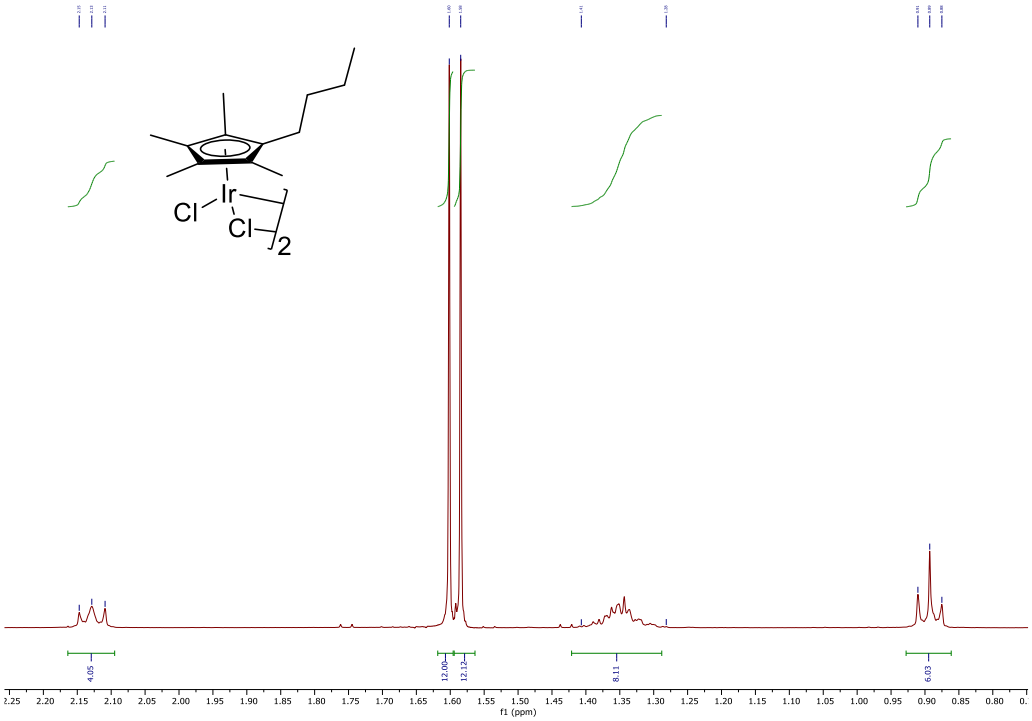

Figure S13. ^{1}H NMR spectrum of **2d** in $CDCl_3$ at 400 MHz.

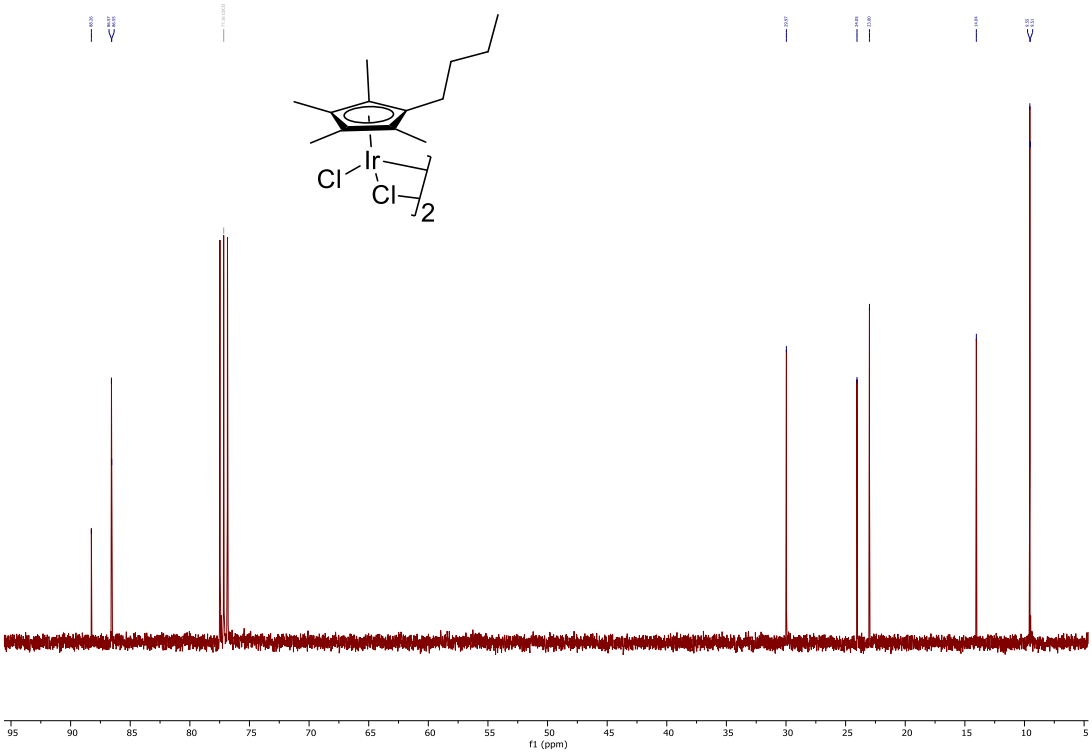

Figure S14. $^{13}C\{^1H\}$ NMR spectrum of **2d** in $CDCl_3$ at 101 MHz.

[Cp*^{isobutyl}IrCl]$_2$(μ^2-Cl)$_2$ (**2e**)

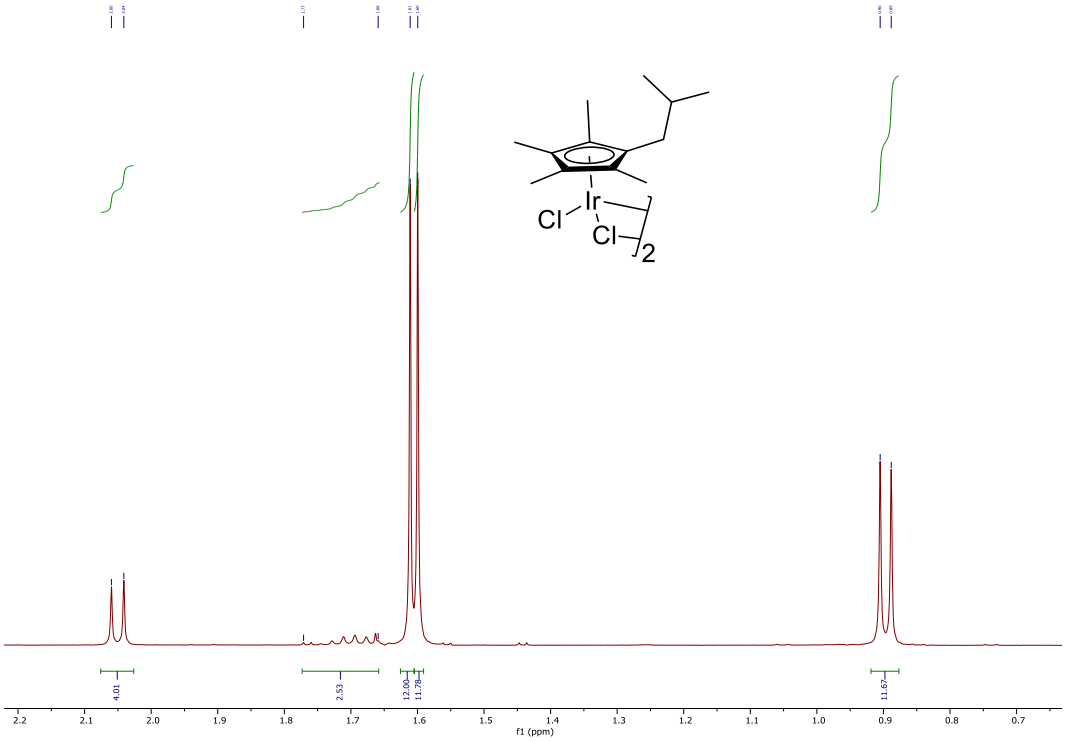

Figure S15. ^{1}H NMR spectrum of **2e** in $CDCl_3$ at 400 MHz.

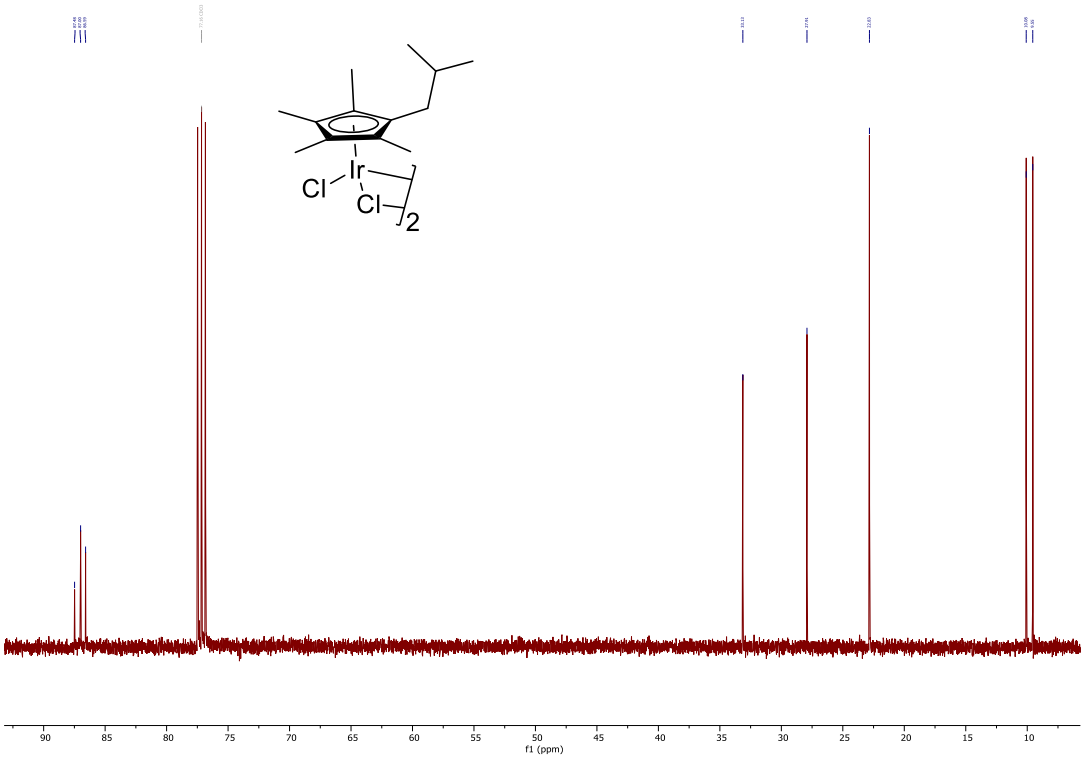

Figure S16. $^{13}C\{^1H\}$ NMR spectrum of **2e** in $CDCl_3$ at 101 MHz.

[Cp*$^{sec\text{-butyl}}$IrCl]$_2$(μ^2-Cl)$_2$ (**2f**)

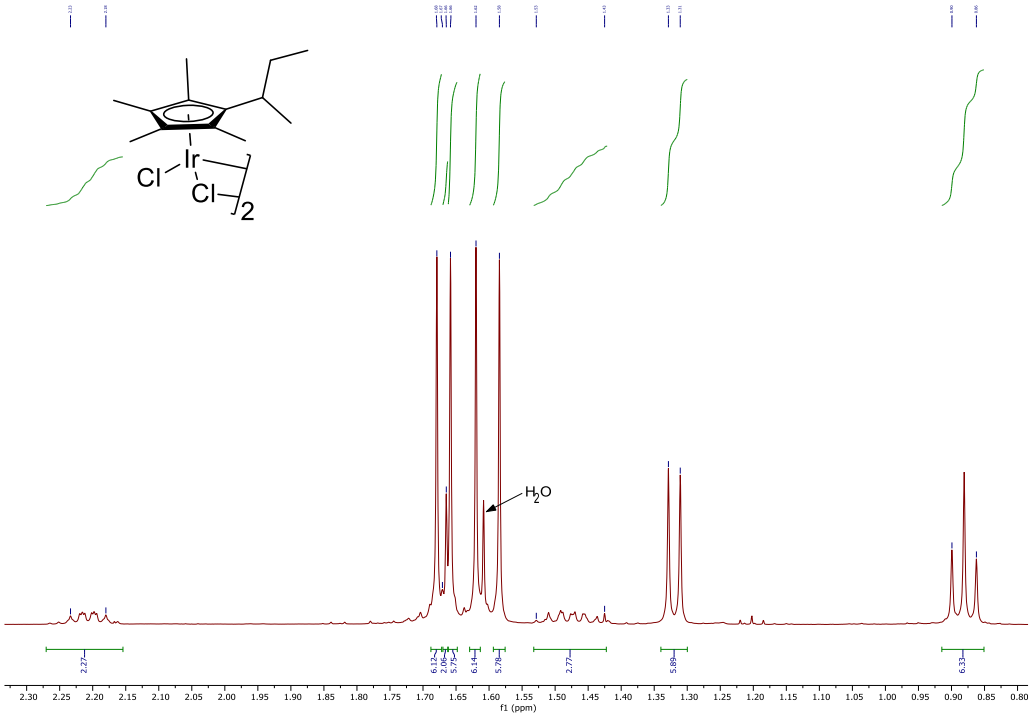

Figure S17. ^{1}H NMR spectrum of **2f** in $CDCl_3$ at 400 MHz.

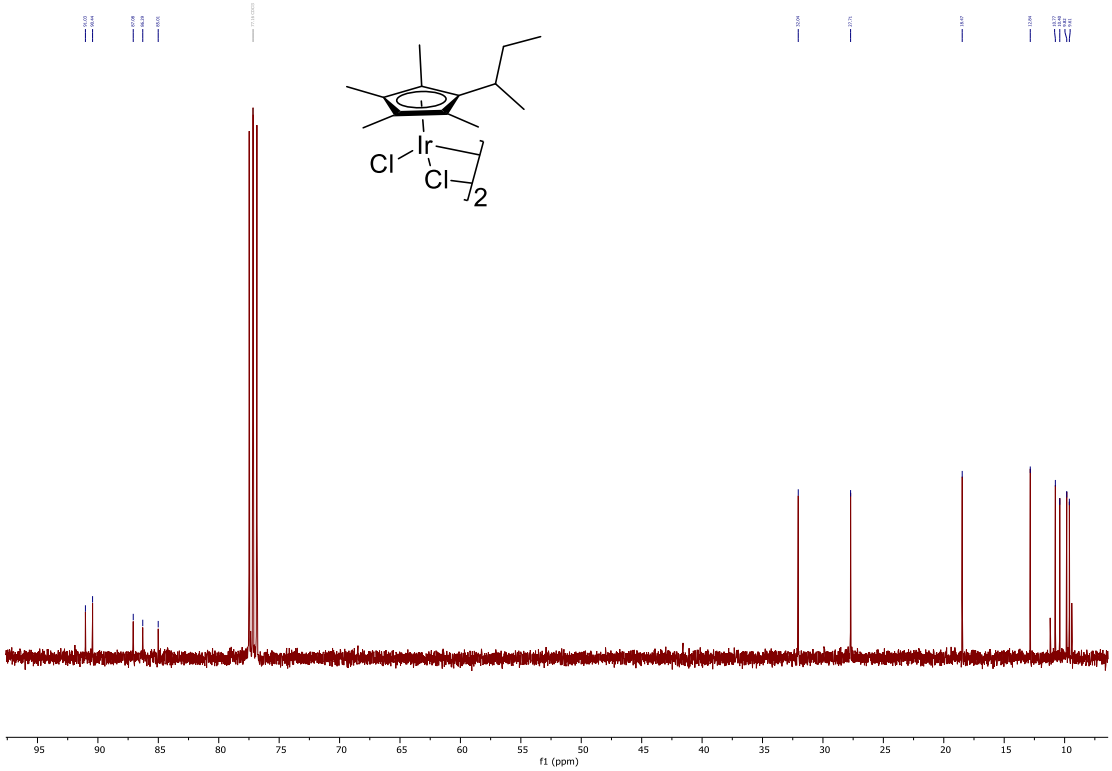

Figure S18. $^{13}C\{^1H\}$ NMR spectrum of **2f** in $CDCl_3$ at 101 MHz.

[Cp*$^{n\text{-pentyl}}$IrCl]$_2$(μ^2-Cl)$_2$ (**2g**)

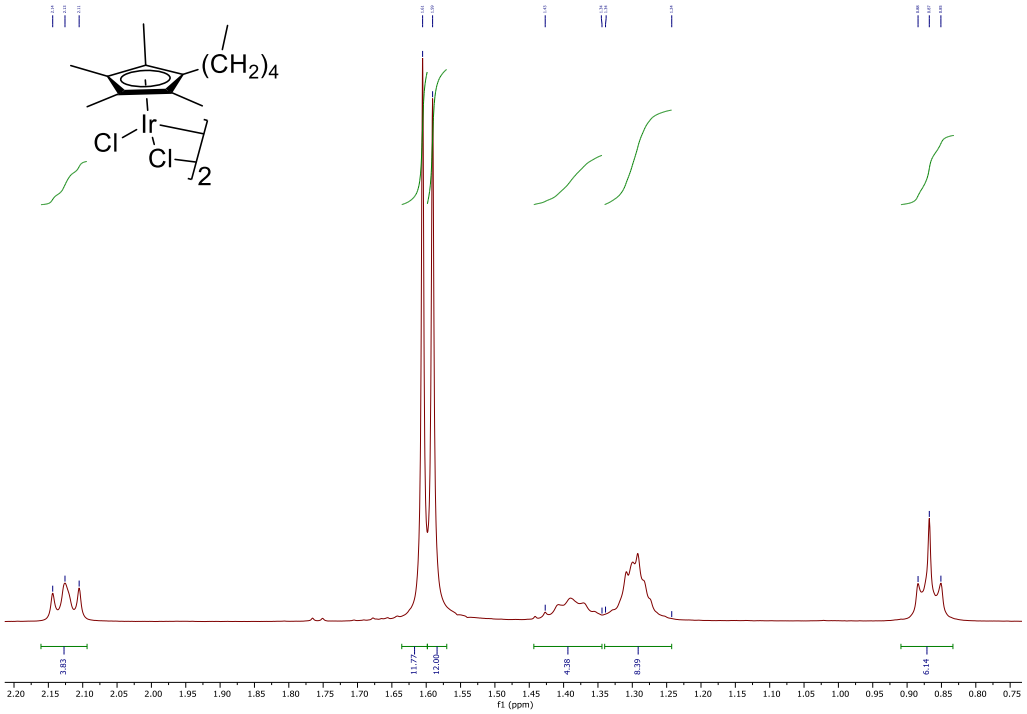

Figure S19. ^{1}H NMR spectrum of **2g** in $CDCl_3$ at 400 MHz.

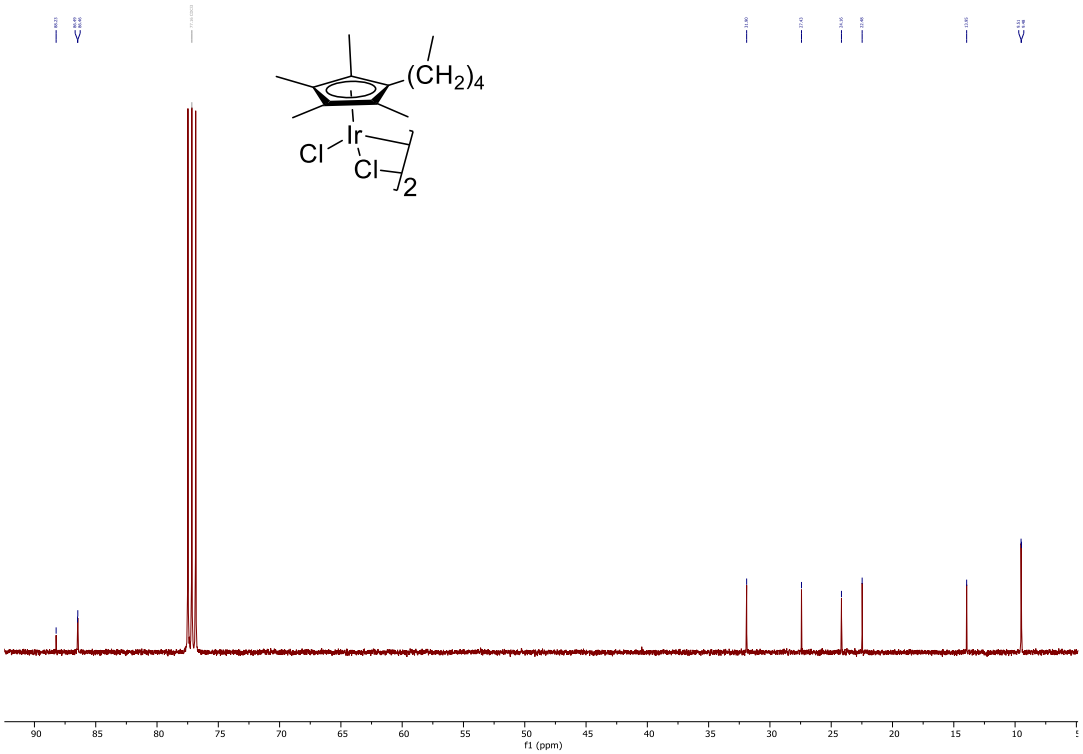

Figure S20. ^{13}C{^{1}H} NMR spectrum of **2g** in $CDCl_3$ at 101 MHz.

[Cp*$^{n\text{-hexyl}}$IrCl]$_2$(μ^2-Cl)$_2$ (**2h**)

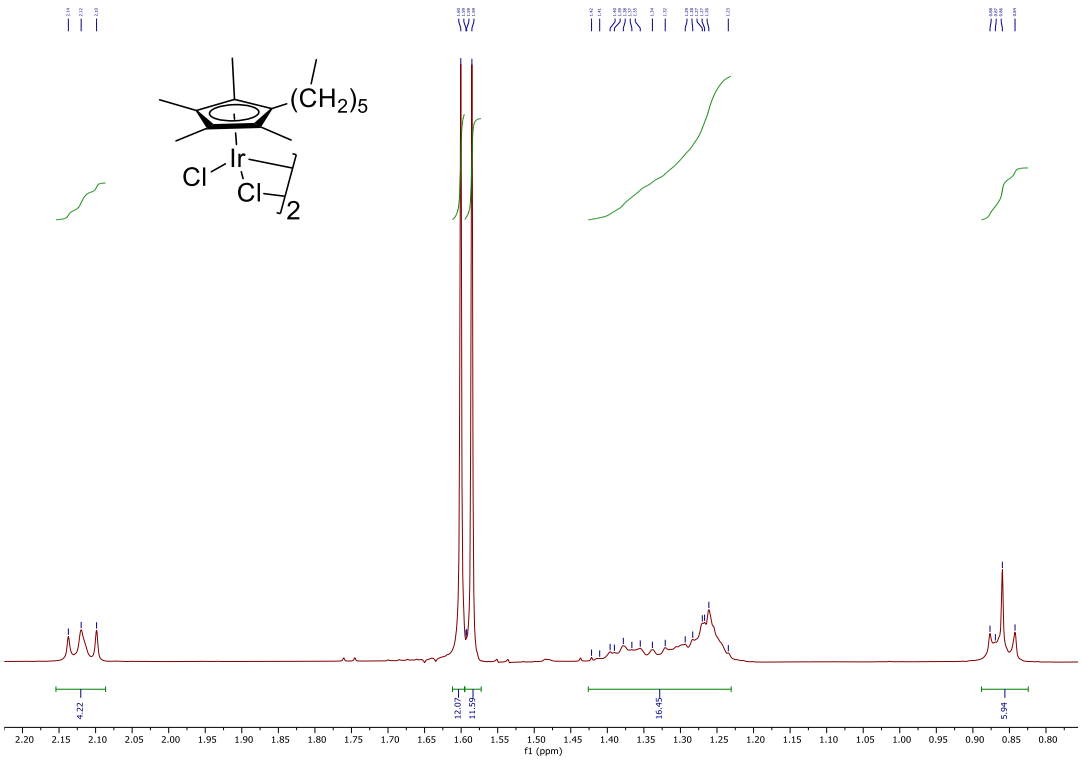

Figure S21. ^{1}H NMR spectrum of **2h** in $CDCl_3$ at 400 MHz.

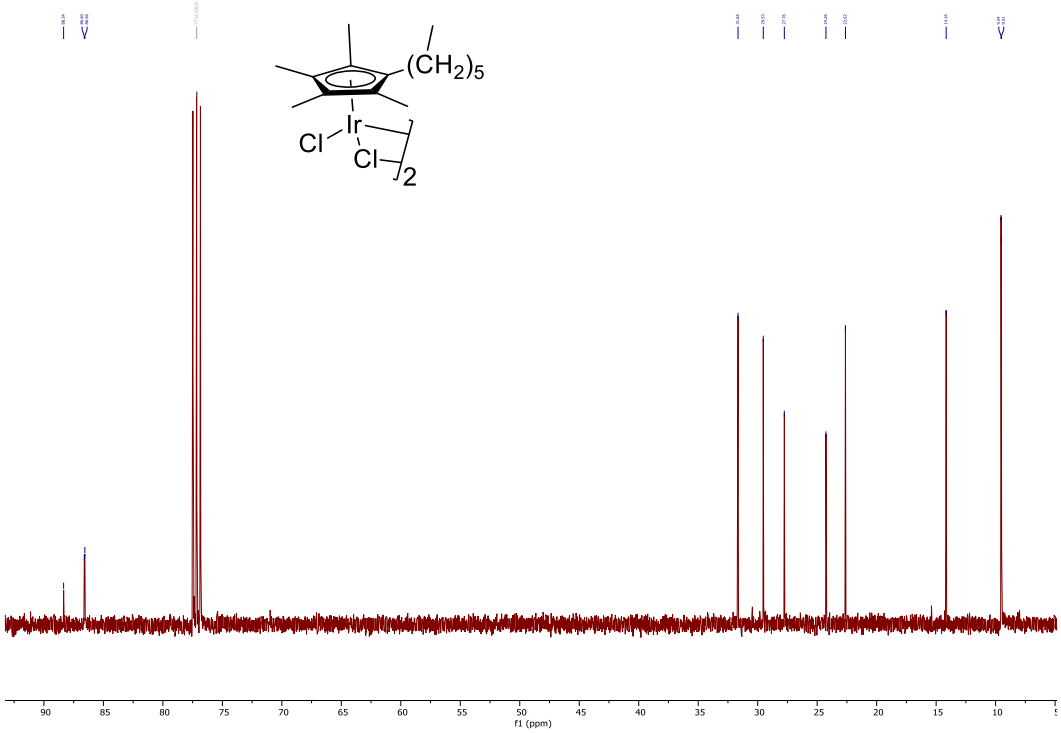

Figure S22. $^{13}C\{^1H\}$ NMR spectrum of **2h** in $CDCl_3$ at 101 MHz.

[Cp*$^{n\text{-heptyl}}$IrCl]$_2$(μ^2-Cl)$_2$ (**2i**)

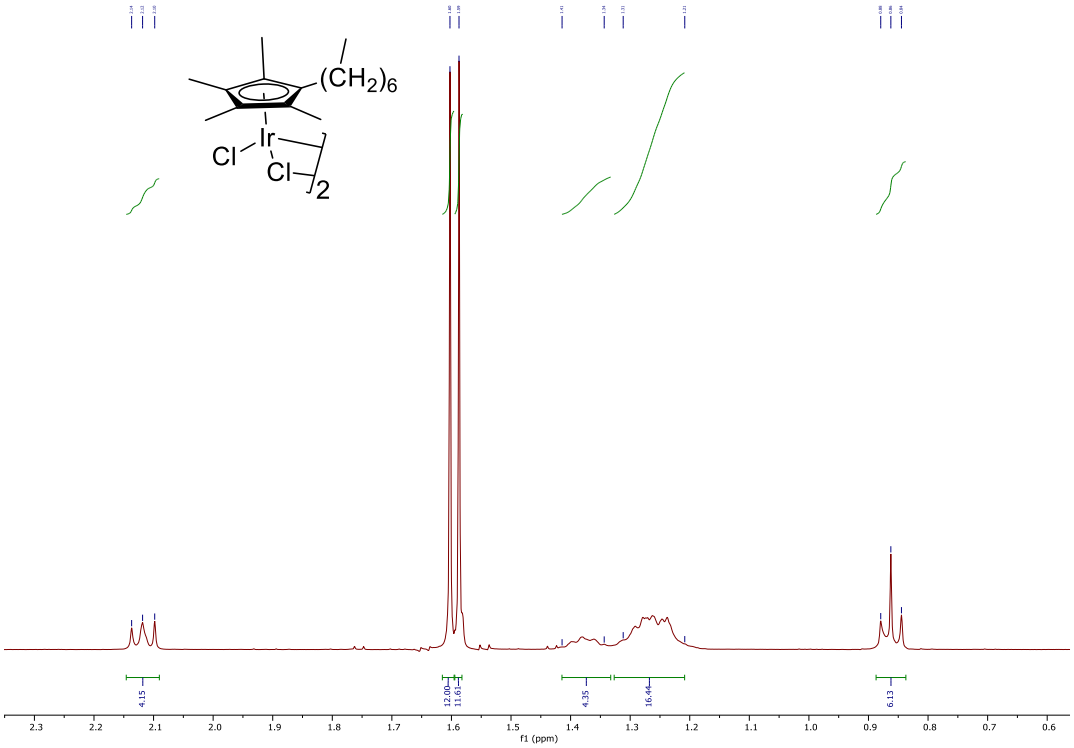

Figure S23. ^{1}H NMR spectrum of **2i** in $CDCl_3$ at 400 MHz.

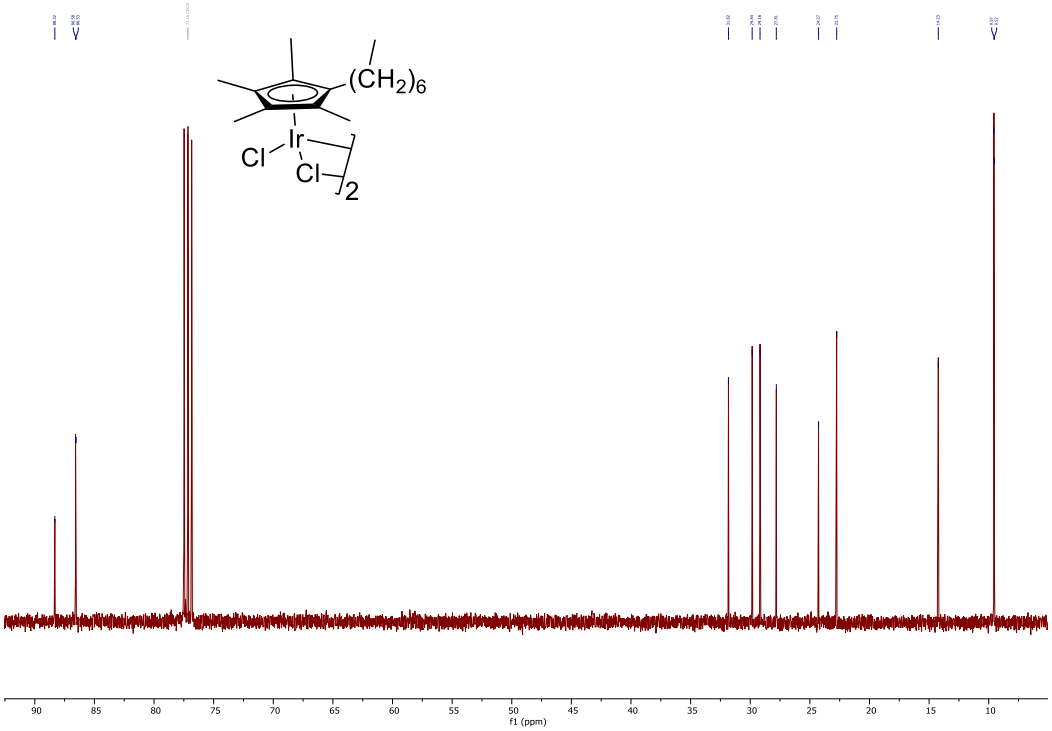

Figure S24. $^{13}C\{^1H\}$ NMR spectrum of **2i** in $CDCl_3$ at 101 MHz.

[Cp*$^{n\text{-octyl}}$IrCl]$_2$(μ^2-Cl)$_2$ (**2j**)

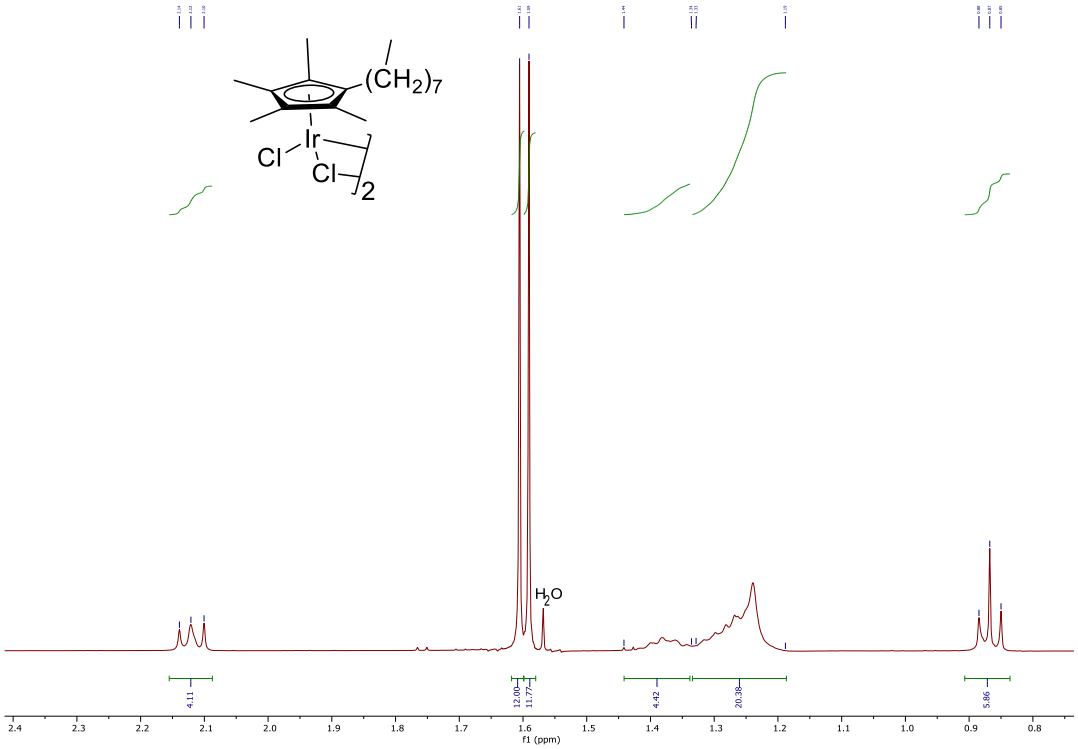

Figure S25. ^{1}H NMR spectrum of **2j** in $CDCl_3$ at 400 MHz.

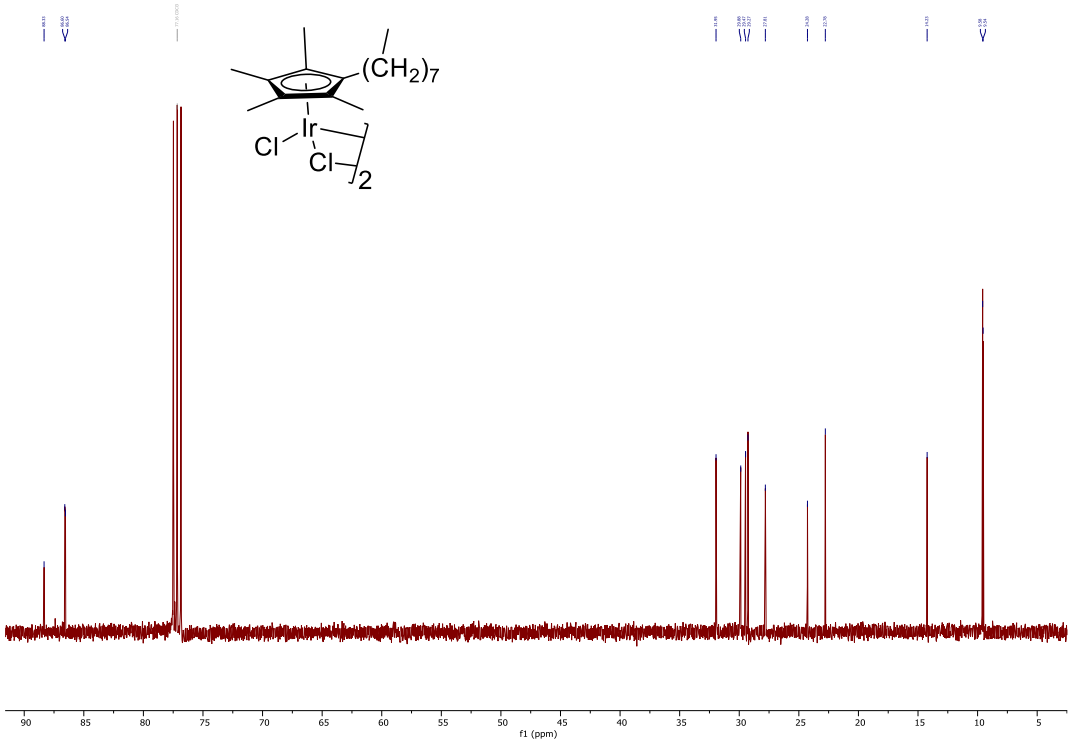

Figure S26. $^{13}C\{^1H\}$ NMR spectrum of **2j** in $CDCl_3$ at 101 MHz.

$[Cp^{*phenyl}IrCl]_2(\mu^2\text{-}Cl)_2$ (**2k**)

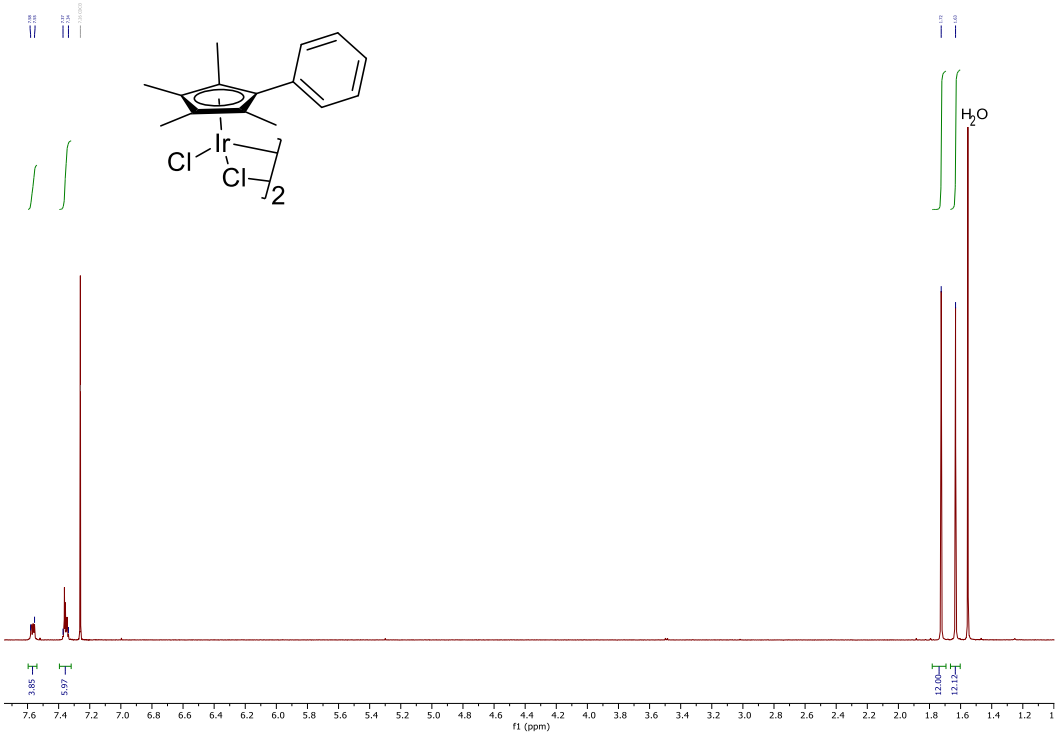

Figure S27. ^{1}H NMR spectrum of **2k** in $CDCl_3$ at 400 MHz.

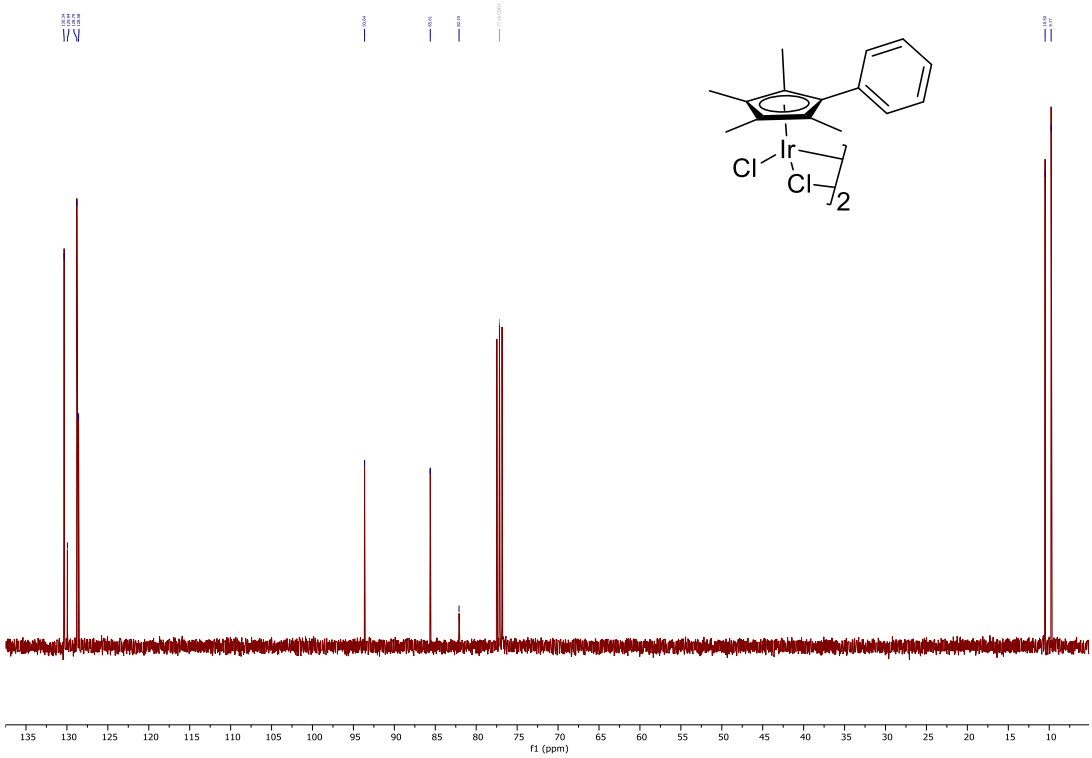

Figure S28. $^{13}C\{^{1}H\}$ NMR spectrum of **2k** in $CDCl_3$ at 101 MHz.

$[Cp^{*benzyl}IrCl]_2(\mu^2\text{-}Cl)_2$ (**2l**)

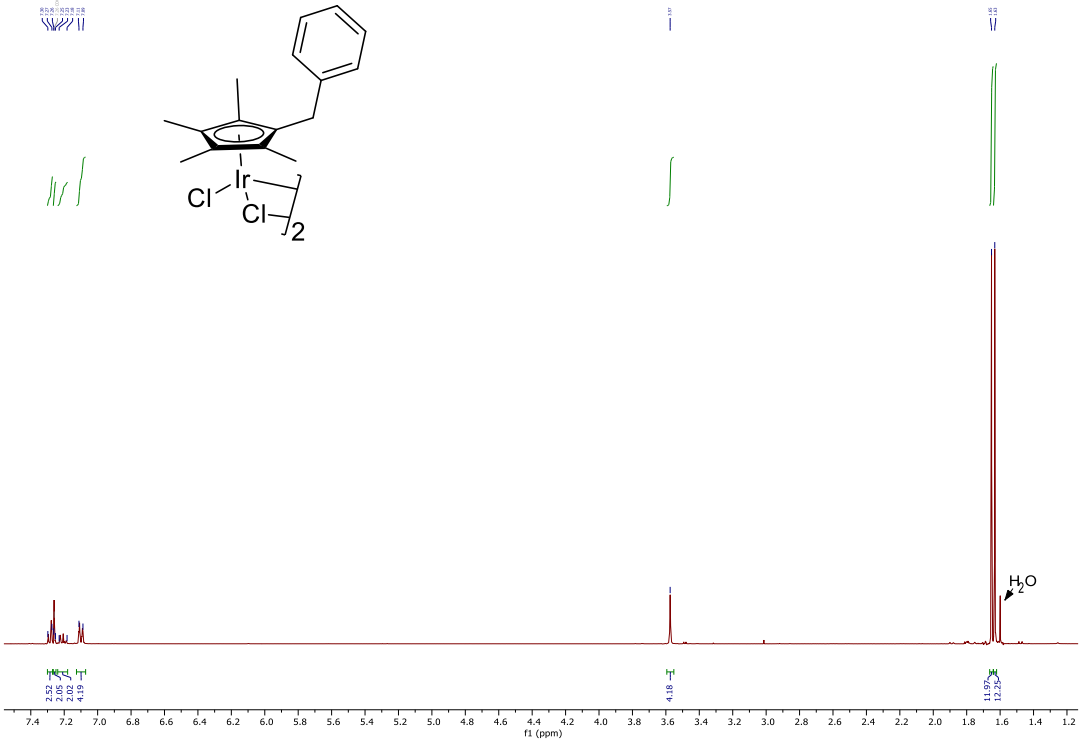

Figure S29. ^{1}H NMR spectrum of **2l** in $CDCl_3$ at 400 MHz.

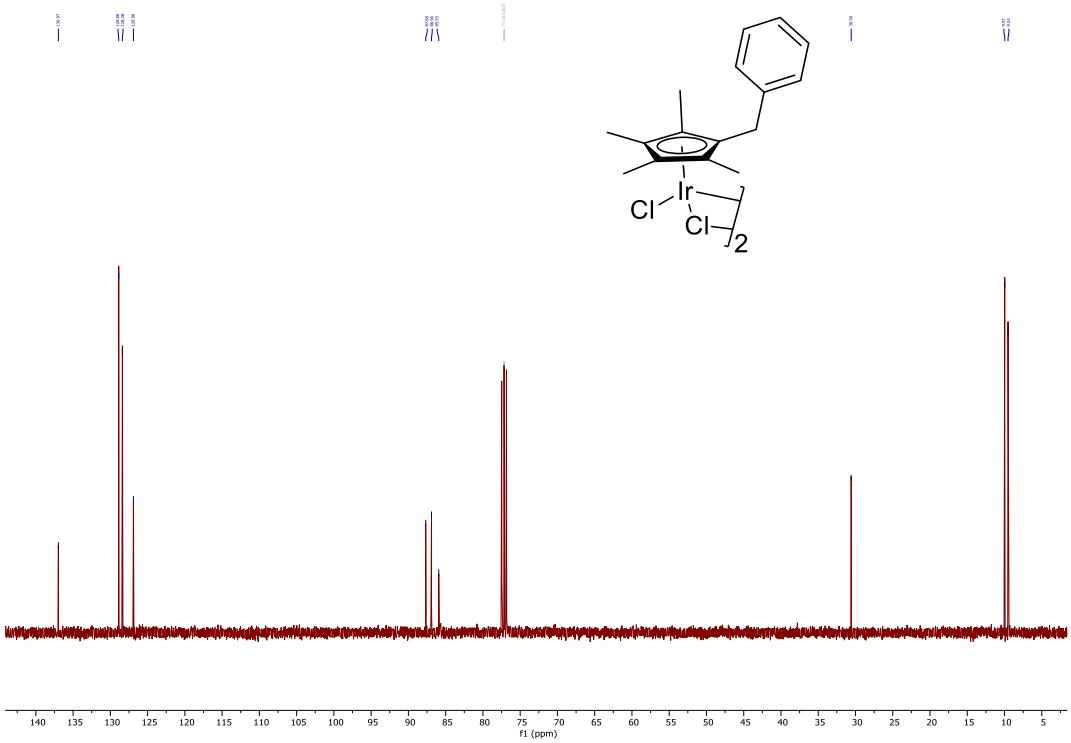

Figure S30. $^{13}C\{^{1}H\}$ NMR spectrum of **2l** in $CDCl_3$ at 101 MHz.

[Cp*^{phenethyl}IrCl]$_2$(μ^2-Cl)$_2$ (**2m**)

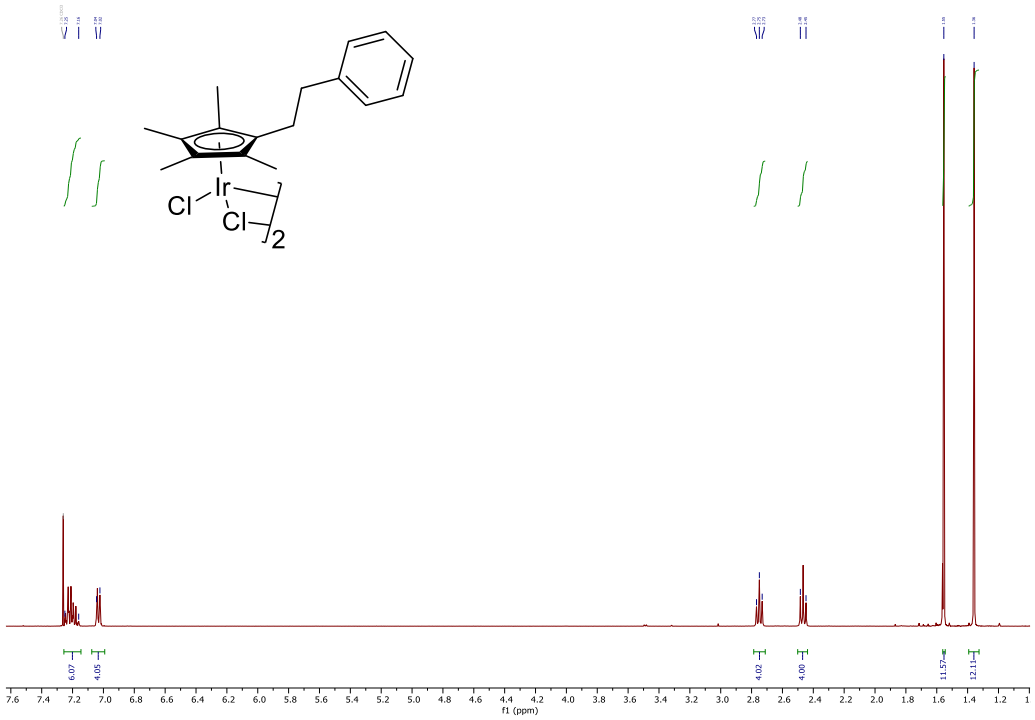

Figure S31. ^{1}H NMR spectrum of **2m** in $CDCl_3$ at 400 MHz.

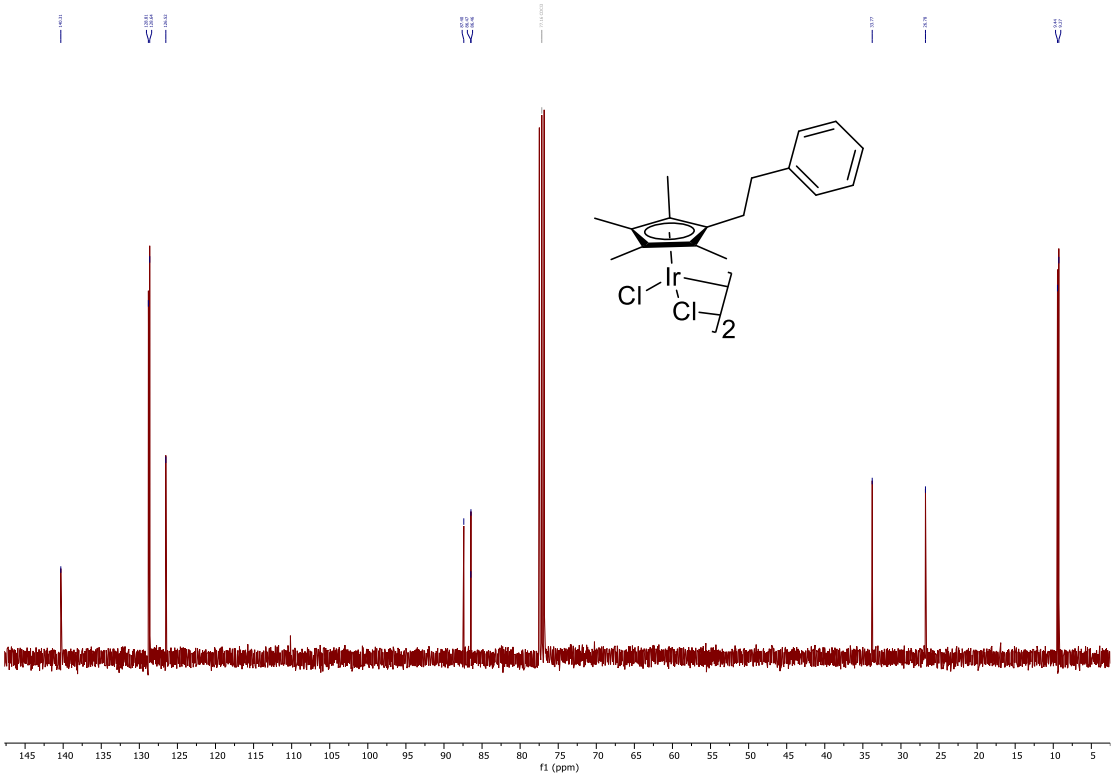

Figure S32. $^{13}C\{^1H\}$ NMR spectrum of **2m** in $CDCl_3$ at 101 MHz.

$[Cp*^{cyclohexyl}IrCl]_2(\mu^2\text{-}Cl)_2$ (**2n**)

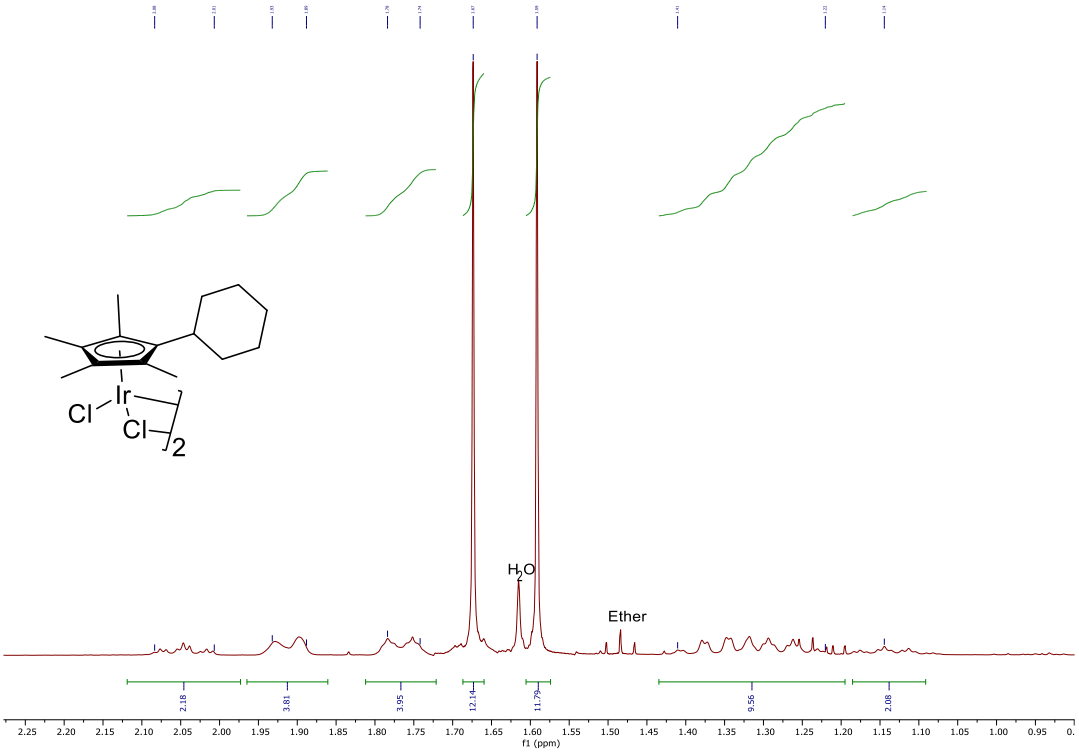

Figure S33. ^{1}H NMR spectrum of **2n** in $CDCl_3$ at 400 MHz.

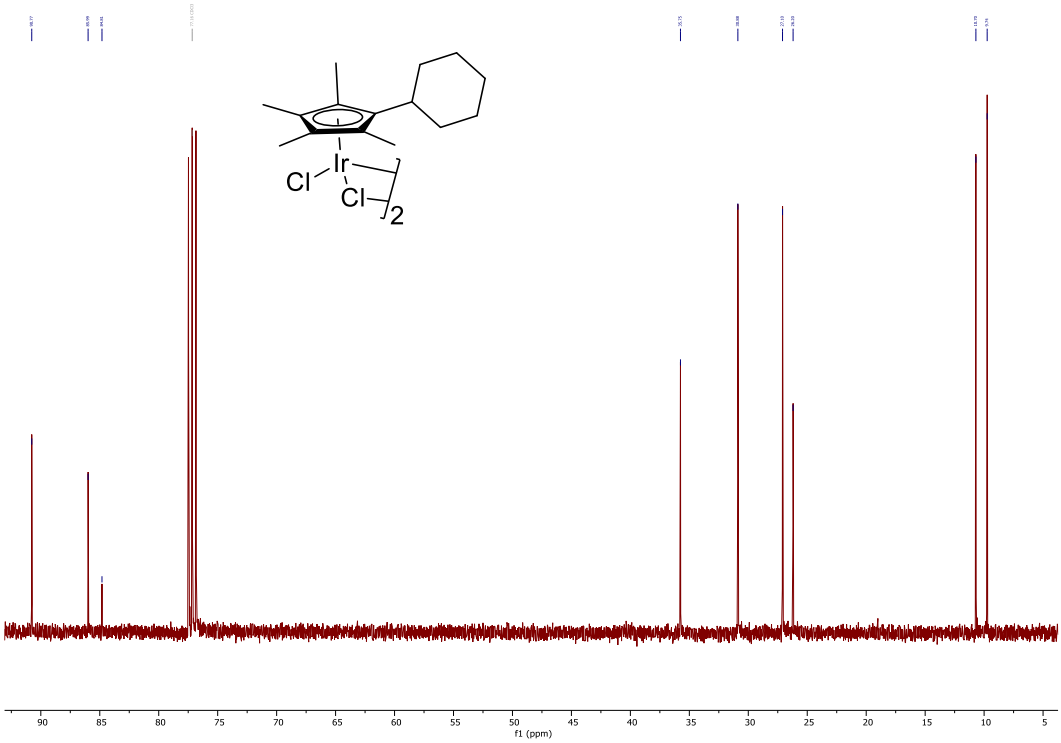

Figure S34. $^{13}C\{^{1}H\}$ NMR spectrum of **2n** in $CDCl_3$ at 101 MHz.

$[Cp^{*cyclopentyl}IrCl]_2(\mu^2\text{-}Cl)_2$ (**2o**)

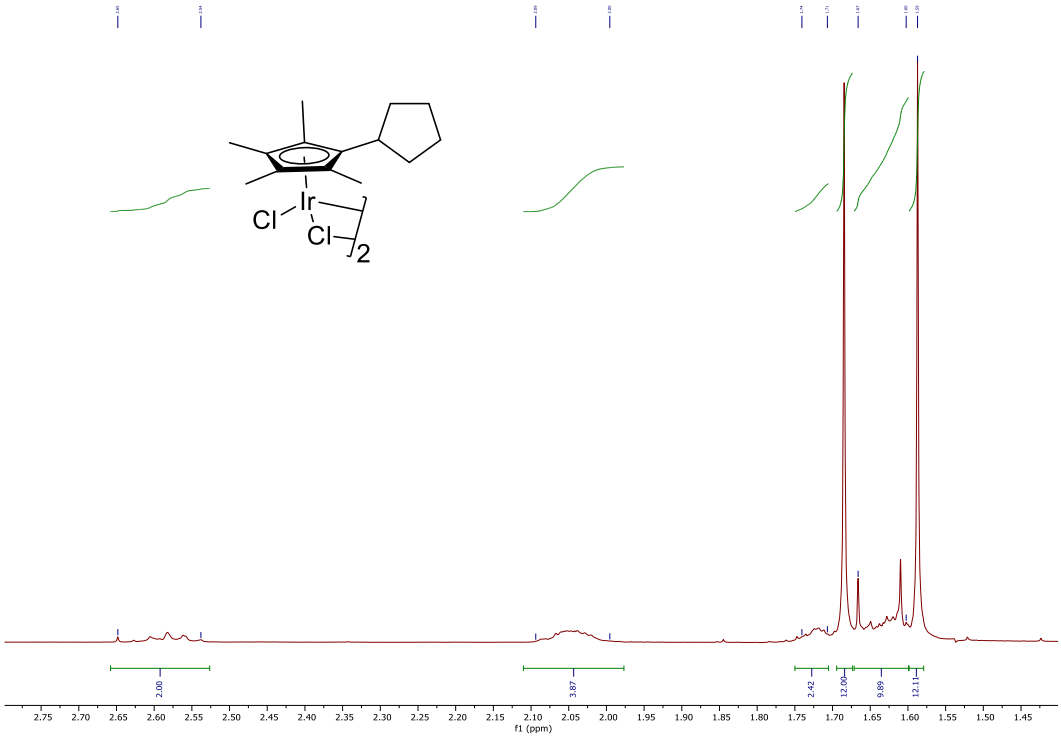

Figure S35. ^{1}H NMR spectrum of **2o** in $CDCl_3$ at 400 MHz.

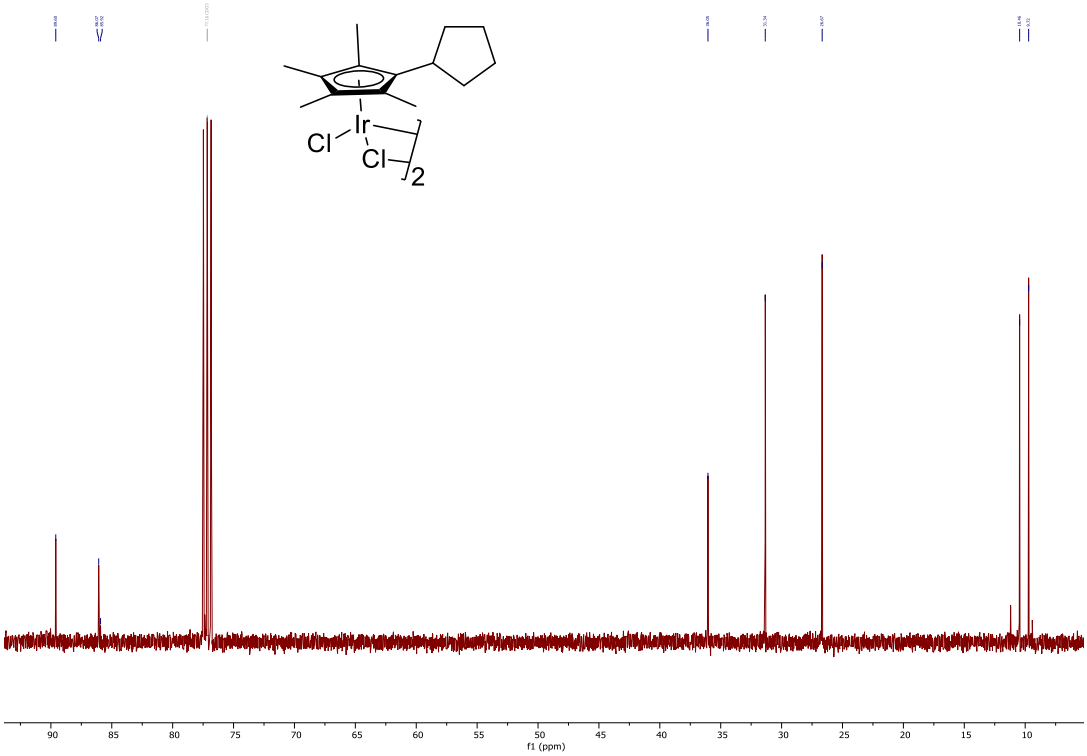

Figure S36. $^{13}C\{^{1}H\}$ NMR spectrum of **2n** in $CDCl_3$ at 101 MHz.

$[Cp^{*ethyl}RhCl]_2(\mu^2\text{-}Cl)_2$ (**3a**)

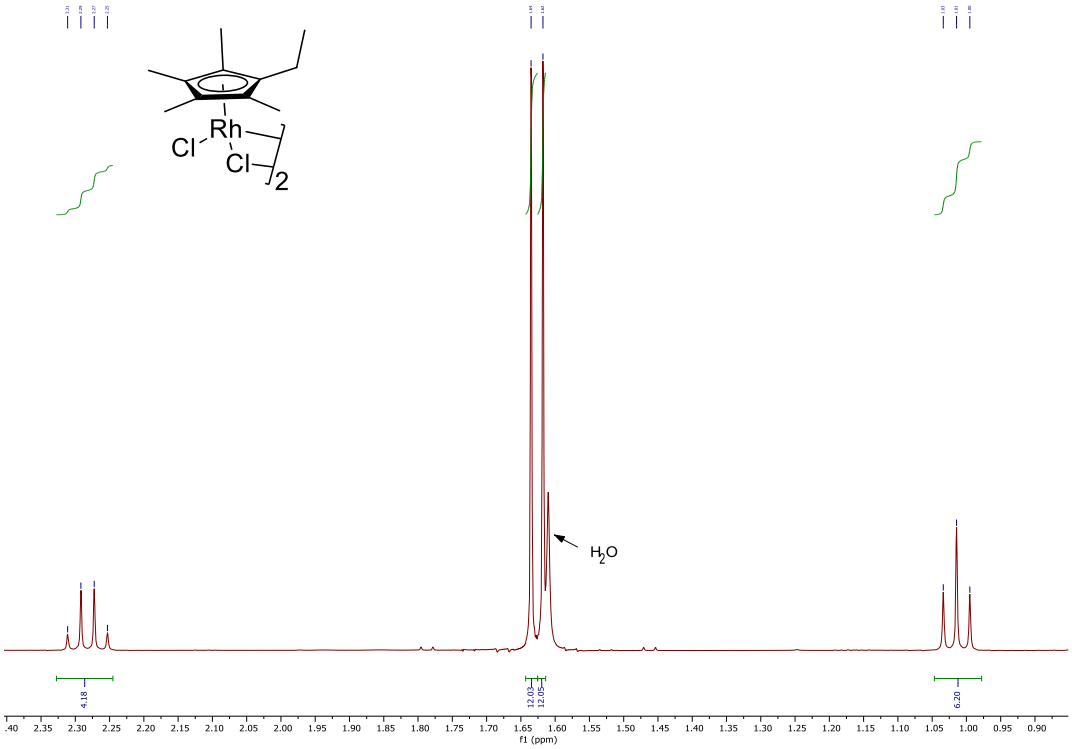

Figure S37. ^{1}H NMR spectrum of **3a** in $CDCl_3$ at 400 MHz.

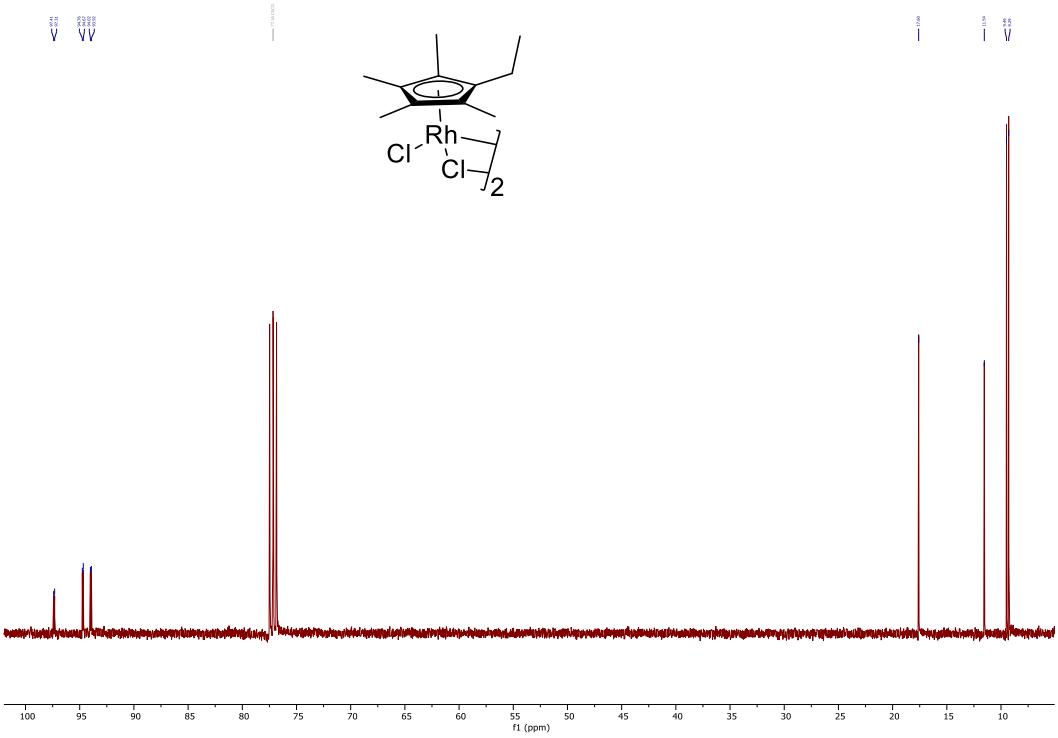

Figure S38. $^{13}C\{^{1}H\}$ NMR spectrum of **3a** in $CDCl_3$ at 101 MHz.

[Cp*$^{n\text{-propyl}}$RhCl]$_2$(μ^2-Cl)$_2$ (**3b**)

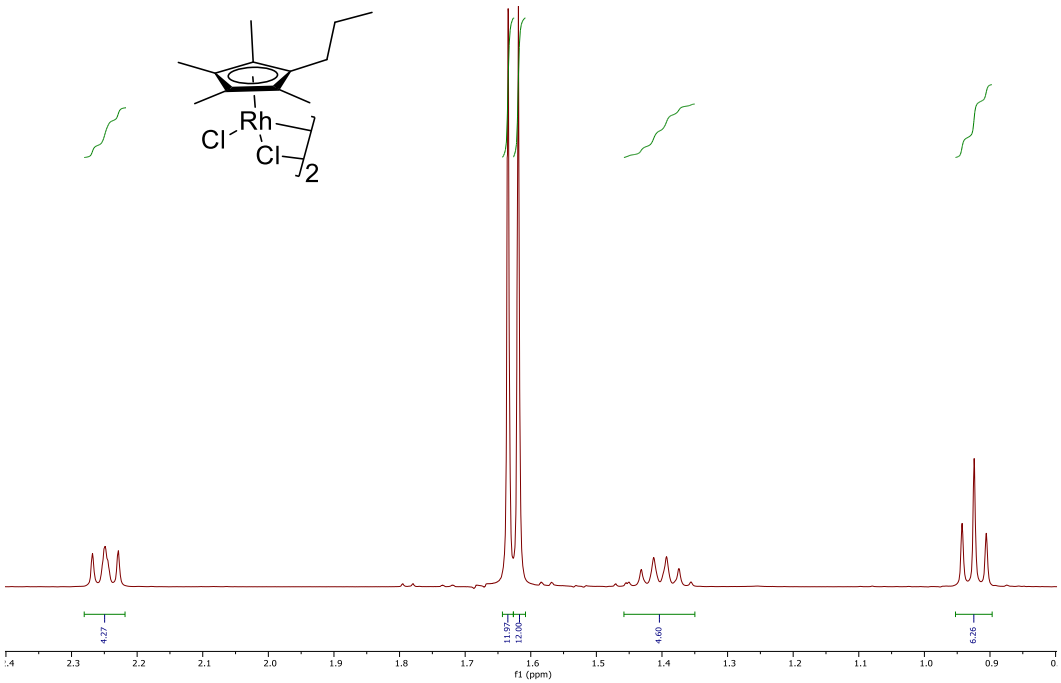

Figure S39. ^{1}H NMR spectrum of **3b** in $CDCl_3$ at 400 MHz.

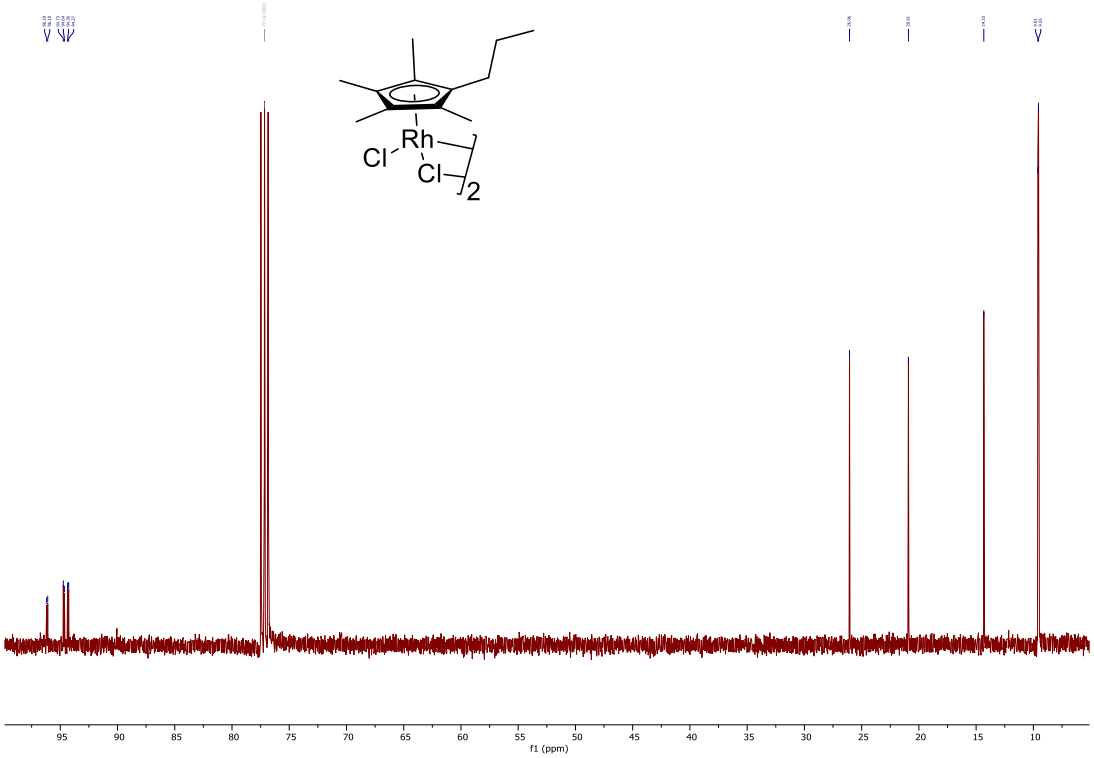

Figure S40. $^{13}C\{^1H\}$ NMR spectrum of **3b** in $CDCl_3$ at 101 MHz.

[Cp*^{isopropyl}RhCl]$_2$(μ^2-Cl)$_2$ (**3c**)

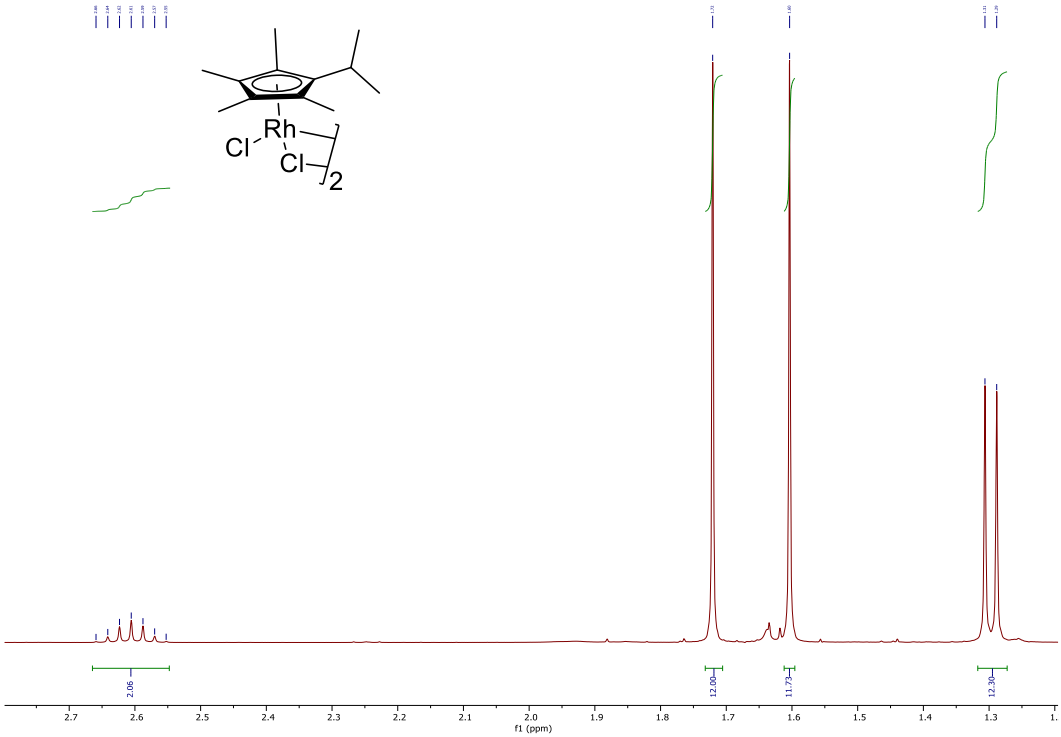

Figure S41. ^{1}H NMR spectrum of **3c** in $CDCl_3$ at 400 MHz.

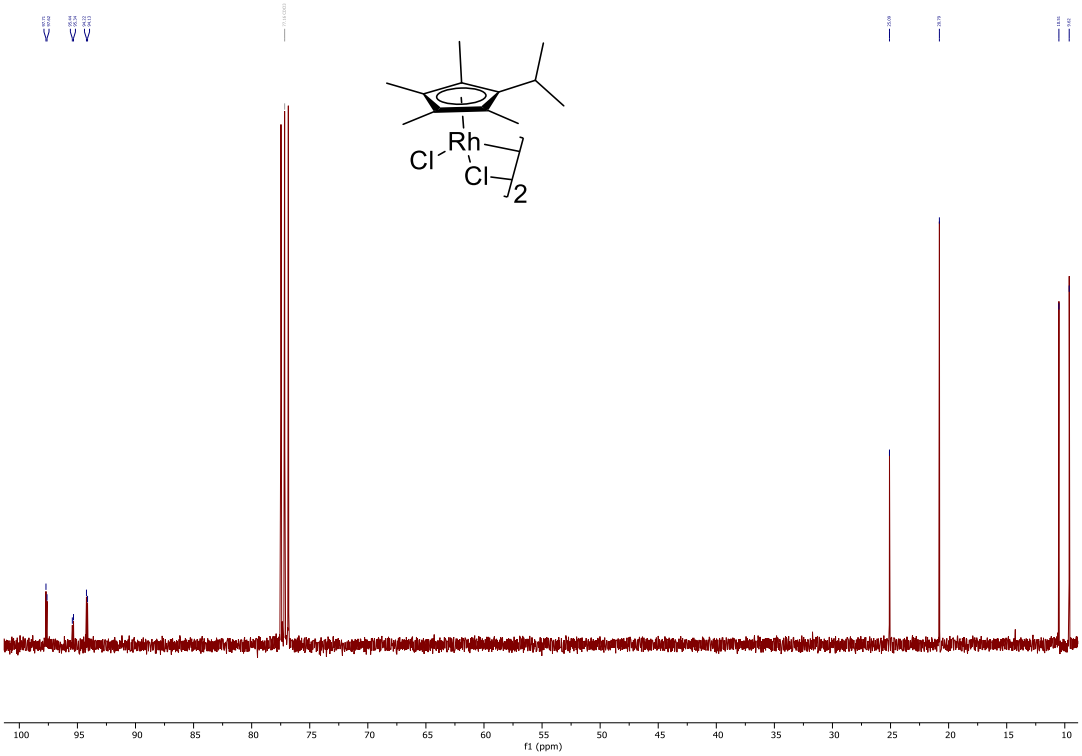

Figure S42. $^{13}C\{^1H\}$ NMR spectrum of **3c** in $CDCl_3$ at 101 MHz.

[Cp*$^{n\text{-butyl}}$RhCl]$_2$(μ^2-Cl)$_2$ (**3d**)

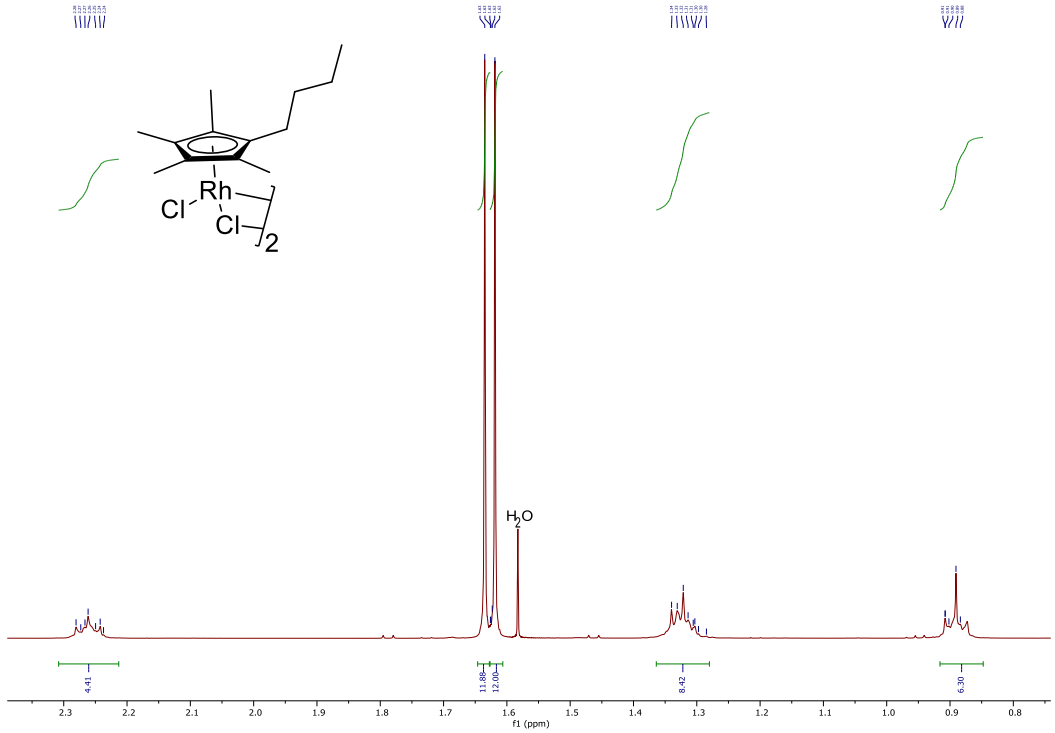

Figure S43. ^{1}H NMR spectrum of **3d** in $CDCl_3$ at 400 MHz.

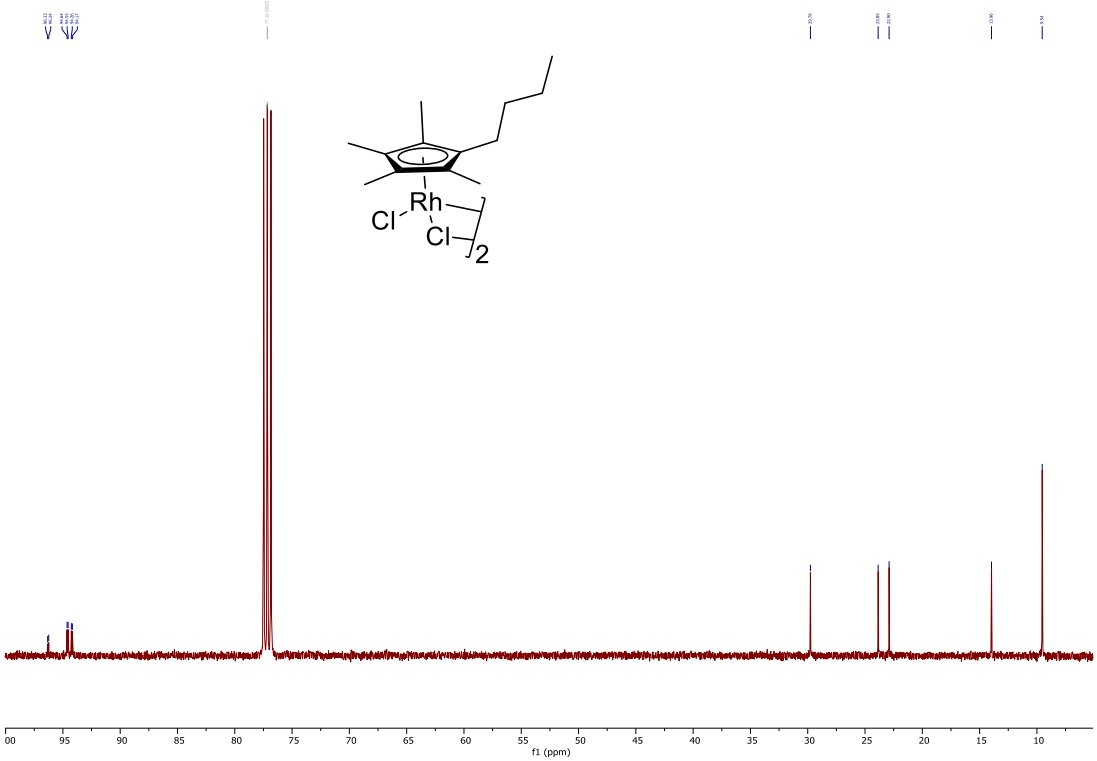

Figure S44. ^{13}C{^{1}H} NMR spectrum of **3d** in $CDCl_3$ at 101 MHz.

[Cp*^{isobutyl}RhCl]$_2$(μ^2-Cl)$_2$ (**3e**)

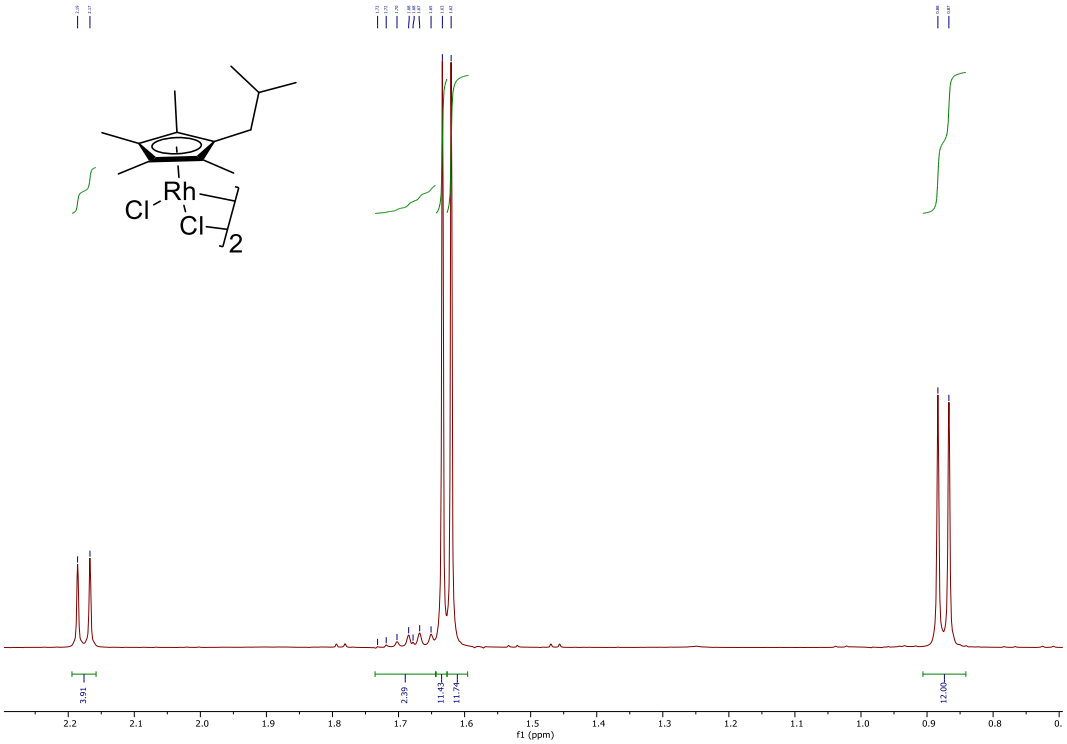

Figure S45. ^{1}H NMR spectrum of **3e** in $CDCl_3$ at 400 MHz.

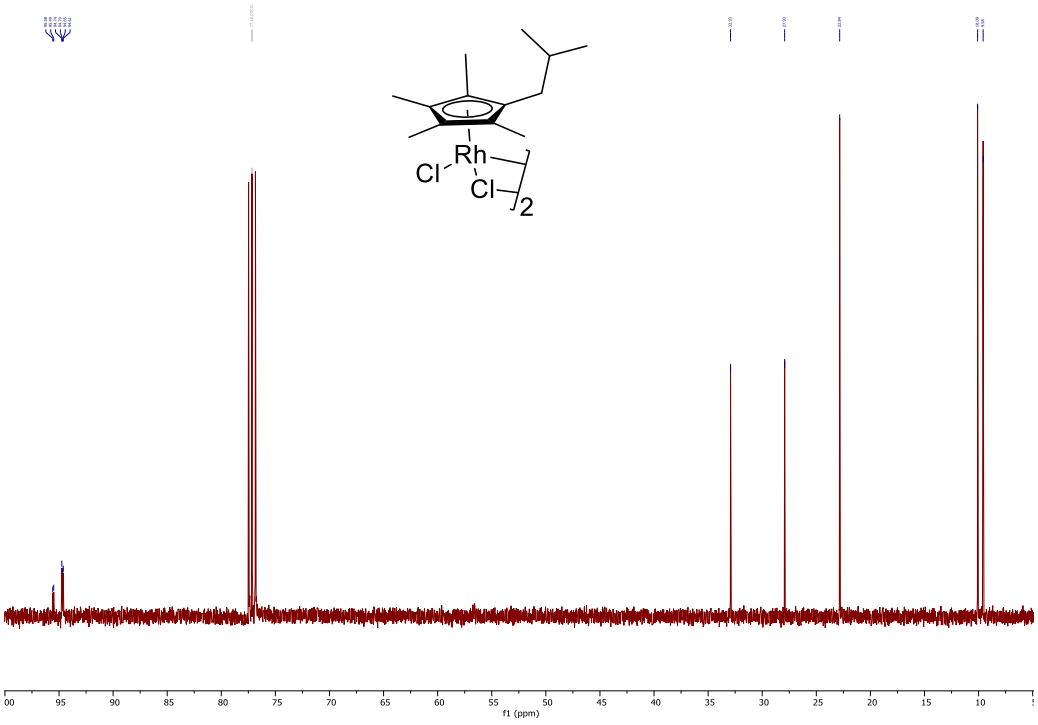

Figure S46. $^{13}C\{^1H\}$ NMR spectrum of **3e** in $CDCl_3$ at 101 MHz.

[Cp*$^{sec\text{-butyl}}$RhCl]$_2$(μ^2-Cl)$_2$ (**3f**)

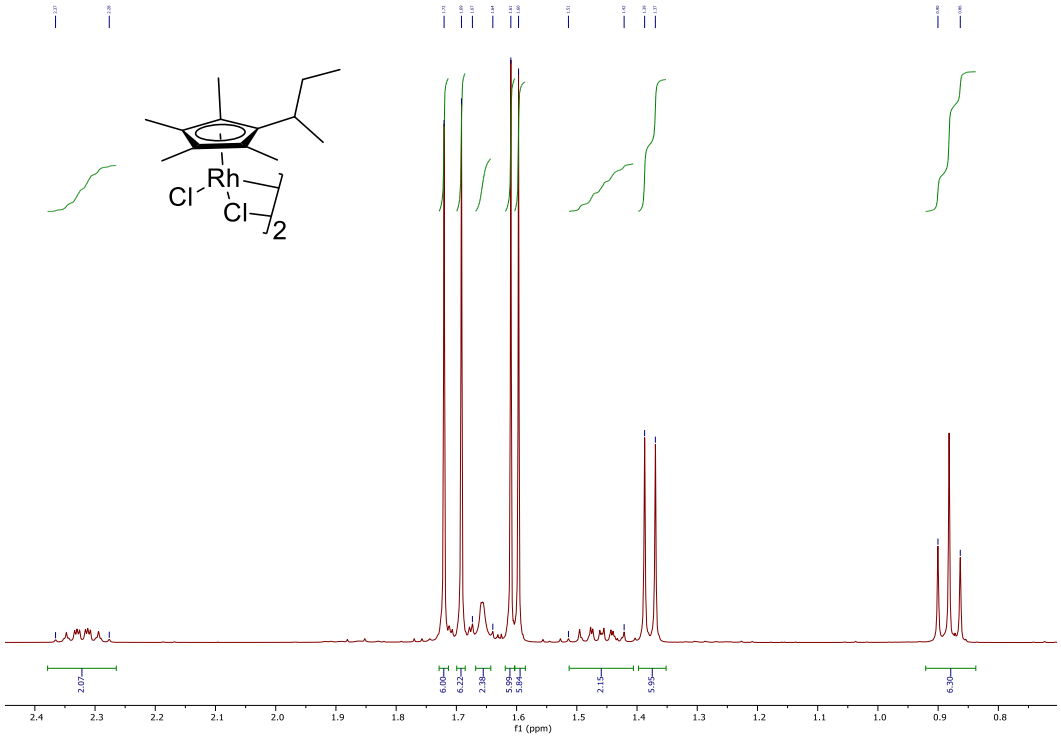

Figure S47. ^{1}H NMR spectrum of **3f** in $CDCl_3$ at 400 MHz.

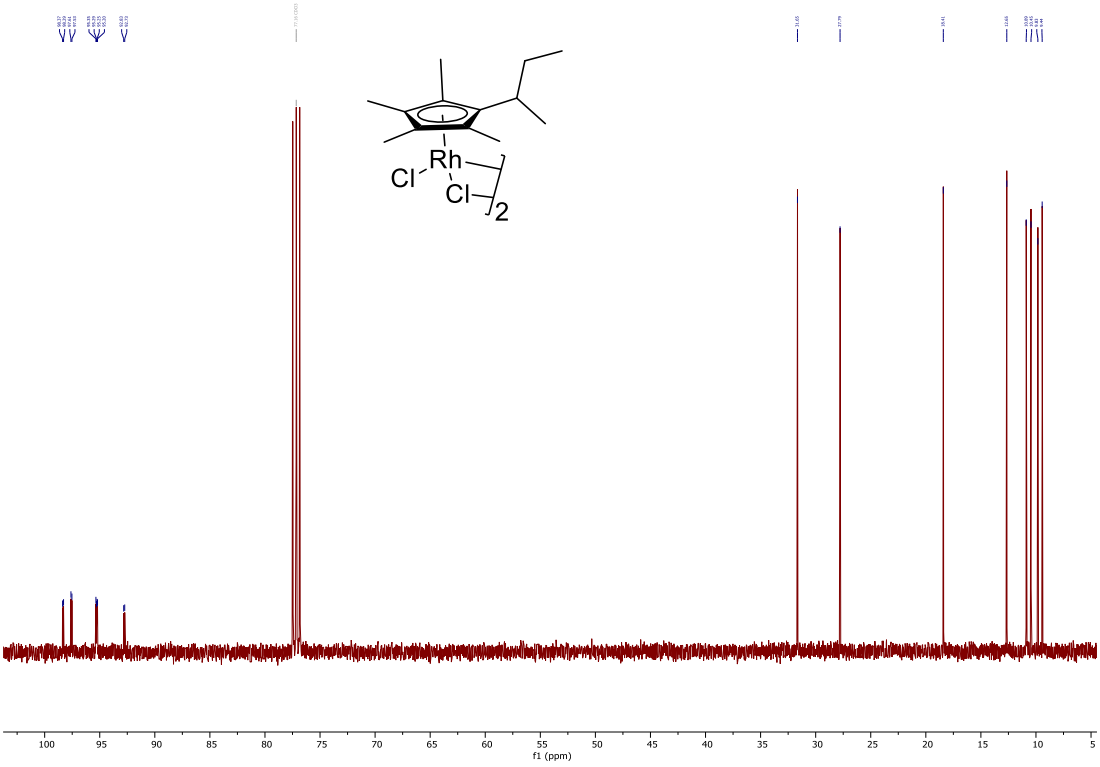

Figure S48. $^{13}C\{^1H\}$ NMR spectrum of **3f** in $CDCl_3$ at 101 MHz.

[Cp*$^{n\text{-pentyl}}$RhCl]$_2$(μ^2-Cl)$_2$ (**3g**)

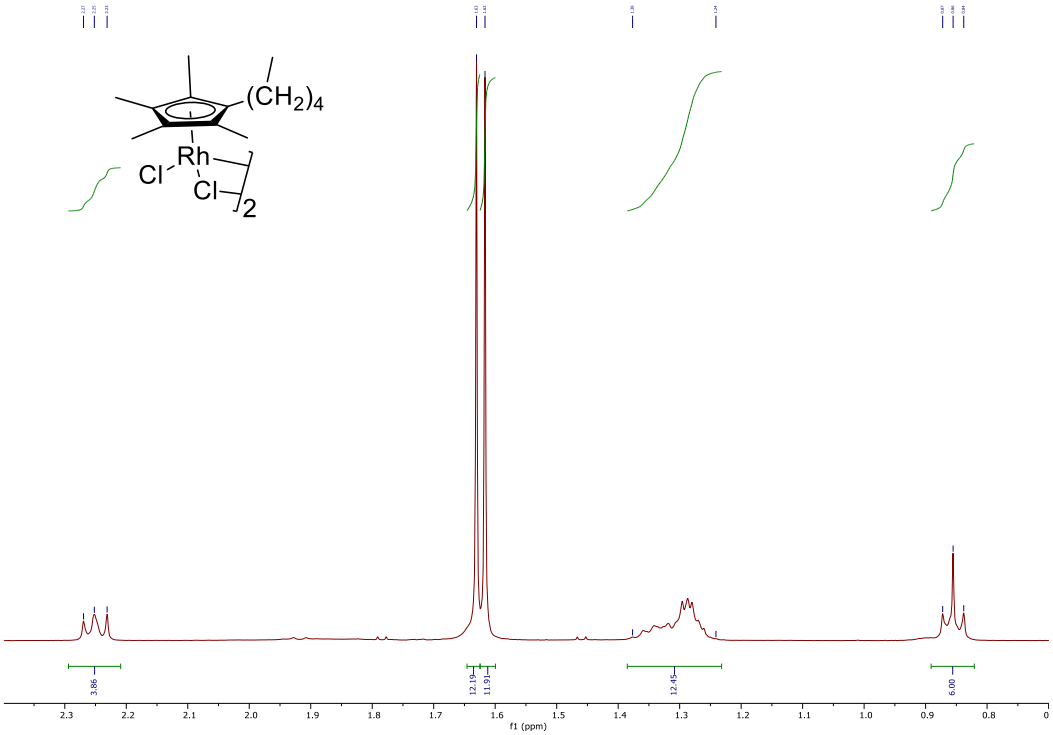

Figure S49. ^{1}H NMR spectrum of **3g** in $CDCl_3$ at 400 MHz.

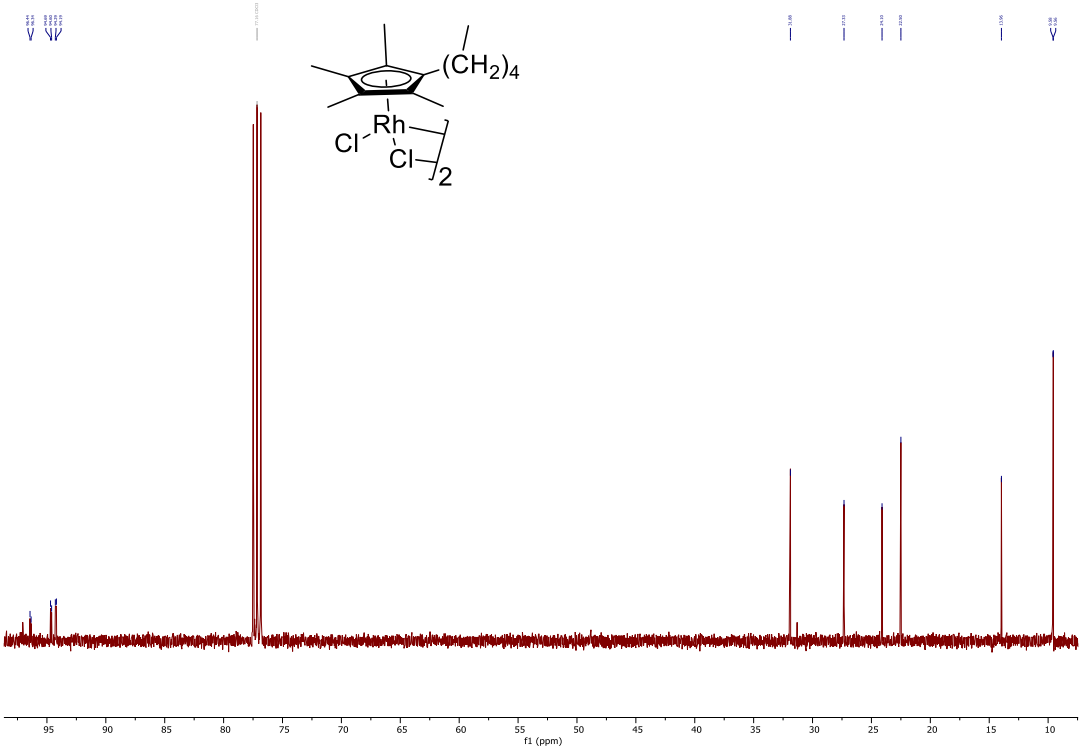

Figure S50. ^{13}C{^{1}H} NMR spectrum of **3g** in $CDCl_3$ at 101 MHz.

[Cp*$^{n\text{-hexyl}}$RhCl]$_2$(μ^2-Cl)$_2$ (**3h**)

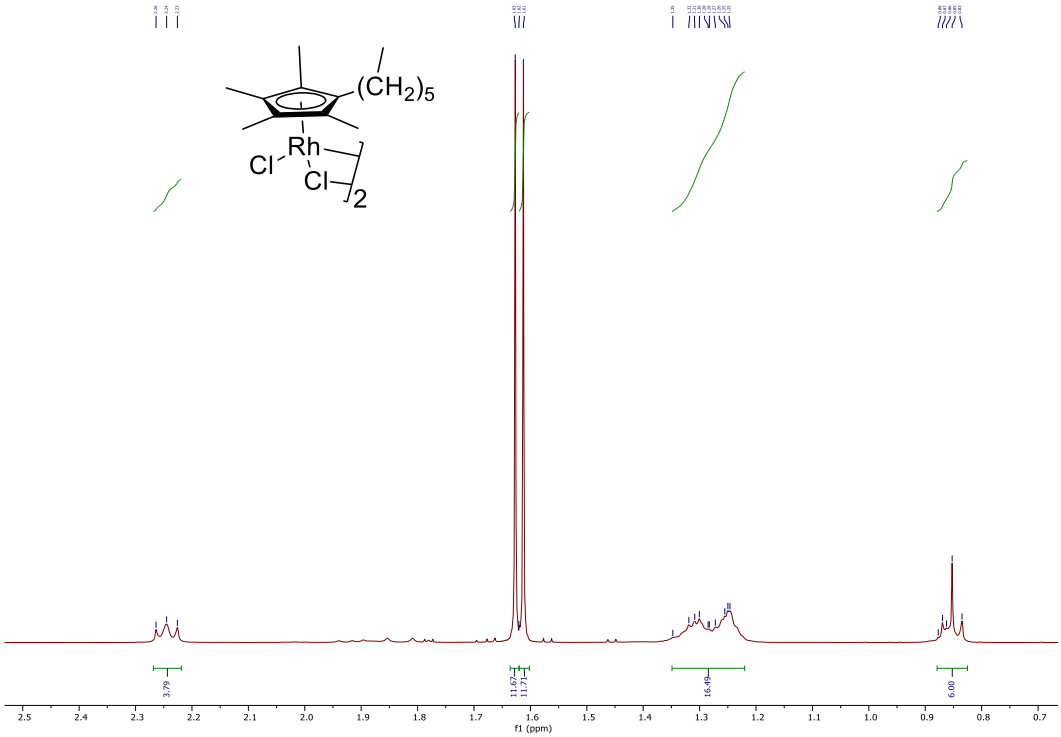

Figure S51. ^{1}H NMR spectrum of **3h** in $CDCl_3$ at 400 MHz.

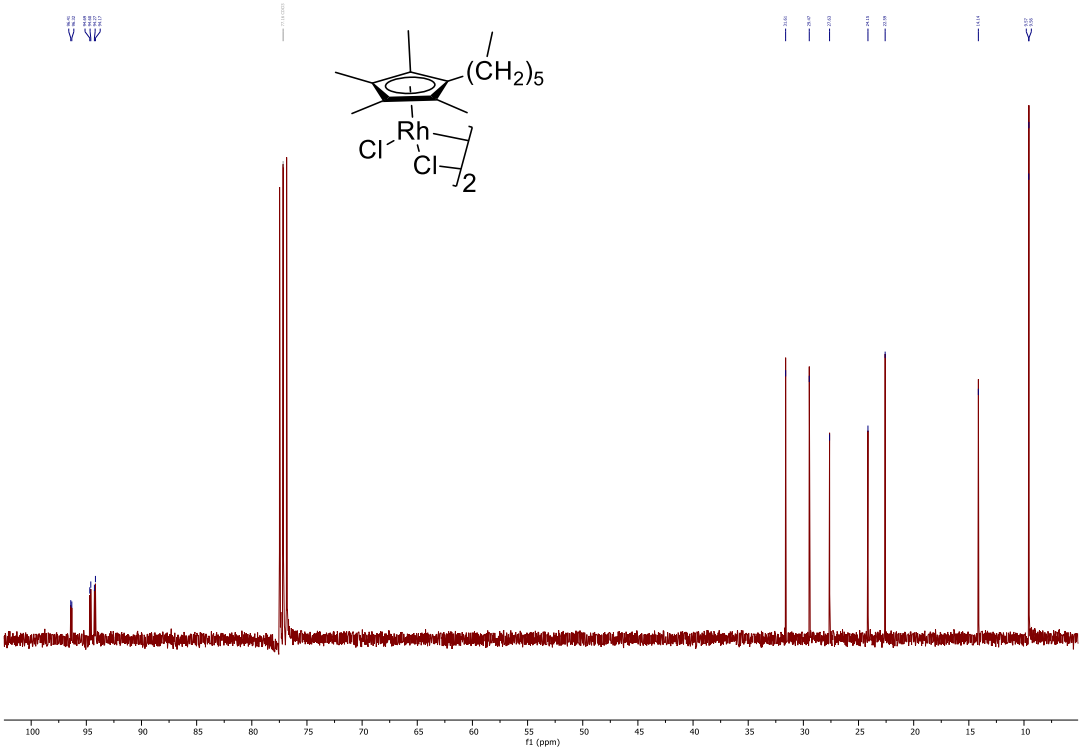

Figure S52. ^{13}C{^{1}H} NMR spectrum of **3h** in $CDCl_3$ at 101 MHz.

[Cp*$^{n\text{-heptyl}}$RhCl]$_2$(μ^2-Cl)$_2$ (**3i**)

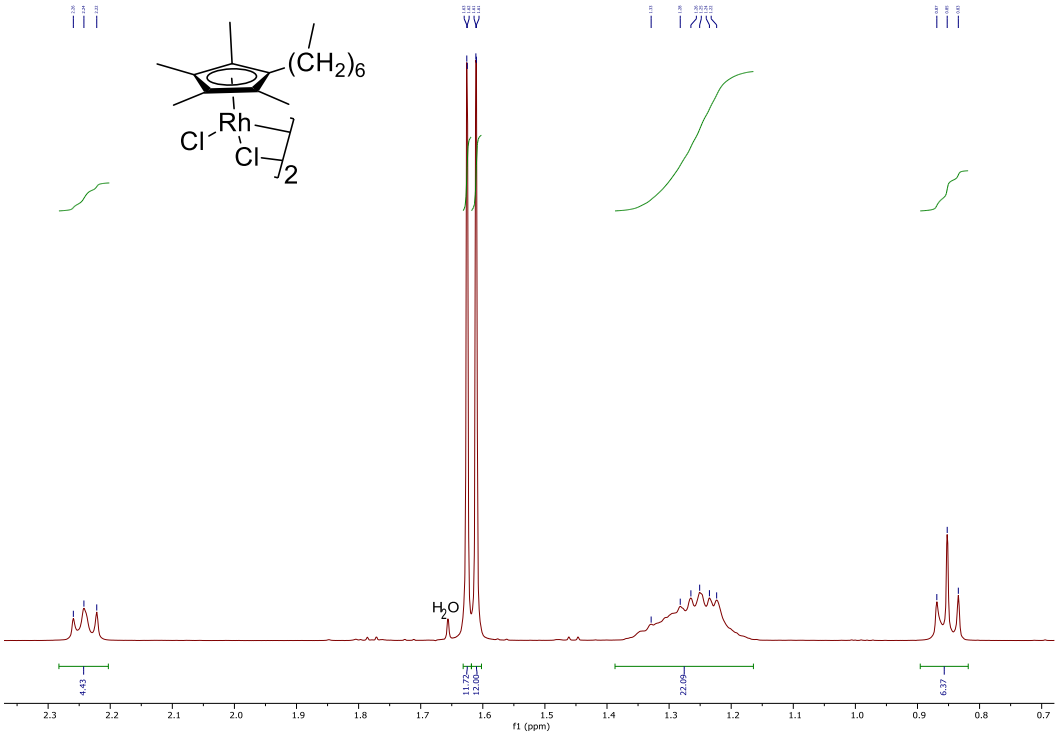

Figure S53. ^{1}H NMR spectrum of **3i** in $CDCl_3$ at 400 MHz.

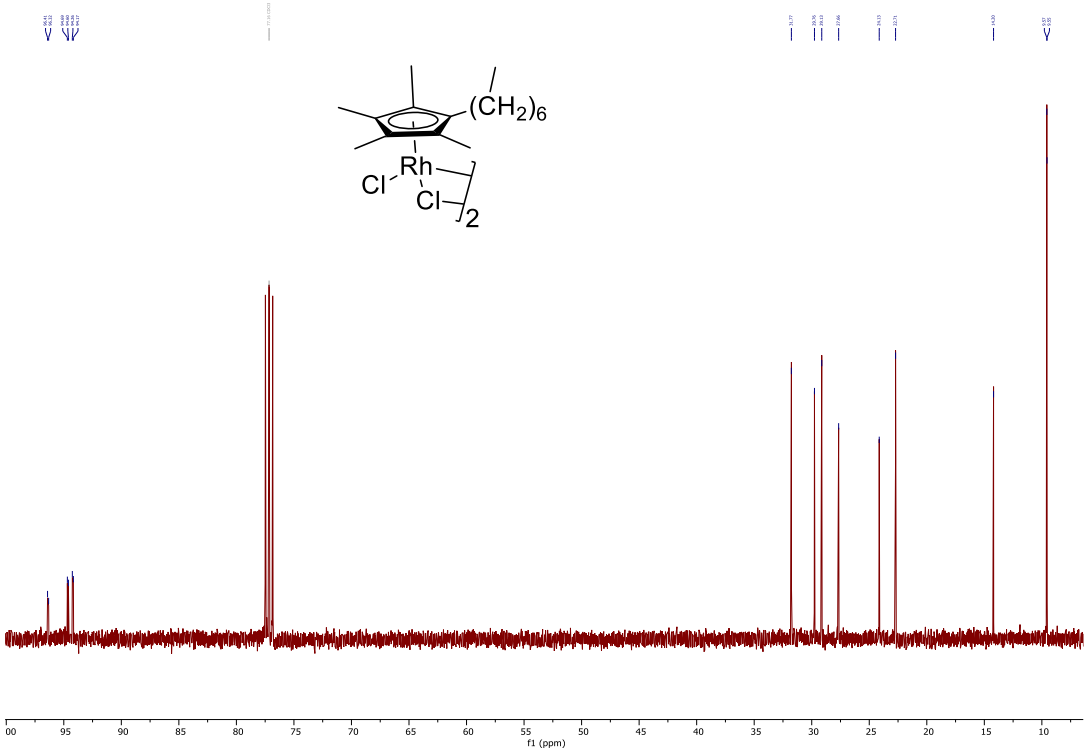

Figure S54. $^{13}C\{^1H\}$ NMR spectrum of **3i** in $CDCl_3$ at 101 MHz.

[Cp*$^{n\text{-octyl}}$RhCl]$_2$(μ^2-Cl)$_2$ (**3j**)

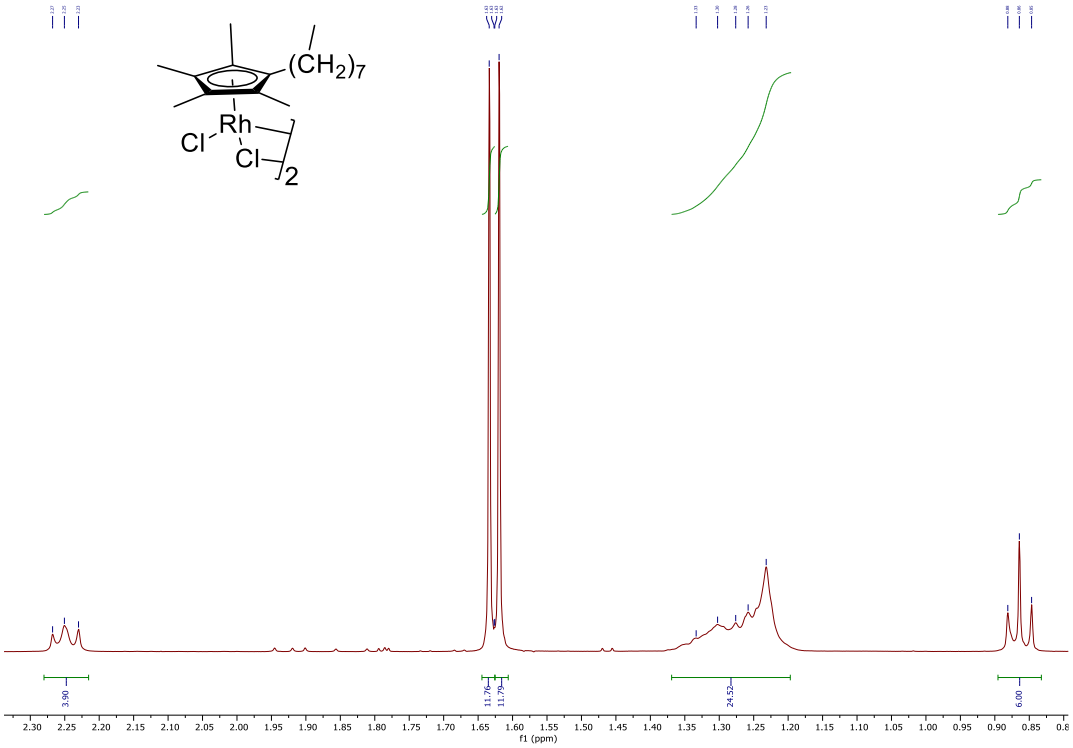

Figure S55. ^{1}H NMR spectrum of **3j** in $CDCl_3$ at 400 MHz.

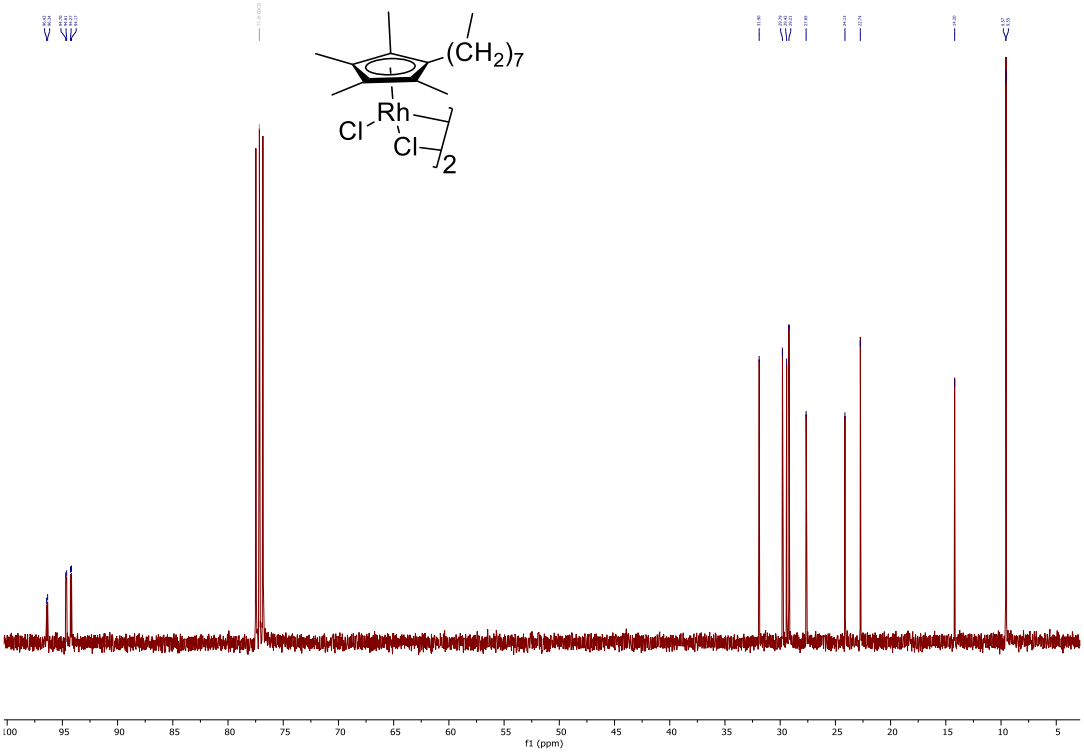

Figure S56. ^{13}C{^{1}H} NMR spectrum of **3j** in $CDCl_3$ at 101 MHz.

$[Cp^{*phenyl}RhCl]_2(\mu^2\text{-}Cl)_2$ (**3k**)

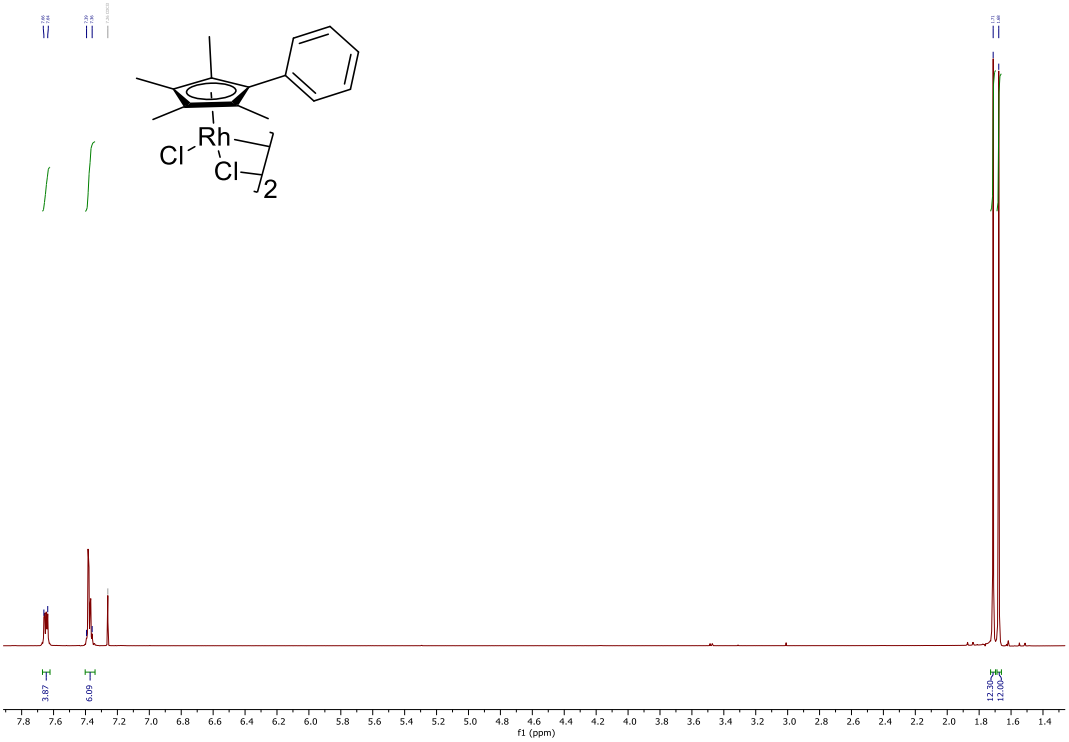

Figure S57. ^{1}H NMR spectrum of **3k** in $CDCl_3$ at 400 MHz.

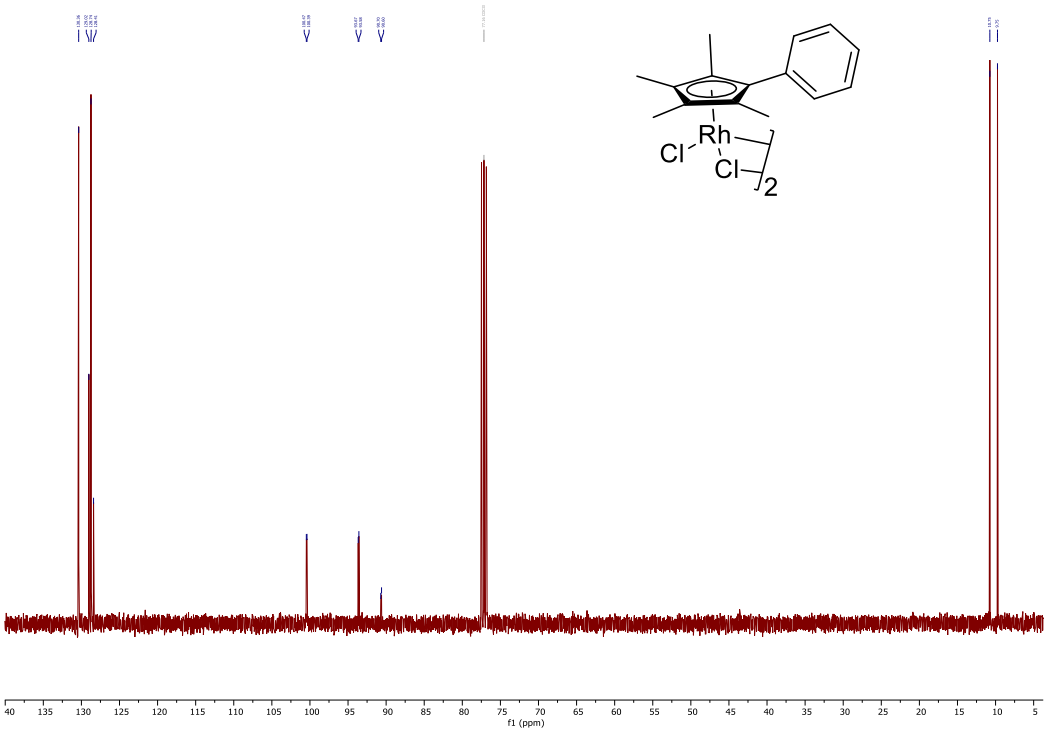

Figure S58. $^{13}C\{^{1}H\}$ NMR spectrum of **3k** in $CDCl_3$ at 101 MHz.

$[Cp^{*benzyl}RhCl]_2(\mu^2\text{-}Cl)_2$ (**3l**)

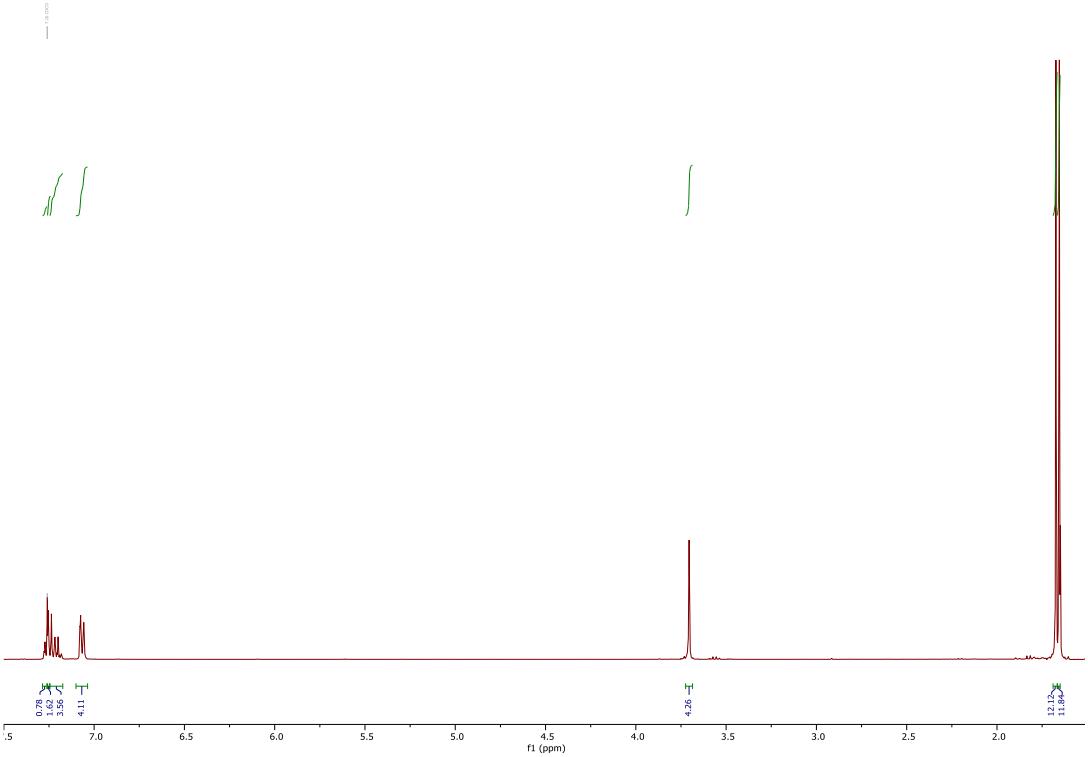

Figure S59. ^{1}H NMR spectrum of **3l** in $CDCl_3$ at 400 MHz.

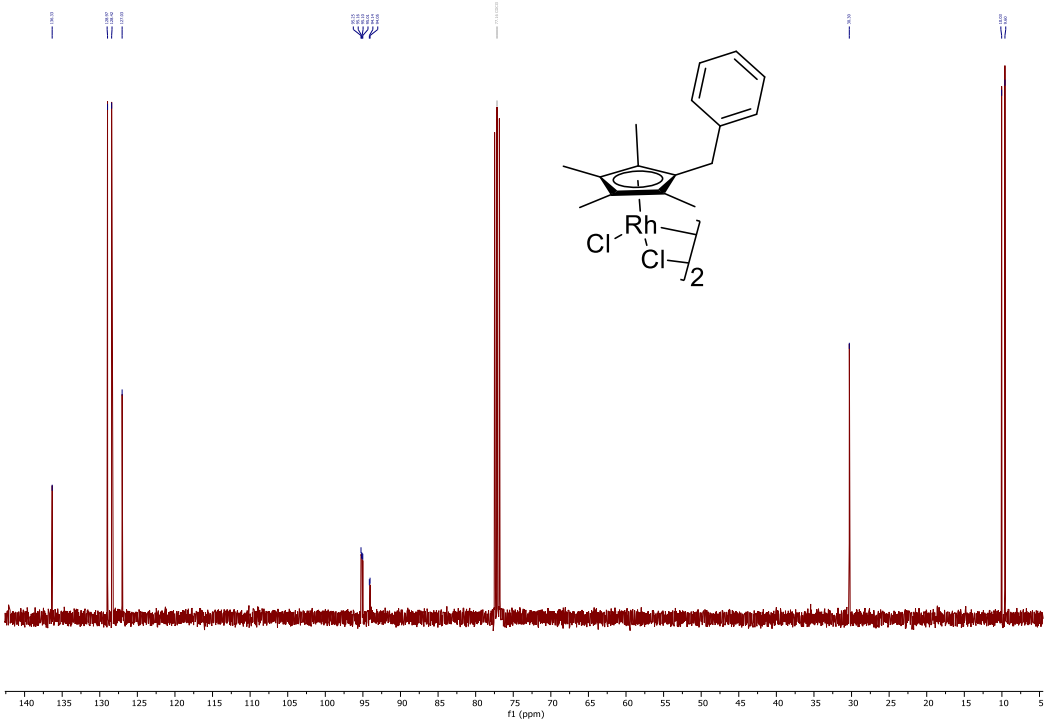

Figure S60. $^{13}C\{^{1}H\}$ NMR spectrum of **3l** in $CDCl_3$ at 101 MHz.

[Cp*^{phenethyl}RhCl]$_2$(μ^2-Cl)$_2$ (**3m**)

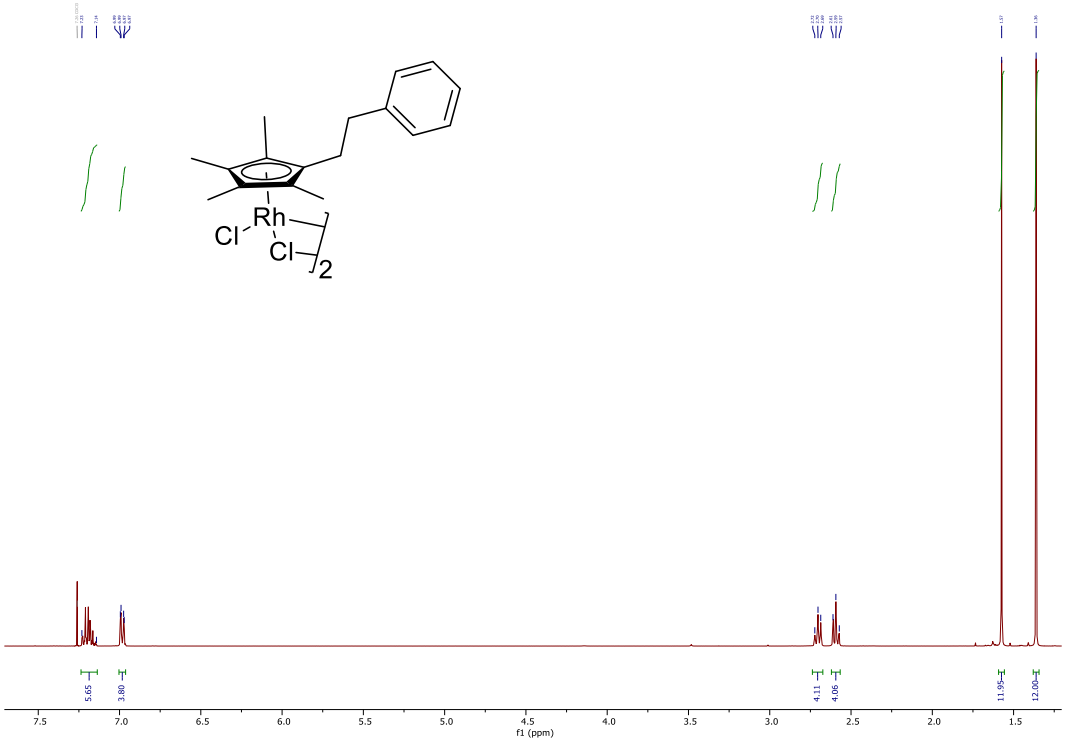

Figure S61. ^{1}H NMR spectrum of **3m** in $CDCl_3$ at 400 MHz.

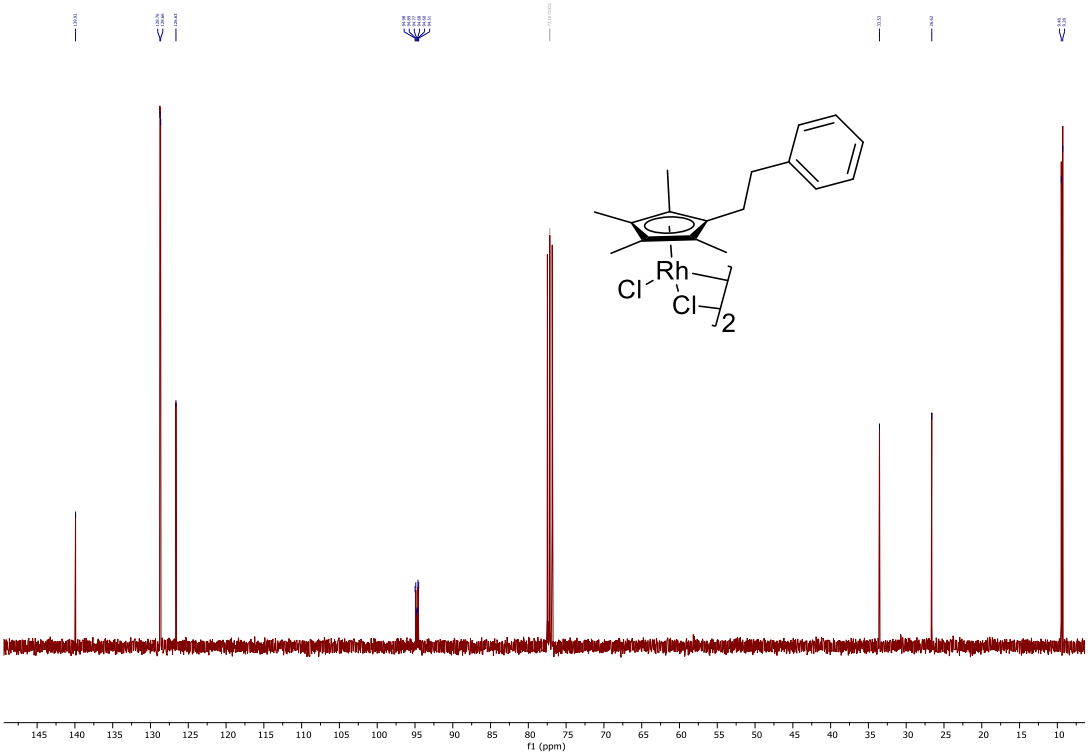

Figure S62. $^{13}C\{^1H\}$ NMR spectrum of **3m** in $CDCl_3$ at 101 MHz.

[Cp*^{cyclohexyl}RhCl]$_2$(μ^2-Cl)$_2$ (**3n**)

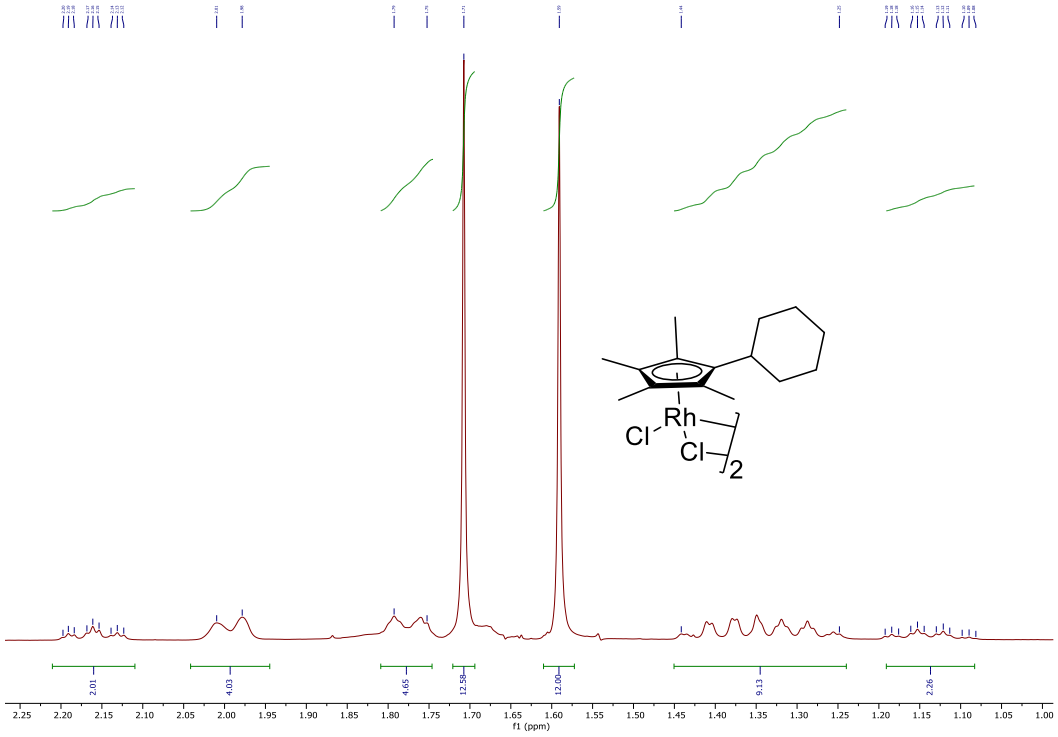

Figure S63. ^{1}H NMR spectrum of **3n** in $CDCl_3$ at 400 MHz.

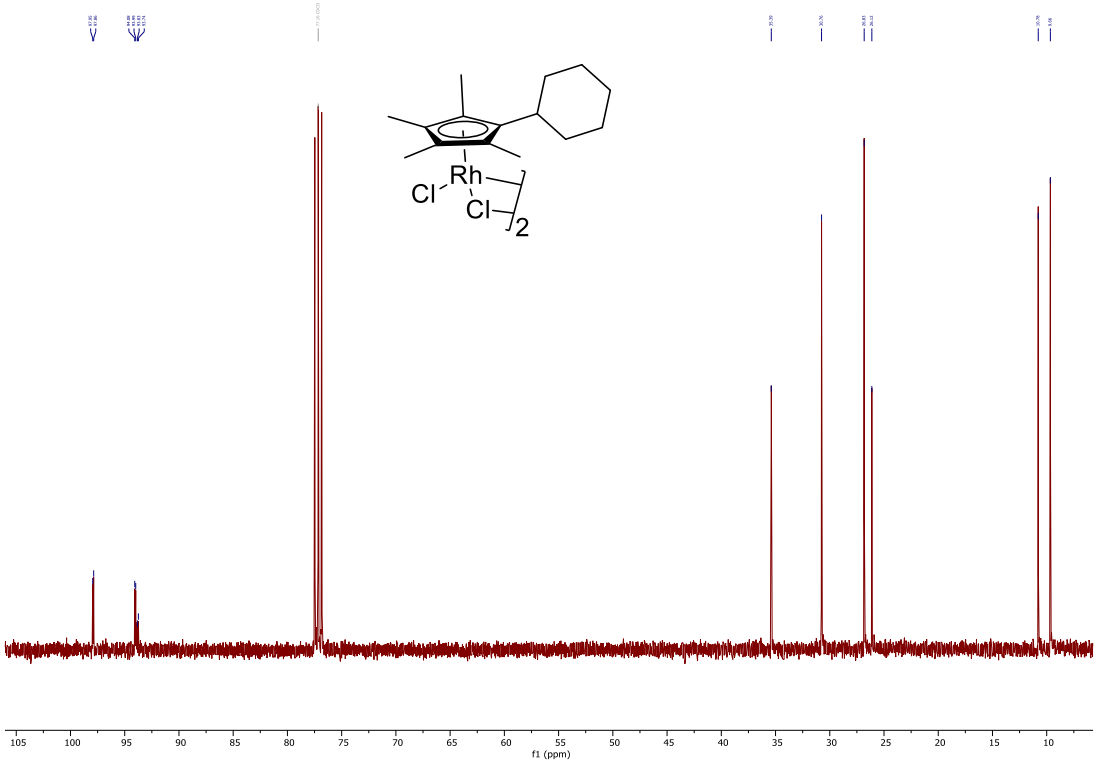

Figure S64. $^{13}C\{^1H\}$ NMR spectrum of **3n** in $CDCl_3$ at 101 MHz.

[Cp*^{cyclopentyl}RhCl]$_2$(μ^2-Cl)$_2$ (**3o**)

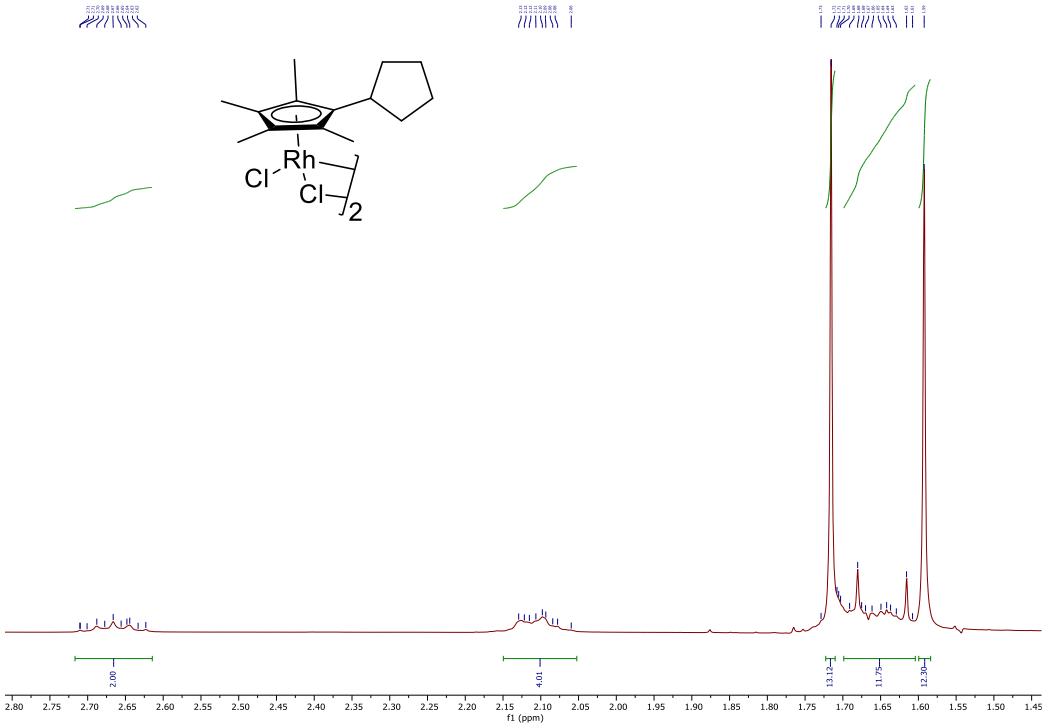

Figure S65. ^{1}H NMR spectrum of **3o** in $CDCl_3$ at 400 MHz.

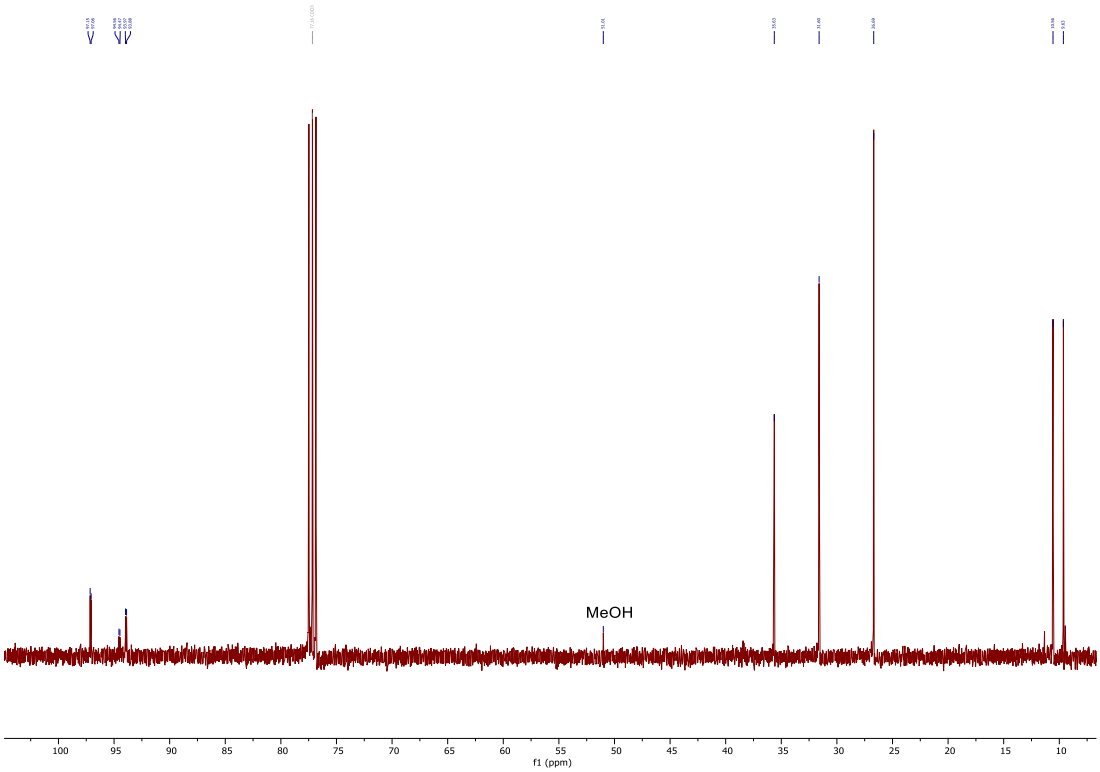

Figure S66. $^{13}C\{^1H\}$ NMR spectrum of **3o** in $CDCl_3$ at 101 MHz.

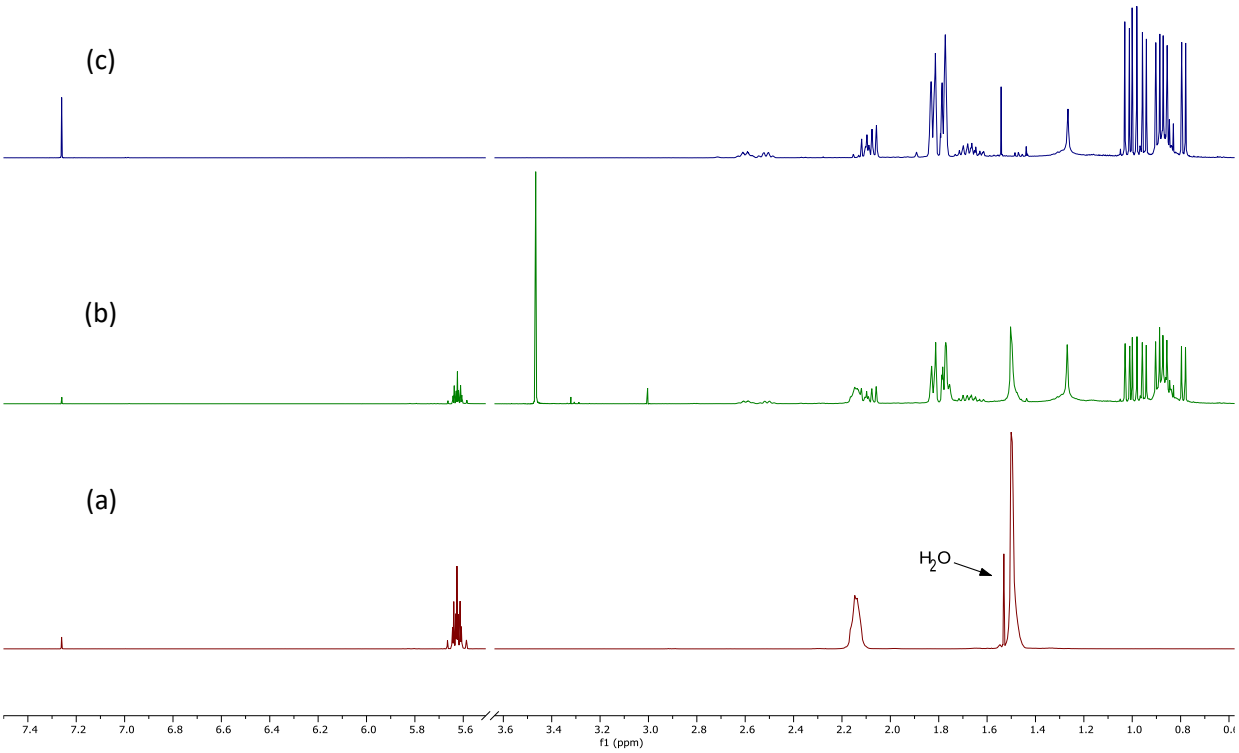

Figure S67. ^{1}H NMR spectrum of byproducts of the reaction: (a) cyclooctene, (b) cyclooctene and unreacted **1f**, and (c) **1f** in $CDCl_3$ at 400 MHz.

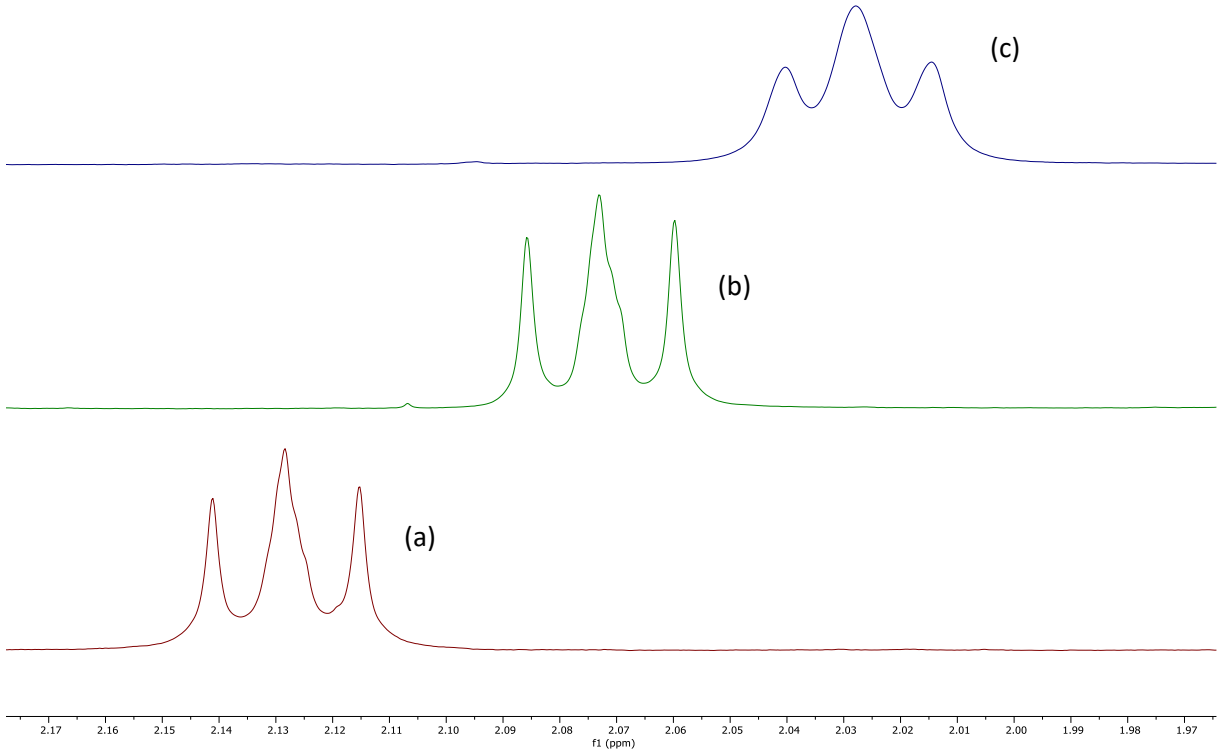

Figure S68. ^{1}H NMR (500 MHz) spectrum of the methylene adjacent to the η^5-ring (**2b**) in $Cl_2CDCDCl_2$ at (a) 70˚C, (b) RT, and (c) -10˚C.

Table S1. Selected bond lengths (Å) and angles (˚) for derivatized chain length iridium(III) complexes.

	2a	**2d**	**2e**	**2f**	**[a]2g**
Ir-C(η^5-ring)	2.139(3)	2.149(4)	2.153(4)	2.134(4)	2.143(4)
	2.157(4)	2.153(4)	2.116(5)	2.142(4)	2.142(3)
	2.132(4)	2.142(4)	2.145(4)	2.156(4)	2.152(4)
	2.146(3)	2.150(4)	2.153(4)	2.152(4)	2.149(4)
	2.134(3)	2.151(4)	2.122(4)	2.132(4)	2.138(4)
Ir-C(centroid)	1.7547(13)	1.7591(18)	1.7489(18)	1.7580(16)	1.7579(16)
Ir-X_1	2.4439(9)	2.4519(10)	2.4499(10)	2.4408(9)	2.4541(9)
Ir-X_2	2.4448(9)	2.4604(10)	2.4512(10)	2.4525(10)	2.4455(8)
Ir-Cl	2.3879(10)	2.3911(10)	2.3902(11)	2.3828(11)	2.4041(9)
Ir-Ir	3.7025(5)	3.7803(4)	3.6844(6)	3.7218(6)	3.7371(6)
X_1-Ir-X_2	81.54(3)	79.37(3)	82.52(3)	80.97(3)	80.59(3)
X_1-Ir-Cl	87.86(3)	89.31(4)	87.72(4)	87.42(4)	88.20(3)
X_2-Ir-Cl	87.55(3)	88.95(4)	87.93(4)	87.78(4)	88.18(3)
Ir-Cl-Ir	98.46(3)	100.63(3)	97.48(3)	99.04(3)	99.41(3)

[a] DCM present in the crystal lattice. [b] X_1 = first bridging Cl and X_2 = second bridging Cl

Table S2. Selected bond lengths (Å) and angles (˚) for ring derivatized iridium(III) complexes.

	2m	**2o**
Ir-C(η^5-ring)	2.155(3)	2.154(2)
	2.134(3)	2.160(2)
	2.149(3)	2.145(2)
	2.128(3)	2.151(2)
	2.139(3)	2.124(2)
Ir-C(centroid)	1.7531(12)	1.7568(8)
Ir-X_1	2.4590(7)	2.4731(5)
Ir-X_2	2.4567(7)	2.4484(5)
Ir-Cl	2.3919(8)	2.3977(5)
Ir-Ir	3.7446(5)	3.7558(3)
X_1-Ir-X_2	80.77(2)	80.516(18)
X_1-Ir-Cl	88.26(3)	88.32(2)
X_2-Ir-Cl	88.86(3)	90.06(2)
Ir-Cl-Ir	99.24(2)	99.483(18)

[a] X_1 = first bridging Cl and X_2 = second bridging Cl

Table S3. Selected bond lengths (Å) and angles (˚) for derivatized chain length rhodium(III) complexes.

	3a	**3b**	**3b**[a]	**3d**	**3e**	[a]**3g**	**3h**
Rh-C(η^5-ring)	2.152(3)	2.1429(14)	2.145(2)	2.122(3)	2.1540(13)	2.136(2)	2.156(2)
	2.162(3)	2.1574(14)	2.148(2)	2.147(3)	2.1182(14)	2.142(2)	2.152(2)
	2.133(3)	2.1420(14)	2.146(2)	2.146(3)	2.1399(14)	2.146(2)	2.133(2)
	2.152(3)	2.1351(14)	2.154(2)	2.132(3)	2.1517(13)	2.147(2)	2.147(2)
	2.111(3)	2.1443(14)	2.114(2)	2.141(3)	2.1193(13)	2.134(2)	2.117(2)
Rh-C(centroid)	1.7566(13)	1.7586(7)	1.7569(10)	1.7511(14)	1.7490(6)	1.7557(9)	1.7591(11)
Rh-X_1	2.4458(7)	2.4608(4)	2.4478(6)	2.4642(8)	2.4558(3)	2.4489(5)	2.4612(6)
Rh-X_2	2.4623(7)	2.4522(4)	2.4546(6)	2.4720(8)	2.4529(3)	2.4579(5)	2.4569(6)
Rh-Cl	2.4102(8)	2.4096(4)	2.4040(6)	2.3973(8)	2.4529(3)	2.4102(5)	2.4019(6)
Rh-Rh	3.7024(6)	3.7192(4)	3.6583(4)	3.6174(6)	3.5948(6)	3.6782(6)	3.6814(6)
X_1-Rh-X_2	82.51(3)	81.595(13)	83.47(2)	85.75(3)	85.839(11)	82.8876(19)	83.286(19)
X_1-Rh-Cl	91.22(3)	91.425(13)	89.53(2)	89.62(3)	89.561(12)	90.446(19)	88.79(2)
X_2-Rh-Cl	91.02(3)	92.288(14)	89.68(2)	91.02(3)	89.997(12)	90.832(18)	91.76(2)
Rh-Cl-Rh	97.77(3)	98.405(13)	96.53(2)	94.25(3)	94.161(11)	97.123(19)	96.38(2)

[a] DCM present in the crystal lattice. [b] X_1 = first bridging Cl and X_2 = second bridging Cl

Table S4. Selected bond lengths (Å) and angles (˚) for ring derivatized rhodium(III) complexes.

	3l	**3m**	[a]**3n**	**3o**
Rh-C(η^5-ring)	2.118(3)	2.1413(17)	2.125(2)	2.157(2)
	2.157(3)	2.1245(18)	2.149(2)	2.149(2)
	2.167(3)	2.1491(18)	2.126(2)	2.138(2)
	2.145(3)	2.1199(17)	2.149(2)	2.153(2)
	2.139(3)	2.1391(16)	2.139(2)	2.121(2)
Rh-C(centroid)	1.7533(11)	1.7486(7)	1.7531(10)	1.7573(9)
Rh-X_1	2.4657(7)	2.4586(4)	2.4442(5)	2.4813(5)
Rh-X_2	2.4609(7)	2.4636(4)	2.4517(5)	2.4522(5)
Rh-Cl	2.3984(6)	2.3947(4)	2.4001(6)	2.4085(6)
Rh-Rh	3.6502(8)	3.6811(5)	3.6364(7)	3.7122(3)
X_1-Rh-X_2	84.568(19)	83.189(14)	84.063(18)	82.400(18)
X_1-Rh-Cl	90.05(2)	91.146(15)	90.26(2)	90.59(2)
X_2-Rh-Cl	89.50(2)	90.909(15)	90.36(2)	92.92(2)
Rh-Cl-Rh	95.43(2)	91.146(15)	95.939(18)	97.600(18)

[a] DCM present in the crystal lattice. [b] X_1 = first bridging Cl and X_2 = second bridging Cl

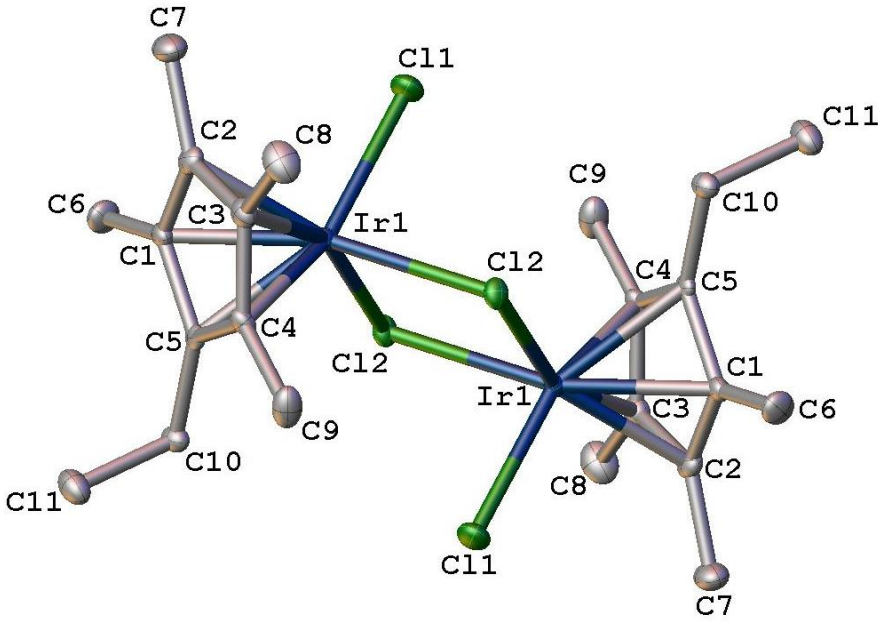

Figure S69. ADP Plot of **2a** (**CSD: 1492610**). Hydrogen atoms omitted for clarity. Ellipsoids shown at 50% probability.

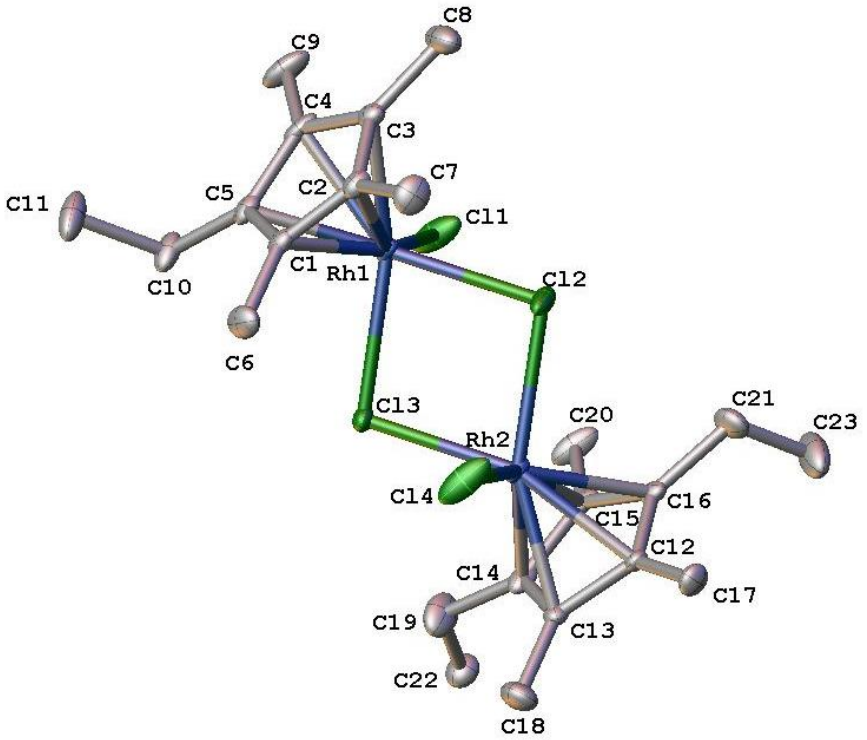

Figure S70. ADP Plot of **3a** (**CSD: 1492614**). Hydrogen atoms omitted for clarity. Ellipsoids shown at 50% probability. Note: Atoms C19, C22, C21, and C23 represent disorder in the chain.

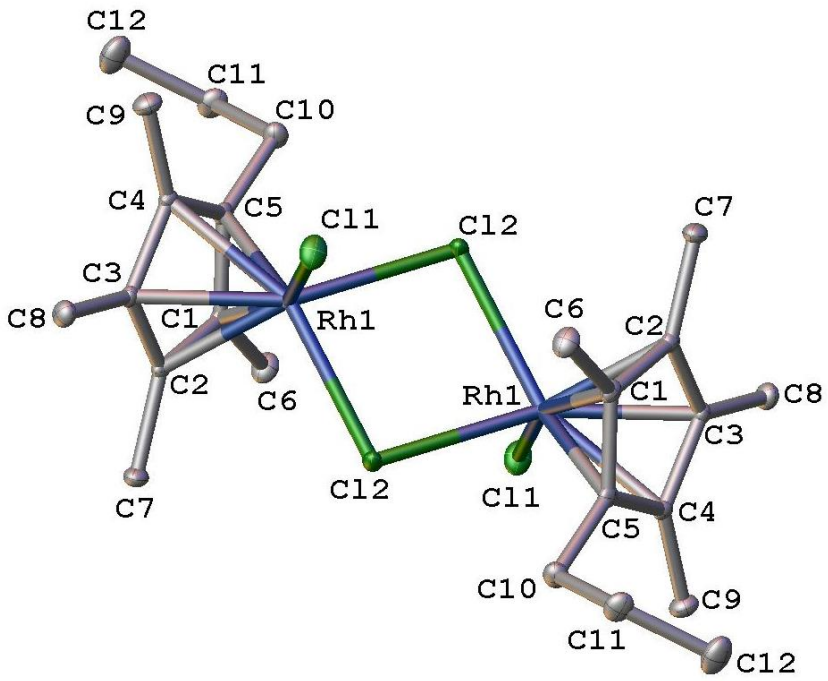

Figure S71. ADP Plot of **3b** (**CSD: 1492622**). Hydrogen atoms omitted for clarity. Ellipsoids shown at 50% probability.

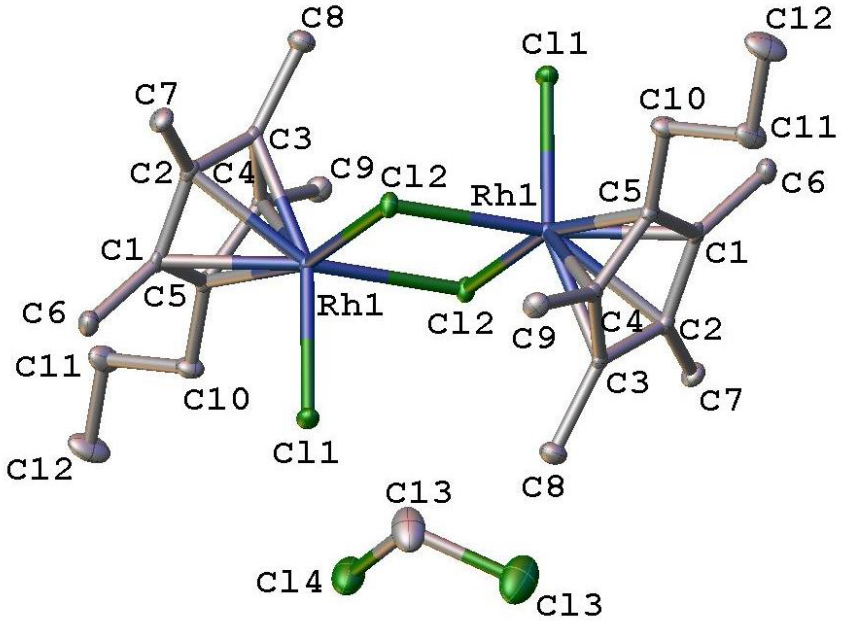

Figure S72. ADP Plot of **3b** (**CSD: 1492611**) with a dichloromethane molecule. Hydrogen atoms omitted for clarity. Ellipsoids shown at 50% probability.

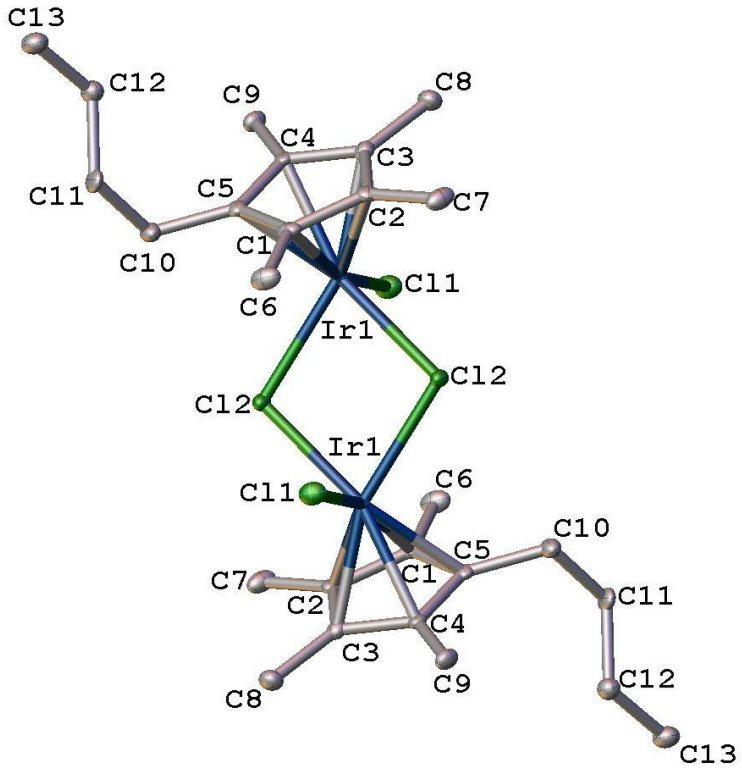

Figure S73. ADP Plot of **2d** (**CSD: 1492609**). Hydrogen atoms omitted for clarity. Ellipsoids shown at 50% probability.

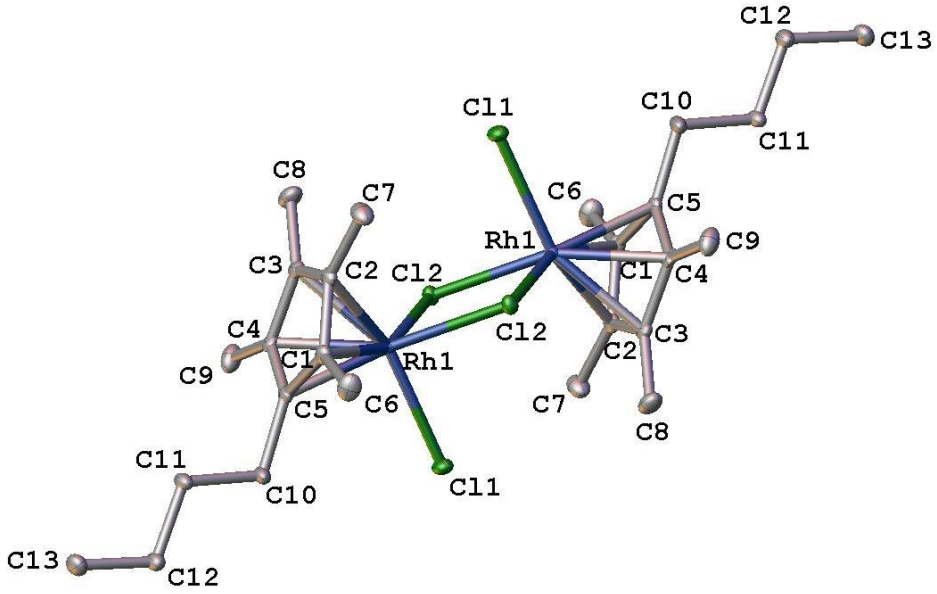

Figure S74. ADP Plot of **3d** (**CSD: 1492625**). Hydrogen atoms omitted for clarity. Ellipsoids shown at 50% probability.

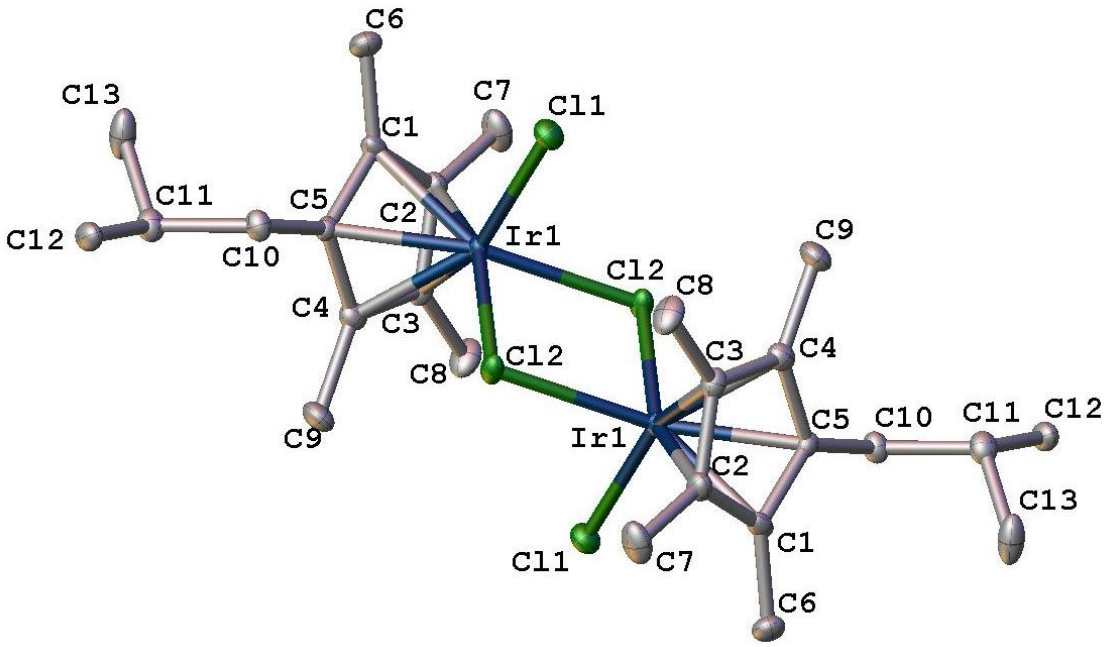

Figure S75. ADP Plot of **2e** (**CSD: 1492615**). Hydrogen atoms omitted for clarity. Ellipsoids shown at 50% probability.

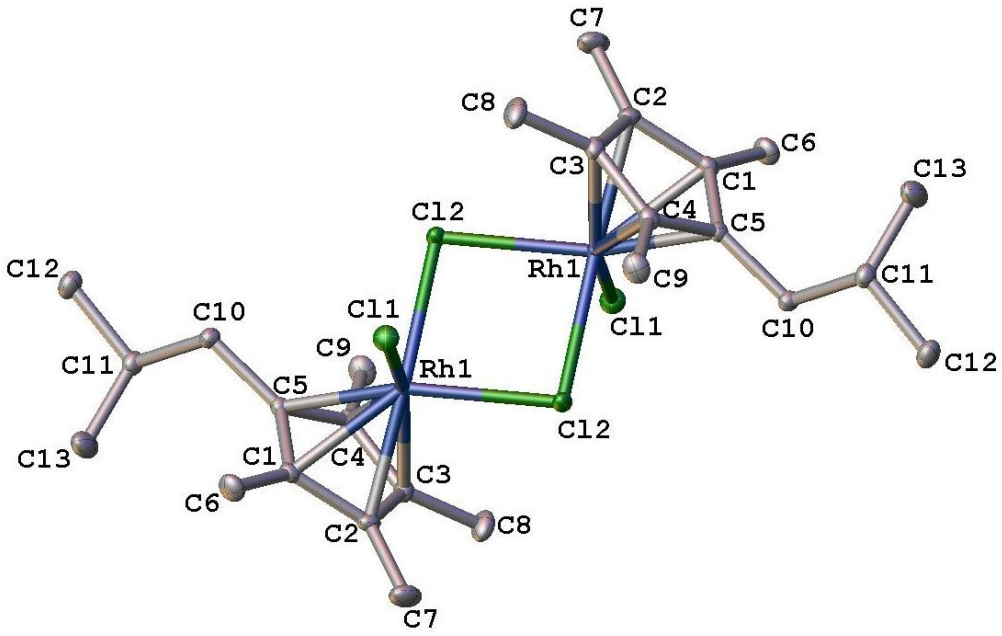

Figure S76. ADP Plot of **3e** (**CSD: 1492617**). Hydrogen atoms omitted for clarity. Ellipsoids shown at 50% probability.

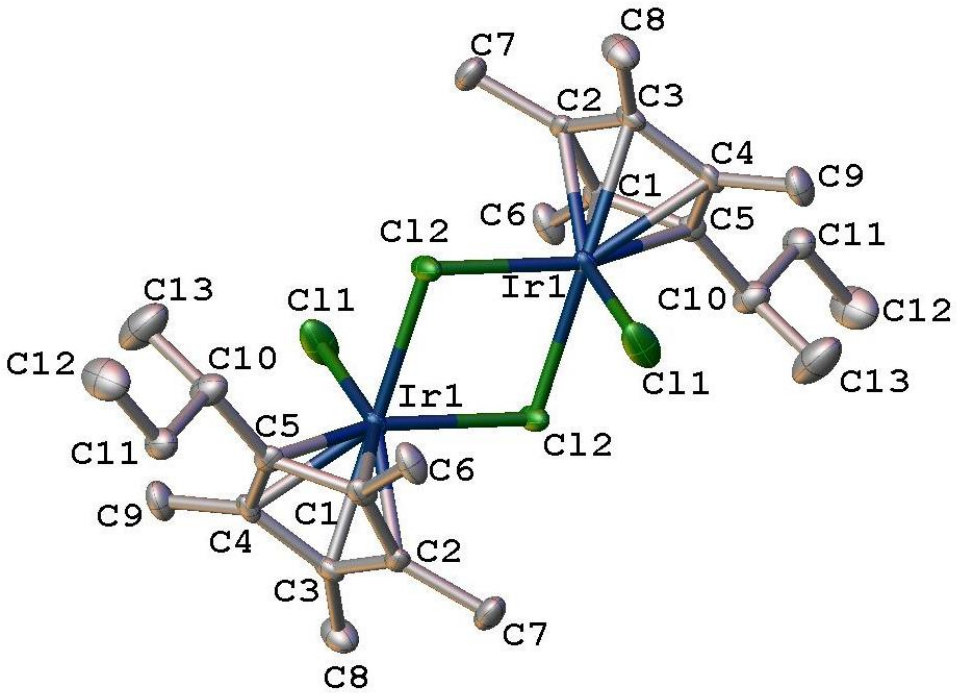

Figure S77. ADP Plot of **2f** (**CSD: 1492624**). Hydrogen atoms omitted for clarity. Ellipsoids shown at 50% probability.

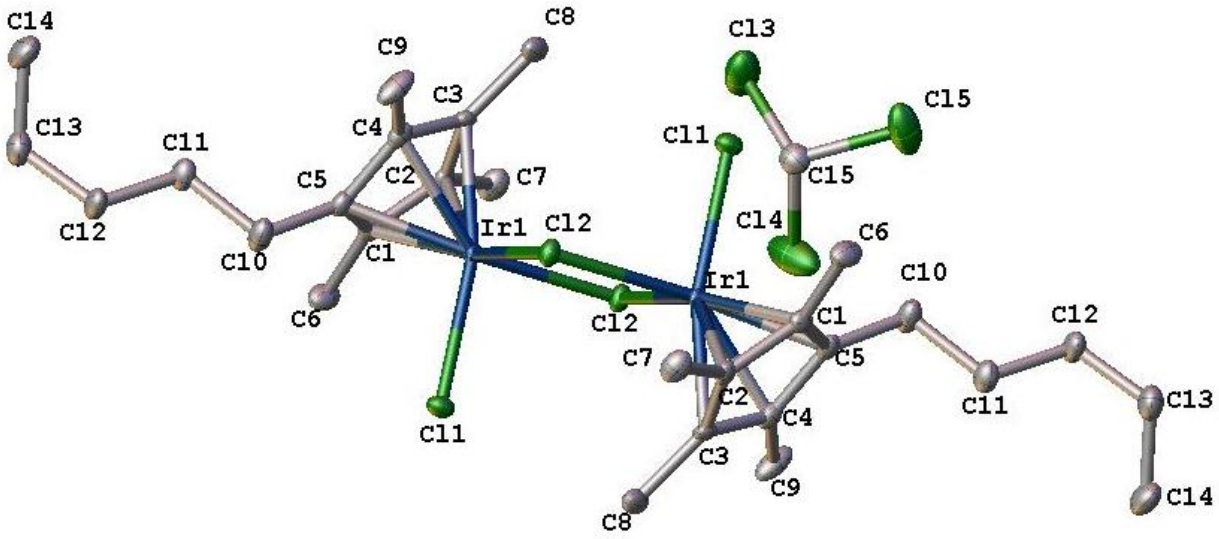

Figure S78. ADP Plot of **2g** (**CSD: 1492612**) with a chloroform molecule. Hydrogen atoms omitted for clarity. Ellipsoids shown at 50% probability.

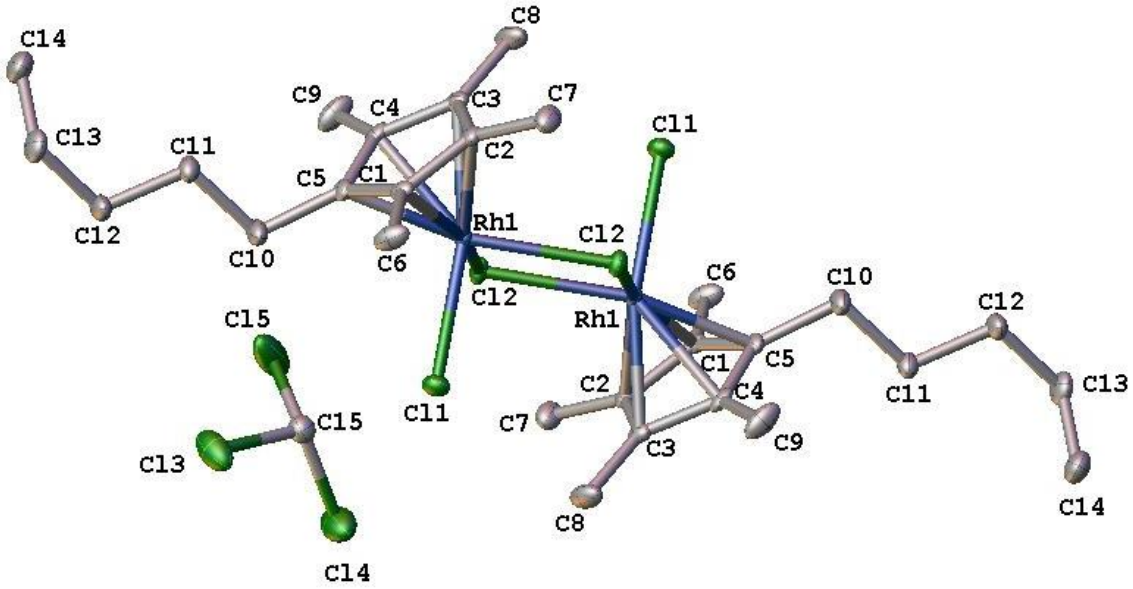

Figure S79. ADP Plot of **3g** (**CSD: 1492621**) with a chloroform molecule. Hydrogen atoms omitted for clarity. Ellipsoids shown at 50% probability.

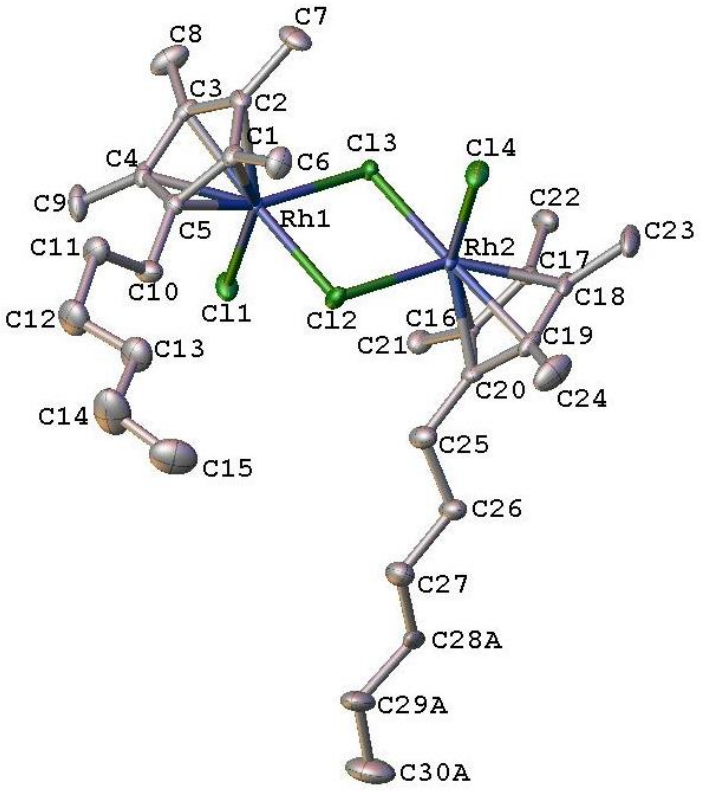

Figure S80. ADP Plot of **3h** (**CSD: 1492616**). Hydrogen atoms omitted for clarity. Ellipsoids shown at 50% probability. Note: Atoms C28A, C29A, and C30A represent disorder in the chain.

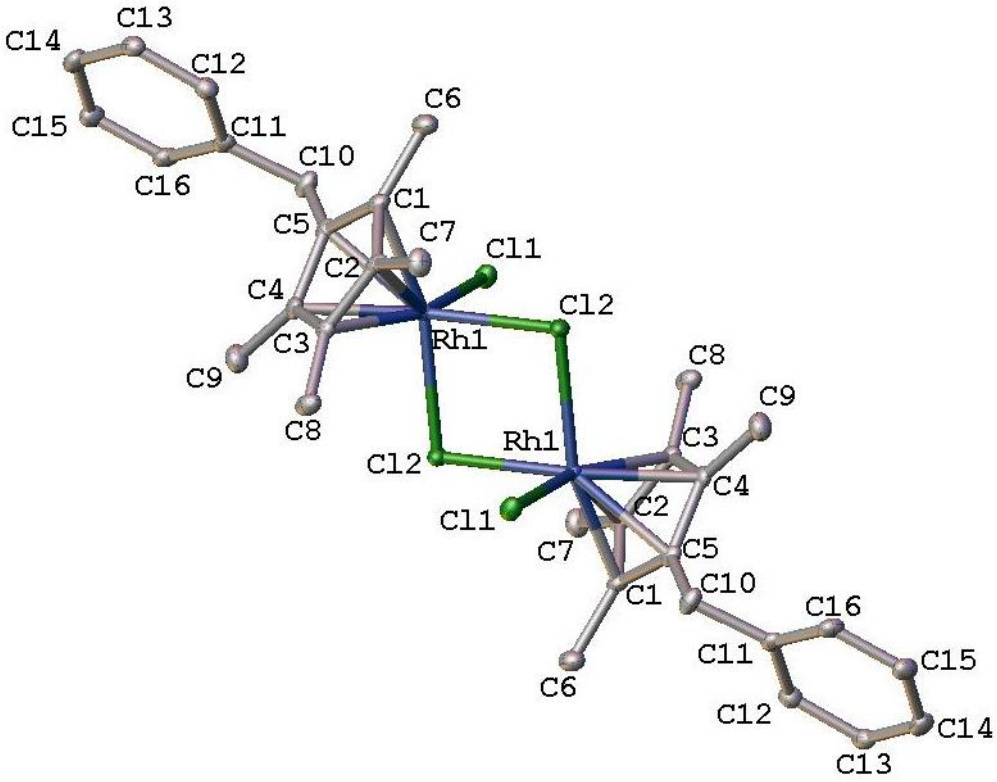

Figure S81. ADP Plot of **3l** (**CSD: 1492613**). Hydrogen atoms omitted for clarity. Ellipsoids shown at 50% probability.

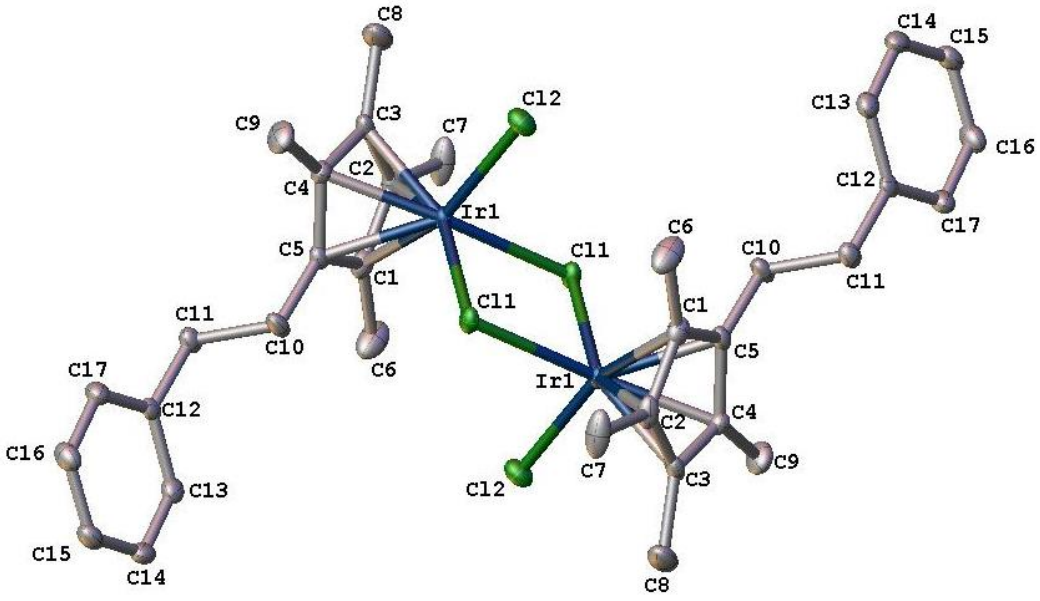

Figure S82. ADP Plot of **2m** (**CSD: 1492618**). Hydrogen atoms omitted for clarity. Ellipsoids shown at 50% probability.

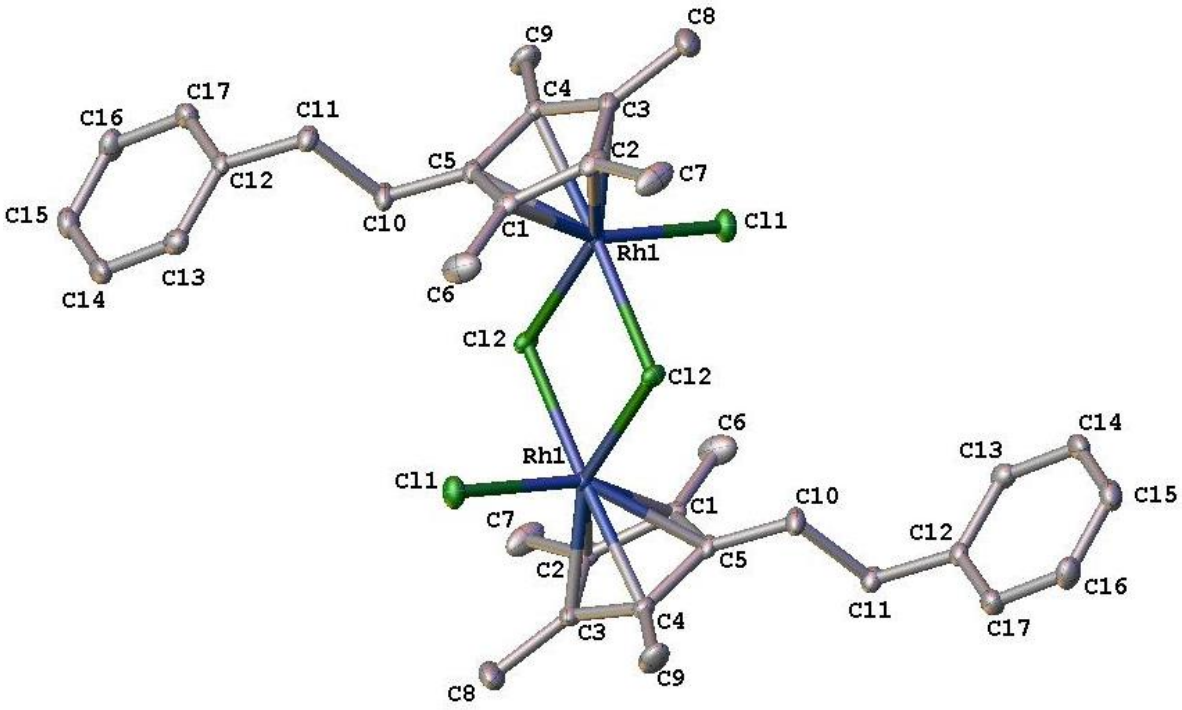

Figure S83. ADP Plot of **3m** (**CSD: 1492619**). Hydrogen atoms omitted for clarity. Ellipsoids shown at 50% probability.

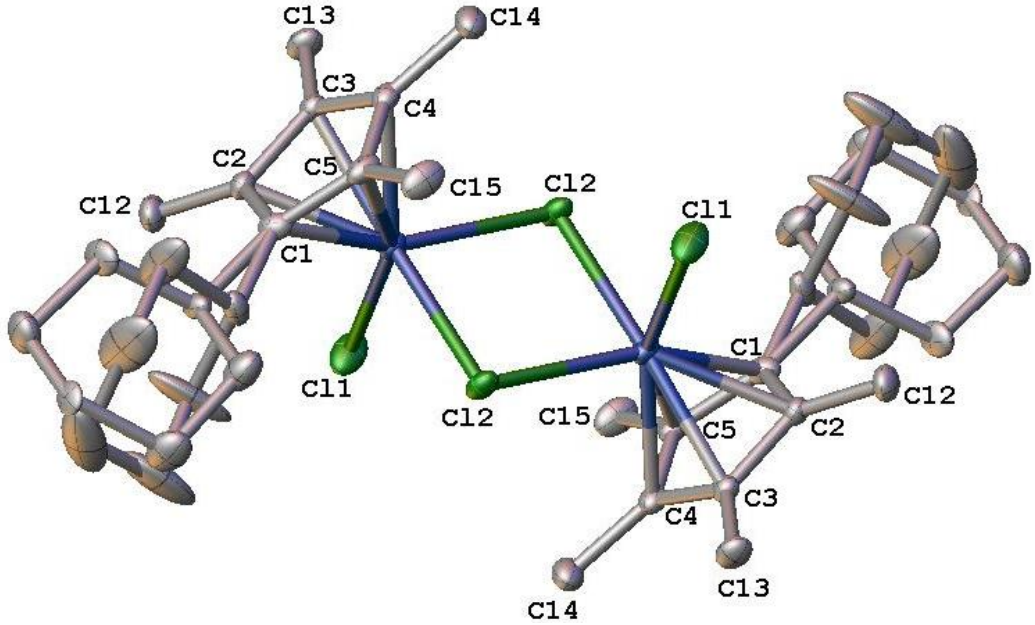

Figure S84. ADP Plot of **3n** (**CSD: 1492620**). Hydrogen atoms omitted for clarity. Ellipsoids shown at 50% probability. Note: dichloromethane molecule was “solvent masked”.

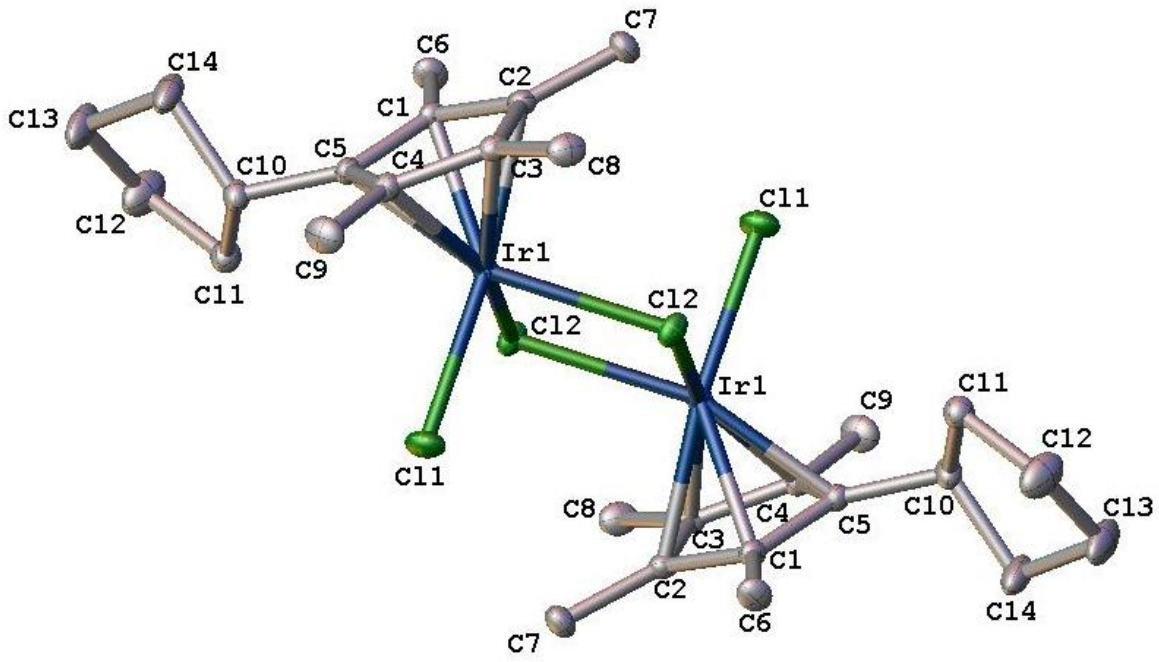

Figure S85. ADP Plot of **2o** (**CSD: 1492623**). Hydrogen atoms omitted for clarity. Ellipsoids shown at 50% probability.

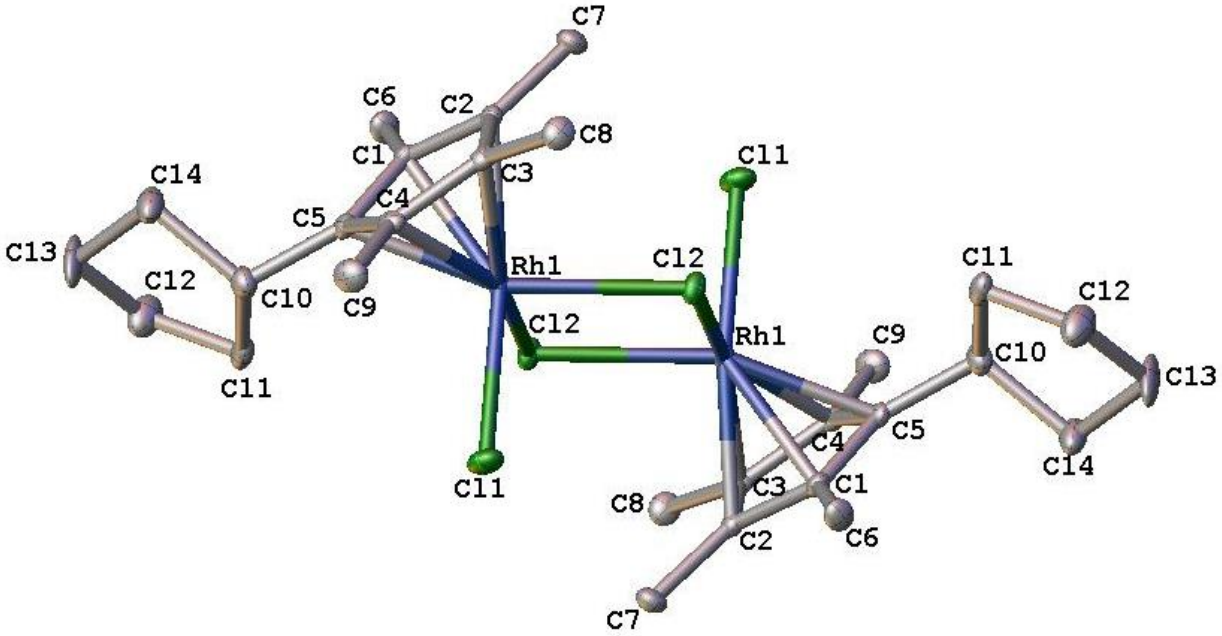

Figure S86. ADP Plot of **3o** (**CSD: 1509390**). Hydrogen atoms omitted for clarity. Ellipsoids shown at 50% probability.

5.4 Synthetic procedures and characterization of products from Chapter 3

5.4.1 General procedure for the microwave synthesis of $[(\eta^5\text{-}Me_4C_5R)IrCl]_2(\mu^2\text{-}Cl)_2$

A microwave pressure tube was charged with the appropriate amounts of $[Ir(COD)]_2(\mu^2\text{-}Cl)_2$, ligand HMe_4C_5R, 4 mL of methanol, and 0.5 mL of 12 M aqueous hydrochloric acid. The reaction mixture was heated to 115 °C at 50 W and 150 psi and held there for 1 h, yielding an orange solution. After cooling, the tube was cautiously opened, and the reaction mixture was transferred to a small flask. The solvent was removed by rotary evaporation,, and the resulting powder was recrystallized from dichloromethane , collected on a filter, washed with cold hexanes, and dried under air or vacuum Complexes **1a-1d** were prepared according to an established literature procedure.[1,2]

5.4.2 Synthesis of $[(\eta^5\text{-}Me_4C_5(C_6F_5)IrCl]_2(\mu^2\text{-}Cl)_2$ (1e)

Following the general procedure, $[Ir(COD)]_2(\mu^2\text{-}Cl)_2$ (0.430 g, 0.298 mmol), $HMe_4C_5(C_6F_5)$ (0.342 g, 1.2 mmol),[3] and 0.5 mL of 12 M aqueous HCl were reacted in methanol (4 mL) to give **1e** (0.579 g, 82% yield). ^{1}H NMR (400 MHz, $CDCl_3$) δ 1.79 (s, 12H, 4 CpCH_3), 1.63 – 1.62 (s, 12H, 4 CpCH_3), (Figure S1). ^{19}F NMR (376 MHz, $CDCl_3$) δ -127.47 (m, 1F), -138.81 (m, 1F), -151.21 (m, 1F), -158.90 (m, 1F), -161.54 (m, 1F), (Figure S2). HRMS/ESI+ (m/z): Calc. for $C_{30}H_{24}[^{193}Ir]_2F_{10}Cl_3$ 1065.0042; Found 1065.0102. Anal. Calc. for $C_{30}H_{24}Ir_2F_{10}Cl_4$, C, 32.74; H, 2.20; Found, C, 32.91; H, 2.22

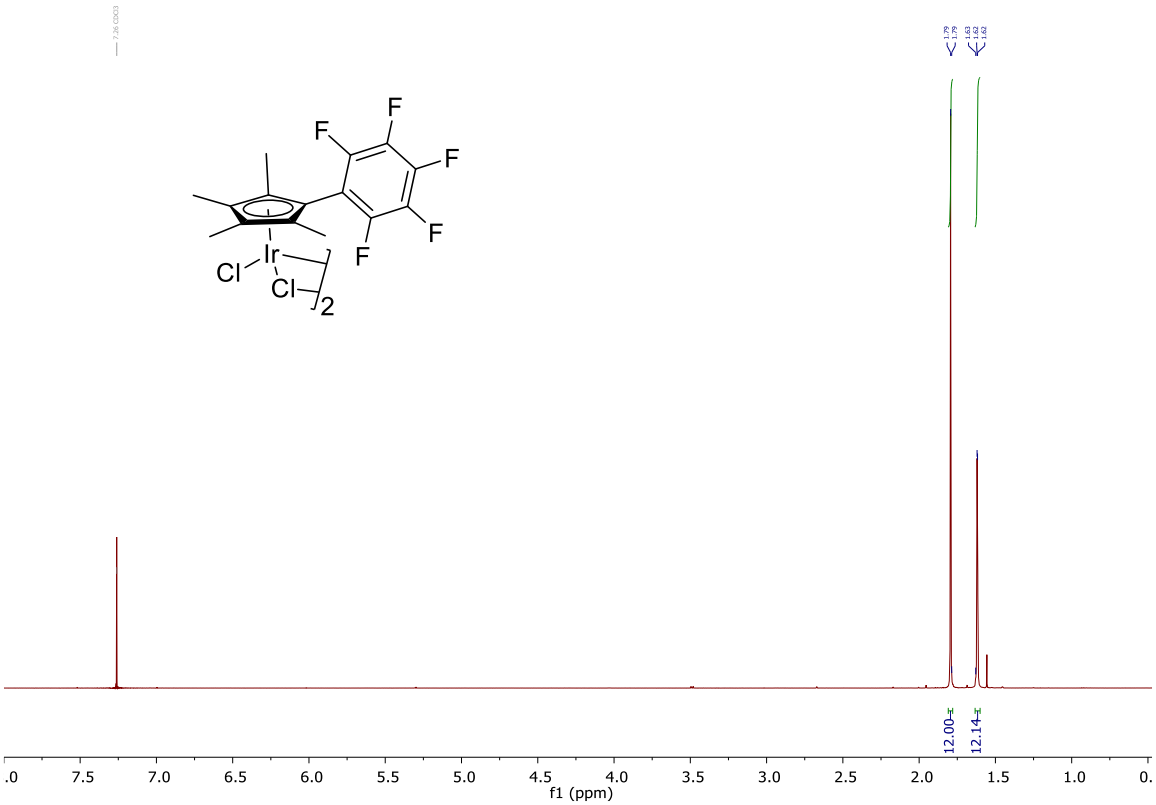

Figure S1. ^{1}H NMR spectrum of **1e** in $CDCl_3$ at 400 MHz.

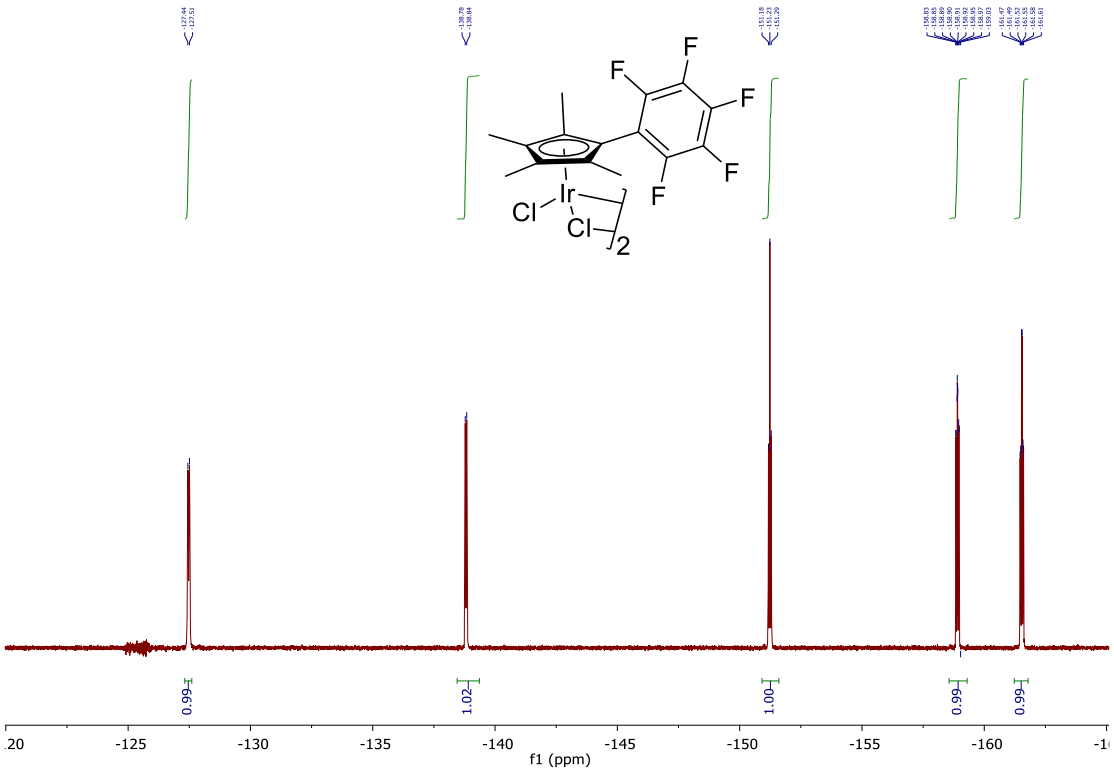

Figure S2. ^{19}F NMR spectrum of **1e** in $CDCl_3$ at 376 MHz.

5.4.3 General Considerations

Chemicals and solvents were used as received unless otherwise stated. HPLC grade acetone was purchased from Alfa Aesar, Ward Hill, MA 01835. Methylsuccinic acid, 2,2-dimethylsuccinic acid, 3-benzoylpriopionic acid, (+/-)-phenylsuccinic acid, 2-methylglutaric acid, 2,2-dimethylglutaric acid, 3-phenylglutaric acid, 4-benzoylbutyric acid, and 3,3-dimethylglutaric acid were purchased from Fisher Scientific, Ward Hill, MA 01835. 1,1-Cyclohexanediacetic anhydride and 3-methyl-1,5-pentanediol were purchased from TCI America, Portland, OR, 97203. Substrates 1,4-butanediol, 1,4-pentanediol, 1,5-pentanediol, and 1,5-hexanediol were purchased from Sigma-Aldrich, St. Louis, MO 63013. Substrate 1,1-dideuterio-1,4-butanediol was prepared according to an established literature procedure.[4] Deuterated solvents for NMR spectroscopy were obtained from Cambridge Isotope Laboratories. ^{1}H NMR (400 MHz) and ^{13}C NMR spectra (101 MHz) were collected on an Agilent (Varian) MR-400 NMR spectrometer. HRMS were collected using direct infusion methods on an Agilent 6220 instrument using electrospray ionization (ESI) and time-of-flight (TOF) mass analysis.

5.4.4 General procedure for the synthesis of diol substrates

Following an adaption of a modified procedure, a solution of the carboxylic acid or ester in 25 mL of anhydrous THF was added dropwise to a stirred suspension of $LiAlH_4$ in 25 mL of THF maintained under a nitrogen atmosphere and at -78 ˚C. The reaction was allowed to warm to room temperature and stirred for 16 h. The reaction was cooled to 0 ˚C and quenched with water. Sodium hydroxide (2 M, 3 mL) and water (8 mL) were then added to the reaction. The reaction was filtered through a pad of diatomaceous earth, using ethyl acetate to wash the reaction flask and filter. The solvent was removed by rotary evaporation and the resulting oil was used without further purification.[5]

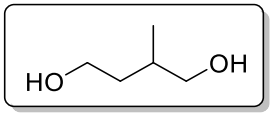

2-Methyl-1,4-butanediol (Table 2 entry 3). ^{1}H NMR (400 MHz, $CDCl_3$) δ 0.93 (d, 3H, J_{HH} = 6.9 Hz), 1.55 – 1.67 (m, 2H), 1.76 – 1.87 (m, 1H), 2.45 – 2.57 (m, 2H), 3.42 – 3.47 (m, 1H), 3.55 – 3.59 (m, 1H), 3.64 – 3.69 (m, 1H), 3.75 – 3.81 (m, 1H).[6]

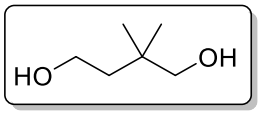

2,2-dimethyl-1,4-butanediol (Table 2 entry 4). ^{1}H NMR (400 MHz, $CDCl_3$) δ 0.90 (s, 6H), 1.49 – 1.61 (m, 2H), 3.17 (br s, 2H), 3.32 (s, 2H), 3.64 – 3.76 (m, 2H).[7]

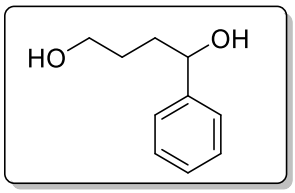

1-Phenyl-1,4-butanediol (Table 2 entry 5). ^{1}H NMR (400 MHz, $CDCl_3$) δ 1.57 – 1.72 (m, 2H), 1.83 (td, 2H, J_{HH} = 7.3, 6.3 Hz), 2.63 – 3.37 (br s, 2H), 3.58 – 3.68 (m, 2H), 4.68 (t, 1H, J_{HH} = 6.3 Hz), 7.24 – 7.30 (m, 1H), 7.31 – 7.37 (m, 4H).[8]

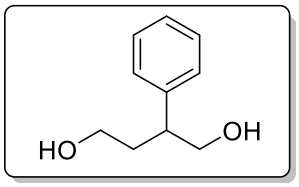

2-Phenyl-1,4-butanediol (Table 2 entry 6). ^{1}H NMR (400 MHz, $CDCl_3$) δ 1.85 – 2.07 (m, 4H), 2.93 – 3.00 (m, 1H), 3.55 – 3.61 (m, 1H), 3.66 – 3.72 (m, 1H), 3.78 (d, 2H, J_{HH} = 6.6 Hz), 7.20 – 7.27 (m, 3H), 7.29 – 7.37 (m, 2H).[9]

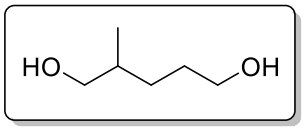

2-Methyl-1,5-pentanediol (Table 2 entry 9). ^{1}H NMR (400 MHz, $CDCl_3$) δ 0.90 (d, 3H, J_{HH} = 6.7 Hz), 1.09 – 122 (m, 1H), 1.45 – 1.70 (m, 4H), 2.46 (br s, 2H), 3.45 (d, 2H, J_{HH} = 6.3 Hz), 3.62 (t, 2H, J_{HH} = 6.3 Hz).[10]

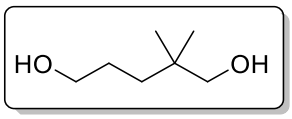

2,2-dimethyl-1,5-pentanediol (Table 2 entry 11). ^{1}H NMR (400 MHz, $CDCl_3$) δ 0.88 (s, 6H), 1.26 – 1.35 (m, 2H), 1.51 – 1.58 (m, 2H), 1.61 (br s, 2H), 3.32 (s, 2H), 3.64 (t, 2H, J_{HH} = 6.5 Hz).[11]

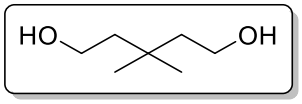

3,3-dimethyl-1,5-pentanediol (Table 2 entry 12). ^{1}H NMR (400 MHz, $CDCl_3$) δ 0.93 (s, 6H), 1.56 (t, 4H, J_{HH} = 7.1 Hz), 2.28 (br s, 2H), 3.71 (t, 4H, J_{HH} = 7.1 Hz).[12]

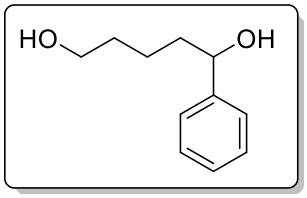

1-Phenyl-1,5-pentanediol (Table 2 entry 13). ^{1}H NMR (400 MHz, $CDCl_3$) δ 1.24 – 1.36 (m, 1H), 1.38 – 1.55 (m, 3H), 1.60 – 1.77 (m, 2H), 1.79 (br s, 2H), 3.55 (t, 2H, J_{HH} = 6.4 Hz), 4.60 (dd, 1H, J_{HH} = 7.6, 5.6 Hz), 7.17 – 7.23 (m, 1H), 7.25 – 7.30 (m, 4H).[11]

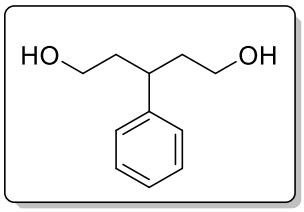

3-Phenyl-1,5-pentanediol (Table 2 entry 14). ^{1}H NMR (400 MHz, $CDCl_3$) δ 1.35 (br s, 2H), 1.81 – 1.90 (m, 2H), 1.92 – 2.00 (m, 2H), 2.92 (tt, 1H, J_{HH} = 10.0, 5.2 Hz), 3.41 – 3.63 (m, 4H), 7.24 – 7.30 (m, 3H), 7.28 – 7.34 (m, 2H).[9]

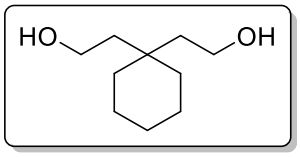

1,1-Bis(2-hydroxyethyl)cyclohexane (Table 2 entry 15). ^{1}H NMR (400 MHz, $CDCl_3$) δ 1.31 – 1.33 (m, 4H), 1.37 – 1.47 (m, 4H), 1.64 (t, 4H, J_{HH} = 7.0 Hz), 2.00 – 2.12 (m, 2H), 3.73 (t, 4H, J_{HH} = 7.0 Hz).[13]

5.4.5 General procedure for the dehydrogenative lactonization of various diols

In a sealed 1-dram vial, a mixture of catalyst (0.010 mol), diol (1.0 mmol), base (0.10 mmol), and acetone (1.0 mL) was stirred at 50 ˚C for 24 h. Catalysts, diols, and bases used in specific experiments are summarized in **Tables 1** and **2**. After evaporation of the acetone solvent, the crude product mixture was analyzed using ^{1}H NMR with anisole as an internal standard to determine conversion and yield.

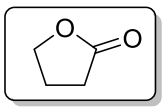

γ-Butyrolactone (Table 2 entry 1). ^{1}H NMR (400 MHz, $CDCl_3$) δ 2.08 – 2.16 (m, 2H), 2.34 (t, 2H, J_{HH} = 8.1 Hz), 4.20 (t, 2H, J_{HH} = 7.1 Hz).[14]

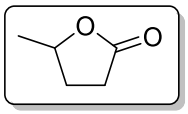

γ-Valerolactone (Table 2 entry 2). ^{1}H NMR (400 MHz, $CDCl_3$) δ 1.21 (d, 3H, J_{HH} = 6.2 Hz), 1.58 – 1.67 (m, 1H), 2.13 – 2.22 (m, 1H), 2.33 – 2.39 (m, 2H), 4.42 – 4.50 (m, 1H).[14]

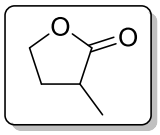

3-Methyldihydrofuran-2(3H)-one (Table 2 entry 3). ^{1}H NMR (400 MHz, $CDCl_3$) δ 1.04 (d, 3H, J_{HH} = 7.1 Hz), 1.64 – 1.75 (m, 1H), 2.19 – 2.26 (m, 1H), 2.34 – 2.48 (m, 1H), 3.93 – 3.99 (m, 1H), 4.08 – 4.13 (m, 1H).[15]

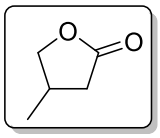

4-Methyldihydrofuran-2(3H)-one (Table 2 entry 3). ^{1}H NMR (400 MHz, $CDCl_3$) δ 0.91 – 0.94 (m, 3H), 1.64 – 1.82 (m, 1H), 2.33 – 2.50 (m, 2H), 3.61 – 3.67 (m, 1H), 4.16 – 4.20 (m, 1H).[15]

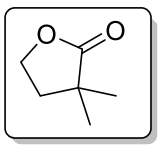

3,3-Dimethyldihydrofuran-2(3H)-one (Table 2 entry 4). ^{1}H NMR (400 MHz, $CDCl_3$) δ 1.08 (s, 6H), 1.94 (t, 2H, J_{HH} = 7.0 Hz), 4.08 (t, 2H, J_{HH} = 7.0 Hz).[16]

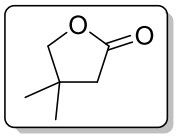

4,4-Dimethyldihydrofuran-2(3H)-one (Table 2 entry 4). ^{1}H NMR (400 MHz, $CDCl_3$) δ 1.01 (s, 6H), 2.14 (s, 2H), 3.80 (s, 2H).[16]

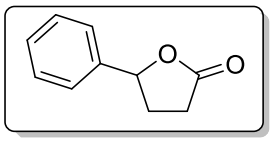

5-Phenyldihydrofuran-2(3H)-one (Table 2 entry 5). ^{1}H NMR (400 MHz, $CDCl_3$) δ 2.42 – 2.52 (m, 3H), 3.47 – 3.53 (m, 1H), 5.33 (dd, 1H, J_{HH} = 8.2, 6.0 Hz), 7.10 – 7.41 (m, 5H).[15]

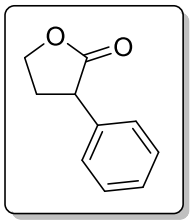

3-Phenyldihydrofuran-2(3H)-one (Table 2 entry 6). ^{1}H NMR (400 MHz, $CDCl_3$) δ 2.22 – 2.33 (m, 1H), 2.47 – 2.58 (m, 1H), 3.55 – 364 (m, 1H), 4.19 (td, 1H, J_{HH} = 9.1, 6.7 Hz), 4.32 (ddd, 1H, J_{HH} = 9.1, 8.2, 3.4 Hz), 7.21 – 7.41 (m, 5H).[15]

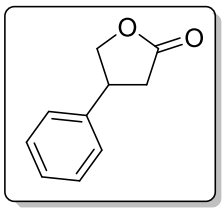

4-Phenyldihydrofuran-2(3H)-one (Table 2 entry 6). ^{1}H NMR (400 MHz, $CDCl_3$) δ 2.51 (dd, 1H, J_{HH} = 17.5, 9.1 Hz), 2.75 (dd, 1H, J_{HH} = 17.5, 8.7 Hz), 3.557 – 3.64 (m, 1H), 4.11 (dd, 1H, J_{HH} = 9.1, 8.0 Hz), 4.50 (dd, 1H, J_{HH} = 9.1, 7.8 Hz), 7.21 – 7.41 (m, 5H).[15]

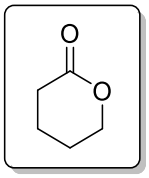

δ-Valerolactone (Table 2 entry 7). ^{1}H NMR (400 MHz, $CDCl_3$) δ 1.65 – 1.78 (m, 4H), 2.37 (t, 2H, J_{HH} = 7.0 Hz), 4.16 (t, 2H, J_{HH} = 5.6 Hz).[14]

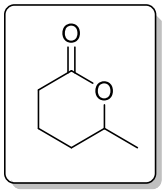

δ-Hexanolactone (Table 2 entry 8). ^{1}H NMR (400 MHz, $CDCl_3$) δ 1.33 (d, 3H, J_{HH} = 6.3 Hz), 1.47 – 1.55 (m, 1H), 1.75 – 1.93 (m, 3H), 2.35 – 2.41 (m, 1H), 2.48 – 2.58 (m, 1H), 4.37 – 4.45 (m, 1H).[17]

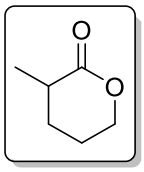

3-Methyltetrahydro-2H-pyran-2-one (Table 2 entry 9). ^{1}H NMR (400 MHz, $CDCl_3$) δ 1.07 (d, 3H, J_{HH} = 6.7 Hz), 1.31 – 1.43 (m, 1H), 1.69 – 1.95 (m, 3H), 2.38 – 2.48 (m, 1H), 4.08 – 4.16 (m, 2H).[18]

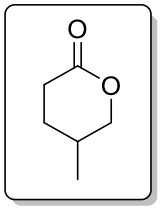

5-Methyltetrahydro-2H-pyran-2-one (Table 2 entry 9). ^{1}H NMR (400 MHz, $CDCl_3$) δ 0.82 (d, 3H, J_{HH} = 6.7 Hz), 1.31 – 1.43 (m, 1H), 1.69 – 1.95 (m, 2H), 2.26 – 2.37 (m, 1H), 2.38 – 2.48 (m, 1H), 3.72 (dd, 1H, J_{HH} = 11.1, 10.0 Hz), 4.10 – 4.14 (m, 1H).[18]

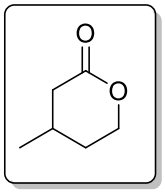

4-Methyltetrahydro-2-pyranone (Table 2 entry 10). ^{1}H NMR (400 MHz, $CDCl_3$) δ 0.86 (d, 3H, J_{HH} = 8.4 Hz), 1.27 – 1.37 (m, 1H), 1.70 – 1.76 (m, 1H), 1.86 – 1.95 (m, 2H), 2.42 – 2.50 (m, 1H), 4.04 – 4.10 (m, 1H), 4.19 – 4.24 (m, 1H).[19]

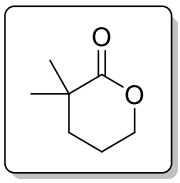

3,3-Dimethyltetrahydro-2H-pyran-2-one (Table 2 entry 11). ^{1}H NMR (400 MHz, $CDCl_3$) δ 1.15 (s, 6H), 1.59 – 1.64 (m, 2H), 1.73 – 1.79 (m, 2H), 4.20 (t, 2H, J_{HH} = 5.8 Hz).[18]

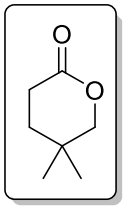

5,5-Mimethyltetrahydro-2H-pyran-2-one (Table 2 entry 11). ^{1}H NMR (400 MHz, $CDCl_3$) δ 0.91 (s, 6H), 1.55 (t, 2H, J_{HH} = 7.4 Hz), 2.40 (t, 2H, J_{HH} = 7.4 Hz), 3.83 (s, 2H).[18]

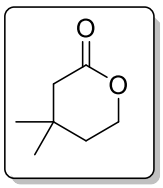

4,4-Dimethyltetrahydro-2H-pyran-2-one (Table 2 entry 12). ^{1}H NMR (400 MHz, $CDCl_3$) δ 0.96 (s, 6H), 1.57 (t, 2H, J_{HH} = 6.1 Hz), 2.19 (s, 2H), 4.23 (t, 2H, J_{HH} = 6.1 Hz).[20]

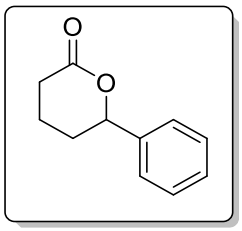

6-Phenyltetrahydro-2H-pyran-2-one (Table 2 entry 13). ^{1}H NMR (400 MHz, $CDCl_3$) δ 1.73 – 1.83 (m, 3H), 1.93 – 1.96 (m, 1H), 2.33 – 2.42 (m, 1H), 2.52 (dtd, 1H, J_{HH} = 17.8, 6.4, 1.1 Hz), 5.16 (dd, 1H, J_{HH} = 10.4, 3.4 Hz), 7.10 – 7.40 (m, 5H).[21]

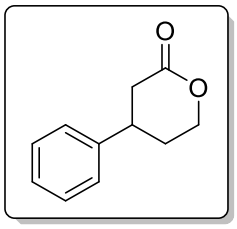

4-Phenyltetrahydro-2H-pyran-2-one (Table 2 entry 14). ^{1}H NMR (400 MHz, $CDCl_3$) δ 1.85 – 1.94 (m, 1H), 1.97 – 2.02 (m, 1H), 2.48 (dd, 1H, J_{HH} = 17.6, 10.7 Hz), 2.75 (ddd, 1H, J_{HH} = 17.6, 5.9, 1.7 Hz), 3.06 – 3.14 (m, 1H), 4.24 (ddd, 1H, J_{HH} = 11.4, 10.4, 3.8 Hz), 4.35 (ddd, 1H, J_{HH} = 11.4z, 4.9, 3.9 Hz), 7.05 – 7.26 (m, 5H).[15]

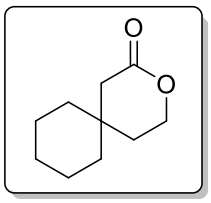

3-Oxaspiro[5.5]undecan-2-one (Table 2 entry 15). ^{1}H NMR (400 MHz, $CDCl_3$) δ 1.13 – 1.37 (m, 10H), 1.54 (t, 2H, J_{HH} = 6.1 Hz), 2.16 (s, 2H), 4.11 (t, 2H, J_{HH} = 6.1 Hz).[22]

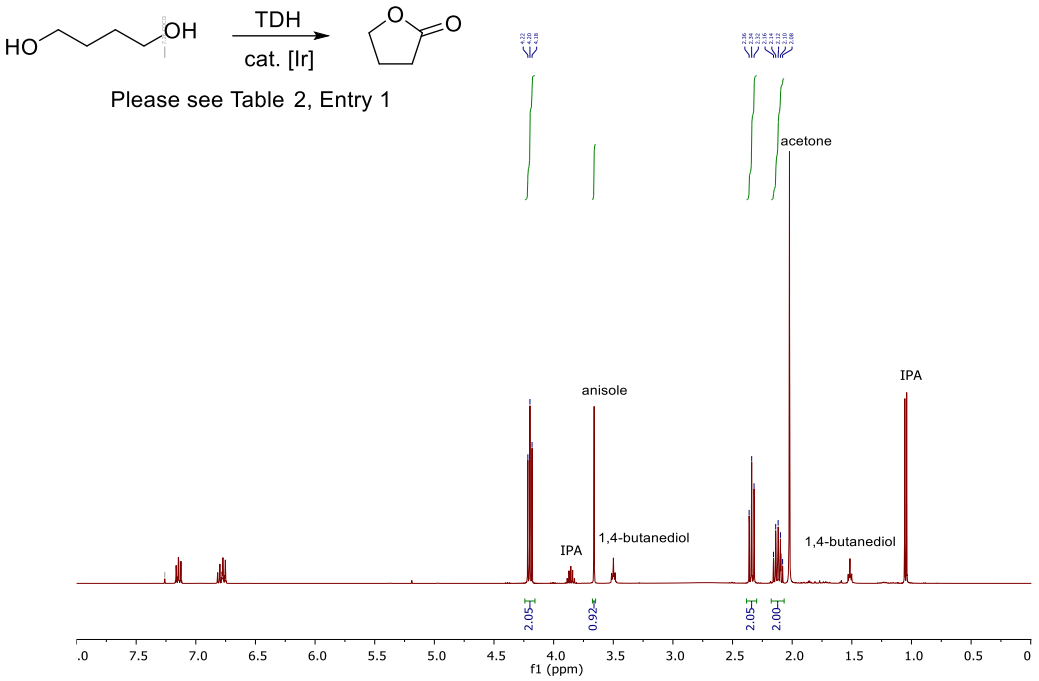

Figure S3. ^{1}H NMR spectrum ($CDCl_3$, 400 MHz) of the crude TDH reaction mixture (Table 2, entry 1) with 1,4-butanediol as the substrate, showing the quantification of γ-butyrolactone (OCH_2 at 4.2 ppm) against the internal standard, anisole (OCH_3 at 3.7 ppm).

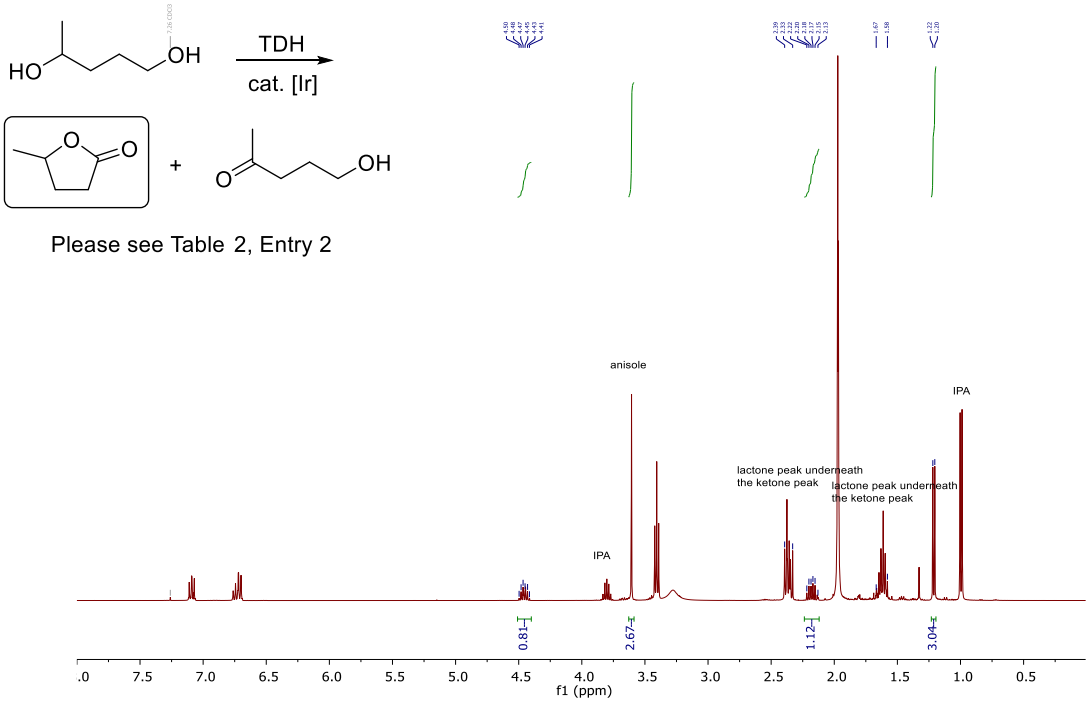

Figure S4. ^{1}H NMR spectrum ($CDCl_3$, 400 MHz) of the crude TDH reaction mixture (Table 2, entry 2) with 1,4-pentanediol as the substrate, showing the quantification of γ-valerolactone (CH_3 at 1.2 ppm) against the internal standard, anisole (OCH_3 at 3.6 ppm).

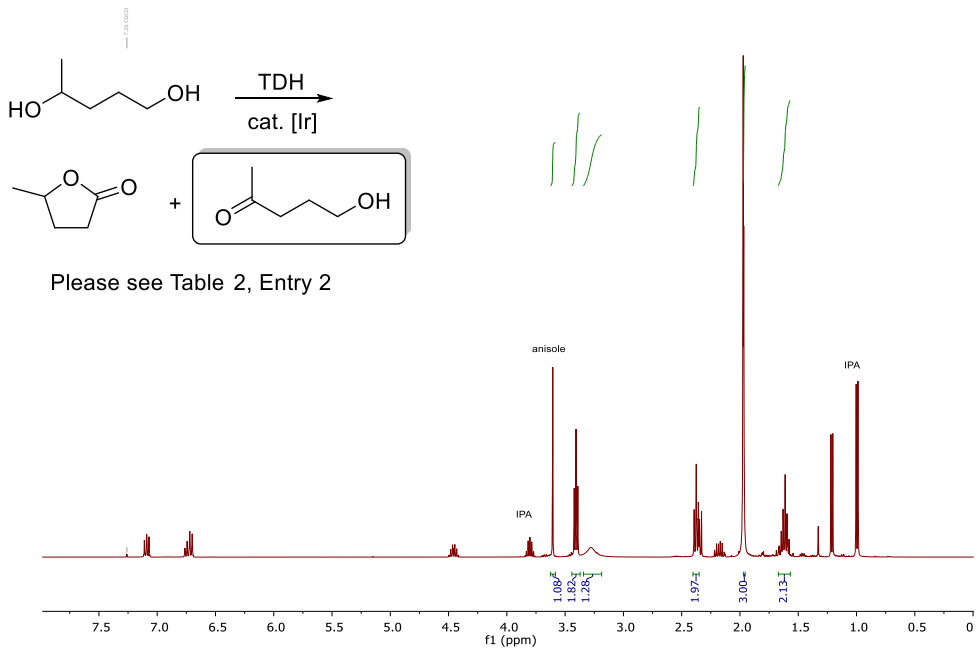

Figure S5. ^{1}H NMR spectrum ($CDCl_3$, 400 MHz) of the crude TDH reaction mixture (Table 2, entry 2) with 1,4-pentanediol as the substrate, showing the quantification of 5-hydroxy-2-pentanone ($HOC\underline{H}_2$ at 3.4 ppm) against the internal standard, anisole (OCH_3 at 3.6 ppm). Chemical shifts for 5-hydroxy-2-pentanone were confirmed by comparison to a commercial sample.[23]

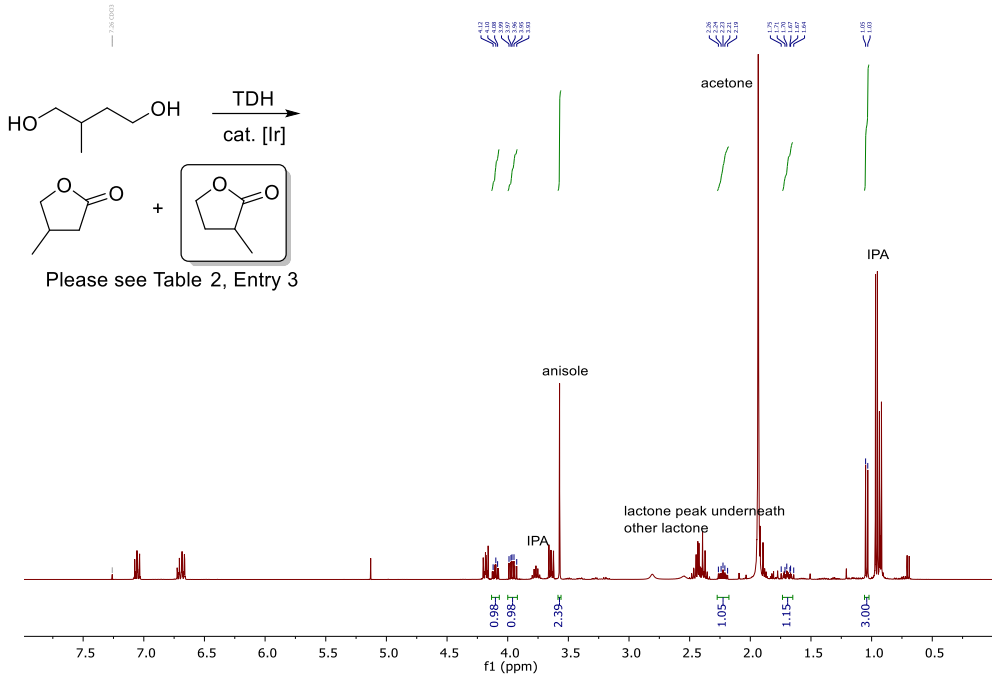

Figure S6. ^{1}H NMR spectrum ($CDCl_3$, 400 MHz) of the crude TDH reaction mixture (Table 2, entry 3) with 2-methyl-1,4-butanediol as the substrate, showing the quantification of 3-methyldihydrofuran-2(3H)-one (CH_3 at 1.04 ppm) against the internal standard, anisole (OCH_3 at 3.6 ppm).

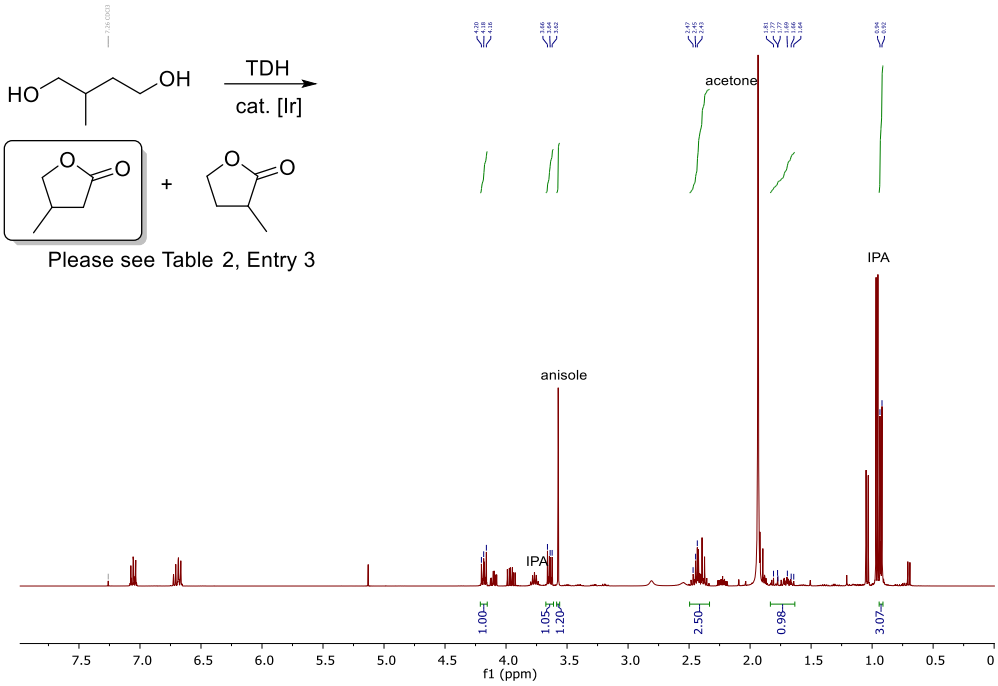

Figure S7. ^{1}H NMR spectrum ($CDCl_3$, 400 MHz) of the crude TDH reaction mixture (Table 2, entry 3) with 2-methyl-1,4-butanediol as the substrate, showing the quantification of 4-methyldihydrofuran-2(3H)-one (CH*H* at 4.18 ppm) against the internal standard, anisole (OCH_3 at 3.6 ppm).

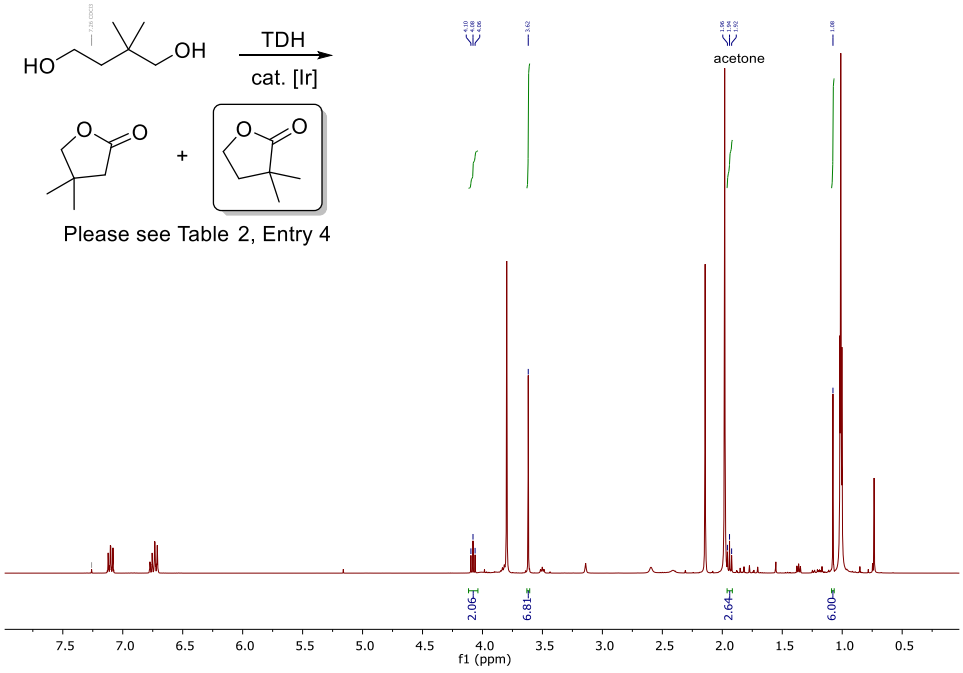

Figure S8. ^{1}H NMR spectrum ($CDCl_3$, 400 MHz) of the crude TDH reaction mixture (Table 2, entry 4) with 2,2-dimethyl-1,4-butanediol as the substrate, showing the quantification of 3,3-dimethyldihydrofuran-2(3H)-one (CH_2 at 4.08 ppm) against the internal standard, anisole (OCH_3 at 3.6 ppm).

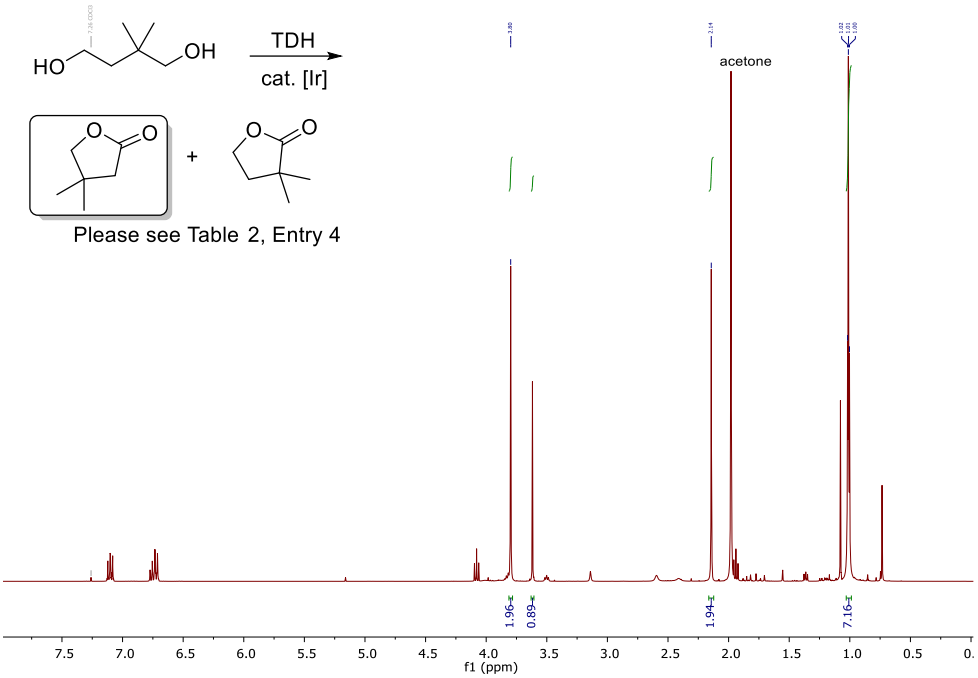

Figure S9. ^{1}H NMR spectrum ($CDCl_3$, 400 MHz) of the crude TDH reaction mixture (Table 2, entry 4) with 2,2-dimethyl-1,4-butanediol as the substrate, showing the quantification of 4,4-dimethyldihydrofuran-2(3H)-one (CH_2 at 2.14 ppm) against the internal standard, anisole (OCH_3 at 3.6 ppm).

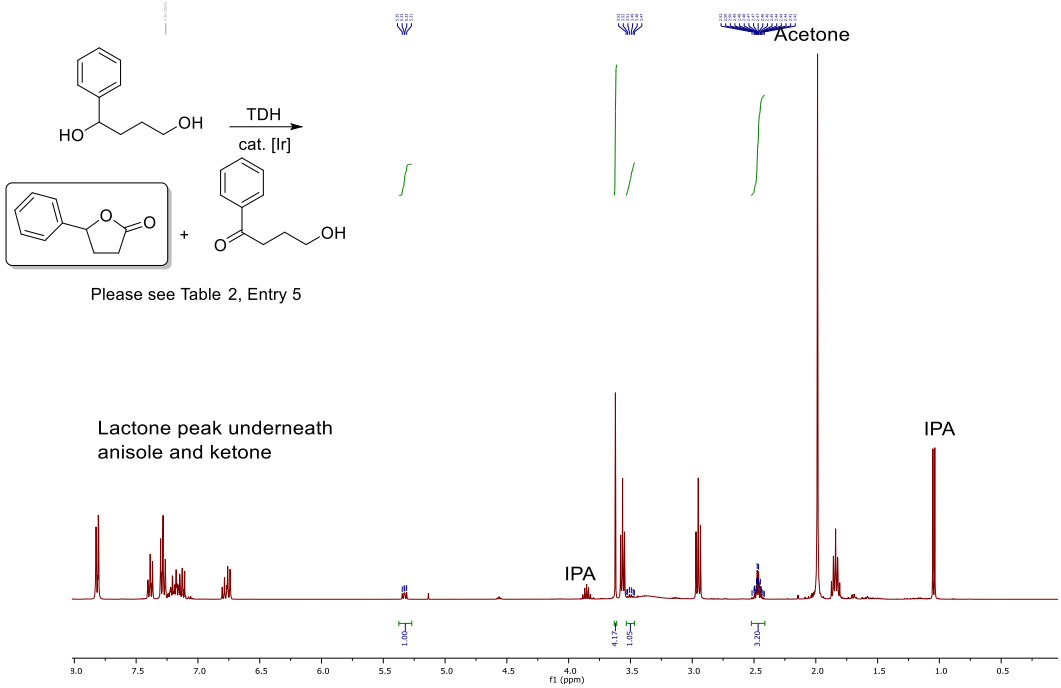

Figure S10. ^{1}H NMR spectrum ($CDCl_3$, 400 MHz) of the crude TDH reaction mixture (Table 2, entry 5) with 1-phenyl-1,4-butanediol as the substrate, showing the quantification of 5-phenyldihydrofuran-2(3H)-one (PhC*H* at 5.33 ppm) against the internal standard, anisole (OCH_3 at 3.6 ppm).

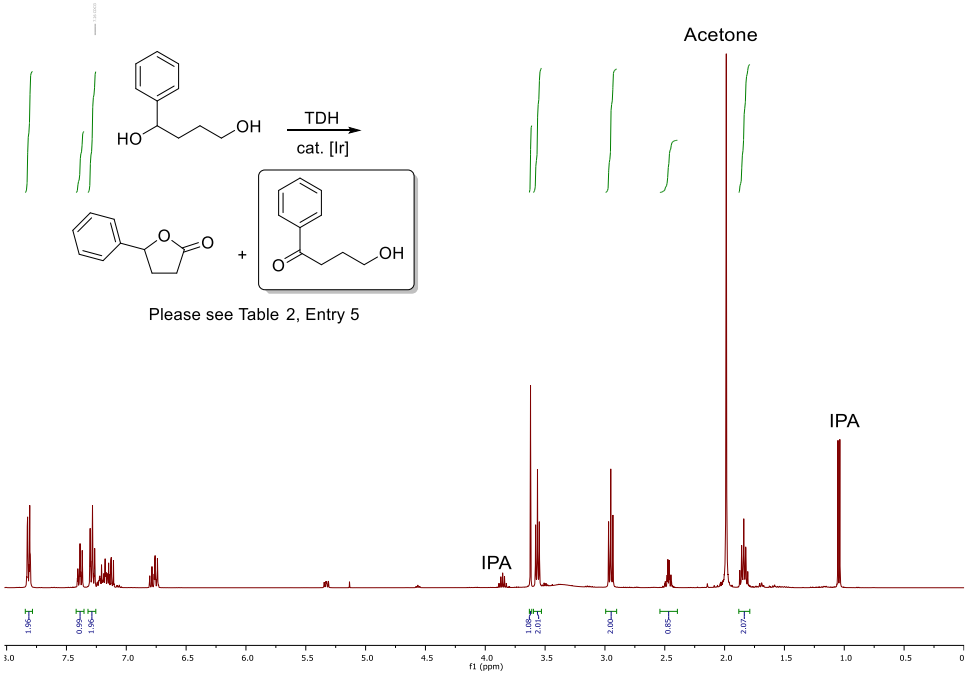

Figure S11. ^{1}H NMR spectrum ($CDCl_3$, 400 MHz) of the crude TDH reaction mixture (Table 2, entry 5) with 1-phenyl-1,4-butanediol as the substrate, showing the quantification of 4-hydroxy-1-phenylbutanone (CH_2 at 2.95 ppm) against the internal standard, anisole (OCH_3 at 3.6 ppm).[24]

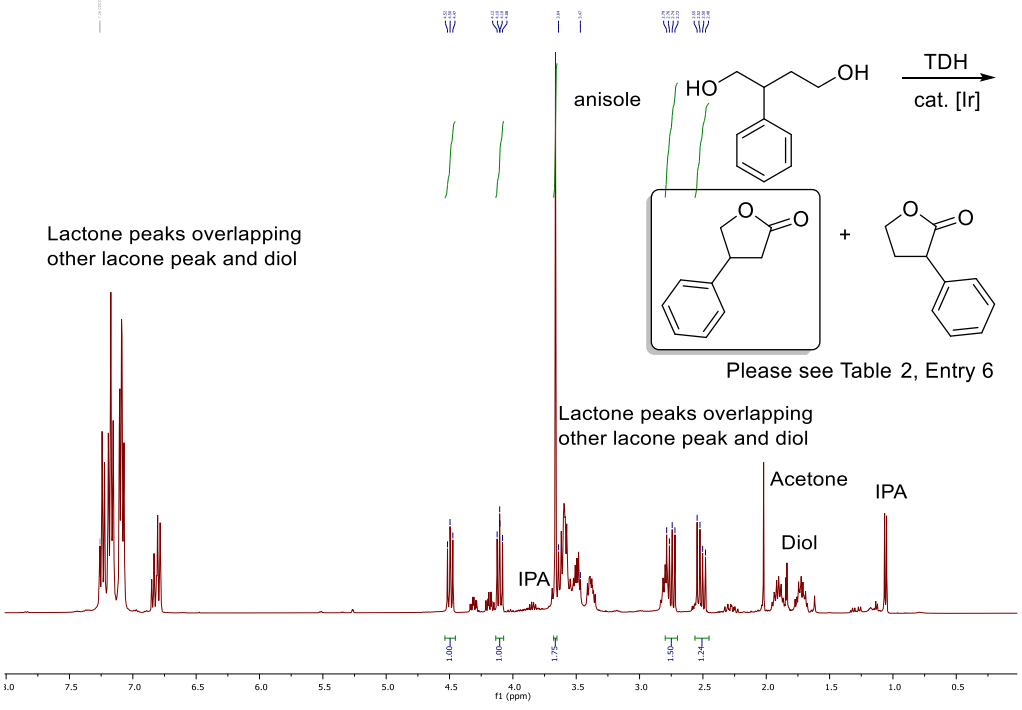

Figure S12. ^{1}H NMR spectrum ($CDCl_3$, 400 MHz) of the crude TDH reaction mixture (Table 2, entry 6) with 2-phenyl-1,4-butanediol as the substrate, showing the quantification of 4-phenyldihydrofuran-2(3H)-one (CH*H* at 4.50 ppm) against the internal standard, anisole (OCH_3 at 3.6 ppm).

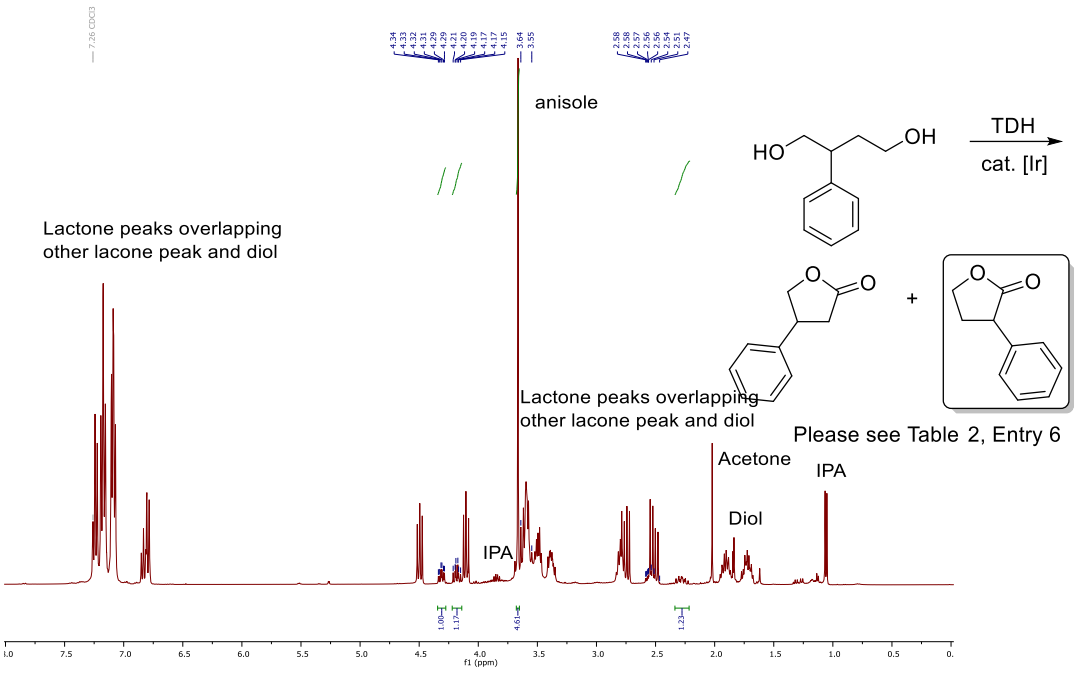

Figure S13. ^{1}H NMR spectrum ($CDCl_3$, 400 MHz) of the crude TDH reaction mixture (Table 2, entry 6) with 2-phenyl-1,4-butanediol as the substrate, showing the quantification of 3-phenyldihydrofuran-2(3H)-one (CH*H* at 4.18 ppm) against the internal standard, anisole (OCH_3 at 3.6 ppm).

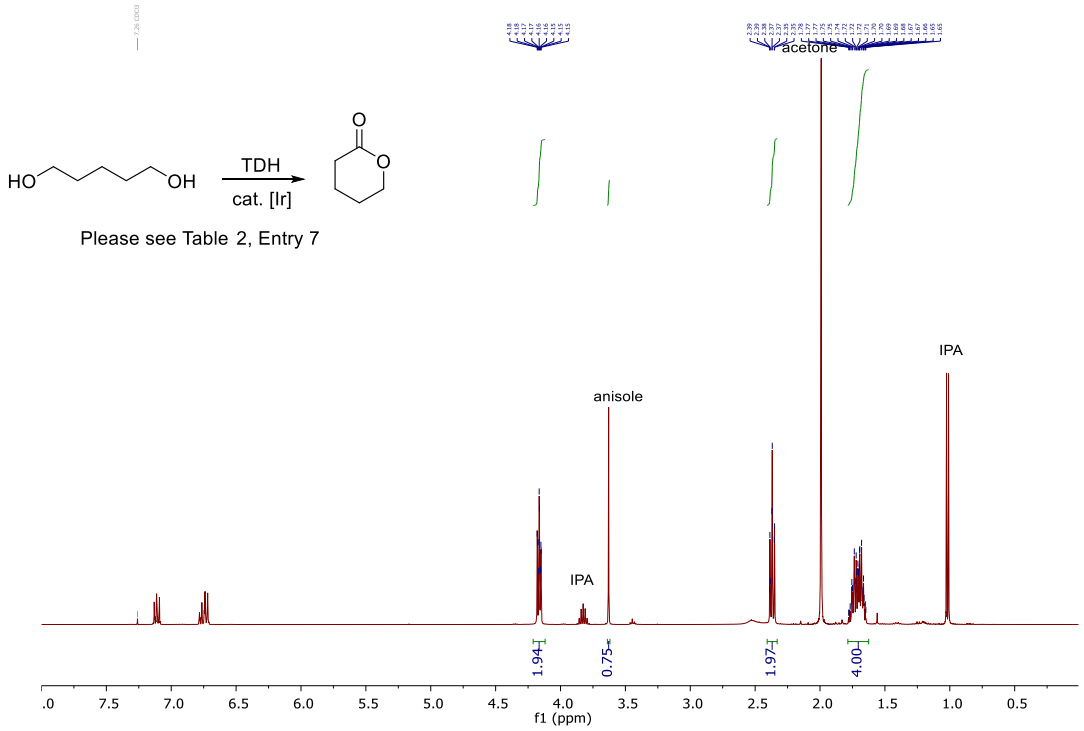

Figure S14. ^{1}H NMR spectrum ($CDCl_3$, 400 MHz) of the crude TDH reaction mixture (Table 2, entry 7) with 1,5-pentanediol as the substrate, showing the quantification of □-valerolactone ($OC\underline{H}_2$ at 4.2 ppm) against the internal standard, anisole (OCH_3 at 3.6 ppm).

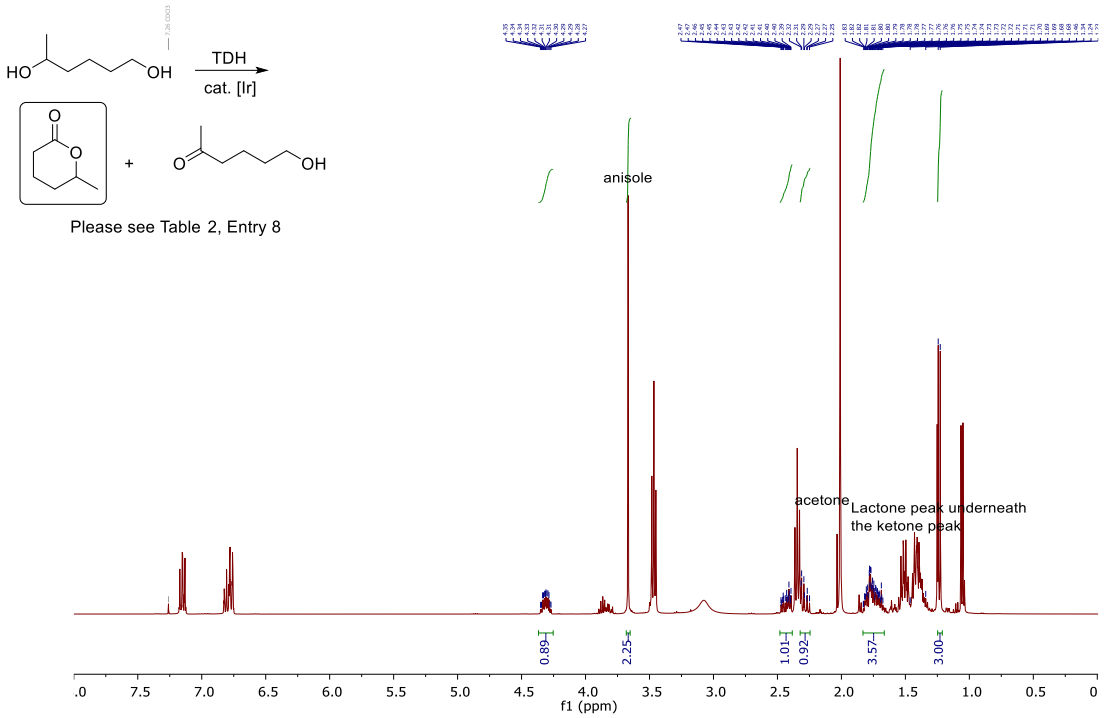

Figure S15. ^{1}H NMR spectrum ($CDCl_3$, 400 MHz) of the crude TDH reaction mixture (Table 2, entry 8) with 1,5-hexanediol as the substrate, showing the quantification of δ-hexanolactone ($OC\underline{H}CH_3$ at 4.3 ppm) against the internal standard, anisole (OCH_3 at 3.6 ppm).

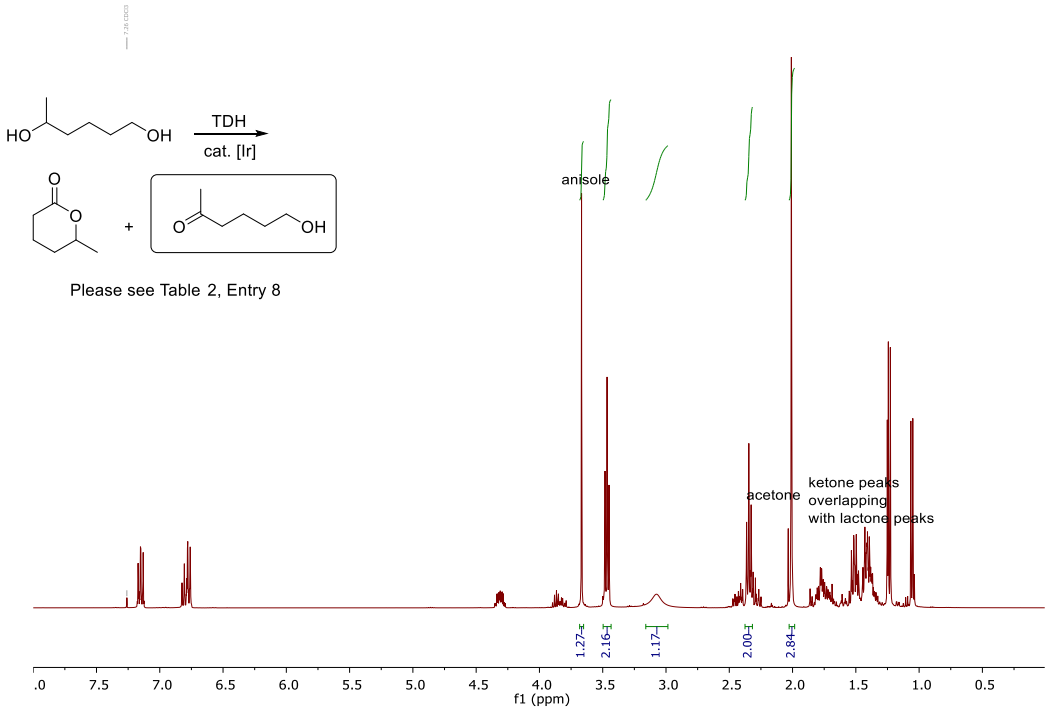

Figure S16. ^{1}H NMR spectrum ($CDCl_3$, 400 MHz) of the crude TDH reaction mixture (Table 2, entry 8) with 1,5-hexanediol as the substrate, showing the quantification of 6-hydroxy-2-hexanone ($HOC\underline{H}_2$ at 3.5 ppm) against the internal standard, anisole (OCH_3 at 3.6 ppm).[25]

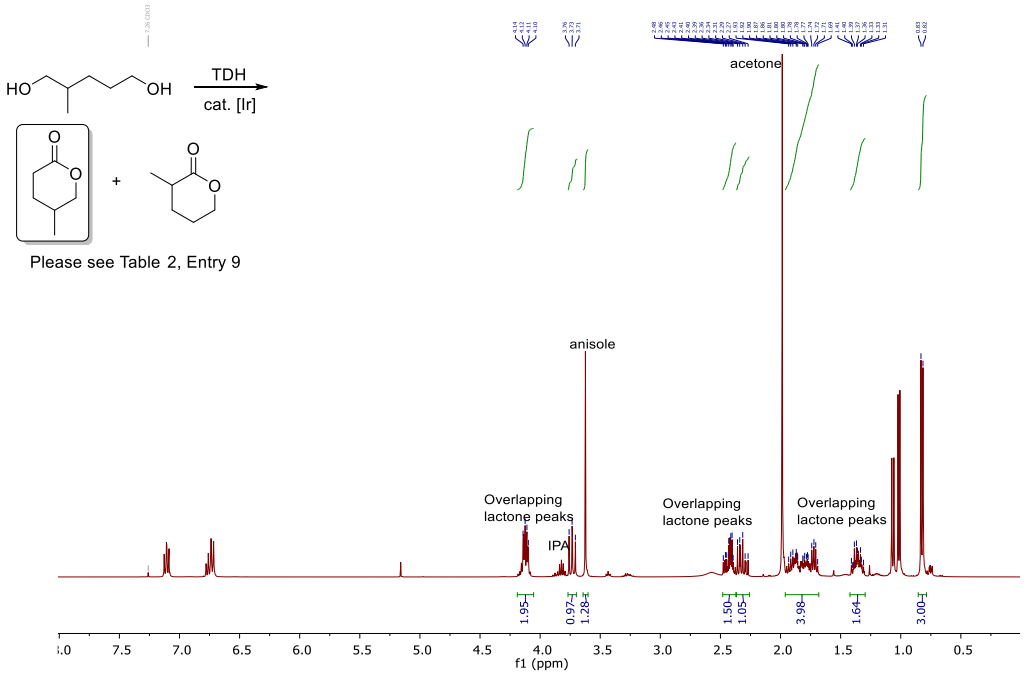

Figure S17. ^{1}H NMR spectrum ($CDCl_3$, 400 MHz) of the crude TDH reaction mixture (Table 2, entry 9) with 2-methyl-1,5-pentanediol as the substrate, showing the quantification of 5-methyltetrahydro-2H-pyran-2-one (CH_3 at 0.82 ppm) against the internal standard, anisole (OCH_3 at 3.6 ppm).

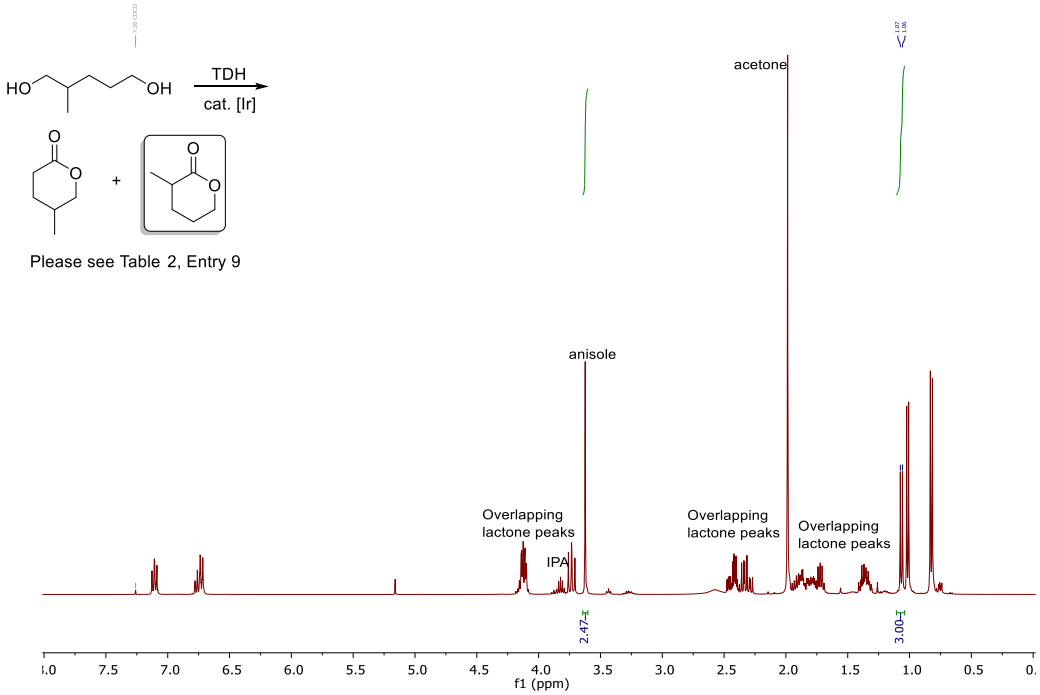

Figure S18. ^{1}H NMR spectrum ($CDCl_3$, 400 MHz) of the crude TDH reaction mixture (Table 2, entry 9) with 2-methyl-1,5-pentanediol as the substrate, showing the quantification of 3-methyltetrahydro-2H-pyran-2-one (CH_3 at 1.06 ppm) against the internal standard, anisole (OCH_3 at 3.6 ppm).

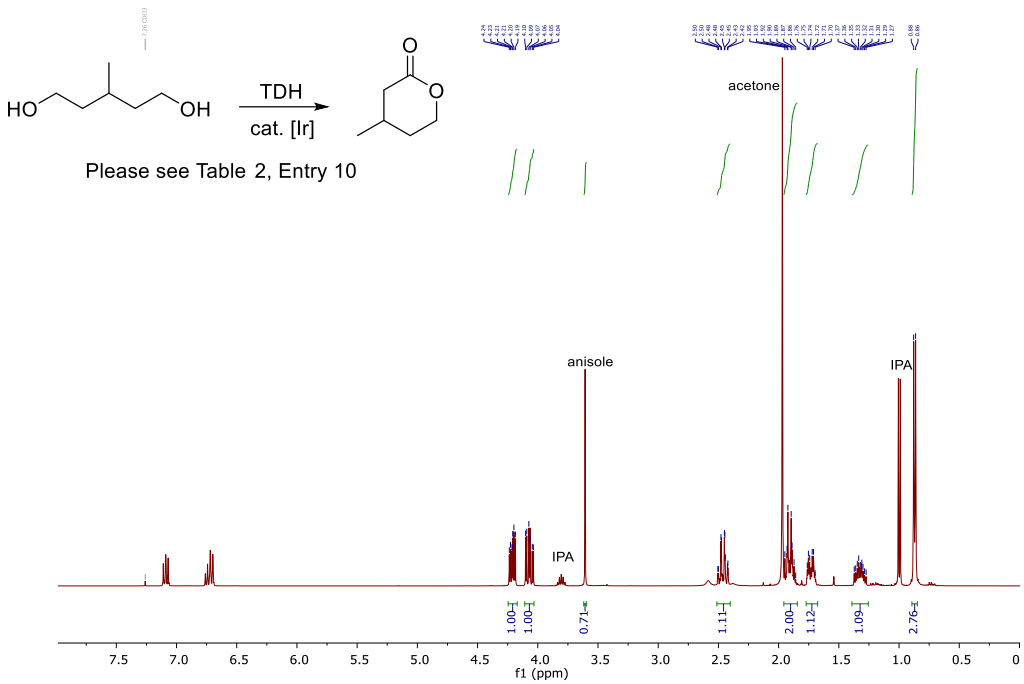

Figure S19. ^{1}H NMR spectrum ($CDCl_3$, 400 MHz) of the crude TDH reaction mixture (Table 2, entry 10) with 3-methyl-1,5-pentanediol as the substrate, showing the quantification of 4-methyltetrahydro-2-pyranone (CH_3 at 0.9 ppm) against the internal standard, anisole (OCH_3 at 3.6 ppm).

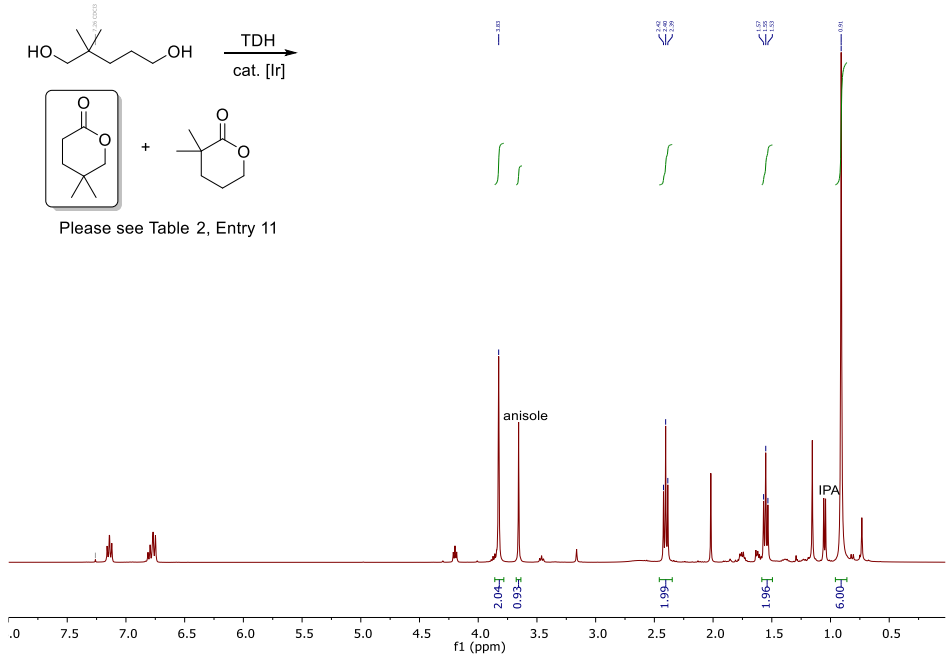

Figure S20. ^{1}H NMR spectrum ($CDCl_3$, 400 MHz) of the crude TDH reaction mixture (Table 2, entry 11) with 2,2-dimethyl-1,5-pentanediol as the substrate, showing the quantification of 5,5-dimethyltetrahydro-2H-pyran-2-one (CH_3 at 0.91 ppm) against the internal standard, anisole (OCH_3 at 3.6 ppm).

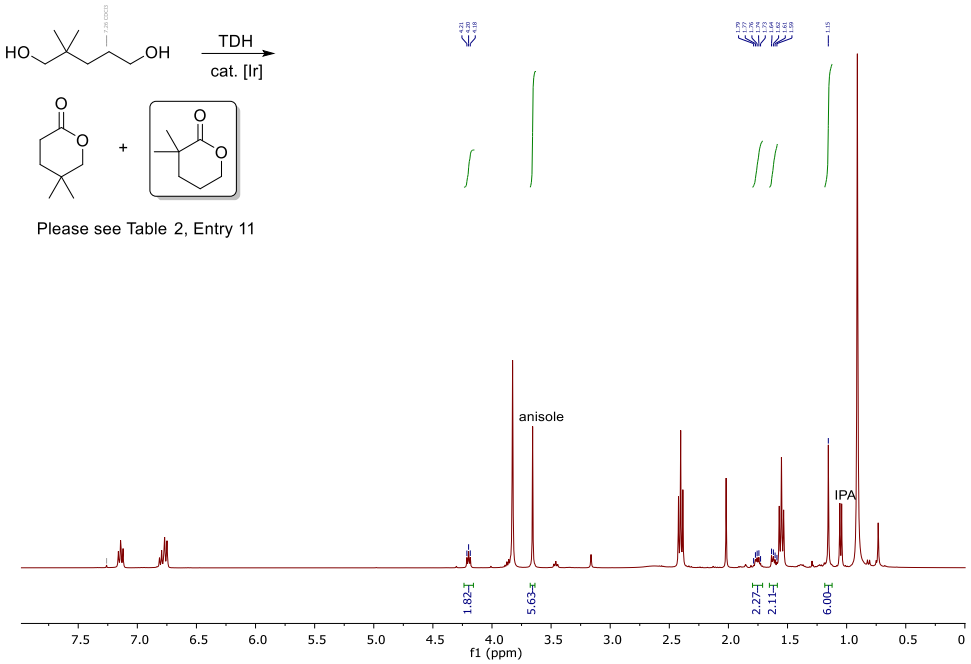

Figure S21. ^{1}H NMR spectrum ($CDCl_3$, 400 MHz) of the crude TDH reaction mixture (Table 2, entry 11) with 2,2-dimethyl-1,5-pentanediol as the substrate, showing the quantification of 3,3-dimethyltetrahydro-2H-pyran-2-one (CH_3 at 0.91 ppm) against the internal standard, anisole (OCH_3 at 3.6 ppm).

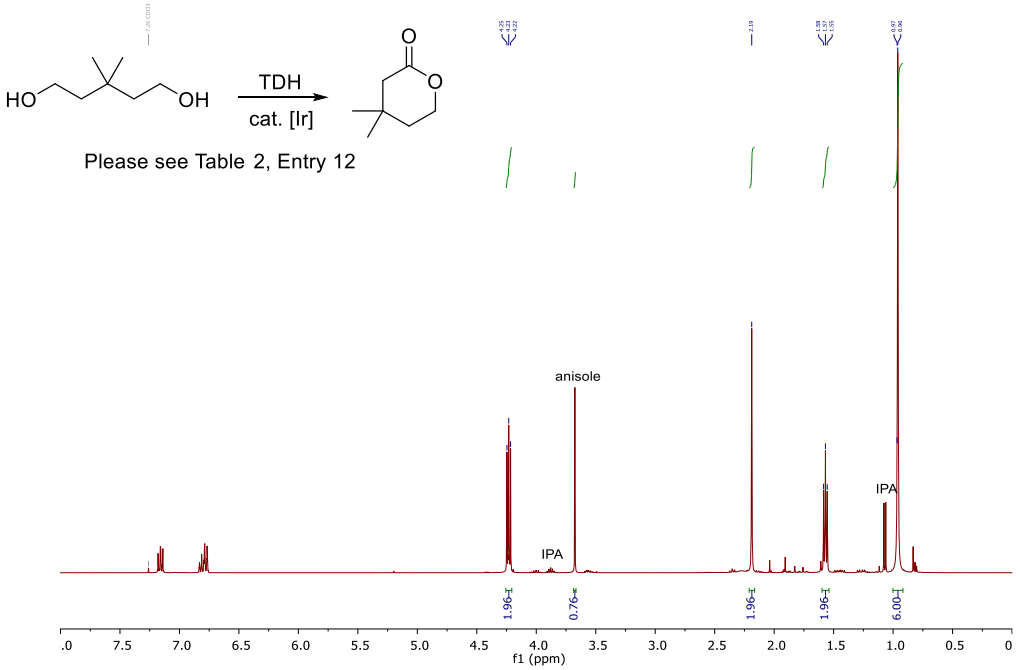

Figure S22. ^{1}H NMR spectrum ($CDCl_3$, 400 MHz) of the crude TDH reaction mixture (Table 2, entry 12) with 3,3-dimethyl-1,5-pentanediol as the substrate, showing the quantification of 4,4-dimethyltetrahydro-2-pyranone (CH_3 at 0.96 ppm) against the internal standard, anisole (OCH_3 at 3.6 ppm).

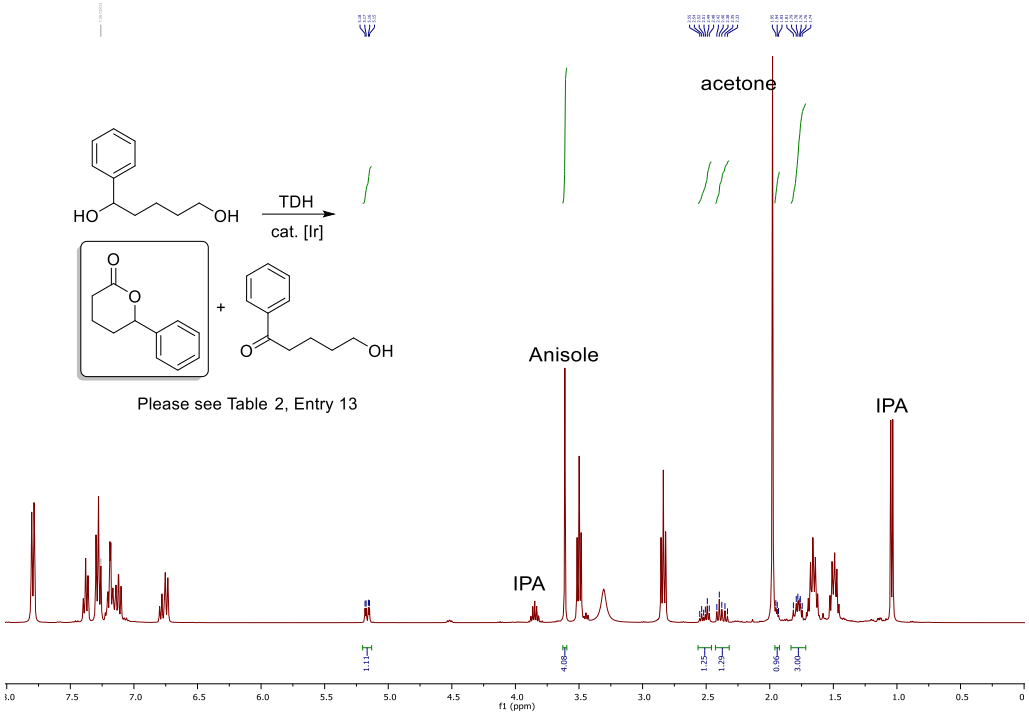

Figure S23. ^{1}H NMR spectrum ($CDCl_3$, 400 MHz) of the crude TDH reaction mixture (Table 2, entry 13) with 1-phenyl-1,5-pentanediol as the substrate, showing the quantification of 6-phenyltetrahydro-2H-pyran-2-one (CH*H* at 5.15 ppm) against the internal standard, anisole (OCH_3 at 3.6 ppm).

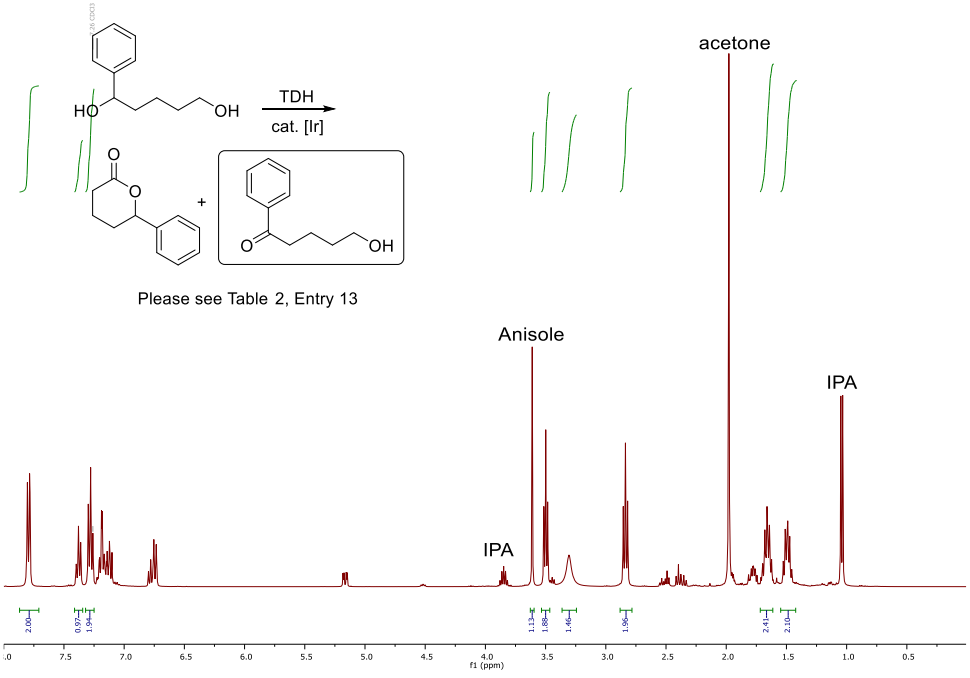

Figure S24. ^{1}H NMR spectrum ($CDCl_3$, 400 MHz) of the crude TDH reaction mixture (Table 2, entry 13) with 1-phenyl-1,5-pentanediol as the substrate, showing the quantification of 5-hydroxy-1-phenylpentanone (CH_2 at 3.50 ppm) against the internal standard, anisole (OCH_3 at 3.6 ppm).[24]

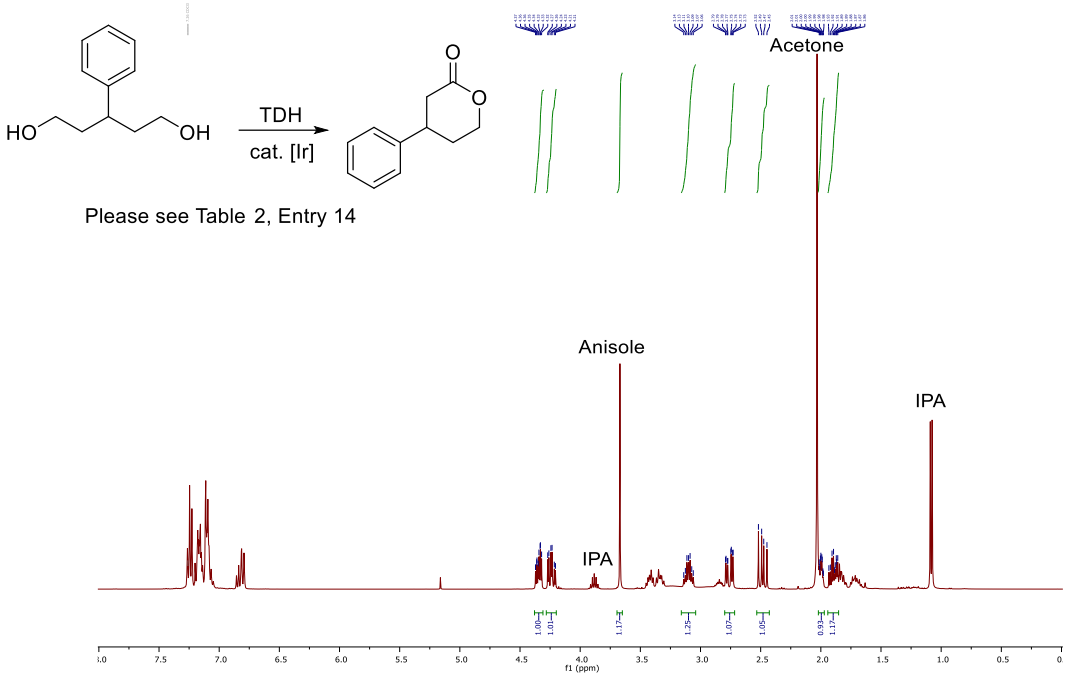

Figure S25. ^{1}H NMR spectrum ($CDCl_3$, 400 MHz) of the crude TDH reaction mixture (Table 2, entry 14) with 3-phenyl-1,5-pentanediol as the substrate, showing the quantification of 4-phenyltetrahydro-2-pyranone (CH*H* at 4.24 ppm) against the internal standard, anisole (OCH_3 at 3.6 ppm).

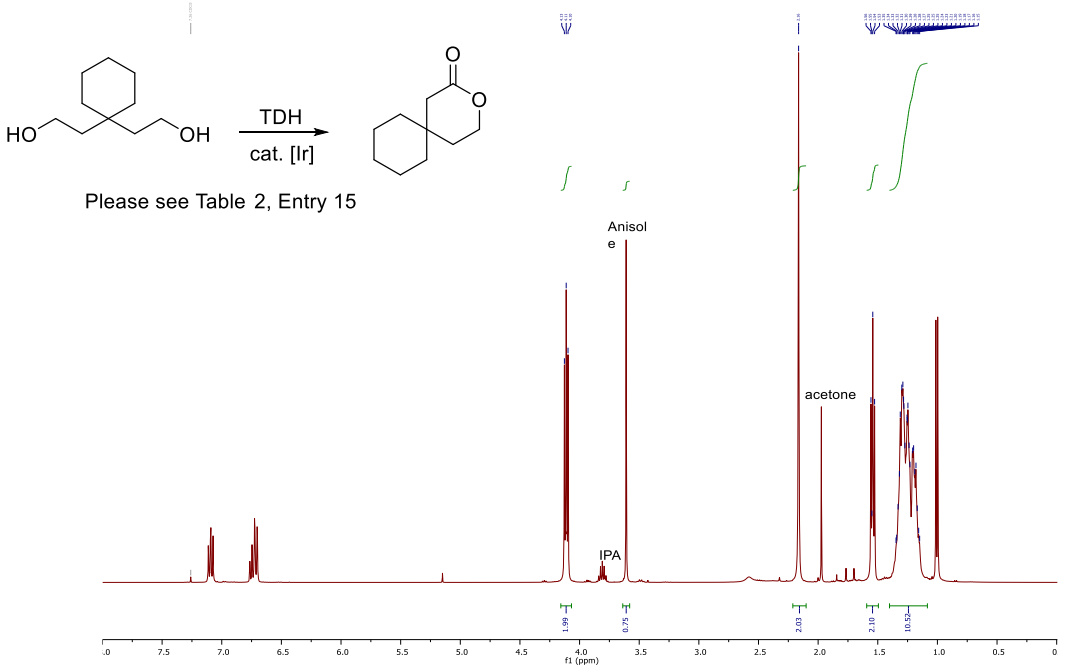

Figure S26. ^{1}H NMR spectrum ($CDCl_3$, 400 MHz) of the crude TDH reaction mixture (Table 2, entry 15) with 1,1-bis(2-hydroxyethyl)cyclohexane) as the substrate, showing the quantification of 3-oxaspiro[5.5]undecan-2-one (CH_2 at 4.11 ppm) against the internal standard, anisole (OCH_3 at 3.6 ppm).

5.4.5.1 Kinetics

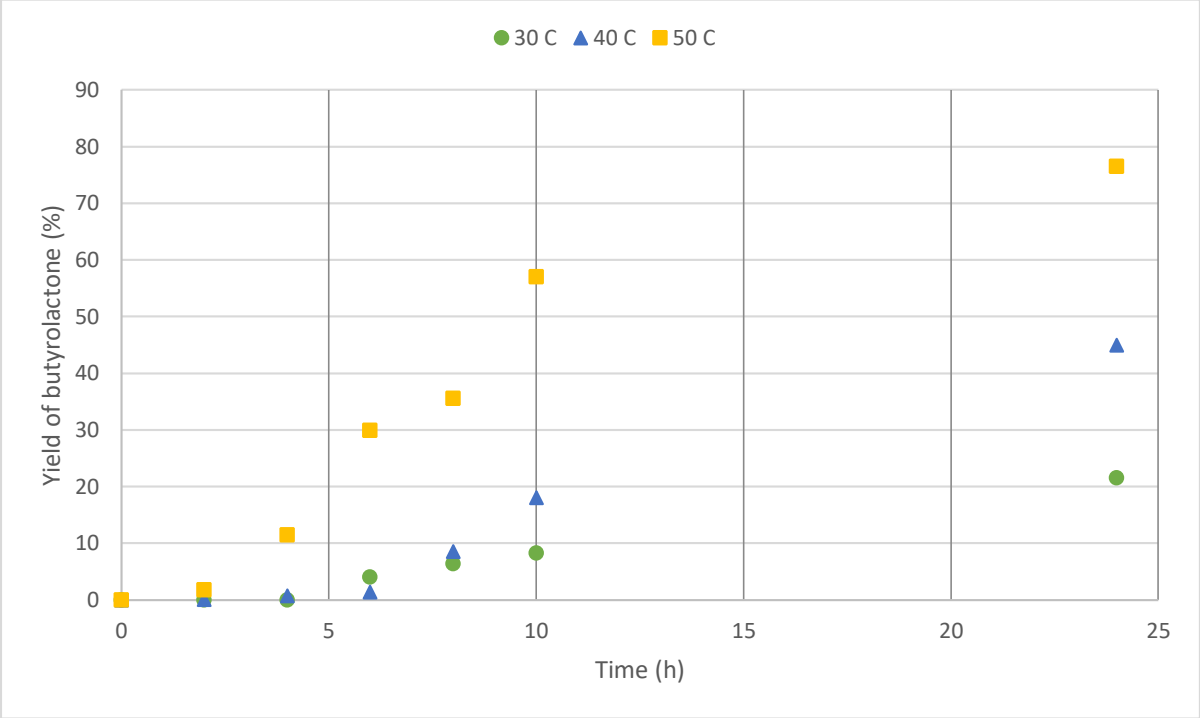

Figure S27. Formation of γ-butyrolactone from 1,4-butanediol (2.0 mmol), $NaHCO_3$ (0.20 mmol), and iridium catalyst **1a** (0.02 mmol) in acetone (2.0 mL) for 24 h at three different temperatures. Yields were determined by ^1H NMR analysis using anisole as an internal standard. A significant induction period is noted.

5.4.5.2 Kinetic isotope effect (KIE) studies

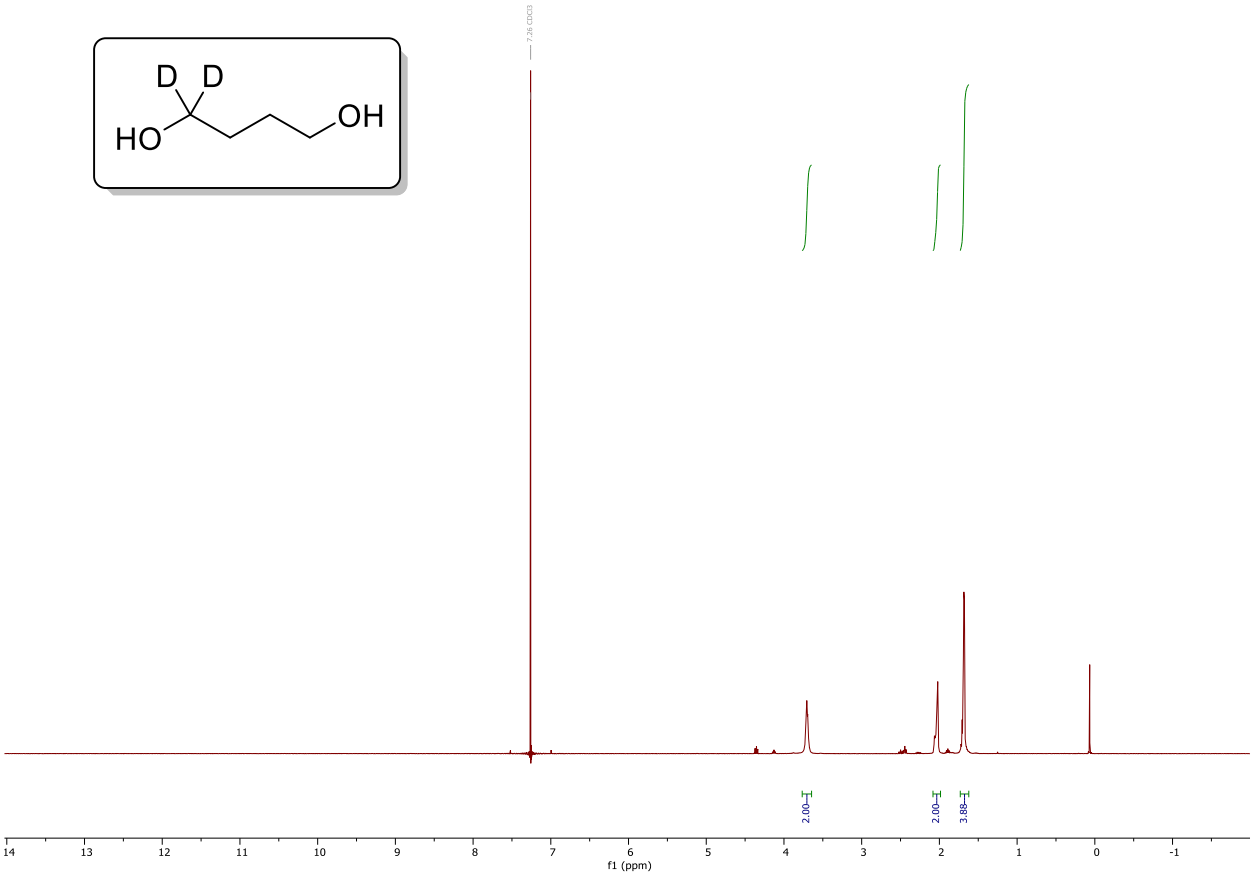

Figure S28. ^{1}H NMR spectrum ($CDCl_3$, 400 MHz) of 1,1-dideuterio-1,4-butanediol.

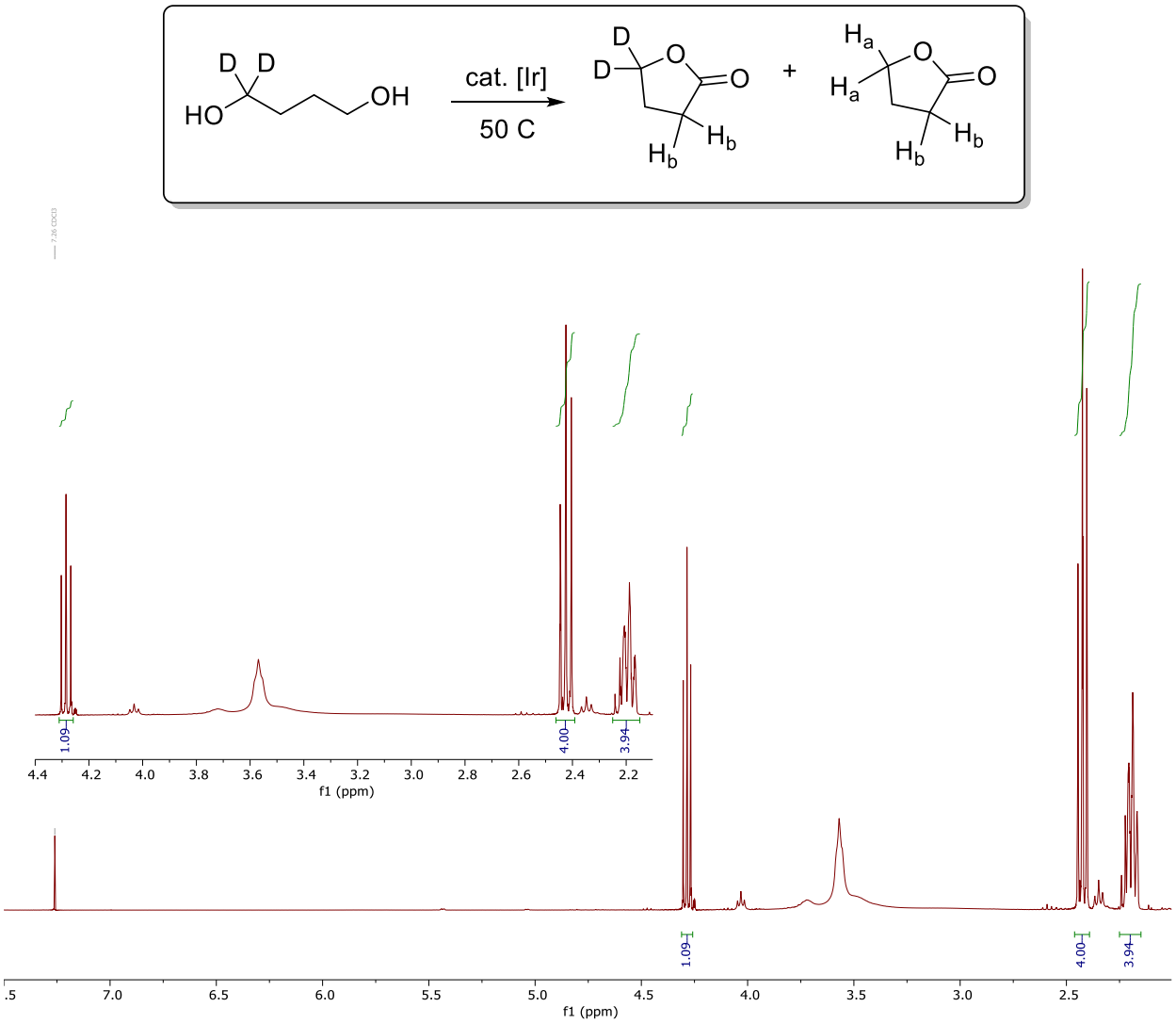

Figure S29. ^{1}H NMR spectrum ($CDCl_3$, 400 MHz) of the crude oxidative lactonization reaction mixture with 1,1-dideuterio-1,4-butanediol as the substrate. If the mole fraction of deuterated lactone (arising from beta-^{1}H transfer) is χ, then $\frac{Ia}{Ib} = 1 - \chi$, where I_a is the intensity of the CH_2O signal (γ-butyrolactone), and I_b is the intensity of the alpha CH_2 signal (γ-butyrolactone + γ-butyrolactone-d_2). Using the integrals I_a = 1.09 and I_b = 4.00, we find χ = 0.73. To determine the kinetic isotope effect (KIE), we used the following equation $\frac{\chi}{1-\chi} = \frac{kH}{kD} = \frac{0.73}{0.27} = 2.7$.

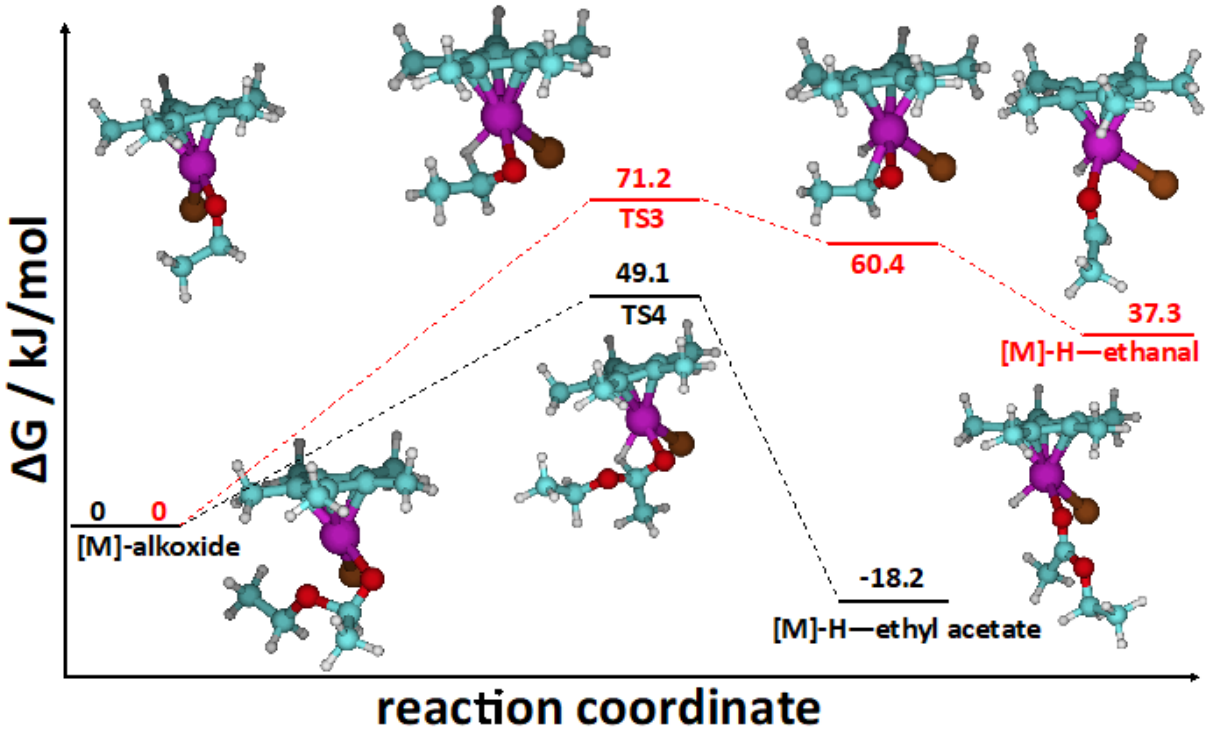

Figure S30. Reaction pathways for β-hydrogen elimination of ethanol (red) and the hemiacetal resulting from addition of ethanol to ethanal (black) as catalyzed by $[(\eta^5\text{-}Me_5C_5)IrCl]_2(\mu^2\text{-}Cl)_2$. For each pathway, the alkoxide bound to the catalyst following ligand substitution is taken as the zero of energy. Energies were calculated using M06-L/def2TZVP//def2SVP; refer to Experimental Section of text for further details. Top insets are for the ethanol reaction, and bottom insets for the hemiacetal one.

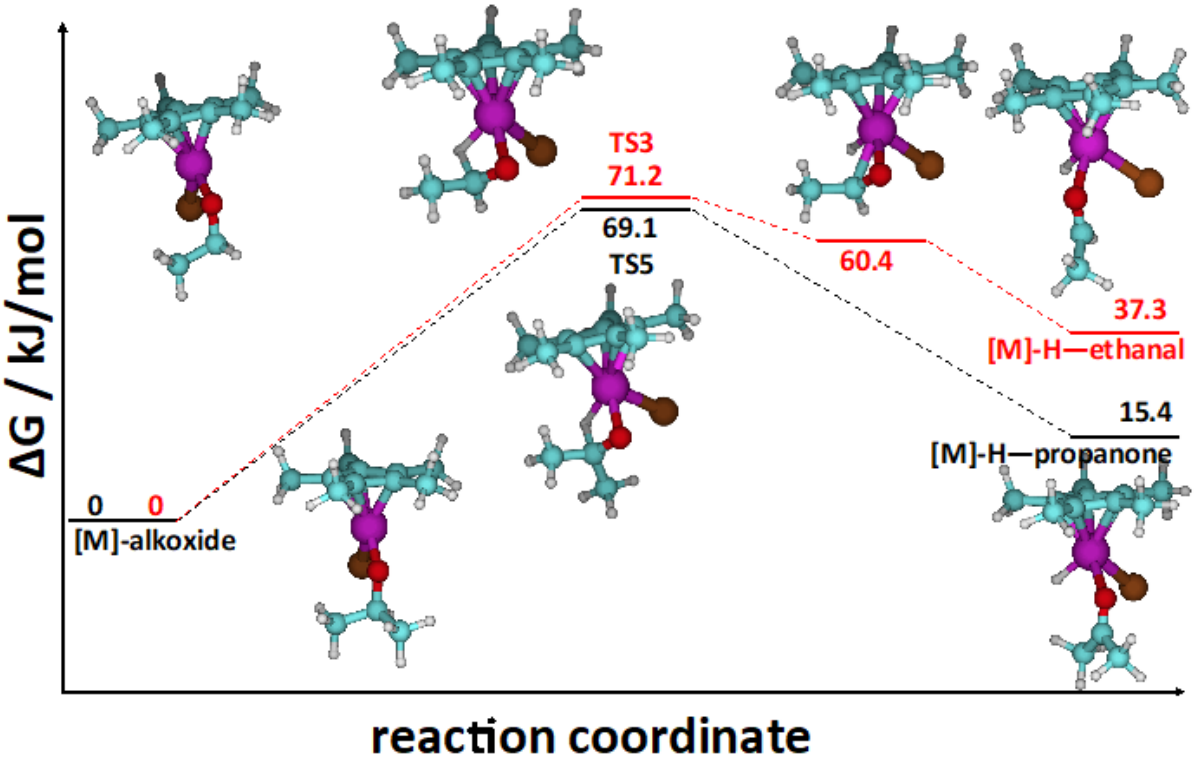

Figure S31. Reaction pathways for β-hydrogen elimination of ethanol (red) and isopropanol (black) as catalyzed by $[(\eta^5\text{-}Me_5C_5)IrCl]_2(\mu^2\text{-}Cl)_2$. For each pathway, the alkoxide bound to the catalyst following ligand substitution is taken as the zero of energy. Energies were calculated using M06-L/def2TZVP//def2SVP; refer to Experimental Section of text for further details. Top insets are for the ethanol reaction, and bottom insets for the isopropanol one. Same color scheme as in Figure 3.

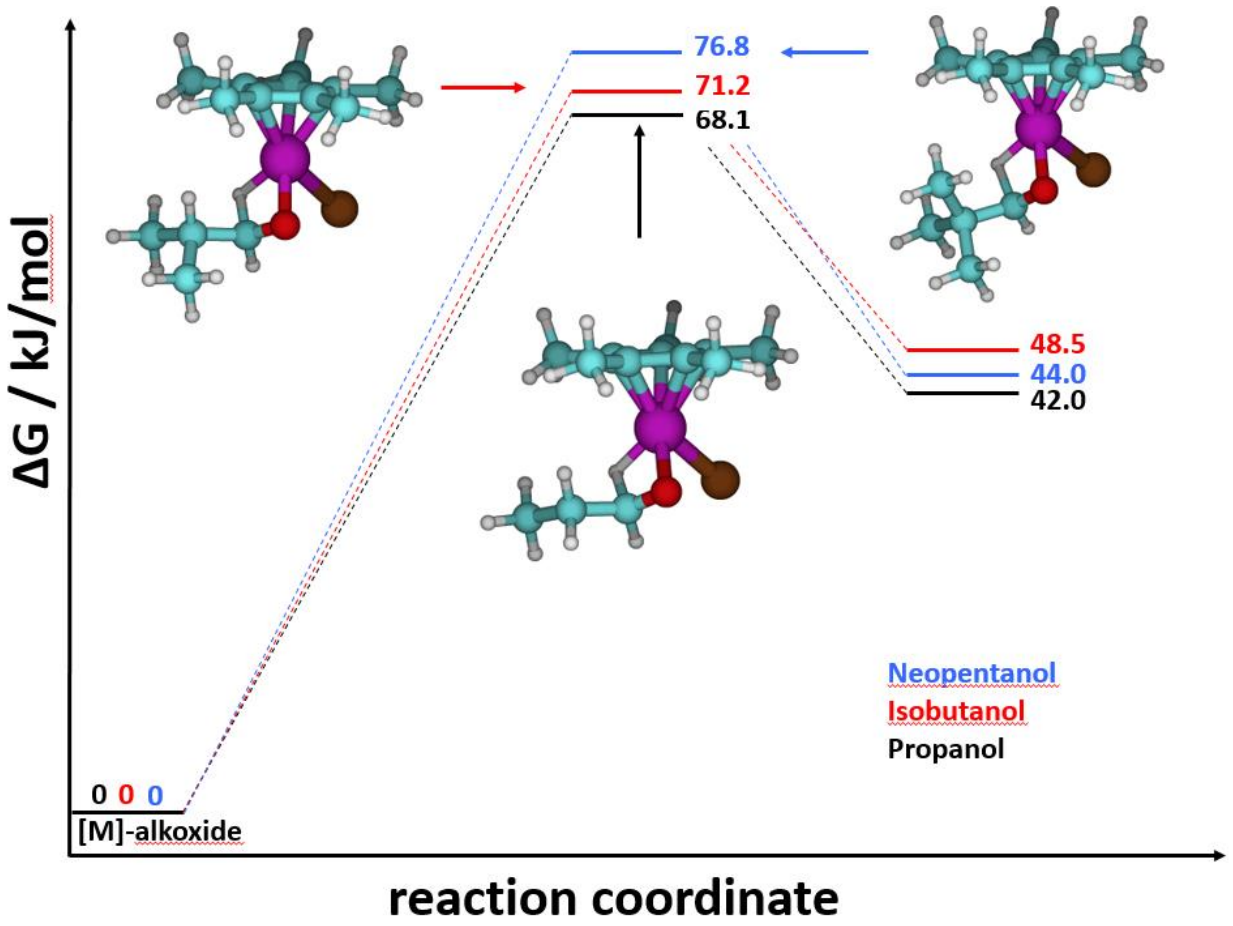

Figure S32. Reaction pathways for β-hydrogen elimination of propanol (black), isobutanol (red), and neopentanol (blue) as catalyzed by $[(\eta^5\text{-}Me_5C_5)IrCl]_2(\mu^2\text{-}Cl)_2$. For each pathway, the alkoxide bound to the catalyst following ligand substitution is taken as the zero of energy. Energies were calculated using M06-L/def2TZVP//def2SVP; refer to Experimental Section of text for further details. Insets are for transition-state structures. Same color scheme as in Figure 3.

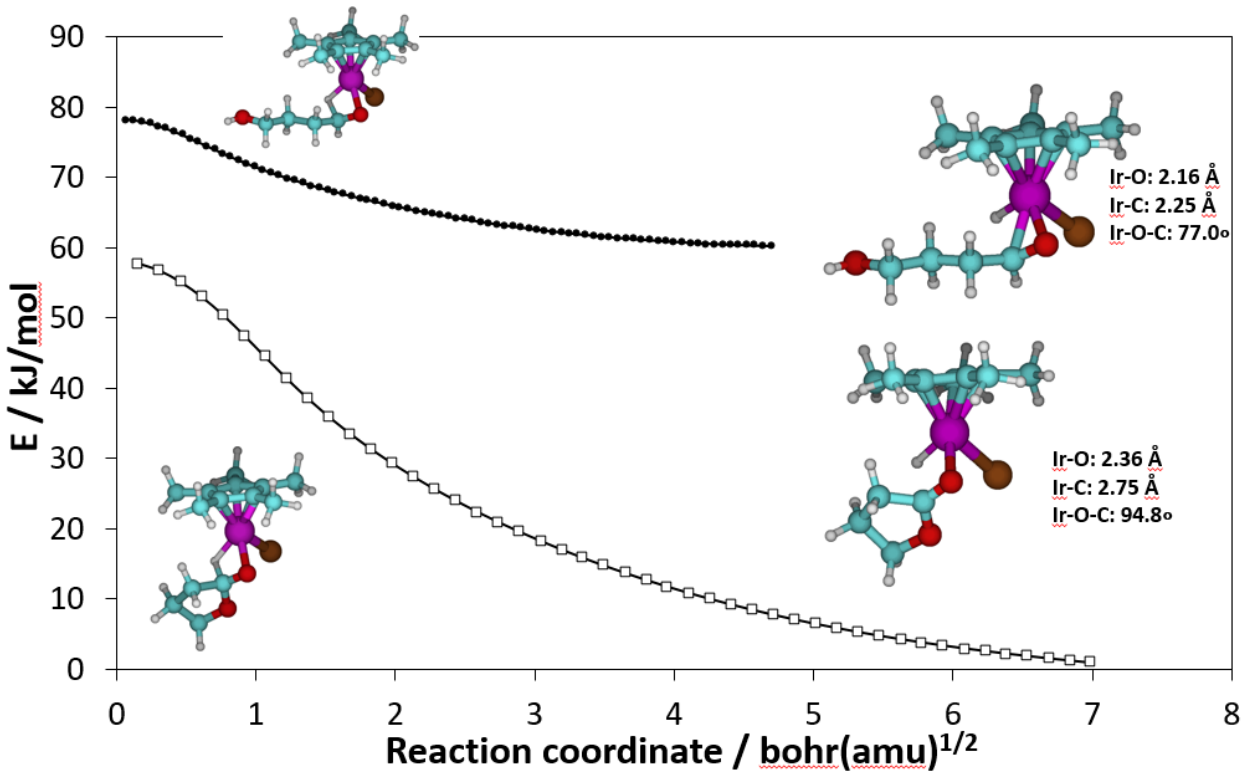

Figure S33. Minimum energy reaction paths (MERP) from the beta hydrogen elimination transition states from 1,4-butanediol (top) and butyrolactol (bottom) toward products. The MERP for the reaction with the normal alcohol finishes in an η2-aldehyde minimum. There is no η2 minimum in the reaction with the lactol. The insets show the transition states, the η2-aldehyde minimum for the 1,4-butanediol reaction, and an intermediate structure for the lactol reaction showing the absence of η2 lactone coordination.

[M]=Cp*IrCl

M06-L/def2tzvp (PCM) // M06-L/def2svp

[M]Cl-[M]Cl → 2[M]Cl ΔG = -31.5 kJ/mol Monomerization

Mechanism

[M]Cl + $HO(CH_2)_4OH$ + HCO_3^- → [M]-$O(CH_2)_4OH$ + H_2CO_3 + Cl^- ΔG = +45.8 kJ/mol	Diol binding. Base removes proton. Cl^- leaves
[M]-$O(CH_2)_4OH$ → [M](H)-$O{=}CH(CH_2)_3OH$ ΔG = +43.8 kJ/mol	Beta elimination
[M](H)-$O{=}CH(CH_2)_3OH$ + $(CH_3)_2C{=}O$ + H_2CO_3 + Cl^- → [M]-Cl + $O{=}CH(CH_2)_3OH$ + $(CH_3)_2CHOH$ + HCO_3^- ΔG = -69.8 kJ/mol	Aldehyde dissociation acetone reduction, catalyst and base regeneration
$O{=}CH(CH_2)_3OH$ → HO-(cyclo-C_4H_7O) ΔG = +7.6 kJ/mol	Lactolization
[M]Cl + HO-(cyclo-C_4H_7O) + HCO_3^- → [M]-O-(cyclo-C_4H_7O) + H_2CO_3 + Cl^- ΔG = +49.2 kJ/mol	Lactol binding. Base removes proton. Cl^- leaves
[M]-O-(cyclo-C_4H_7O) → [M](H)-lactone ΔG = -32.3 kJ/mol	Beta elimination
[M](H)-lactone + $(CH_3)_2C{=}O$ + H_2CO_3 + Cl^- → [M]-Cl + lactone + $(CH_3)_2CHOH$ + HCO_3^- ΔG = -66.8 kJ/mol	Lactone dissociation, acetone reduction, catalyst and base regeneration

Overall: Diol + $2(CH_3)_2C{=}O$ → Lactone + $2(CH_3)_2CHOH$ ΔG = -22.6 kJ/mol

Figure S34. Mechanistic catalytic sequence of the 1,4-butanediol → butyrolactone reaction as catalyzed by $[(\eta^5\text{-}Me_5C_5)IrCl]_2(\mu^2\text{-}Cl)_2$ including the Gibbs energies (298 K, 1 atm) for the individual steps.

Table S1. Activation Gibbs energies (298 K, 1 atm) for beta-elimination of 1,4-butanediol and ensuing lactol product (kJ/mol).[a]

	1,4-butanediol → 4-hydroxybutanal	butyrolactol→butyrolactone
M06-L	69.2	48.3
B3LYP	79.5	63.0
wB97X-D	56.2	49.2
M06	62.3	48.4
PBE1PBE	60.0	45.8
B97D	54.7	45.1

[a] Single-point calculations with the def2TZVP basis set using geometries and thermal corrections at the M06-L/def2SVP level.

5.4.5.3 XYZ Coordinates of Stationary Points in Angstroms

β-hydrogen elimination of 1,4-butanediol as catalyzed by (η^5-Me_5C_5)$IrCl_2$

[M]—alkoxide

C,0,1.6738060198,-1.4910755,-0.8139597013
C,0,2.414165404,-0.6058924912,0.0361955574
C,0,2.1889239042,-1.0200363708,1.4246167357
C,0,1.3392481673,-2.1740361335,1.4225032109
C,0,0.9716733917,-2.4335037698,0.0534855557
Ir,0,0.359638906,-0.4637291594,0.5038147908
O,0,-0.3424292859,0.9618851244,-0.6680926098
C,0,-1.5165012066,1.7021413356,-0.4950636248
C,0,-2.7548561126,0.9337523395,-0.9178336986
C,0,-4.0370820413,1.7073964736,-0.6853884869
C,0,-5.2720332274,0.9659432907,-1.1327598675
O,0,-6.3984025165,1.7722803452,-0.8833257118
C,0,3.2671572311,0.525617698,-0.4073020254
C,0,2.7751895576,-0.371772878,2.6248288791
C,0,0.8484189567,-2.9054092726,2.6189851082
C,0,0.0724271125,-3.5190548281,-0.4122341583
C,0,1.609064739,-1.4400008923,-2.2966486719
Cl,0,-1.3482898483,-0.0890691401,2.1159413086
H,0,3.3085049249,1.3203339039,0.3481503951
H,0,4.3008437487,0.1942550866,-0.5946583677
H,0,2.8860151309,0.9742667719,-1.3331535211
H,0,3.746763075,-0.8231066539,2.882539805
H,0,2.9435482739,0.7007528717,2.4655551676
H,0,2.1182228807,-0.4751437108,3.4972531009
H,0,-0.1343591783,-3.3582597404,2.4384483798
H,0,1.5405660157,-3.7108166612,2.9101637957
H,0,0.7308549262,-2.2340512227,3.4784680379
H,0,0.647975419,-4.4309853127,-0.6386203928
H,0,-0.6747269369,-3.779536849,0.3472367198
H,0,-0.4665020312,-3.2360325361,-1.3251792461
H,0,1.6506251848,-0.4053319578,-2.6600701856
H,0,2.4416169824,-1.9944390969,-2.7576385667
H,0,0.6745257903,-1.8746271214,-2.6732304848
H,0,-1.4213763317,2.6131733937,-1.1187499843
H,0,-2.6570283568,0.6533632782,-1.9820996148
H,0,-2.7790002889,-0.012681552,-0.3498988669
H,0,-4.1414578681,1.9474316287,0.3863121283
H,0,-4.0066385727,2.6793999126,-1.2075995074
H,0,-5.181441862,0.7125930591,-2.2105986772
H,0,-5.3340949012,-0.0032390091,-0.5951490842
H,0,-7.1816143849,1.2817639134,-1.149238016
H,0,-1.6437787913,2.0478264329,0.5475653956

TS1
C,0,-2.40402493,-0.7035816742,0.7696029773
C,0,-2.3954680465,0.4430357319,1.6797582395
C,0,-2.0664221959,1.6130988408,0.9029388451
C,0,-1.8006099459,1.1953599968,-0.4560972407
C,0,-2.0378876178,-0.2366792703,-0.5248650548
Ir,0,-0.4363960356,0.2326279158,0.9094921872
C,0,1.7579436774,0.7189685928,0.442639361
C,0,2.020116063,1.996307709,-0.3216134565
C,0,2.0065437791,3.2577788674,0.514472421
C,0,2.3952414736,4.4940724829,-0.258710711
O,0,2.2711558299,5.6044346117,0.5919043141
C,0,-2.7793524316,0.3867081581,3.1141081913
C,0,-2.0437983244,3.0114714449,1.4079873855
C,0,-1.4994364275,2.0771165141,-1.6144074719
C,0,-1.8397050604,-1.0589811232,-1.7463646717
C,0,-2.7090105101,-2.0955954489,1.1874432962
Cl,0,0.4270917841,-1.243535998,2.644329785
O,0,1.3304995582,-0.3235831405,-0.1907086973
H,0,-2.094780003,-2.3842887227,2.0529986705
H,0,-3.7674804591,-2.1975794545,1.4726902816
H,0,-2.5066521429,-2.8169808356,0.3869376596
H,0,-2.4364519402,1.2743189182,3.6599205362
H,0,-3.8727223113,0.320996983,3.2323662108
H,0,-2.3292742637,-0.4880201913,3.602028084
H,0,-1.3846200067,3.6558374581,0.8122425556
H,0,-3.052211709,3.4522215658,1.3679064556
H,0,-1.7038817065,3.0627953989,2.4500027296
H,0,-2.4193211731,2.3834359285,-2.1389278298
H,0,-0.982915926,2.9963723624,-1.3050916654
H,0,-0.8617581216,1.570048924,-2.3515330958
H,0,-1.7791712441,-2.1283513222,-1.5136603378
H,0,-2.6699902665,-0.9153524366,-2.4552960086
H,0,-0.9110612466,-0.7852534679,-2.2648408468
H,0,2.4520596188,0.5422945058,1.2960366169
H,0,3.0112866756,1.8636357623,-0.7934622333
H,0,1.3020343944,2.0563261917,-1.1551496351
H,0,0.9998663285,3.4149295112,0.9397434516
H,0,2.6777532493,3.1551837479,1.3838428886
H,0,3.4295695487,4.380948713,-0.6447069919
H,0,1.7447566036,4.5862788578,-1.1554054456
H,0,2.5587796347,6.387101552,0.1123646023
H,0,0.7257618274,1.2492298388,1.546280648

[M]-H-eta2-4hydroxybutanal

C	0	1.41085	1.18635	1.35698
C	0	2.24843	0.97261	0.24571
C	0	1.47542	1.23899	-0.97161
C	0	0.1681	1.72468	-0.5609
C	0	0.09589	1.59946	0.87136
Ir	0	0.40253	-0.33601	-0.06511
O	0	-0.27348	-1.6289	1.52846
C	0	-1.2141	-1.7127	0.66424
C	0	-2.56483	-1.09877	0.90793
C	0	-3.27865	-0.62294	-0.34055
C	0	-4.66298	-0.08613	-0.07264
O	0	-5.17446	0.43293	-1.27386
C	0	3.64449	0.47097	0.23579
C	0	2.04592	1.23928	-2.34537
C	0	-0.86292	2.31854	-1.4533
C	0	-1.02369	2.03303	1.74808
C	0	1.72217	0.9469	2.78926
Cl	0	1.64863	-2.26966	-0.83492
H	0	3.70063	-0.49753	-0.28614
H	0	4.3095	1.17242	-0.28979
H	0	4.03753	0.32595	1.24875
H	0	1.25857	1.20323	-3.10836
H	0	2.65008	2.14214	-2.5296
H	0	2.69003	0.36405	-2.50136
H	0	-1.87185	2.25333	-1.02606
H	0	-0.65102	3.3857	-1.62552
H	0	-0.8884	1.82643	-2.43364
H	0	-0.86237	3.05732	2.12228
H	0	-1.98579	2.02768	1.21847
H	0	-1.11974	1.38081	2.62744
H	0	2.72116	0.51763	2.927
H	0	1.67492	1.88348	3.36653
H	0	1.00103	0.25035	3.24042
H	0	-1.19342	-2.57215	-0.03877
H	0	-3.17352	-1.87491	1.4116
H	0	-2.45634	-0.2866	1.64392
H	0	-2.68293	0.1682	-0.82525
H	0	-3.34194	-1.43384	-1.08536
H	0	-5.30611	-0.89215	0.33781
H	0	-4.60853	0.69138	0.72049
H	0	-6.07449	0.73299	-1.11507
H	0	-0.49312	-0.72582	-1.3356

TS eta2→eta1

C	0	1.41085	1.18635	1.35698
C	0	2.24843	0.97261	0.24571
C	0	1.47542	1.23899	-0.97161
C	0	0.1681	1.72468	-0.5609

C	0	0.09589	1.59946	0.87136
Ir	0	0.40253	-0.33601	-0.06511
O	0	-0.27348	-1.6289	1.52846
C	0	-1.2141	-1.7127	0.66424
C	0	-2.56483	-1.09877	0.90793
C	0	-3.27865	-0.62294	-0.34055
C	0	-4.66298	-0.08613	-0.07264
O	0	-5.17446	0.43293	-1.27386
C	0	3.64449	0.47097	0.23579
C	0	2.04592	1.23928	-2.34537
C	0	-0.86292	2.31854	-1.4533
C	0	-1.02369	2.03303	1.74808
C	0	1.72217	0.9469	2.78926
Cl	0	1.64863	-2.26966	-0.83492
H	0	3.70063	-0.49753	-0.28614
H	0	4.3095	1.17242	-0.28979
H	0	4.03753	0.32595	1.24875
H	0	1.25857	1.20323	-3.10836
H	0	2.65008	2.14214	-2.5296
H	0	2.69003	0.36405	-2.50136
H	0	-1.87185	2.25333	-1.02606
H	0	-0.65102	3.3857	-1.62552
H	0	-0.8884	1.82643	-2.43364
H	0	-0.86237	3.05732	2.12228
H	0	-1.98579	2.02768	1.21847
H	0	-1.11974	1.38081	2.62744
H	0	2.72116	0.51763	2.927
H	0	1.67492	1.88348	3.36653
H	0	1.00103	0.25035	3.24042
H	0	-1.19342	-2.57215	-0.03877
H	0	-3.17352	-1.87491	1.4116
H	0	-2.45634	-0.2866	1.64392
H	0	-2.68293	0.1682	-0.82525
H	0	-3.34194	-1.43384	-1.08536
H	0	-5.30611	-0.89215	0.33781
H	0	-4.60853	0.69138	0.72049
H	0	-6.07449	0.73299	-1.11507
H	0	-0.49312	-0.72582	-1.3356

[M]-H—4-hydroxybutanal

C,0,0.4351665338,-2.0263844894,-0.2686294172

C,0,1.7734429282,-1.5957925916,-0.6860068246

C,0,2.2247044437,-0.6159336145,0.2138067763

C,0,1.1670056675,-0.3830783958,1.2066208669

C,0,0.1084509187,-1.3497446929,0.9596984563

Ir,0,0.2170988974,0.0695746353,-0.5913063368

Cl,0,0.9082606287,2.3616983978,-1.0969739564

C,0,2.4506324671,-2.088930527,-1.9136981565

C,0,3.4766525145,0.179466159,0.1469547847

C,0,1.305794359,0.5066308237,2.3904870696

C,0,-1.0654662751,-1.6068485366,1.834796258

C,0,-0.3354181419,-3.120856508,-0.9173319534

O,0,-0.3987558365,0.1058871502,-2.7546563096

C,0,-0.9317084347,1.0837240395,-3.263780779

C,0,-1.1384279737,1.2142408649,-4.7293973886

C,0,-2.5130443582,1.7426898998,-5.1055555456

C,0,-2.65458398,1.9948277935,-6.5875506511

O,0,-3.9565705894,2.4561287085,-6.8277282028

H,0,3.2494407785,1.2490242842,0.0133263036

H,0,4.0635951692,0.0755016574,1.0722425356

H,0,4.1150868568,-0.1272537772,-0.690448754

H,0,0.3289361189,0.7585901322,2.8219367966

H,0,1.9104217069,0.0346319832,3.1825942846

H,0,1.7922729354,1.4520384459,2.1163282899

H,0,-1.9250517156,-1.9797146086,1.2636898477

H,0,-0.8251723183,-2.3579954108,2.6043256005

H,0,-1.388983793,-0.6950306197,2.3523896161

H,0,0.0545119263,-4.1121304896,-0.6321784171

H,0,-1.3963290473,-3.091242941,-0.638683046

H,0,-0.2824473081,-3.0545944077,-2.012905539

H,0,3.3554664163,-1.5136746331,-2.1440031124

H,0,2.7437216132,-3.1463034036,-1.8138480288

H,0,1.7888019703,-2.0226836777,-2.7897246984

H,0,-1.2581601499,1.9296659573,-2.6211873239

H,0,-0.3646364764,1.9291025037,-5.0700225748

H,0,-0.9055366003,0.2542000089,-5.2150600992

H,0,-3.2969102084,1.0342728245,-4.7929415225

H,0,-2.7243084362,2.679796574,-4.5652919717

H,0,-1.8860711126,2.728866519,-6.9094079021

H,0,-2.4355979249,1.0592064937,-7.143721482

H,0,-4.0531466798,2.6171563917,-7.7711326701

H,0,-1.25541349,0.6967870765,-0.3480498226

β-hydrogen elimination of lactol resulting from ring closure of 4-hydroxybutanal, as catalyzed by (η5-Me5C5)IrCl2

[M]—alkoxide

C,0,2.911299223,-1.0895877697,-0.1123529947

C,0,2.0592132042,0.0098980348,-0.4573154902

C,0,2.7844638607,1.2474396539,-0.1596312785

C,0,4.0901050255,0.9067714037,0.329180735

C,0,4.1555844397,-0.5287352856,0.411396815

Ir,0,2.5272739498,0.1007219948,1.6032773738

O,0,1.0732402004,-0.8802420946,2.5066512343

C,0,0.6079919777,-0.7458427997,3.8142601031

O,0,-0.6545881173,-1.3711231754,3.8933475939

C,0,-0.4304013381,-2.7239455621,4.2302115791

C,0,0.6480926077,-2.6635346028,5.2984008926

C,0,1.503932442,-1.488131728,4.8280123655

C,0,0.6855598463,-0.085255268,-1.0128233086

C,0,2.2643641776,2.621970087,-0.3697179255

C,0,5.142767747,1.861853442,0.7615838605

C,0,5.3148162949,-1.3193864263,0.8959967428

C,0,2.5831564509,-2.5320927668,-0.2415208175

Cl,0,2.973953854,1.3004698899,3.6040370794

H,0,1.1756713681,2.6684300139,-0.2413057405

H,0,2.7101088136,3.33322765,0.3363989847

H,0,2.4912945678,2.9762729979,-1.3880609

H,0,5.7678841623,1.4378919784,1.5571386126

H,0,5.8037881129,2.137830277,-0.0746448636

H,0,4.7062291262,2.7841061815,1.164455845

H,0,4.9989255637,-2.2651921214,1.3539896869

H,0,5.9922268232,-1.5677330097,0.0631999508

H,0,5.897647464,-0.7671218262,1.6431050498

H,0,2.8517861925,-2.9190170958,-1.237141968

H,0,3.1196015751,-3.1352710522,0.5019844703

H,0,1.5111386173,-2.7111225195,-0.0897842763

H,0,0.0783785997,0.7864467353,-0.7387890463

H,0,0.7036083645,-0.1434676982,-2.112592172

H,0,0.1638560405,-0.9742418497,-0.6370007308

H,0,2.4232562918,-1.8160454164,4.3220453181

H,0,1.8162678952,-0.825252258,5.6453199927

H,0,0.1894696162,-2.4480195699,6.2755640353

H,0,1.2099913487,-3.6025345058,5.4038786129

H,0,-1.3826100856,-3.1590659585,4.5647933335

H,0,-0.0880195725,-3.2993096965,3.3464014985

H,0,0.4512862688,0.3156427166,4.0717237462

TS2

O,0,3.0699029396,-1.0512026039,-0.465792008

C,0,2.1647357819,-0.0173684283,-0.5580309975

C,0,2.9050300928,1.2368503082,-0.0968855277

C,0,3.8378635989,0.6791601213,0.9557795558

C,0,4.149151536,-0.7085424133,0.3966850144

Ir,0,-0.2224556239,-0.1675895543,-0.1286513889

Cl,0,0.0858256461,-2.5721498802,-0.1661306041

C,0,-1.8330836885,0.9423783391,-1.0401918255

C,0,-2.356254403,-0.2121106136,-0.3717934338

C,0,-1.9868087958,-0.1247859766,1.0374144464

C,0,-1.2579193668,1.1092392006,1.2158196452

C,0,-1.1432335476,1.7689875125,-0.0677496326

C,0,-1.9116304573,1.2442506488,-2.492528706

C,0,-3.1167893641,-1.3383375813,-0.9701996334

C,0,-2.3753531191,-1.109624998,2.0797037593

C,0,-0.720182668,1.6207505375,2.5044908211

C,0,-0.5365425208,3.0970727868,-0.3487933509

H,0,-3.1009610861,-1.3056179484,-2.066046377

H,0,-2.6845470862,-2.3021901725,-0.6663691732

H,0,-4.1690911614,-1.3157121866,-0.6469556855

H,0,-1.7564913687,-1.0118102736,2.9803414252

H,0,-3.4276074315,-0.9833253574,2.380617303

H,0,-2.2457434237,-2.1350409568,1.7087671185

H,0,0.1955626259,2.2097741935,2.3607091286

H,0,-1.4536400222,2.2717159997,3.0056790362

H,0,-0.4811557963,0.8021409459,3.1948174582

H,0,-1.3061165349,3.8805034607,-0.4414502537

H,0,0.1474202069,3.4129991988,0.4497240846

H,0,0.0331660333,3.08833645,-1.2887759366

H,0,-2.1941403652,0.361766848,-3.0782285419

H,0,-2.6553963466,2.0317777404,-2.6910650695

H,0,-0.9450538479,1.5963617626,-2.8773869784

H,0,3.4506162815,1.6197235712,-0.9750837184

H,0,2.2227268817,2.0237571377,0.2471272816

H,0,3.3143942545,0.5982990706,1.9221164133

H,0,4.7405301979,1.2799142821,1.1278239866

H,0,4.2516311379,-1.4810458795,1.1732385649

H,0,5.0764582805,-0.7141870758,-0.2003622197

O,0,1.3720777501,-0.0289727016,-1.572005737

H,0,1.3843447803,-0.2323165144,0.5849547561

[M(Ir)]-H—butyrolactone

C,0,-1.4805225552,1.8729066484,-0.1682395276
C,0,-1.825559987,0.7810171221,-1.0855341933
C,0,-2.3509919298,-0.28503969,-0.3351926416
C,0,-2.3141177442,0.0954088967,1.0836382559
C,0,-1.8778765324,1.4819434613,1.1600242129
Ir,0,-0.3202512561,0.2300234036,0.5199450775
O,0,1.5550031792,0.5620855983,-0.7506379866
C,0,2.7083217992,0.312150075,-0.4517791343
O,0,3.6816603709,0.4986685915,-1.3500108746
C,0,4.9666367089,0.2281522465,-0.7617623574
C,0,4.6742109387,-0.6194680542,0.4643840088
C,0,3.2750198774,-0.1707492606,0.8460236327
C,0,-1.552893379,0.8211863226,-2.5458734671
C,0,-2.7534839138,-1.6311071912,-0.8152559495
C,0,-2.874457058,-0.7263231272,2.1891902671
C,0,-1.8789773495,2.3349349251,2.3774489779
C,0,-0.9908763904,3.2096184763,-0.5988288385
Cl,0,0.4701957294,-2.0899643439,0.6725900109
H,0,-2.6654492843,-1.7221481068,-1.9046818785
H,0,-2.1152856206,-2.4091501862,-0.3674947806
H,0,-3.7960834642,-1.855450263,-0.5425567045
H,0,-2.4866570802,-0.40774636,3.1649258057
H,0,-3.9742368623,-0.656512376,2.2258902249
H,0,-2.6094130357,-1.784378201,2.064112678
H,0,-1.1101836617,3.1163726537,2.3264669597
H,0,-2.8530036584,2.8334126163,2.5076523064
H,0,-1.6853692574,1.7452180982,3.2823674358
H,0,-1.8106700672,3.8312047207,-0.9959530289
H,0,-0.5324266839,3.7606577902,0.2321567988
H,0,-0.2351578211,3.1232445249,-1.3916882201

H,0,-1.7508890117,-0.1434972428,-3.0281803511

H,0,-2.1729996578,1.5806015902,-3.0480397845

H,0,-0.5027482917,1.0783929331,-2.7476464793

H,0,3.2592689479,0.6825607313,1.5457303035

H,0,2.6207123501,-0.9425746786,1.273883706

H,0,4.6649015798,-1.6863051104,0.1967498284

H,0,5.4219369824,-0.4886857782,1.2561178522

H,0,5.5840141744,-0.259662441,-1.5257695866

H,0,5.4332505713,1.1950394546,-0.5120891789

H,0,0.6671413438,0.5429945306,1.7716716205

β-hydrogen elimination of ethanol as catalyzed by (η^5-Me_5C_5)$IrCl_2$

[M]—alkoxide

C,0,-1.6084284353,-0.1767638617,-1.0313454275

C,0,-1.5993191841,-1.6091532551,-0.9982287864

C,0,-1.9071695526,-2.0160163103,0.3735331748

C,0,-2.16308623,-0.8414470647,1.1608619005

C,0,-1.9278760907,0.2972320545,0.3173881566

Ir,0,-0.1457366598,-0.8415780044,0.343862992

Cl,0,1.0803957509,-0.6711288378,2.3739480271

C,0,-1.3161684168,-2.5144634993,-2.1406256108

C,0,-1.9925218037,-3.4185145025,0.8526689165

C,0,-2.504621584,-0.8084790872,2.6064096107

C,0,-2.0387214526,1.7205412543,0.7252230519

C,0,-1.3354001215,0.6771378268,-2.2150549239

O,0,1.5100283095,-0.9344658359,-0.7233120111

C,0,2.8344487125,-0.8019409972,-0.28198072

C,0,3.2313656281,0.6458815946,-0.1053018375

H,0,4.2924352548,0.740053946,0.1679872534

H,0,-1.7577747292,-3.4953134418,1.9212896687

H,0,-3.0080318876,-3.8199834028,0.705414076

H,0,-1.2989784754,-4.0755432611,0.3130356809

H,0,-2.0907508181,0.0815278897,3.0962935245

H,0,-3.5946267587,-0.8040988532,2.7626799029

H,0,-2.0930133484,-1.6764043959,3.1362993913

H,0,-1.3625170948,2.3624480303,0.1465775502

H,0,-3.0630132662,2.0955183998,0.5688840048

H,0,-1.7938436013,1.8555737163,1.7858933648

H,0,-2.2583430657,0.8883156823,-2.777979812

H,0,-0.8991962837,1.6412466963,-1.924080165

H,0,-0.6272185501,0.1940628258,-2.8998304057

H,0,-0.9009359606,-3.4720089014,-1.8020257484

H,0,-2.2289692052,-2.7346683104,-2.7164228201

H,0,-0.5841516694,-2.0706968542,-2.8272194765

H,0,3.473878894,-1.2720647264,-1.0541371585

H,0,3.0677919231,1.2136880741,-1.0332206543

H,0,2.6358913262,1.1108120991,0.6935261948

H,0,3.0161214464,-1.3543866867,0.6572801151

TS3

C,0,-1.5159900956,-1.6037867754,-0.9922327723

C,0,-1.8832033406,-2.0155072196,0.3179878797

C,0,-1.865574886,-0.8393487106,1.1881815052

C,0,-1.5304471264,0.3013722977,0.3641415251

C,0,-1.2685757773,-0.1700321845,-0.9767103009

Ir,0,0.0901031303,-1.0752353729,0.4239817441

O,0,1.87715674,-1.4866262391,-0.7138658849

C,0,2.2884296226,-0.5127793912,0.0310412941

C,0,2.5836785016,0.824103872,-0.5958855543

H,0,2.69596094,1.6218386252,0.1500803859

C,0,-2.1896211065,-3.3904652515,0.7867802434

C,0,-2.2584388044,-0.8433548034,2.6214669266

C,0,-1.4773623322,1.7175509377,0.814670841

C,0,-0.9506419733,0.6511234744,-2.1743570566

C,0,-1.3296457269,-2.4687660879,-2.1855940221

Cl,0,0.9905256754,-2.6200270958,2.07860361

H,0,-1.5529873928,-3.6595144115,1.6423591311

H,0,-3.2403965055,-3.4684015193,1.1052496074

H,0,-2.0191429667,-4.1380845895,0.0032984925

H,0,-1.9013387137,0.0540033941,3.1418963613

H,0,-3.3531693468,-0.885567076,2.7392528021

H,0,-1.8275441711,-1.7105811692,3.1390151507

H,0,-0.7279647822,2.295540242,0.2579342139

H,0,-2.4503508293,2.2117357153,0.6674850449

H,0,-1.2274932762,1.7930485582,1.8802309321

H,0,-1.8433310376,0.8114819915,-2.8004137677

H,0,-0.566126981,1.6423993033,-1.9014435754

H,0,-0.1948886462,0.1634390482,-2.8061959547

H,0,-1.2890044934,-3.5311622931,-1.9191605393

H,0,-2.1557594726,-2.3331556599,-2.9012293407

H,0,-0.3962510425,-2.2272541917,-2.7116448165

H,0,2.9477273752,-0.780977865,0.8863656395

H,0,3.5351452062,0.7430036687,-1.1429221048

H,0,1.8092525228,1.1068018568,-1.3201819712

H,0,1.2150941129,-0.0538410785,1.1162233306

M-H-eta2-ethanal

C	0	-1.18567	-0.1789	-0.93971
C	0	-1.48496	-1.6097	-0.97111
C	0	-1.8712	-2.00979	0.32161
C	0	-1.81254	-0.8417	1.20468
C	0	-1.47912	0.31217	0.38074

Ir	0	0.17672	-1.0128	0.52268
Cl	0	1.10536	-2.72576	1.96818
C	0	-1.30103	-2.46325	-2.17251
C	0	-2.18762	-3.37924	0.79587
C	0	-2.26636	-0.8398	2.62146
C	0	-1.49295	1.73654	0.80848
C	0	-0.84788	0.62333	-2.14467
O	0	1.79705	-1.48715	-0.83334
C	0	2.2769	-0.53614	-0.12396
C	0	2.51523	0.83063	-0.68827
H	0	2.51893	1.5982	0.09644
H	0	-1.44399	-3.70874	1.53895
H	0	-3.1767	-3.40921	1.27646
H	0	-2.18539	-4.10908	-0.02195
H	0	-1.89467	0.03848	3.16357
H	0	-3.36595	-0.83656	2.6924
H	0	-1.89743	-1.72773	3.15125
H	0	-0.74384	2.33118	0.26946
H	0	-2.47722	2.19307	0.61894
H	0	-1.2832	1.83906	1.88035
H	0	-1.72466	0.737	-2.80251
H	0	-0.50402	1.6326	-1.88532
H	0	-0.05935	0.13885	-2.7382
H	0	-1.44335	-3.52652	-1.94783
H	0	-2.01356	-2.18851	-2.96609
H	0	-0.29084	-2.34846	-2.5906
H	0	2.90165	-0.81585	0.74905
H	0	3.50829	0.85185	-1.16686
H	0	1.77392	1.09166	-1.4533
H	0	0.83306	-0.05678	1.63137

TS eta2→eta1

C	0	1.5957	1.24941	1.30776
C	0	2.41086	0.98767	0.19551
C	0	1.65107	1.34316	-1.01402
C	0	0.40151	1.96982	-0.59
C	0	0.32397	1.81265	0.8359
Ir	0	0.44506	-0.08322	-0.13516
O	0	-0.61876	-1.24224	1.73156
C	0	-1.46389	-1.72743	0.98333
C	0	-2.8929	-1.31235	0.96941
H	0	-3.25109	-1.1927	-0.06157
C	0	3.7416	0.33094	0.16794
C	0	2.20385	1.3047	-2.39302
C	0	-0.57497	2.66111	-1.47146
C	0	-0.76749	2.2753	1.73281
C	0	1.87795	0.94288	2.73319
Cl	0	1.36257	-2.24089	-0.71627
H	0	3.68553	-0.63729	-0.35449
H	0	4.48111	0.95325	-0.3581
H	0	4.12328	0.13627	1.17718
H	0	1.40778	1.30996	-3.1477
H	0	2.85498	2.17344	-2.58424
H	0	2.80048	0.39715	-2.5519
H	0	-1.59199	2.62158	-1.06115
H	0	-0.30825	3.72253	-1.59787
H	0	-0.6078	2.20725	-2.46994
H	0	-0.51069	3.2281	2.22416
H	0	-1.70522	2.43043	1.18364
H	0	-0.96466	1.54019	2.52563
H	0	2.80835	0.37618	2.8553

H	0	1.96538	1.86666	3.32663
H	0	1.0695	0.34655	3.17865
H	0	-1.18187	-2.57539	0.31571
H	0	-3.49895	-2.11688	1.41508
H	0	-3.0525	-0.38998	1.54019
H	0	-0.78662	-0.48001	-1.1225

[M]-H—ethanal

C,0,0.4325853337,-2.0222065324,-0.2724892568

C,0,1.7457519395,-1.5964163074,-0.682069479

C,0,2.2137485396,-0.5817606626,0.2676017756

C,0,1.1833974742,-0.3260481112,1.187588876

C,0,0.0265372741,-1.1549145678,0.8222836409

Ir,0,0.3333971763,-0.0128504113,-0.8925922655

O,0,1.2834304549,1.1809483545,-2.5443402503

C,0,0.6722024559,2.0184953715,-3.1961897796

C,0,1.3387613866,2.9117052999,-4.1690693375

H,0,0.8648345547,2.8190529867,-5.1570752469

C,0,2.5870978069,-2.1991807683,-1.75030292

C,0,3.5379757816,0.0863156259,0.172906808

C,0,1.1579460089,0.6870063611,2.2727376014

C,0,-1.2259944834,-1.2492351498,1.6187654154

C,0,-0.3529066149,-3.1535818622,-0.8317948588

Cl,0,-0.7575661895,2.1219339701,-0.4088103304

H,0,0.3768100768,1.4400087445,2.0824196123

H,0,0.9424247641,0.2210059778,3.2462940632

H,0,2.1127020484,1.219597725,2.3606346813

H,0,-2.0468360497,-1.6771360659,1.0296877902

H,0,-1.0901565497,-1.8805731148,2.5124886403

H,0,-1.5525551258,-0.2567965697,1.9563700491

H,0,-0.1081524709,-3.3371534654,-1.8856194559

H,0,-0.1527884458,-4.0837632832,-0.2760594217

H,0,-1.4316719349,-2.9607204757,-0.7763761955

H,0,3.2984084384,-2.9335855763,-1.3372176962

H,0,1.9787532809,-2.7165058123,-2.5028774098

H,0,3.177703228,-1.4354433513,-2.2750945641

H,0,3.6173670132,0.9409884595,0.855533958

H,0,4.3570452714,-0.6102088231,0.4136556124

H,0,3.7266964325,0.4605540777,-0.8439193256

H,0,-0.4221254134,2.133027019,-3.0493579464

H,0,1.1842945655,3.956281885,-3.8600351642

H,0,2.4118524704,2.7045389842,-4.2440932675

H,0,-0.8488294985,-0.2314839316,-1.9770083524

β-hydrogen elimination of hemiacetal resulting from addition of ethanol to ethanal, as catalyzed by (η^5-Me_5C_5)$IrCl_2$

[M]—alkoxide

C,0,0.4416884099,-1.8290559297,-0.943674253

C,0,1.5445172972,-0.9176981256,-1.1364721803

C,0,2.104161537,-0.5954421001,0.1659318825

C,0,1.3720468972,-1.3431244597,1.172612067

C,0,0.3391221675,-2.0730615295,0.487411526

Ir,0,0.1047991796,-0.0029107742,0.0792545457

C,0,-1.9743620345,1.516929857,-0.8045029057

O,0,-2.1986655686,0.4023686115,0.1782892456

C,0,-2.926191664,0.7509885319,1.3500881369

C,0,-2.7046862505,-0.2911947729,2.4081281933

C,0,1.9745524065,-0.3522860278,-2.4398733772

C,0,3.2532834124,0.3043307978,0.441264323

C,0,1.6407996075,-1.302748594,2.6337067575

C,0,-0.678329619,-2.9555963649,1.1129252443

C,0,-0.4119371752,-2.4205963344,-2.0057686072

Cl,0,0.1719643048,1.876252151,1.6307270736

O,0,-0.7914902629,1.2102574446,-1.3590393626

C,0,-3.1089545657,1.5598490476,-1.7945766735

H,0,3.0948685068,0.8697470947,1.3681274748

H,0,4.1861191723,-0.2718707309,0.5457251081

H,0,3.3988187199,1.0351465936,-0.3634063358

H,0,0.8166769326,-1.7426675767,3.2094249788

H,0,2.556930089,-1.8564023939,2.8925219517

H,0,1.7594190552,-0.2664149463,2.9802861365

H,0,-1.6535582352,-2.8604096464,0.6169516965

H,0,-0.3721781261,-4.0106519342,1.032835904

H,0,-0.8213138933,-2.7324809511,2.1770457429

H,0,-1.4287826923,-2.6158308654,-1.640033021

H,0,-0.5031171614,-1.7422070585,-2.8639345504

H,0,-0.0044015328,-3.3751382002,-2.3760223563

H,0,2.5216139172,0.5890594973,-2.3097380841

H,0,2.6332343497,-1.0536030304,-2.9751266014

H,0,1.1105323318,-0.1384046517,-3.0817299527

H,0,-2.5889378065,1.7400548997,1.7071987622

H,0,-3.997154085,0.8345622409,1.0874116505

H,0,-3.257589284,-0.0392603175,3.3227503963

H,0,-3.0361639476,-1.2851057971,2.0758917272

H,0,-1.6347695203,-0.3389769565,2.6639103807

H,0,-3.1644825838,0.6087396349,-2.3412789739

H,0,-4.0739702723,1.7494542048,-1.3039662774

H,0,-2.9346234224,2.3646378742,-2.5204132146

H,0,-1.9556645905,2.4318245883,-0.1642581782

TS4

C,0,1.5109490811,-1.1947190451,-1.112054184

C,0,2.3304272002,-0.5883393135,-0.1079335774

C,0,1.7103026498,-0.8227612794,1.1924035334

C,0,0.5176779232,-1.6078538775,0.9613112018

C,0,0.3711379839,-1.8196879606,-0.461561402

Ir,0,0.3613524664,0.2706979109,-0.0150899159

Cl,0,1.1048342855,2.5492729392,0.4337634426

C,0,3.583437987,0.1818670074,-0.3116459369

C,0,2.2845581504,-0.4066084431,2.4982448483

C,0,-0.4028283606,-2.1134847255,2.0135781697

C,0,-0.6952919264,-2.5867423371,-1.1555202996

C,0,1.7220759738,-1.1571602645,-2.5816785141

O,0,-0.9544864323,1.1152385934,-1.5032970973

C,0,-1.795749739,1.1595705915,-0.525912696

C,0,-2.3289163056,2.5190031561,-0.1328651704

O,0,-2.728694953,0.1268126275,-0.5503469736

C,0,-3.5807689998,-0.0066720969,0.5684305627

C,0,-4.3325429427,-1.3036099387,0.4520509122

H,0,3.5450051496,1.1387786044,0.2269442745

H,0,4.4525942895,-0.3854847021,0.0554938734

H,0,3.7541970193,0.4117533648,-1.3699225587

H,0,1.5247209685,-0.3950737667,3.2897217136

H,0,3.0908793417,-1.0853393095,2.8200994722

H,0,2.7013872134,0.6071332348,2.4356761531

H,0,-1.4281733352,-2.2257109647,1.6375113169

H,0,-0.0766951896,-3.100867568,2.3761208526

H,0,-0.4369272778,-1.4399467626,2.8794624813

H,0,-1.5850973505,-2.7036336416,-0.5254884226

H,0,-1.0208425884,-2.0737830162,-2.0703925932

H,0,-0.3502006154,-3.5943752739,-1.4376340434

H,0,2.4332100624,-0.3752417706,-2.8724735994

H,0,2.1133550201,-2.1198193965,-2.9467023979

H,0,0.7814693305,-0.9598055066,-3.1126762661

H,0,-1.1155144021,0.8761344801,0.696614694

H,0,-2.9755915437,0.0231888678,1.5000324341

H,0,-4.2882918566,0.8408473583,0.627235644

H,0,-5.0380848022,-1.4219140801,1.284452407

H,0,-4.9032741421,-1.338340554,-0.4852561008

H,0,-3.6533747685,-2.1671008182,0.4581578638

H,0,-2.9939637139,2.8594425936,-0.9395310802

H,0,-2.8866630221,2.5188033556,0.8110738856

H,0,-1.4834108288,3.2094167277,-0.0480489073

[M]-H—ethyl acetate

C,0,-1.5016208947,1.9379967051,-0.0962904522

C,0,-1.7033053332,0.848403867,-1.0579789881

C,0,-2.2124758462,-0.2663986707,-0.3702146993

C,0,-2.3093113748,0.0820024216,1.0544420945

C,0,-1.9736135707,1.4922771011,1.1894217997

Ir,0,-0.2919539405,0.3580387481,0.6517247645

O,0,1.6226431063,0.8044931741,-0.5125841252

C,0,2.7813018107,0.4760934633,-0.3024535938

O,0,3.6149090886,0.5772769642,-1.3407940578

C,0,4.98541078,0.1767624321,-1.2367479288

C,0,3.3079667351,-0.0046004871,1.0019363647

C,0,-1.3214398777,0.9393454895,-2.4911787526

C,0,-2.4858631778,-1.624401403,-0.904444645

C,0,-2.9002088538,-0.7987451192,2.0967712516

C,0,-2.1249939397,2.3152718126,2.4180322149

C,0,-1.0650125146,3.3114809404,-0.4631675591

Cl,0,0.6497607579,-1.9030692887,0.7900660623

H,0,-2.3319386213,-1.6775194497,-1.9891277911

H,0,-1.816002602,-2.3654275999,-0.4396143488

H,0,-3.5219102395,-1.9323541605,-0.6963941856

H,0,-2.6120260478,-0.4780864371,3.1057782475

H,0,-4.0017405692,-0.8002567634,2.0467411136

H,0,-2.5574646981,-1.8347151121,1.9748510217

H,0,-1.4041206704,3.1422682658,2.4442194851

H,0,-3.1352590352,2.7511306694,2.4779301551

H,0,-1.9681596571,1.717023943,3.3244904998

H,0,-1.8868079366,3.8881840064,-0.9194992758

H,0,-0.7140511935,3.8729111673,0.4119672102

H,0,-0.2410673073,3.2877846298,-1.1896599048

H,0,-1.41891298,-0.0249371633,-3.0042405295

H,0,-1.948029515,1.6696213193,-3.0274632868

H,0,-0.2770486623,1.2654113728,-2.6037195879

H,0,2.5751746555,0.2130189353,1.7855891756

H,0,3.4193140998,-1.097261425,0.9707620794

H,0,0.5529759137,0.6950665405,1.99576583

H,0,4.2821523635,0.441827476,1.2402580905

C,0,5.5778132772,0.2134748787,-2.6150028769

H,0,5.5172329894,0.8612078649,-0.5540220861

H,0,5.0439617786,-0.8333175645,-0.7995351281

H,0,6.6349372714,-0.0780230782,-2.5846886381

H,0,5.0511480437,-0.4754367551,-3.2872630842

H,0,5.5126273876,1.2212102894,-3.0444329355

β-hydrogen elimination of i-propanol as catalyzed by (η^5-Me_5C_5)$IrCl_2$

[M]—alkoxide

C,0,0.7300204275,-2.1525155092,-0.3960015648

C,0,1.7379923966,-1.2946325044,-1.019490305

C,0,2.3175199852,-0.4925361963,0.0167500098

C,0,1.6739867576,-0.865197488,1.2796130391

C,0,0.7384835734,-1.9224270186,1.0241338204

Ir,0,0.2369537671,-0.1208747725,-0.0896190675

O,0,0.0954206249,1.4333613973,-1.2921477201

C,0,-0.9900137882,2.32076556,-1.473349845

C,0,-0.426621683,3.5977145115,-2.0669822974

C,0,2.08202639,-1.2517342631,-2.463375347

C,0,3.3778923354,0.5325888365,-0.1550831717

C,0,1.9786374618,-0.2747440376,2.6073117389

C,0,-0.135757355,-2.5837253509,2.0269986716

C,0,-0.1180526275,-3.1386197045,-1.1119444746

Cl,0,-1.8823039149,0.336751349,0.8890069122

C,0,-2.0404352428,1.6888378752,-2.3672311168

H,0,1.1081198363,-0.3121506189,3.2736519984

H,0,2.7996885839,-0.819610323,3.1004008524

H,0,2.2854439994,0.7754860628,2.5243934295

H,0,-1.0872397711,-2.901637724,1.5831397981

H,0,0.3485580091,-3.4735241931,2.4585320382

H,0,-0.3870391934,-1.9040877807,2.8506189426

H,0,-0.3526183462,-2.8080098317,-2.1316352333

H,0,0.3947012031,-4.1107804225,-1.1907874075

H,0,-1.0689027569,-3.3068219072,-0.5917787704

H,0,1.2286246842,-1.5426273341,-3.0890198499

H,0,2.3779943796,-0.2411245708,-2.7717530658

H,0,2.9135881863,-1.934230807,-2.6998603825

H,0,3.3089589356,1.3160769289,0.6100550429

H,0,4.3821723927,0.0861653119,-0.0812373452

H,0,3.3005723713,1.0256935009,-1.1322463341

H,0,0.0520365144,3.3956978416,-3.0370937436

H,0,-1.2152912397,4.3477186521,-2.22471666

H,0,0.3324269391,4.0356181446,-1.4046691332

H,0,-1.4616014459,2.5556616304,-0.5001877508

H,0,-1.6042938004,1.4198718708,-3.3419243278

H,0,-2.4428270336,0.7788108849,-1.9015776984

H,0,-2.8811315559,2.3748049998,-2.5481316818

TS5
C,0,-1.5012435201,-1.5944993796,-0.9946175206
C,0,-1.9170775133,-2.0176786353,0.2990904274
C,0,-1.9164186789,-0.8519647734,1.182965121
C,0,-1.5379084573,0.2924774161,0.3860705752
C,0,-1.2446506206,-0.1641657786,-0.9544291861
Ir,0,0.0582522806,-1.1090836801,0.4740813514
O,0,1.8895452435,-1.5501691344,-0.5777988741
C,0,2.3290745052,-0.5308579027,0.0976999017
C,0,2.4563838889,0.7926160165,-0.6300462288
H,0,2.5051530982,1.6501740279,0.0545156194
C,0,-2.2669417034,-3.3931338874,0.7341717853
C,0,-2.348951599,-0.8684457923,2.6045774843
C,0,-1.478917214,1.7022306167,0.8557097383
C,0,-0.9194077871,0.6729708079,-2.1388575741
C,0,-1.2877373128,-2.4466276063,-2.1926428666
Cl,0,0.8010972837,-2.6867412514,2.1901864753
H,0,-1.7007517092,-3.6723664976,1.6341561541
H,0,-3.3402604927,-3.4648811641,0.9684968199
H,0,-2.0409475366,-4.1370995792,-0.0388155408
H,0,-2.0044553321,0.0233778349,3.1428032497
H,0,-3.4466554901,-0.9090073947,2.6910597225
H,0,-1.9332297882,-1.7414800794,3.1250587799
H,0,-0.7081459725,2.2770143493,0.3255170547
H,0,-2.4414973034,2.2110548066,0.6902878816
H,0,-1.25510105,1.7613142417,1.9280905184
H,0,-1.8146506951,0.8506750118,-2.7568987813
H,0,-0.5261870962,1.6574413079,-1.8539538719
H,0,-0.1739214192,0.187895679,-2.7846766494
H,0,-1.2724455155,-3.5128502059,-1.9389094461
H,0,-2.0858592432,-2.2894837907,-2.9351763013
H,0,-0.3322187462,-2.2128980367,-2.6815857494
C,0,3.408901891,-0.7955138833,1.1189488205
H,0,3.3968472089,0.7739795003,-1.2030317602

H,0,1.6351743219,0.9391803787,-1.340399037
H,0,1.2372825164,-0.1177515906,1.1648801964
H,0,4.3246060733,-1.0457250625,0.5614134817
H,0,3.6193224374,0.0809516176,1.745940566
H,0,3.1432290479,-1.6506205064,1.7490556629

[M]-H—acetone
C,0,0.7842003609,-2.1463596311,-0.4926096629
C,0,1.8042474402,-1.2675187278,-1.0064359944
C,0,2.3860461237,-0.5366351392,0.1229408825
C,0,1.6873393834,-0.8928326936,1.2901213097
C,0,0.6277006054,-1.840295427,0.9194895501
Ir,0,0.16712884,-0.1540276913,-0.2172022846
O,0,0.400817335,1.7346620934,-1.3905229476
C,0,-0.4239133128,2.5462257502,-1.8163337895
C,0,0.0628568008,3.8083910964,-2.4473225732
C,0,2.3370127334,-1.2333864913,-2.394753353
C,0,3.473492754,0.4661122519,-0.0187150333
C,0,1.8603516714,-0.3489171445,2.6606751723
C,0,-0.2611906075,-2.5309416289,1.891455165
C,0,0.0518085844,-3.1967609441,-1.2478995567
Cl,0,-1.049440417,1.2604124131,1.3822556314
C,0,-1.8875760293,2.3224452168,-1.720934268
H,0,0.9469395463,0.1713210097,2.9895798673
H,0,2.0655833606,-1.1534298108,3.3833321301
H,0,2.6864610624,0.3703874023,2.7165226866
H,0,-1.1460501512,-2.9530341867,1.3986805043
H,0,0.2623761647,-3.354930375,2.403982558
H,0,-0.6201681655,-1.8327229766,2.6590399908
H,0,-0.0420530417,-2.9426135273,-2.3113399942
H,0,0.5739037341,-4.1648040766,-1.1814381017
H,0,-0.9628996957,-3.3404595435,-0.8558711449
H,0,1.6053803384,-1.6115028805,-3.1200832131
H,0,2.6015774236,-0.2107960042,-2.6977299483
H,0,3.2477060602,-1.8475032653,-2.4928829528
H,0,3.6500737805,1.0155554763,0.91380438
H,0,4.4231878405,-0.0092182777,-0.3118261611
H,0,3.2332654121,1.2077862642,-0.7947104538
H,0,-0.3292205766,3.9003943403,-3.4708191419
H,0,-0.3321139614,4.6729738085,-1.8933730592
H,0,1.1565079815,3.8538870458,-2.4619636082
H,0,-1.2509150609,-0.3365636838,-0.9770902299
H,0,-2.1610685345,2.2966749827,-0.653054653
H,0,-2.4721630913,3.0834707051,-2.2506702395
H,0,-2.1280656923,1.3153622701,-2.0923214632

β-hydrogen elimination of 1-propanol as catalyzed by (η^5-Me_5C_5)$IrCl_2$

[M]—alkoxide

C,0,-1.3033102299,-0.0587763003,1.3808166061
C,0,-1.1140815642,1.3064986096,0.884899462
C,0,-1.42463407,1.3079757111,-0.5139931517
C,0,-1.7995807747,-0.0588217992,-0.8794040837
C,0,-1.7770160205,-0.8786895567,0.3004763095
Ir,0,0.1793476214,-0.0254976029,-0.1265553975
O,0,1.7601940393,1.0748162173,-0.557799779
C,0,3.0803395944,0.638820295,-0.7114931882
C,0,3.7742909243,0.4096312393,0.6194260882
C,0,-0.6711985415,2.4738366987,1.6886778172
C,0,-1.3648395099,2.4766702066,-1.4279911912
C,0,-2.1899673431,-0.5053155348,-2.2402801714
C,0,-2.0856996512,-2.3303333489,0.3693243426
C,0,-1.0869367522,-0.5032901192,2.7808192652
Cl,0,1.4345377076,-2.0411284091,-0.2916550869
C,0,5.1817300528,-0.1235218412,0.4618335933
H,0,-1.9657847453,-1.5674730273,-2.3968104287
H,0,-3.2710773368,-0.3661591013,-2.4013566631
H,0,-1.6667361372,0.0621986545,-3.0200476684
H,0,-1.4764033456,-2.8344614769,1.1295705441
H,0,-3.1448516455,-2.505473519,0.6144050655
H,0,-1.8741751124,-2.8317181895,-0.5832117682
H,0,-0.2915539175,0.0721966972,3.2710622656
H,0,-2.002987392,-0.375711172,3.3798131092
H,0,-0.8041542913,-1.5620939818,2.8275846395
H,0,-1.5301556952,3.0131253138,2.1183895797
H,0,-0.0245910122,2.1676803846,2.5209190412

H,0,-0.0996870603,3.1841020638,1.0782234988

H,0,-1.1713451791,2.1685593374,-2.4631558986

H,0,-2.3102900841,3.0417463365,-1.4220679998

H,0,-0.5597525044,3.1648651062,-1.1409688556

H,0,3.6196657001,1.4272711512,-1.2740541387

H,0,3.7723151548,1.3545064714,1.1899546104

H,0,3.1636414215,-0.3016425719,1.2006752981

H,0,3.1489140001,-0.2823002603,-1.3198520524

H,0,5.6834620428,-0.2603920788,1.4296597591

H,0,5.1787038295,-1.1004748785,-0.04493514

H,0,5.8117678276,0.5516742751,-0.1377982321

TS

C,0,-1.517866457,-1.604996869,-0.993426688

C,0,-1.8862064592,-2.0193688786,0.3161743168

C,0,-1.8679042108,-0.8447928638,1.1884587896

C,0,-1.5320511397,0.2968608231,0.3671343756

C,0,-1.2697557847,-0.1714869262,-0.9749248838

Ir,0,0.087100921,-1.0840871764,0.423071375

O,0,1.872404985,-1.5122213561,-0.7124229181

C,0,2.288568526,-0.5355812373,0.0244466249

C,0,2.5843700477,0.8079823986,-0.6025923943

C,0,2.7529469704,1.9363623571,0.3891878305

C,0,-2.1952852491,-3.3948634431,0.7816189501

C,0,-2.2606454255,-0.849725375,2.6217692227

C,0,-1.4865715276,1.7118755947,0.8212227949

C,0,-0.9495031173,0.6526889134,-2.1697455259

C,0,-1.331048824,-2.4683696483,-2.1879162519

Cl,0,0.9795355986,-2.6289674075,2.0824063839

H,0,-1.5651262047,-3.6641393223,1.6418155057

H,0,-3.2485356391,-3.4738188388,1.0916680562

H,0,-2.018035736,-4.141856848,-0.0009568663

H,0,-1.9030849249,0.0473167646,3.1424728887

H,0,-3.3554398856,-0.8913211483,2.7393409199

H,0,-1.8303587757,-1.7175688767,3.1388091168

H,0,-0.7836574928,2.3097800733,0.2264719391

H,0,-2.4775491595,2.1830649029,0.7282561142

H,0,-1.1823382444,1.7905787849,1.8727008926

H,0,-1.8447595282,0.8326255405,-2.7868225359

H,0,-0.5448473189,1.6351695488,-1.8934558977

H,0,-0.2073464433,0.1570729171,-2.811309491

H,0,-1.2895881709,-3.5310062164,-1.922554228

H,0,-2.1573280538,-2.3325015004,-2.903274512

H,0,-0.397700173,-2.2256663959,-2.7134433608

H,0,2.9558682021,-0.7972060882,0.8786915184

H,0,3.5156887749,0.6626013816,-1.1781184841

H,0,1.8088437019,1.029649657,-1.35223542

H,0,1.225784994,-0.0689782401,1.1108293748

H,0,3.0623976729,2.8697885682,-0.0987414659

H,0,1.8161678617,2.1411478443,0.9303076943

H,0,3.5139506894,1.6969195863,1.1464592388

[M]-H—aldehyde

C,0,0.0243311279,-1.1547093564,0.8306111449

C,0,0.4443273119,-2.04915126,-0.2367355332

C,0,1.7611967626,-1.6311705527,-0.6424306861

C,0,2.2164492292,-0.5908471622,0.2854637922

C,0,1.1751449666,-0.3138220903,1.1868357178

Ir,0,0.34877608,-0.0569204422,-0.9101592474

O,0,1.3139317775,1.1008521004,-2.5785188485

C,0,0.6979815315,1.9119029374,-3.2584596775

C,0,1.3677127708,2.8432350982,-4.2045954108

C,0,-0.3327417487,-3.1964790441,-0.7749364317

C,0,2.6156860951,-2.2594059295,-1.6852717701

C,0,3.5399598766,0.0781791134,0.1876335266

C,0,1.134728997,0.7274032163,2.2444820357

C,0,-1.2367456583,-1.231578653,1.6153781673

Cl,0,-0.7454505061,2.0923452756,-0.4974850576

C,0,0.6273303841,3.0150212174,-5.5176950259

H,0,0.3513087056,1.4706048347,2.0271544627

H,0,0.9129960023,0.2861238324,3.2281329899

H,0,2.0856926032,1.2676173681,2.3266106051

H,0,-2.0501237029,-1.6762155633,1.0283262996

H,0,-1.1096591721,-1.8396744462,2.5263575516

H,0,-1.5691126281,-0.2316713969,1.924106921

H,0,-0.0770462058,-3.4061909377,-1.8212570352

H,0,-0.1361893342,-4.1117424963,-0.1937261252

H,0,-1.4124537459,-3.0049338429,-0.7352305053

H,0,3.3237164208,-2.981267849,-1.2453077719

H,0,2.0169230467,-2.7974082277,-2.431000421

H,0,3.2106992255,-1.5081370223,-2.2229103642

H,0,3.6100900125,0.950033248,0.8492328749

H,0,4.3582617682,-0.6097335615,0.4543579913

H,0,3.7380974614,0.4273355538,-0.8363284001

H,0,-0.4065735712,1.9887199324,-3.156513134

H,0,1.4076004192,3.8111022451,-3.6709188647

H,0,2.4130374811,2.5287831215,-4.3393428095

H,0,-0.8212967566,-0.305463557,-2.0015254919

H,0,1.106130144,3.7758388255,-6.1462091486

H,0,0.6017290808,2.0803534381,-6.0943832684

H,0,-0.4129382521,3.3301040329,-5.3557110519

β-hydrogen elimination of isobutanol as catalyzed by (η^5-Me_5C_5)$IrCl_2$

[M]—alkoxide

C,0,-1.3331513457,0.001056208,1.3872831893

C,0,-1.3032193036,1.3518911773,0.8375553915

C,0,-1.7443280032,1.2596218707,-0.5235812516

C,0,-2.088171016,-0.1395117848,-0.7991449502

C,0,-1.8726013736,-0.8994078065,0.394461285

Ir,0,-0.0362872812,0.0487138371,-0.269858023

O,0,1.5227613692,1.2272647065,-0.5690764405

C,0,2.8470497559,0.8343887839,-0.7748813694

C,0,3.5155565584,0.3245905984,0.5004725223

C,0,-0.8586183746,2.5869597978,1.5331757028

C,0,-1.8549555376,2.3887230263,-1.4812217699

C,0,-2.5982137438,-0.6644506285,-2.0909138159

C,0,-2.074744801,-2.3625334517,0.5548230895

C,0,-0.9246992404,-0.3717553657,2.7652039882

Cl,0,1.1706095108,-1.8710775174,-0.9873383817

C,0,4.9394074893,-0.1156688751,0.2126486682

H,0,-2.3002067482,-1.708826263,-2.2451539286

H,0,-3.6984773761,-0.6208501489,-2.1296655379

H,0,-2.2167879331,-0.086343249,-2.942071377

H,0,-1.3574819538,-2.7923630081,1.265173036

H,0,-3.0877023395,-2.5909122182,0.9212937651

H,0,-1.9316670905,-2.8929152399,-0.3945014742

H,0,-0.0885797506,0.2440612911,3.1212094473

H,0,-1.7600233212,-0.2342997336,3.4704746386

H,0,-0.6112876344,-1.421062844,2.8242951624

H,0,-1.7147316549,3.1977842113,1.8598135507

H,0,-0.2617477305,2.3553076748,2.4239940887

H,0,-0.2320230555,3.2070571011,0.8780400264

H,0,-1.7104737668,2.0573991206,-2.5172130794

H,0,-2.8481530651,2.8615712082,-1.421467922

H,0,-1.1037609794,3.1613748895,-1.2751110583

H,0,3.3988021827,1.7288049615,-1.1326527149

C,0,3.4470112828,1.3570211657,1.6124502253

H,0,2.9362927257,-0.5644645071,0.8146524847

H,0,2.9398540547,0.0650922763,-1.5636305696

H,0,5.4334571172,-0.511988612,1.1116144052

H,0,4.9698411052,-0.9028086912,-0.5549547545

H,0,5.5535893576,0.7246083372,-0.1504170417

H,0,3.8751806546,0.975106484,2.5513314893

H,0,4.0047369413,2.2697321116,1.3450875774

H,0,2.4078303148,1.6578111056,1.8102497262

TS

C,0,-1.5220661175,-1.618297679,-0.9923016659
C,0,-1.8958676346,-2.0176607054,0.3188621186
C,0,-1.865456606,-0.8374501616,1.182933989
C,0,-1.5201050435,0.2961156424,0.3517690552
C,0,-1.2595915191,-0.186648637,-0.9846256558
Ir,0,0.0900168021,-1.0931014254,0.425953771
O,0,1.8777642143,-1.5021880973,-0.7180307483
C,0,2.2793368507,-0.534026548,0.0366942095
C,0,2.5749706309,0.827522384,-0.5744934897
C,0,2.7434633664,1.9034350139,0.481458757
C,0,-2.2173135605,-3.386563857,0.7950334381
C,0,-2.2650546737,-0.8271518742,2.6144504858
C,0,-1.4640128143,1.7147468976,0.7933620431
C,0,-0.9292610934,0.6213519039,-2.1878946323
C,0,-1.3426092824,-2.4915082336,-2.1807491492
Cl,0,0.9765006387,-2.6671724886,2.059193059
H,0,-1.5782963255,-3.6611870583,1.6471015218
H,0,-3.2666750373,-3.4482696088,1.1214464125
H,0,-2.0630800296,-4.1393850452,0.0132080722
H,0,-1.8937176679,0.0662506302,3.1318054962
H,0,-3.3609303434,-0.8483365811,2.7276827996
H,0,-1.8532163259,-1.6995723806,3.1386443601
H,0,-0.7439697402,2.2980966056,0.2044881619
H,0,-2.4473408621,2.1976956102,0.6814585415
H,0,-1.1746481032,1.799002025,1.8486274612
H,0,-1.8142018838,0.7684149411,-2.8280461064
H,0,-0.553089168,1.6178681486,-1.9226174883
H,0,-0.161700167,0.1298916642,-2.8025203332

H,0,-1.3167448594,-3.5530730896,-1.9091829705
H,0,-2.1640113832,-2.3486066826,-2.9004166915
H,0,-0.4042736591,-2.2644516888,-2.7045105564
H,0,2.9533778105,-0.802829747,0.8851431416
C,0,3.8201890502,0.6814975564,-1.4412818279
H,0,1.7239453888,1.0803596317,-1.2313522383
H,0,1.2008976986,-0.0873319907,1.1517213699
H,0,3.0000176025,2.8729748625,0.032462781
H,0,1.8290811186,2.0435182493,1.0775952233
H,0,3.5528157589,1.6467237887,1.1826632918
H,0,4.0662480159,1.6269989474,-1.9447862956
H,0,4.6939412484,0.3948722408,-0.8354881943
H,0,3.6799957051,-0.0910451637,-2.2086865174

[M]-H—aldehyde
C,0,0.0292780103,-1.08538244,0.7950730019

C,0,0.4249136383,-2.0332732345,-0.2347390693

C,0,1.7545145617,-1.6699954253,-0.6526240877

C,0,2.2368076809,-0.6057176182,0.233951016

C,0,1.2024982503,-0.2642042444,1.1213637595

Ir,0,0.3916368162,-0.0689202137,-0.9876159447

O,0,1.3868096365,1.0638881238,-2.6620397167

C,0,0.7186461582,1.8222183319,-3.3541347748

C,0,1.305508633,2.9452922333,-4.1419161874

C,0,-0.383677766,-3.1782393683,-0.7295043565

C,0,2.5933216935,-2.3650686694,-1.6652245106

C,0,3.5771837427,0.0240938514,0.1100275428

C,0,1.1898111603,0.8192115987,2.1365087401

C,0,-1.2367369492,-1.0917018754,1.5753275573

Cl,0,-0.6465430489,2.1353715063,-0.6627900872

C,0,0.7702835189,2.9568938385,-5.5666400137

H,0,0.4291877612,1.5759946836,1.8874480336

H,0,0.9528448652,0.424099444,3.1360944341

H,0,2.1560400927,1.3341646654,2.2006637402

H,0,-2.0604768564,-1.5369284998,1.0034046729

H,0,-1.1312834872,-1.6638498027,2.5119623061

H,0,-1.5404065036,-0.0701594351,1.8397266715

H,0,-0.1315695252,-3.4366288321,-1.7657276756

H,0,-0.2145765,-4.0747341446,-0.1116146769

H,0,-1.4575291891,-2.9545515697,-0.7010372622

H,0,3.2729226894,-3.094052442,-1.1933436247

H,0,1.9812269487,-2.9092742255,-2.3954217231

H,0,3.2175282896,-1.6549221128,-2.2250767444

H,0,3.6734213812,0.914291902,0.7432299981

H,0,4.3779801687,-0.6767555289,0.3952057132

H,0,3.7790657172,0.3358027752,-0.9252528307

H,0,-0.3896979483,1.7193094411,-3.377433239

C,0,0.9598579228,4.2359125522,-3.3951874362

H,0,2.3997517773,2.8085169565,-4.1425579756

H,0,-0.7731172994,-0.327150328,-2.0847431994

H,0,1.1772827374,3.8095175726,-6.1267366137

H,0,1.0320894224,2.0425625369,-6.1165914105

H,0,-0.32592899,3.0519628307,-5.5781465544

H,0,1.3757994079,5.1038609381,-3.9254633487

H,0,-0.129018892,4.3710957156,-3.3216534697

H,0,1.3513982726,4.2277755124,-2.369922654

β-hydrogen elimination of neopentanol as catalyzed by (η^5-Me_5C_5)$IrCl_2$

[M]—alkoxide

C,0,-1.5209510421,-0.2270942301,1.3846621737

C,0,-1.2789748598,1.1496684402,0.9491836847

C,0,-1.6581234428,1.2400821664,-0.429777755

C,0,-2.1380983148,-0.0811055779,-0.8418030326

C,0,-2.1023348565,-0.9611939634,0.2925422871

Ir,0,-0.1256224413,-0.205398578,-0.1960325402

O,0,1.5049212418,0.8306605225,-0.6235123612

C,0,2.8202664827,0.391298008,-0.7574821004

C,0,3.6330356447,0.5643598031,0.5408351968

C,0,-0.7261898876,2.2463862739,1.7839145876

C,0,-1.5700034219,2.4482246955,-1.2884653239

C,0,-2.6250837466,-0.4322932839,-2.1994235436

C,0,-2.5008777602,-2.3922460695,0.3111258004

C,0,-1.2567700151,-0.7600975429,2.745239558

Cl,0,0.9442663876,-2.2932210462,-0.6142226553

C,0,5.0633836421,0.1168448186,0.2565795112

H,0,-2.4723009542,-1.49580394,-2.4197427958

H,0,-3.7028058237,-0.2235742715,-2.2941058329

H,0,-2.10962895,0.1441005376,-2.9778305626

H,0,-1.8820506483,-2.972266759,1.0068174429

H,0,-3.5526366862,-2.5117290907,0.6146028802

H,0,-2.3806835046,-2.8561259057,-0.6755491079

H,0,-0.4226776651,-0.239061846,3.2320159065

H,0,-2.1411705084,-0.6411645548,3.3916693033

H,0,-1.0072277484,-1.8281206847,2.7174746528

H,0,-1.5258263879,2.7889336927,2.3127066944

H,0,-0.0300312332,1.865964239,2.5429185751

H,0,-0.1760931387,2.9734694791,1.1733715933

H,0,-1.4567043381,2.18236439,-2.3468878589

H,0,-2.4731507166,3.0721950854,-1.1986136037

H,0,-0.7050319984,3.0665207806,-1.0168812633

H,0,3.3007650292,1.0069999591,-1.5457904966

C,0,3.6181367796,2.0303629846,0.9641718206

C,0,3.0365558247,-0.297519719,1.6496195704

H,0,2.8894040486,-0.6614415802,-1.0854490893

H,0,5.702764942,0.2293258246,1.1453868971

H,0,5.1016751893,-0.9406090193,-0.0461329093

H,0,5.5177141205,0.7100554814,-0.5522244455

H,0,3.6121402498,-0.1977559371,2.5831777742

H,0,1.9980776596,-0.0006840826,1.8711892815

H,0,3.0158161241,-1.3609438417,1.3692622774

H,0,4.1868541282,2.18629773,1.8941140826

H,0,4.0624612732,2.6763563716,0.1910385109

H,0,2.5889373229,2.37901724,1.131253215

TS

C,0,-1.6148072849,-1.6761249632,-0.9858333162

C,0,-1.9067445547,-2.062210805,0.3482593809

C,0,-1.9107391726,-0.8575905739,1.1795150542

C,0,-1.6810016816,0.2716151005,0.3051696823

C,0,-1.4592797384,-0.2294445935,-1.0314999933

Ir,0,0.0194569639,-1.008854256,0.34356873

O,0,1.8121298359,-1.3949741429,-0.833506341

C,0,2.2723117549,-0.5151386522,-0.0166203892

C,0,2.8200815191,0.8175424035,-0.5285753395

C,0,3.0195826356,1.7803607427,0.6343712867

C,0,-2.1266697165,-3.4339907743,0.8700797692

C,0,-2.2339490888,-0.8339062542,2.6299036577

C,0,-1.7029694279,1.7026415626,0.7085572037

C,0,-1.3410014664,0.5592133935,-2.2857573032

C,0,-1.4318933827,-2.5678258255,-2.1601208404

Cl,0,0.9937423858,-2.4956290173,2.026143294

H,0,-1.4552974354,-3.6418589367,1.715762714

H,0,-3.1638048955,-3.552444413,1.2196634967

H,0,-1.939722099,-4.1977926387,0.1061554585

H,0,-1.9055932474,0.1002740617,3.102287948

H,0,-3.3177862642,-0.9335785931,2.8014444906

H,0,-1.7290546798,-1.6570454867,3.152743771

H,0,-1.055257846,2.3179750696,0.0702493193

H,0,-2.7222681477,2.1132401748,0.6358192922

H,0,-1.3678213675,1.8355357951,1.7449956183

H,0,-2.301037057,0.5673240324,-2.8277127116

H,0,-1.0667685803,1.6046235123,-2.0997698099

H,0,-0.5912958853,0.1342973043,-2.9669029291

H,0,-1.3106109125,-3.6162238193,-1.8641626509

H,0,-2.2977841504,-2.508086467,-2.8382817419

H,0,-0.54204828,-2.2854210739,-2.7389212196

H,0,2.809072613,-0.8906412906,0.8850022575

C,0,4.1772277866,0.4588181484,-1.147048547

C,0,1.9087747932,1.4185187656,-1.5834002627

H,0,1.0985089844,0.107595118,0.9611967197

H,0,3.5402395786,2.6923116867,0.3079125602

H,0,2.0574171174,2.0879458554,1.0735506572

H,0,3.6200183276,1.3262337741,1.4370746347

H,0,2.3605341419,2.3122933572,-2.0381178846

H,0,1.7015527706,0.6923324375,-2.3815949915

H,0,0.9476364855,1.715345379,-1.1376925488

H,0,4.6773144629,1.3611751164,-1.5282197171

H,0,4.8481058639,-0.0064848341,-0.409819659

H,0,4.0566833417,-0.24585538,-1.9814958003

[M]-H—aldehyde

C,0,0.0316972147,-1.0839043157,0.808028715

C,0,0.3961419901,-2.0396532221,-0.2263165039

C,0,1.7238608853,-1.6969330124,-0.6667754456

C,0,2.2363532201,-0.6379633251,0.2093234156

C,0,1.2224411015,-0.2798838559,1.1136163223

Ir,0,0.3801820283,-0.0762622633,-0.9818080162

O,0,1.3783510871,1.0362187687,-2.6718069648

C,0,0.7296504944,1.8211607354,-3.3515127449

C,0,1.3441408757,2.931942983,-4.1517537087

C,0,-0.4377146716,-3.1732095742,-0.7051340854

C,0,2.5351376234,-2.4051936136,-1.6926035142

C,0,3.5827038999,-0.0264059347,0.0603848435

C,0,1.2429008976,0.8052782008,2.1268148528

C,0,-1.2209629205,-1.0704465144,1.6094342356

Cl,0,-0.6157015877,2.1454326521,-0.6468707212

C,0,0.8094031366,2.8516092244,-5.5836018968

H,0,0.4911902917,1.5742432639,1.8881020589

H,0,1.0147377872,0.4156833253,3.1305981623

H,0,2.2183941777,1.3042216563,2.1755089365

H,0,-2.0609498416,-1.5031125027,1.0516980807

H,0,-1.1085047336,-1.6438677555,2.5444800785

H,0,-1.5043625633,-0.044286465,1.8783693325

H,0,-0.2068273285,-3.4374663687,-1.7448044756

H,0,-0.2721219163,-4.07094341,-0.088091783

H,0,-1.5074145441,-2.9330727898,-0.6595097585

H,0,3.2141072387,-3.141513986,-1.2313439264

H,0,1.90286857,-2.9433636651,-2.409959998

H,0,3.1577708335,-1.7043438949,-2.2658694914

H,0,3.6992042447,0.8682570753,0.6839123904

H,0,4.3789795676,-0.7345085519,0.3403494549

H,0,3.7736113786,0.273065757,-0.9807693317

H,0,-0.3809028883,1.7556522642,-3.3667356344

C,0,0.8424324274,4.222781464,-3.4842297029

C,0,2.8627434448,2.8581396024,-4.1194684815

H,0,-0.8042070122,-0.3170164279,-2.0617515801

H,0,1.1627988459,3.712136329,-6.1694126931

H,0,1.1476515778,1.9391313048,-6.0954985558

H,0,-0.2900088533,2.8650900203,-5.6081029076

H,0,1.2188668425,5.0962481889,-4.0366015716

H,0,-0.255440615,4.2734519209,-3.4709208842

H,0,1.1815531548,4.2925121496,-2.4417165781

H,0,3.3013021852,3.6928261791,-4.6842464206

H,0,3.2423895688,2.9071995881,-3.090093475

H,0,3.2300148845,1.9208947955,-4.5604400284

References

(1) Brown, L. C.; Ressegue, E.; Merola, J. S. *Organometallics* **2016**, *35* (24), 4014–4022.

(2) Tönnemann, J.; Risse, J.; Grote, Z.; Scopelliti, R.; Severin, K. *Eur. J. Inorg. Chem.* **2013**, *2013* (26), 4558–4562.

(3) Piou, T.; Romanov-Michailidis, F.; Romanova-Michaelides, M.; Jackson, K. E.; Semakul, N.; Taggart, T. D.; Newell, B. S.; Rithner, C. D.; Paton, R. S.; Rovis, T. *J. Am. Chem. Soc.* **2017**, *139* (3), 1296–1310.

(4) Fier, P. S.; Luo, J.; Hartwig, J. F. *Copper-Mediated Fluorination of Arylboronate Esters. Identification of a Copper(III) Fluoride Complex*; 2013; Vol. 135.

(5) Ascic, E.; Ohm, R. G.; Petersen, R.; Hansen, M. R.; Hansen, C. L.; Madsen, D.; Tanner, D.; Nielsen, T. E. *Chem. - A Eur. J.* **2014**, *20* (12), 3297–3300.

(6) Li, W.; Xie, J. H.; Yuan, M. L.; Zhou, Q. L. *Green Chem.* **2014**, *16* (9), 4081–4085.

(7) Oger, C.; Marton, Z.; Brinkmann, Y.; Burtel-Poncé, V.; Durand, T.; Graber, M.; Galano, J. M. *J. Org. Chem.* **2010**, *75* (6), 1892–1897.

(8) Kim, H.; Lee, C. *Org. Lett.* **2011**, *13* (8), 2050–2053.

(9) Endo, Y.; Bäckvall, J. E. *Chem. - A Eur. J.* **2011**, *17* (45), 12596–12601.

(10) Peng, J.; Place, A. R.; Yoshida, W.; Anklin, C.; Hamann, M. T. *J. Am. Chem. Soc.* **2010**, *132* (10), 3277–3279.

(11) Hoover, J. M.; Stahl, S. S. *J. Am. Chem. Soc.* **2011**, *133* (42), 16901–16910.

(12) Kelly, B. D.; Lambert, T. H. *Org. Lett.* **2011**, *13* (4), 740–743.

(13) Akhtar, W. M.; Armstrong, R. J.; Frost, J. R.; Stevenson, N. G.; Donohoe, T. J. *J. Am. Chem. Soc.* **2018**, *140* (38), 11916–11920.

(14) Mitsudome, T.; Noujima, A.; Mizugaki, T.; Jitsukawa, K.; Kaneda, K. *Green Chem.* **2009**, *11* (6), 793–797.

(15) Fujita, K. I.; Ito, W.; Yamaguchi, R. *ChemCatChem* **2014**, *6* (1), 109–112.

(16) Kayser, M. M.; Salvador, J.; Morand, P. *Can. J. Chem.* **1983**, *61* (3), 439–441.

(17) Matsubara, S.; Takai, K.; Nozaki, H. *Bull. Chem. Soc. Jpn.* **1983**, *56* (7), 2029–2032.

(18) Ishii, Y.; Osakada, K.; Ikariya, T.; Saburi, M.; Yoshikawa, S. *J. Org. Chem.* **1986**, *51* (11), 2034–2039.

(19) Reynolds, N. T.; Rovis, T. *Tetrahedron* **2005**, *61* (26), 6368–6378.

(20) Little, R. D.; Muller, G. W.; Venegas, M. G.; Carroll, G. L.; Bukhari, A.; Patton, L.; Stone, K. *Tetrahedron* **1981**, *37* (25), 4371–4383.

(21) Hoefgen, B.; Decker, M.; Mohr, P.; Schramm, A. M.; Rostom, S. A. F.; El-Subbagh, H.; Schweikert, P. M.; Rudolf, D. R.; Kassack, M. U.; Lehmann, J. *J. Med. Chem.* **2006**, *49* (2), 760–769.

(22) Fukutomi, Ryuuta; Inoue, Hitoshi; Kawamura, Koji; Kishimoto, Takuya; Suzuki, Masashi; Shibayama, Rie; Kojima, Kazuko; Hagihara, K. Novel 4-(2-furoyl)aminopiperidines, intermediates in synthesizing the same, process for producing the same and medicinal use of the same. WO 2003035645, 2003.

(23) Helfer, D. S.; Phaho, D. S.; Atwood, J. D. *Organometallics* **2006**, *25* (2), 410–415.

(24) Miao, L.; Dimaggio, S. C.; Trudell, M. L. *Synthesis (Stuttg).* **2010**, *2010* (1), 91–97.

(25) Ghosh, A. K.; Nicponski, D. R. *Org. Lett.* **2011**, *13* (16), 4328–4331.

5.5 Synthetic procedures and characterization of products from Chapter 4

5.5.1 Synthesis of HMe_4C_5R and $Me_4C_5R_2$ dienes

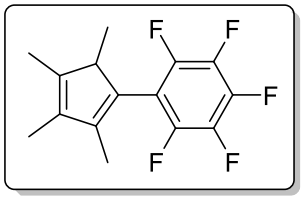

1,2,3,4,5-pentafluoro-6-(2,3,4,5-tetramethylcyclopenta-1,3-dien-1-yl)benzene (**1a**)

Major isomer: ^{1}H NMR (400 MHz, $CDCl_3$) δ 3.23 (br q, 1H, J_{HH} = 7.6 Hz, 1 CpC*H*), 1.92 (d, 3H, J_{HF} = 1.2 Hz, 1 CpCH_3), 1.87 (m, 3H, 1 CpCH_3), 1.86 (m, 3H, 1 CpCH_3), 0.92 (d, 3H, J_{HH} = 7.7 Hz, 1 CpCH_3). ^{19}F NMR (376 MHz, $CDCl_3$) δ -140.59 (br s, 2F, 2 Ar*F*), -157.46 (t, 1F, J_{FF} = 20.8 Hz, 1 Ar*F*), -163.13 – 163.35 (m, 2F, 2 Ar*F*).

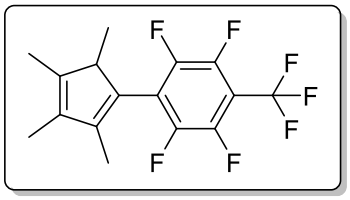

1,2,4,5-tetrafluoro-3-(2,3,4,5-tetramethylcyclopenta-1,3-dien-1-yl)-6-(trifluoromethyl)benzene (**1b**)

$KCpMe_4$ (5.0 g, 0.031 mmol) was slowly added to a solution of octafluorotoluene (8.84 g, 0.037 mol) in THF (60 mL) and the mixture was stirred at 25 °C for 16 h. The solvent was removed under reduced pressure, and the residue was washed with hexanes. Then DI water was added to the hexane layer and separated using a separatory funnel. The organic layer was dried over $MgSO_4$, filtered, and evaporated under reduced pressure. The residue was separated via column chromatography with the monoarylated product eluting first and the diarylated product eluting last. The hexanes fraction containing the monoarylated product was evaporated under reduced pressure

to yield 2.85 g (27 %) and was used without further purification. **Major isomer:** ^{1}H NMR (400 MHz, $CDCl_3$) δ 3.40 – 3.33 (m, 1H, 1 CpC*H*), 1.95 (d, 3H, J_{HF} = 1.3 Hz, 1 CpCH_3), 1.89 (t, 3H, J_{HH} = 1.3 Hz, 1 CpCH_3), 1.86 (q, 3H, J_{HH} = 1.9 Hz, 1 CpCH_3), 0.96 (d, 3H, J_{HH} = 7.7 Hz, 1 CpCH_3). ^{19}F NMR (376 MHz, $CDCl_3$) δ -56.23 (t, 1F, J_{FF} = 21.6 Hz, 1 CF_3), -138.96 (br s, 1F, 1 Ar*F*), -141.88 – 142.39 (m, 3F, 3 Ar*F*).

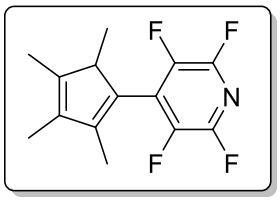

2,3,5,6-tetrafluoro-4-(2,3,4,5-tetramethylcyclopenta-1,3-dien-1-yl)pyridine (**1c**)

$KCpMe_4$ (1.6 g, 0.010 mmol) was slowly added to a solution of C_5F_4N (2.03 g, 0.012 mol) in THF (60 mL) and the mixture was stirred at 25 °C for 16 h. The solvent was removed under reduced pressure, and the residue was washed with hexanes. Then DI water was added to the hexane layer and separated using a separatory funnel. The organic layer was dried over $MgSO_4$, filtered, and evaporated under reduced pressure. The residue was separated via column chromatography with the monoarylated product eluting first and the diarylated product eluting last. The hexanes fraction containing the monoarylated product was evaporated under reduced pressure to yield 730 mg (27 %) and was used without further purification. **Major isomer:** ^{1}H NMR (400 MHz, $CDCl_3$) δ 3.44 – 3.38 (m, 1H, 1 CpC*H*), 1.95 (m, 3H, 1 CpCH_3), 1.90 – 1.88 (m, 6H, 2 CpCH_3), 0.96 (d, 3H, J_{HH} = 7.7 Hz, 1 CpCH_3). ^{19}F NMR (376 MHz, $CDCl_3$) δ -92.39 – 92.59 (m, 2F, Ar*F*), -92.06 (br s, 2F, 2 Ar*F*).

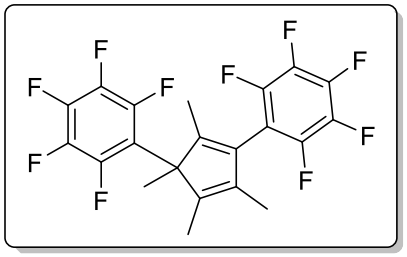

6,6'-(2,3,4,5-tetramethylcyclopenta-1,4-diene-1,3-diyl)bis(1,2,3,4,5-pentafluorobenzene) (**2a**)

^{1}H NMR (400 MHz, *toluene-d*$_8$) δ 1.53 (s, 3H, 1 CpC*H*$_3$), 1.50 (s, 3H, 1 CpC*H*$_3$), 1.46 (s, 3H, 1 CpC*H*$_3$), 1.41 – 1.36 (m, 3H, 1 CpC*H*$_3$). ^{19}F NMR (376 MHz, *toluene-d*$_8$) δ -133.47 (m, 1F, 1 Ar*F*), -134.37 – 134.70 (m, 1F, 1 ArF), -135.82 (dd, 1F, J_{FF} = 23.9, 8.3 Hz, 1 Ar*F*), -136.80 (m, 1F, 1 Ar*F*), -149.81 (t, 1F, J_{FF} = 21.3 Hz, 1 Ar*F*), -157.51 (tt, 1F, J_{FF} = 23.4, 21.2, 8.3 Hz, 1 Ar*F*), -156.96 – 157.11 (m, 2F, 1 Ar*F*), -157.35 – 157.59 (m, 2F, 1 Ar*F*).

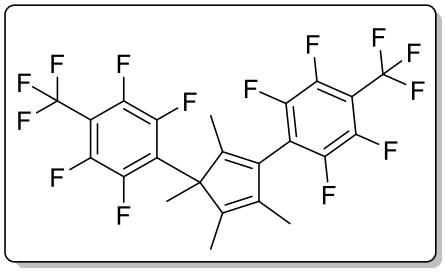

6,6'-(2,3,4,5-tetramethylcyclopenta-1,4-diene-1,3-diyl)bis(1,2,4,5-tetrafluoro-3-(trifluoromethyl) benzene) (**2b**)

Following the procedure from **1b**, the hexanes fraction containing diarylated product was evaporated under reduced pressure to yield 8.46 g (49 %). ^{1}H NMR (400 MHz, $CDCl_3$) δ 1.76 (s, 3H, 1 CpC*H*$_3$), 1.73 (s, 3H, 1 CpC*H*$_3$), 1.71 (s, 3H, 1 CpC*H*$_3$), 1.65 – 1.63 (m, 3H, 1 CpC*H*$_3$). ^{19}F NMR (376 MHz, $CDCl_3$) δ -56.29 (t, 3F, J_{FF} = 21.7 Hz, 1 C*F*$_3$), -56.49 (t, 3F, J_{FF} = 21.2 Hz, 1 C*F*$_3$), -136.23 (dt, 1F, J_{FF} = 21.9, 11.8 Hz, 1 Ar*F*), -137.07 (dt, 1F, J_{FF} = 25.2, 12.8 Hz, 1 Ar*F*), -138.16 (dd, 1F, J_{FF} = 22.6, 12.8 Hz, 1 Ar*F*), -139.31 – 139.52 (m, 1F, 1 Ar*F*), -140.15 – 140.43

(m, 1F, 1 Ar*F*), -140.46 – 140.72 (m, 1F, 1 Ar*F*), -140.73 – 141.01 (m, 1F, 1 Ar*F*), -141.06 – 141.34 (m, 1F, 1 Ar*F*).

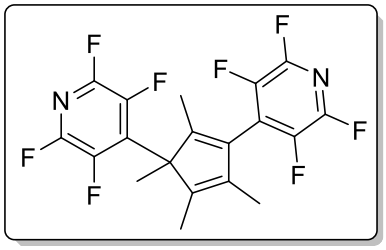

4,4'-(2,3,4,5-tetramethylcyclopenta-1,4-diene-1,3-diyl)bis(2,3,5,6-tetrafluoropyridine) (**2c**)

Following the procedure from **1c**, the hexanes fraction containing diarylated product was evaporated under reduced pressure to yield 0.55 g (13 %). ^{1}H NMR (400 MHz, $CDCl_3$) δ 1.78 – 1.74 (m, 9H, 3 CpCH_3), 1.68 – 1.66 (m, 3H, 1 CpCH_3). ^{19}F NMR (376 MHz, $CDCl_3$) δ -90.37 – 91.04 (m, 3F, Ar*F*), -91.85 – 92.29 (m t, 1 Ar*F*), -139.45 – 139.85 (m, 1F, 1 Ar*F*), -140.31 – 140.58 (m, 1F, 1 Ar*F*), -141.43 (dd, 1F, J_{FF} = 28.6, 21.0 Hz, 1 Ar*F*), -142.15 – 142.52 (m, 1F, 1 Ar*F*).

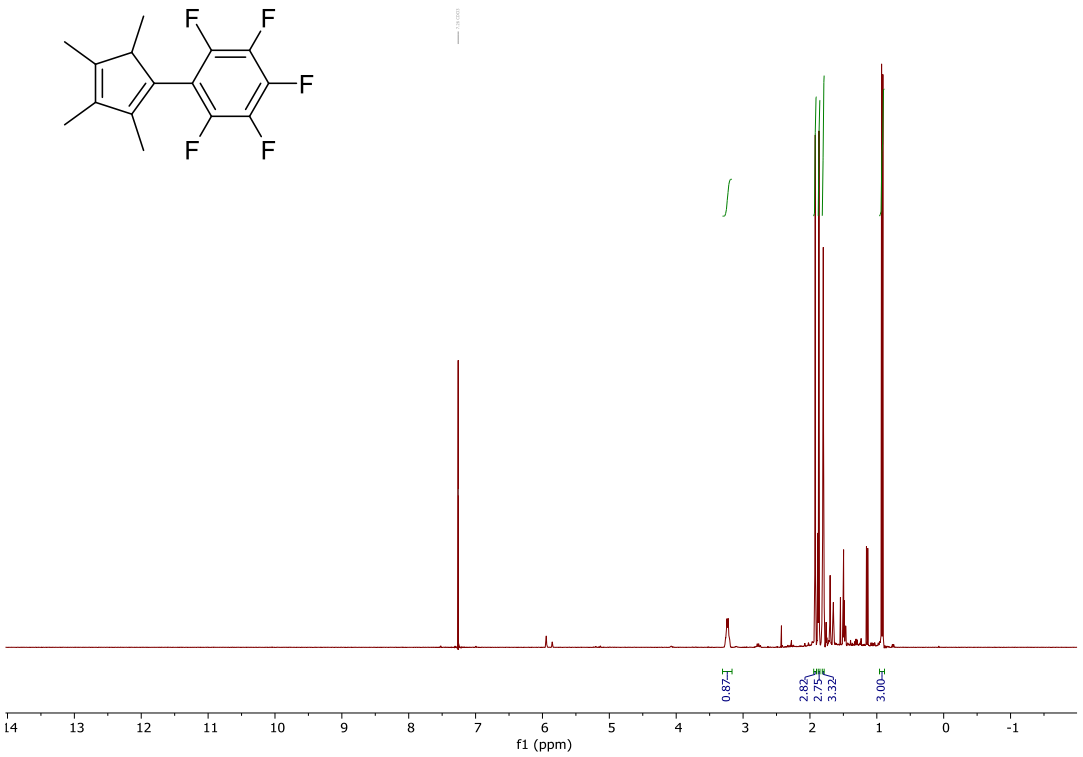

Figure S1. ^{1}H NMR spectrum of **1a** in $CDCl_3$ at 400 MHz.

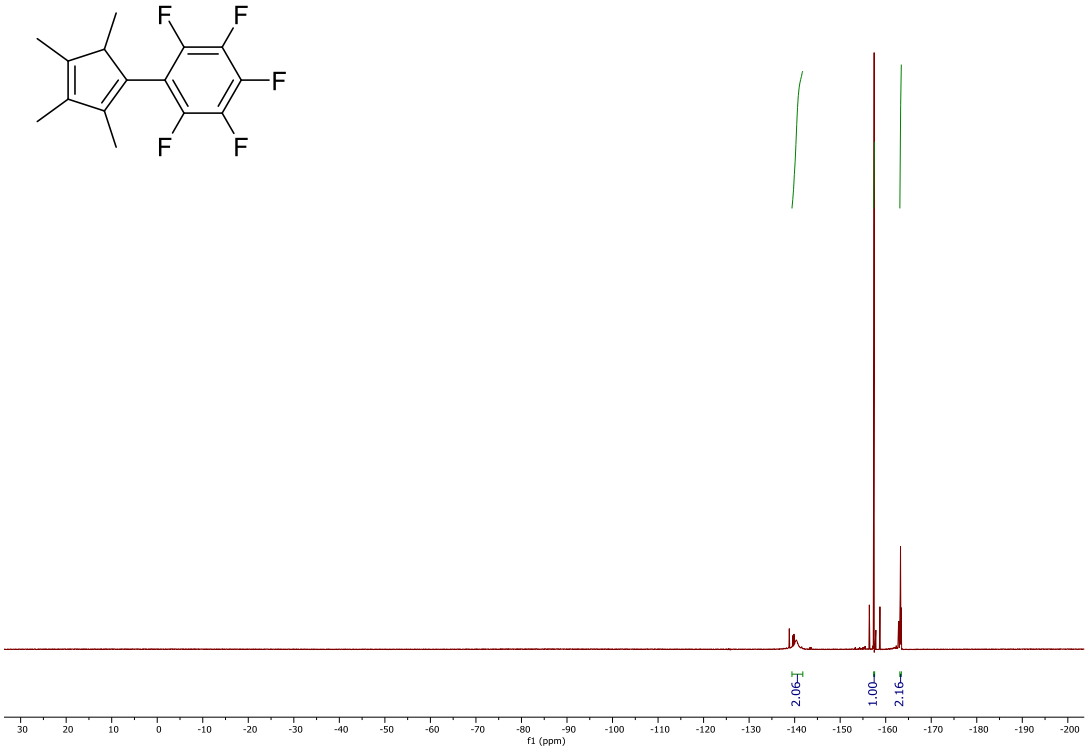

Figure S2. ^{19}F NMR spectrum of **1a** in $CDCl_3$ at 376 MHz.

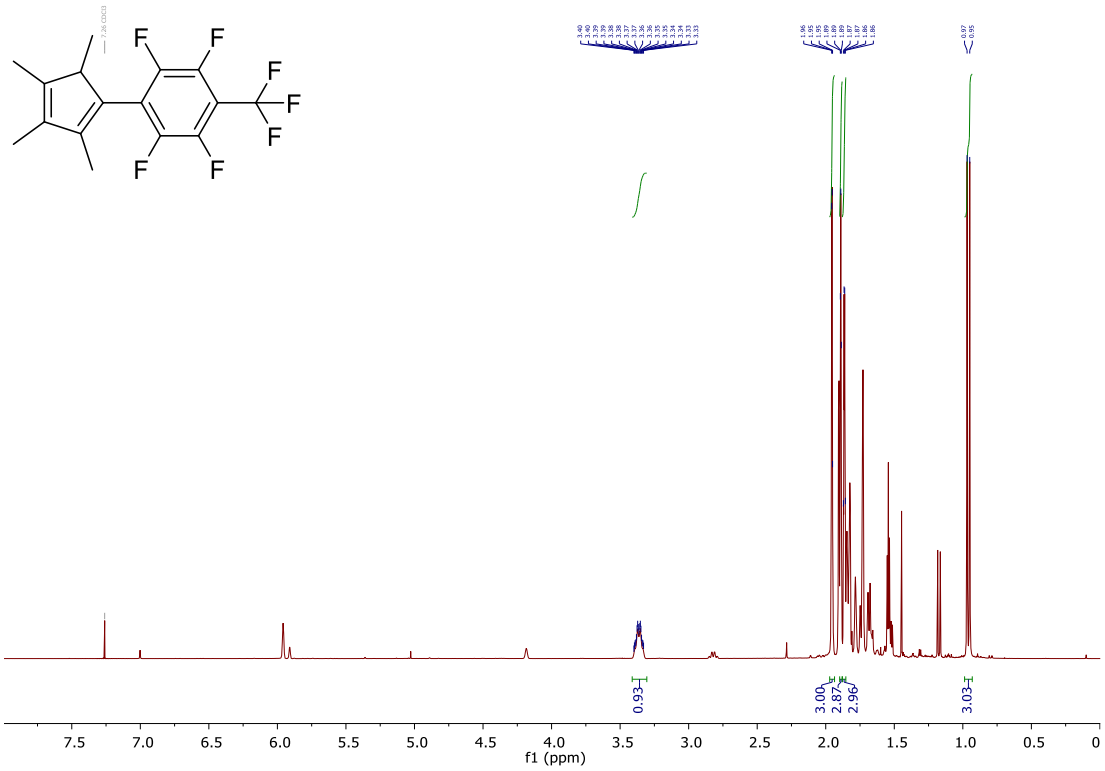

Figure S3. Crude ^{1}H NMR spectrum of **1b** in $CDCl_3$ at 400 MHz.

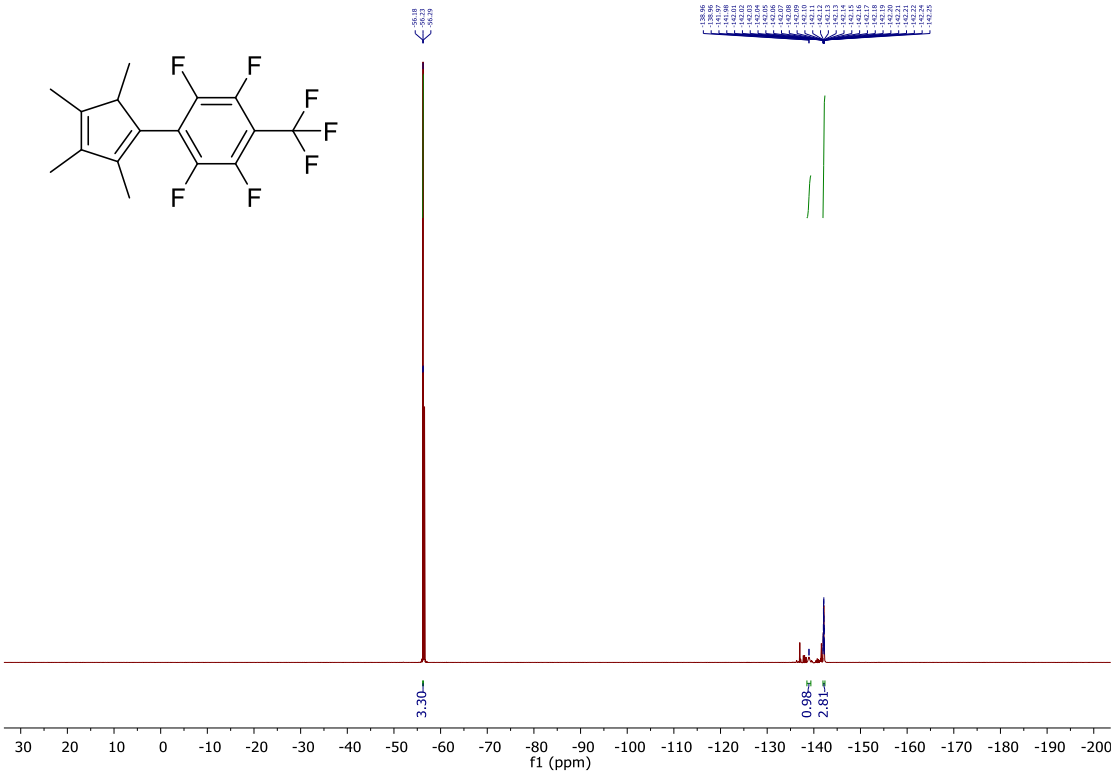

Figure S4. Crude ^{19}F NMR spectrum of **1b** in $CDCl_3$ at 376 MHz.

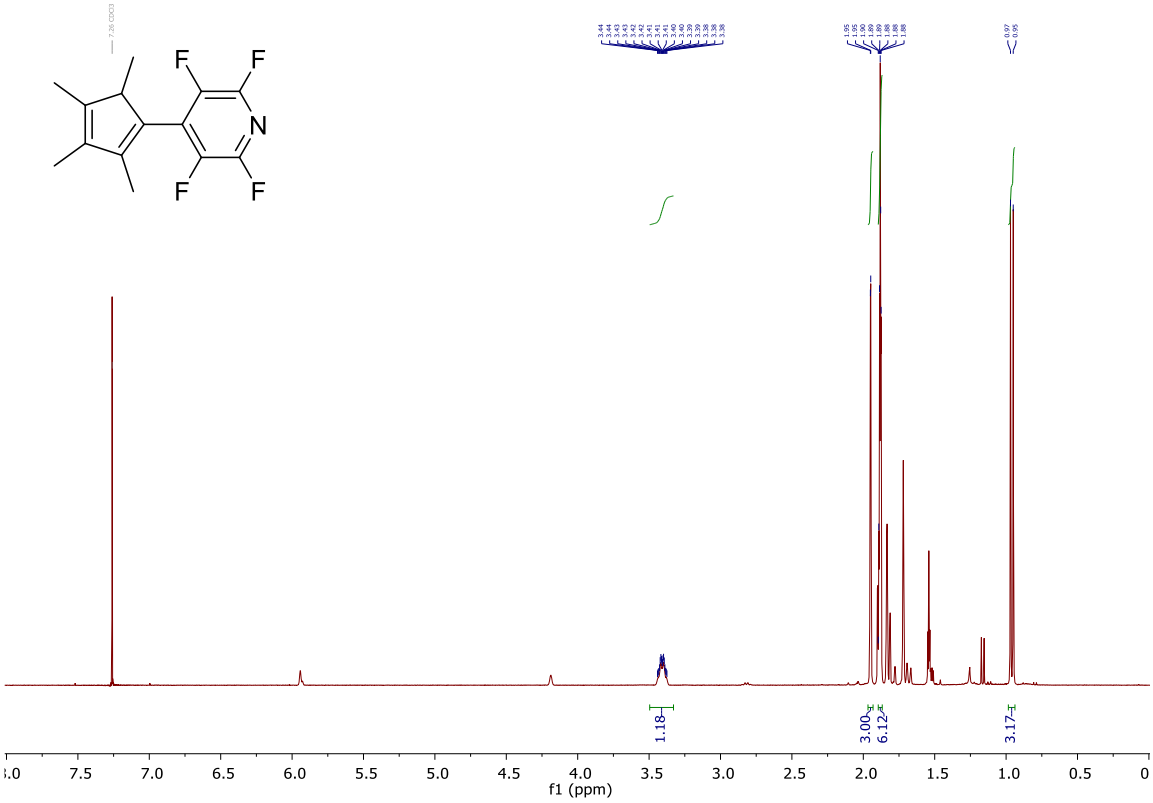

Figure S5. Crude ^{1}H NMR spectrum of **1c** in $CDCl_3$ at 400 MHz.

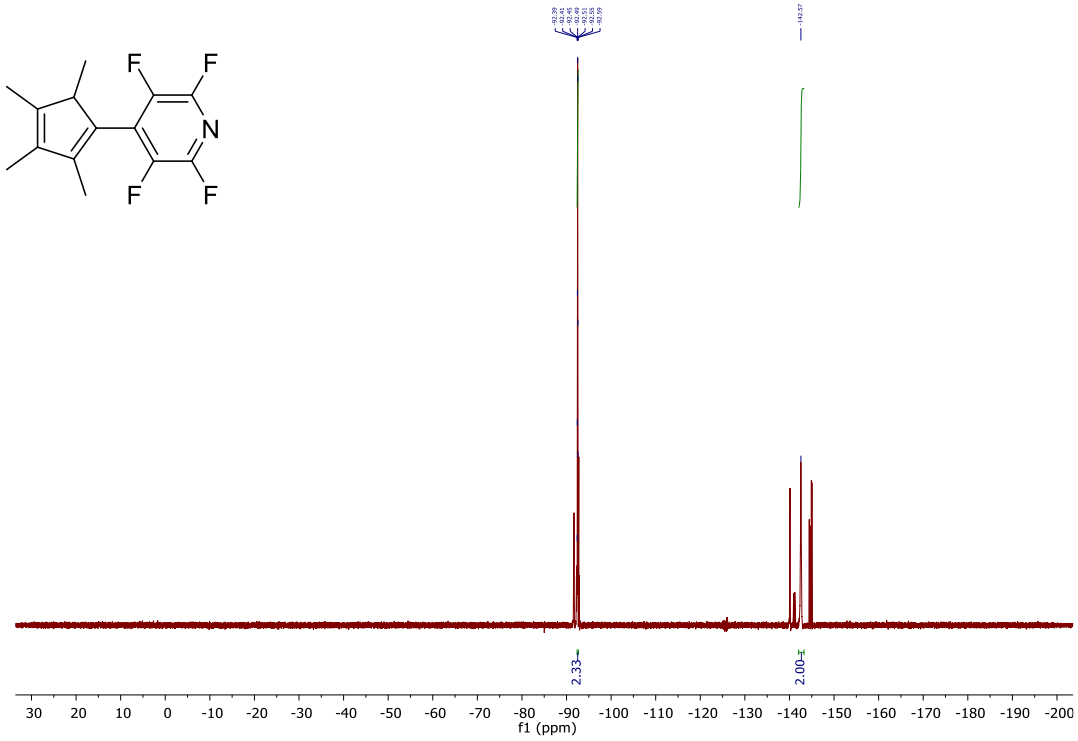

Figure S6. Crude ^{19}F NMR spectrum of **1c** in $CDCl_3$ at 376 MHz.

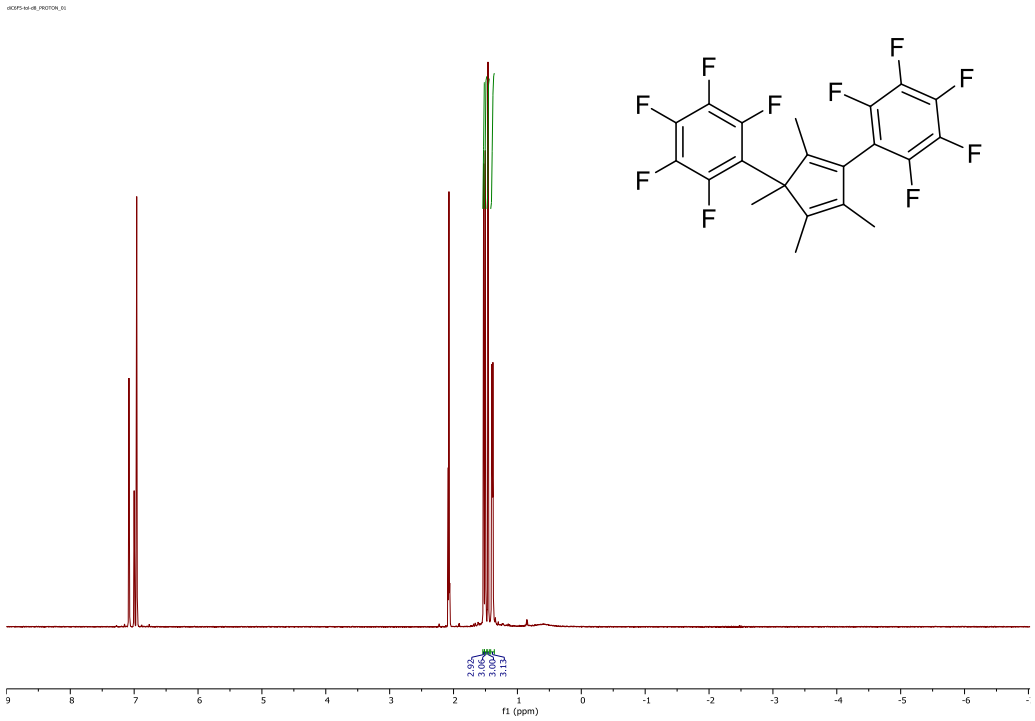

Figure S7. ^{1}H NMR spectrum of **2a** in *toluene-d*$_8$ at 400 MHz.

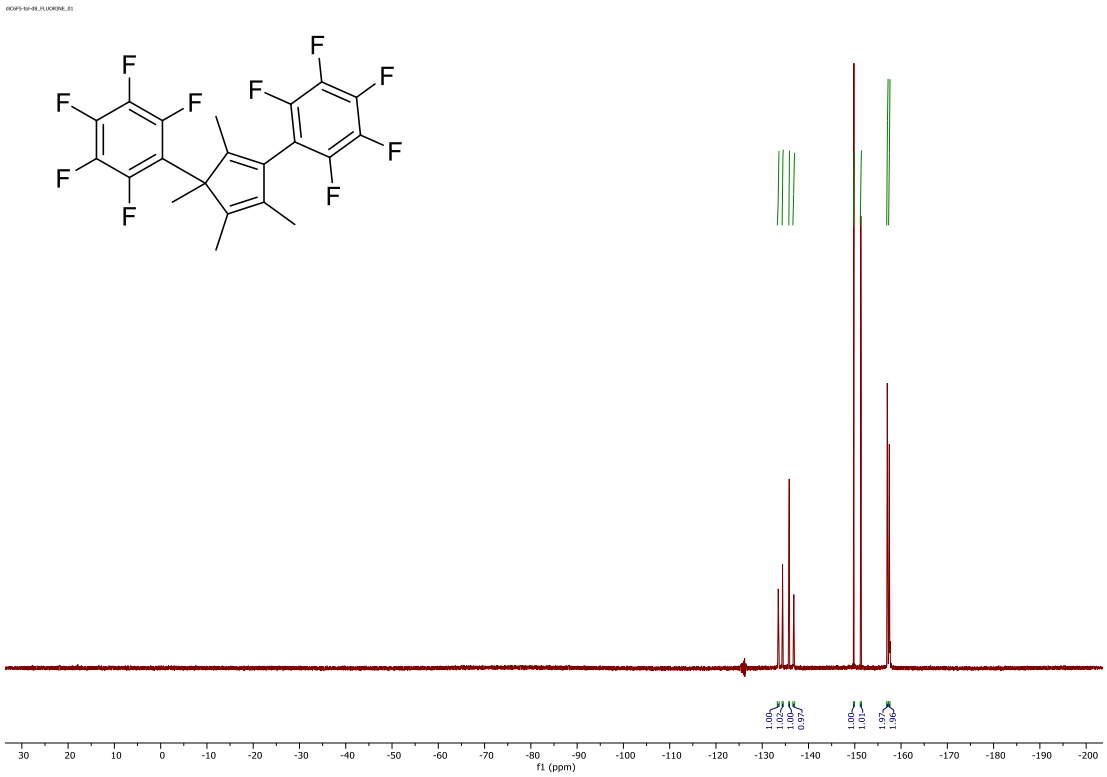

Figure S8. ^{19}F NMR spectrum of **2a** in *toluene-d*$_8$ at 376 MHz.

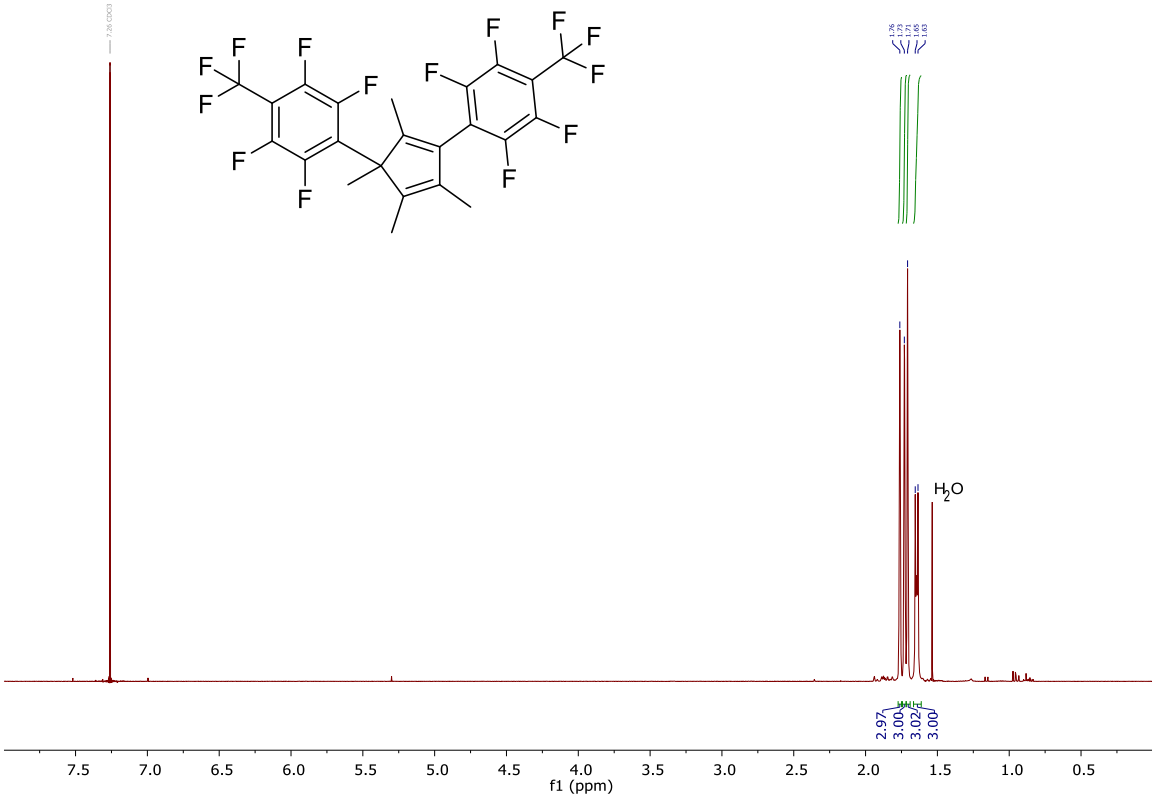

Figure S9. ^{1}H NMR spectrum of **2b** in $CDCl_3$ at 400 MHz.

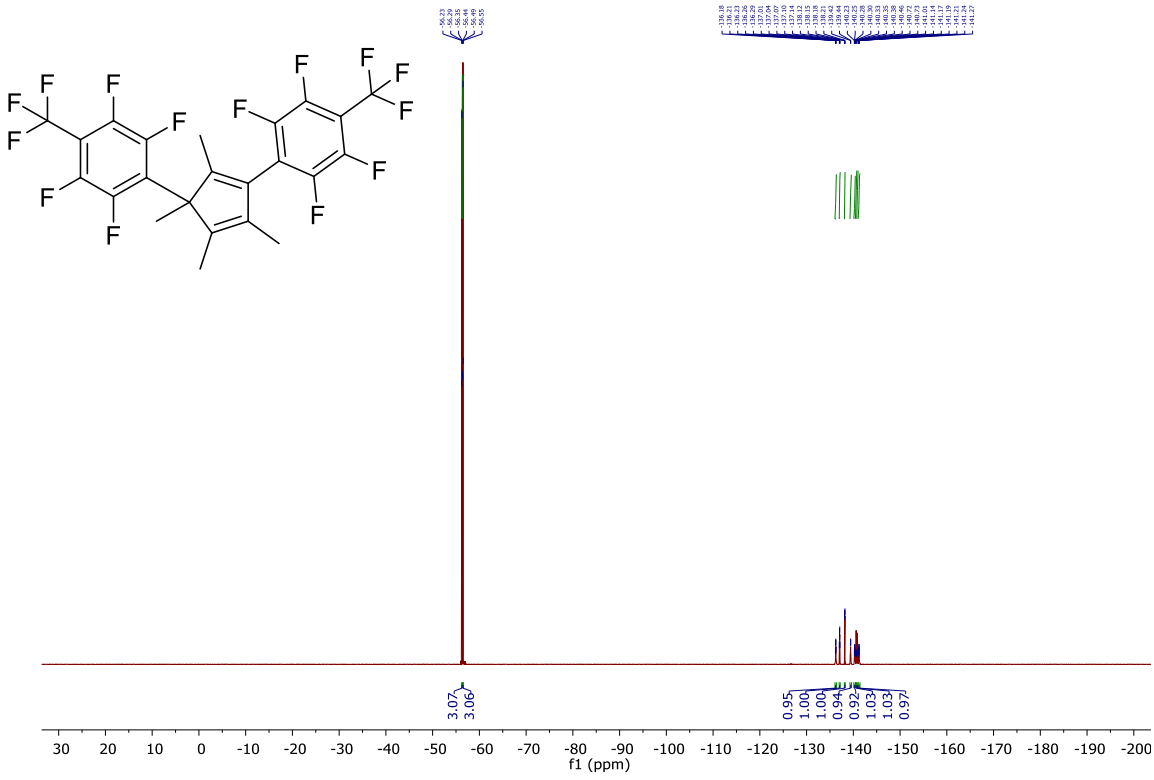

Figure S10. ^{19}F NMR spectrum of **2b** in $CDCl_3$ at 376 MHz.

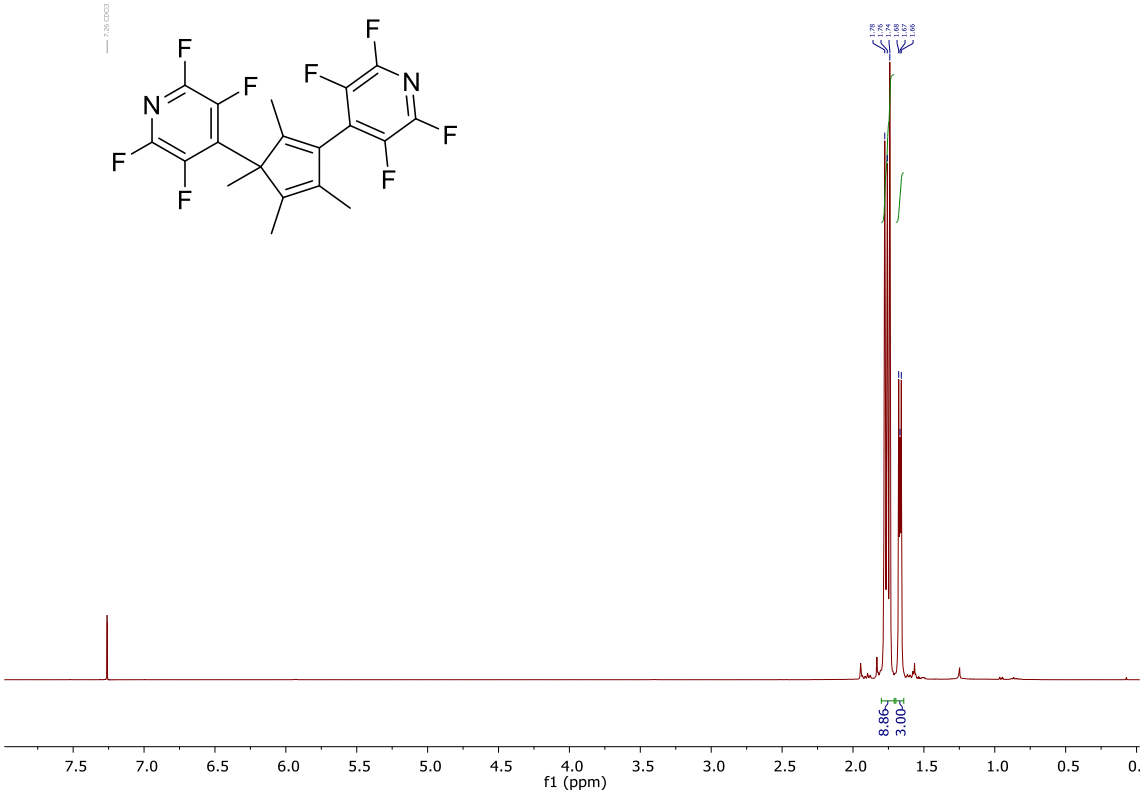

Figure S11. ^{1}H NMR spectrum of **2c** in $CDCl_3$ at 400 MHz.

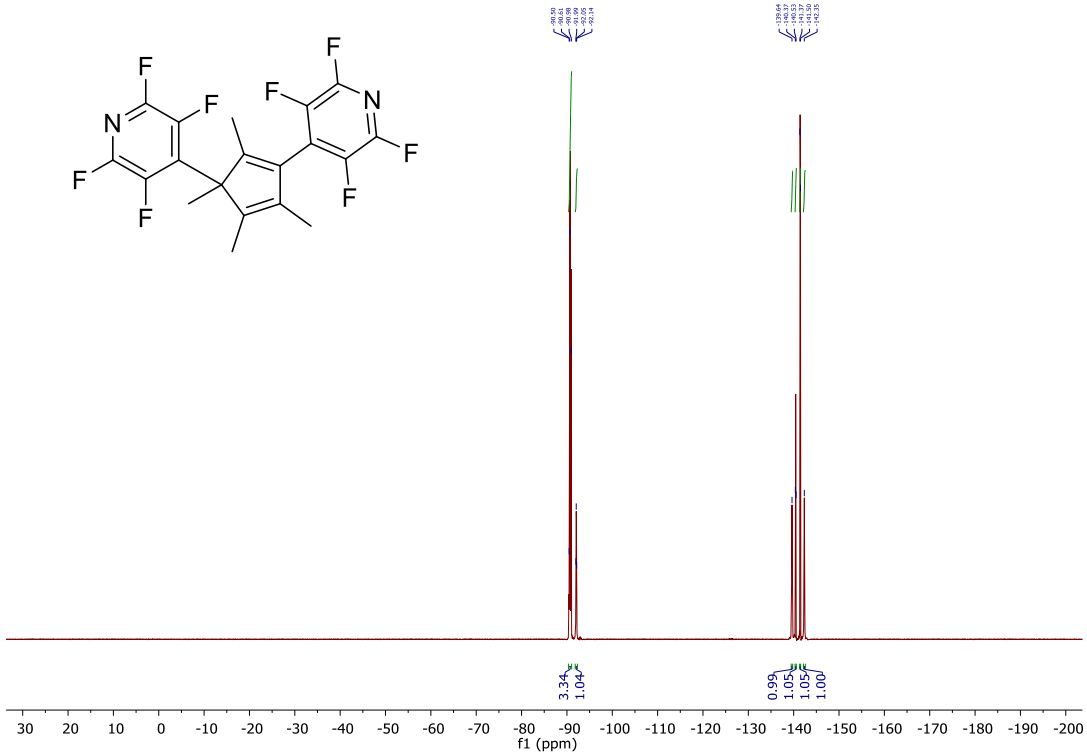

Figure S12. ^{19}F NMR spectrum of **2c** in $CDCl_3$ at 376 MHz.

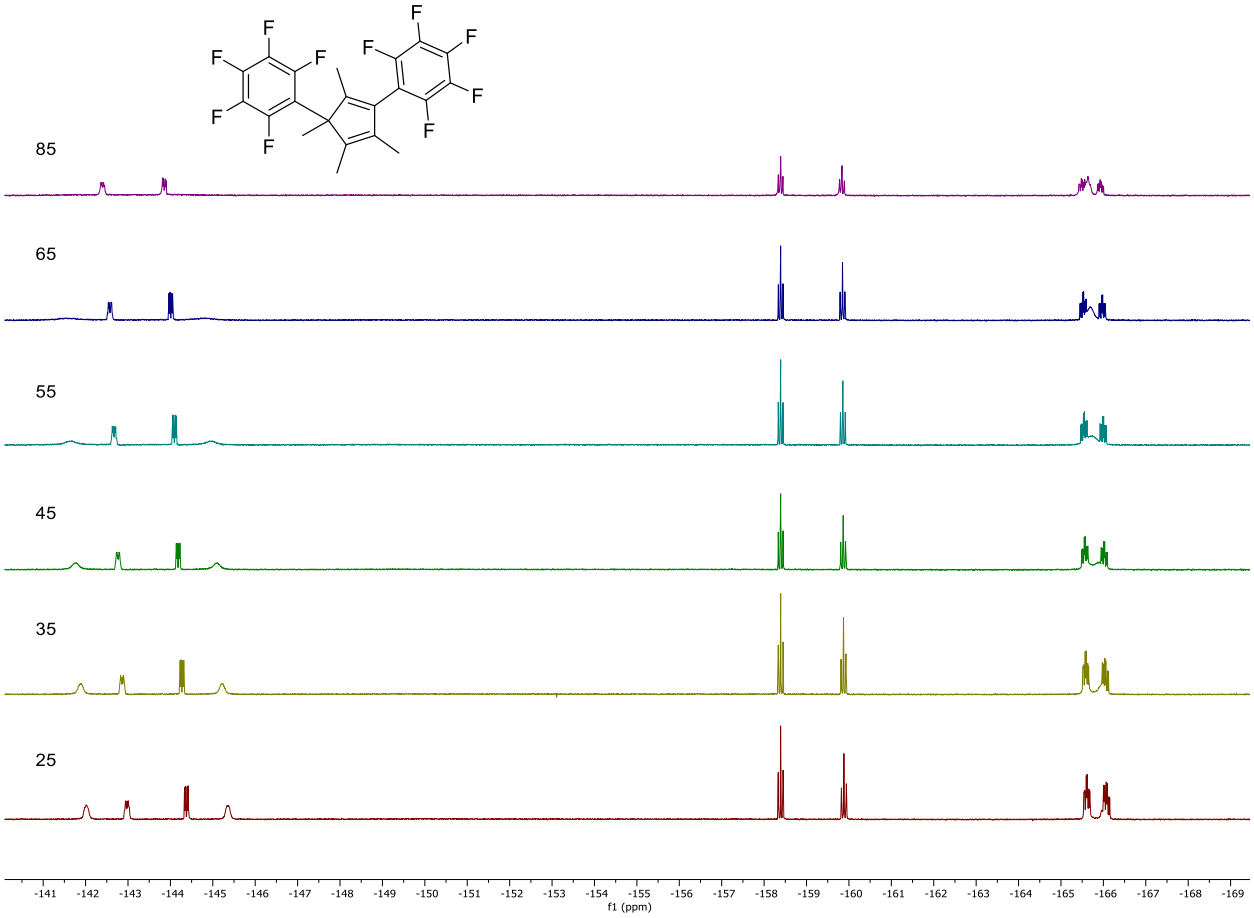

Figure 13. ^{19}F NMR spectra of **2a** at several temperatures (˚C) in *toluene-d*$_8$ at 376 MHz.

5.5.2 General procedure for the microwave synthesis of $[(\eta^5\text{-}Me_4C_5R)RhCl]_2(\mu^2\text{-}Cl)_2$

A microwave pressure tube was fitted with the appropriate amounts of the respective $[Rh(COD)]_2(\mu^2\text{-}Cl)_2$, HMe_4C_5R, in 4 mL of methanol with 0.5 mL of concentrated HCl. The reaction mixture was heated to 115 °C at 50 W and 150 psi and held for 1 h, yielding an orange solution. The solvent was evaporated under reduced pressure, and the resulting powder recrystallized from DCM and cold hexanes, collected via filtration, and washed with cold hexanes. **RhCp*** was prepared according to an established literature procedure.[1]

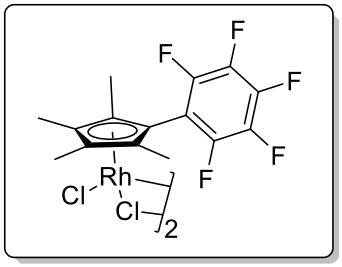

$[(\eta^5\text{-}Me_4C_5(C_6F_5)RhCl]_2(\mu^2\text{-}Cl)_2$ (**3a**)

Following the general procedure, $[Rh(COD)]_2(\mu^2\text{-}Cl)_2$ (0.200 g, 0.406 mmol), **1a** (0.4661 g, 1.62 mmol), and 0.5 mL of HCl were reacted in methanol (4 mL) to give **3a** (0.114 g, 31% yield). ^{1}H NMR (400 MHz, $CDCl_3$) δ 1.76 (s, 12H, 4 CpCH_3), 1.65 (d, 12H, J_{HF} = 1.4 Hz, 4 CpCH_3). ^{19}F NMR (376 MHz, $CDCl_3$) δ -124.02 – 137.33 (m, 1F, 1 Ar*F*), -138.37 (d, 1F, J_{FF} = 22.8 Hz, 1 Ar*F*), -150.23 (tt, 1F, J_{FF} = 21.2, 3.1 Hz, 1 Ar*F*), -158.36 (td, 1F, J_{FF} = 21.2, 7.5 Hz, 1 Ar*F*), -161.27 (td, 1F, J_{FF} = 22.1, 8.6 Hz, 1 Ar*F*).

HRMS/ESI+ (m/z): Calc. for $C_{30}H_{24}Rh_2F_{10}Cl_3$ 884.8894; Found 884.8958

Anal. Calc. for $C_{30}H_{24}Ir_2F_{10}Cl_4$, C, 32.74; H, 2.20; Found, C, 32.91; H, 2.22

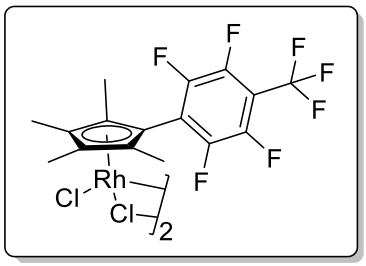

$[(\eta^5\text{-}Me_4C_5(CF_3(C_6F_4))RhCl]_2(\mu^2\text{-}Cl)_2$ (**3b**)

Following a literature procedure,[2] a pressure tube was fitted with $RhCl_3{\cdot}3H_2O$ (150 mg, 0.57 mmol) and **1b** in 3 mL of MeOH and added a few drops of DI water. The mixture was stirred at 65 ˚C for 4 days. The orange-red precipitate was isolated by vacuum filtration and rinsed with cold ethanol and pentane. The solid was dried overnight under vacuum to obtain **3b** (0.070 g, 25% yield). ^{1}H NMR (400 MHz, $CDCl_3$) δ 1.79 (s, 12H, 4 CpC*H*$_3$), 1.68 (d, 12H, J_{HF} = 1.4 Hz, 4 CpC*H*$_3$). ^{19}F NMR (376 MHz, $CDCl_3$) δ -56.52 (t, 3F, J_{FF} = 21.5 Hz, 1 C*F*$_3$), -122.40 (dd, 1F, J_{FF} = 22.7, 12.9 Hz, 1 Ar*F*), -136.45 - -136.57 (m, 1F, 1 Ar*F*), -136.58 – 136.82 (m, 1F, 1 Ar*F*), -140.15 – 140.55 (m, 1F, 1 Ar*F*).

HRMS/ESI+ (m/z): Calc. for $C_{32}H_{24}Rh_2F_{14}Cl_3$ 984.8830; Found 984.8861

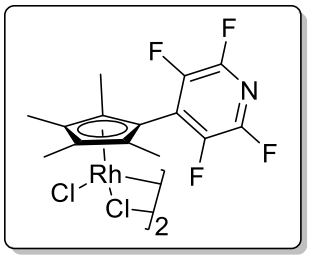

$[(\eta^5\text{-}Me_4C_5(C_5F_4N)RhCl]_2(\mu^2\text{-}Cl)_2$ (**3c**)

Following a literature procedure,[2] a pressure tube was fitted with $RhCl_3{\cdot}3H_2O$ (150 mg, 0.57 mmol) and **4c** in 3 mL of MeOH and added a few drops of DI water. The mixture was stirred at 65 ˚C for 4 days. The orange-red precipitate was isolated by vacuum filtration and rinsed with cold ethanol and pentane. The solid was dried overnight under vacuum to obtain **3c** (0.097 g, 38% yield). ^{1}H NMR (400 MHz, $CDCl_3$) δ 1.80 (s, 12H, 4 CpC*H*$_3$), 1.69 (s, 12H, 4 CpC*H*$_3$). ^{19}F NMR

(376 MHz, $CDCl_3$) δ -86.62 (ddd, 1F, J_{FF} = 29.4, 21.1, 13.7 Hz, 1 Ar*F*), -89.93 (ddd, 1F, J_{FF} = 30.3, 21.4, 13.6 Hz, 1 Ar*F*), -126.19 (dd, 1F, J_{FF} = 30.3, 21.3 Hz, 1 Ar*F*), -139.86 (dd, 1F, J_{FF} = 28.9, 21.8 Hz, 1 Ar*F*).

HRMS/ESI+ (m/z): Calc. for $C_{28}H_{24}Rh_2F_8N_2Cl_3$ 850.8987; Found 850.9067

5.5.3 General procedure for the microwave synthesis of $[(\eta^5\text{-}Me_4C_5R)IrCl]_2(\mu^2\text{-}Cl)_2$

A microwave pressure tube was fitted with the appropriate amounts of the respective $[Ir(COD)]_2(\mu^2\text{-}Cl)_2$, HMe_4C_5R, in 4 mL of methanol with 0.5 mL of concentrated HCl. The reaction mixture was heated to 115 °C at 50 W and 150 psi and held for 1 h, yielding an orange solution. The solvent was evaporated under reduced pressure, and the resulting powder recrystallized from DCM and cold hexanes, collected via filtration, and washed with cold hexanes. **IrCp*** was prepared according to an established literature procedure.[1]

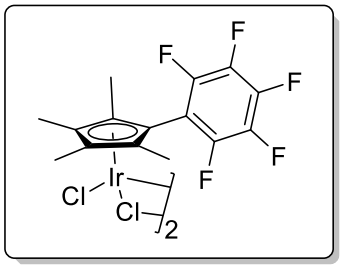

$[(\eta^5\text{-}Me_4C_5(C_6F_5)IrCl]_2(\mu^2\text{-}Cl)_2$ (**4a**)

Following the general procedure, $[Ir(COD)]_2(\mu^2\text{-}Cl)_2$ (0.430 g, 0.298 mmol), **1a** (0.342 g, 1.2 mmol), and 0.5 mL of HCl were reacted in methanol (4 mL) to give **4a** (0.579 g, 82% yield). ^{1}H NMR (400 MHz, $CDCl_3$) δ 1.79 (s, 12H, 4 CpC*H*$_3$), 1.62 (d, 12H, J_{HF} = 1.2 Hz, 4 CpC*H*$_3$). ^{13}C{^{1}H} NMR (101 MHz, $CDCl_3$) δ 110.017 (Cp*C*), 93.18 (Cp*C*), 88.20 (Cp*C*), 10.30 (Cp*C*H$_3$), 9.76 (Cp*C*H$_3$). ^{19}F NMR (376 MHz, $CDCl_3$) δ -127.47 (d, 1F, J_{FF} = 23.9 Hz, 1 Ar*F*), -138.81 (d, 1F, J_{FF} = 22.9 Hz, 1 Ar*F*), -151.21 (t, 1F, J_{FF} = 21.1 Hz, 1 Ar*F*), -158.90 (td, 1F, J_{FF} = 21.5, 7.7 Hz, 1 Ar*F*), -161.54 (td, 1F, J_{FF} = 22.1, 8.7 Hz, 1 Ar*F*).

HRMS/ESI+ (m/z): Calc. for $C_{30}H_{24}[^{193}Ir]_2F_{10}Cl_3$ 1065.0042; Found 1065.0102

Anal. Calc. for $C_{30}H_{24}Ir_2F_{10}Cl_4$, C, 32.74; H, 2.20; Found, C, 32.91; H, 2.22

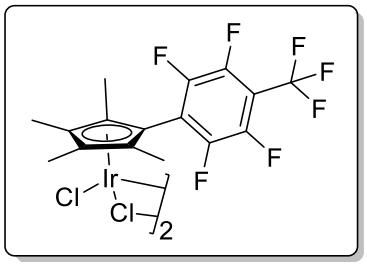

$[(\eta^5\text{-}Me_4C_5(CF_3(C_6F_4))IrCl]_2(\mu^2\text{-}Cl)_2$ (**4b**)

Following the general procedure, $[Ir(COD)]_2(\mu^2\text{-}Cl)_2$ (0.330 g, 0.491 mmol), **1b** (0.582 g, 1.72 mmol), and 0.5 mL of HCl were reacted in methanol (4 mL) to give **4b** (0.292 g, 49% yield). ^{1}H NMR (400 MHz, $CDCl_3$) δ 1.82 (s, 12H, 4 CpC*H*$_3$), 1.65 (d, 12H, J_{HF} = 1.4 Hz, 4 CpC*H*$_3$). ^{19}F NMR (376 MHz, $CDCl_3$) δ -56.50 (t, 3F, J_{FF} = 21.6 Hz, 1 C*F*$_3$), -125.71 (dd, 1F, J_{FF} = 22.3, 13.2 Hz, 1 Ar*F*), -136.91 (dd, 1F, J_{FF} = 21.7, 11.9 Hz, 1 Ar*F*), -137.05 – 137.33 (m, 1F, 1 Ar*F*), -140.52 – 140.69 (m, 1F, 1 Ar*F*).

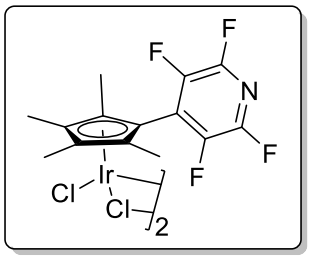

$[(\eta^5\text{-}Me_4C_5(C_5F_4N)IrCl]_2(\mu^2\text{-}Cl)_2$ (**4c**)

Following the general procedure, $[Ir(COD)]_2(\mu^2\text{-}Cl)_2$ (0.150 g, 0.22 mmol), **1c** (0.212 g, 0.78 mmol), and 0.5 mL of HCl were reacted in methanol (4 mL) to give **4c** (0.122 g, 51% yield). ^{1}H NMR (400 MHz, DMSO) δ 1.79 (s, 12H, 4 CpC*H*$_3$), 1.70 (d, 12H, J_{HF} = 1.4 Hz, 4 CpC*H*$_3$). ^{19}F NMR (376 MHz, DMSO) δ -91.82 (ddd, 1F, J_{FF} = 27.9, 22.3, 13.9 Hz, 1 Ar*F*), -92.64 (ddd, 1F, J_{FF} = 28.7, 22.9, 13.8 Hz, 1 Ar*F*), -128.57 (dd, 1F, J_{FF} = 28.7, 22.3 Hz, 1 Ar*F*), -139.53 – 139.63 (m, 1F, 1 Ar*F*),

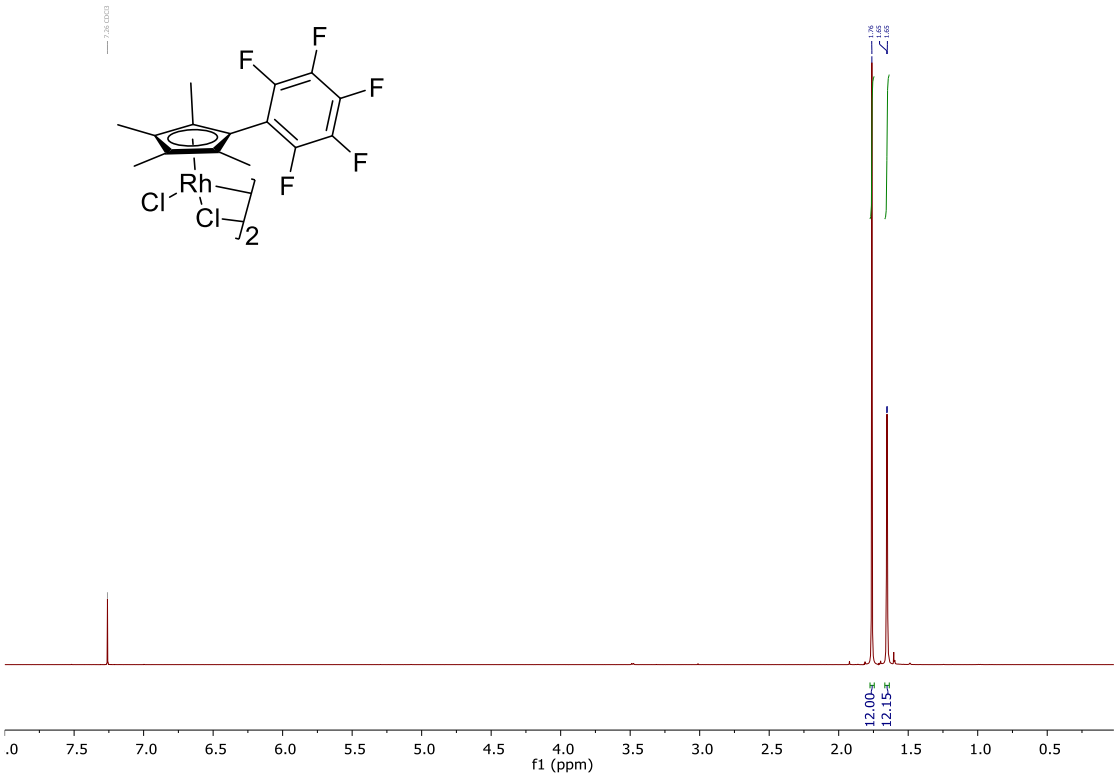

Figure S14. ^{1}H NMR spectrum of **3a** in $CDCl_3$ at 400 MHz.[2]

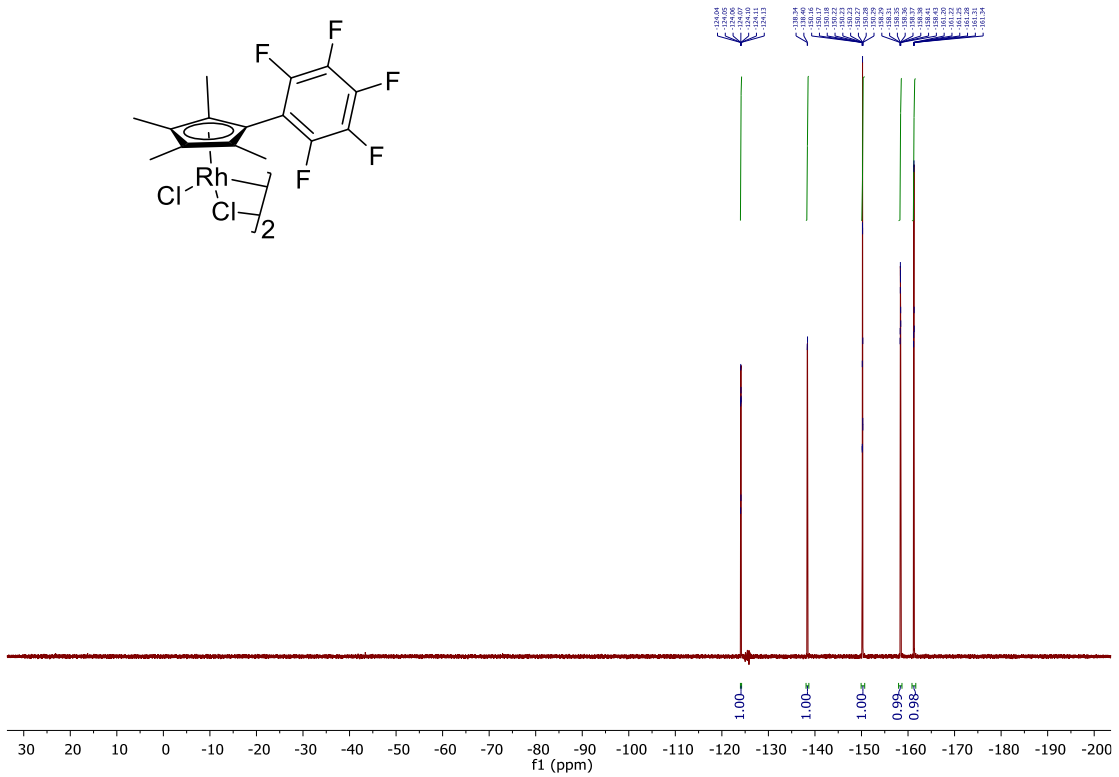

Figure S15. ^{19}F NMR spectrum of **3a** in $CDCl_3$ at 376 MHz.[2]

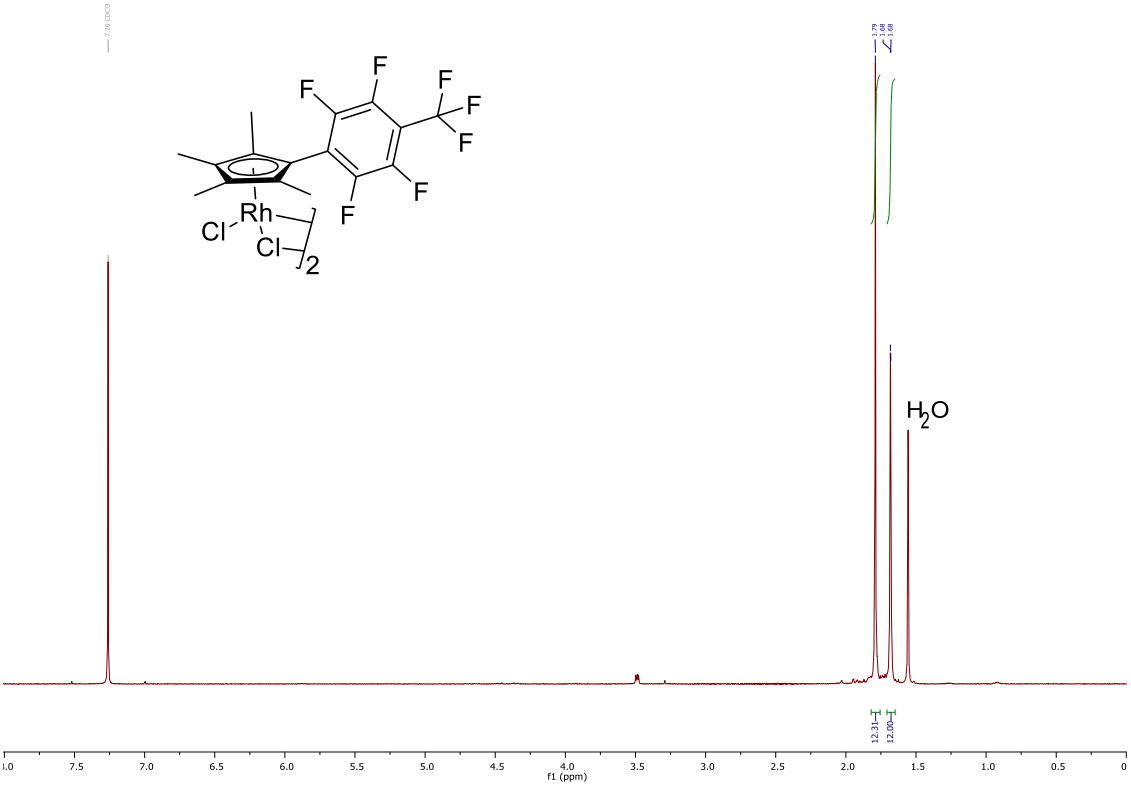

Figure S16. ^{1}H NMR spectrum of **3b** in $CDCl_3$ at 400 MHz.

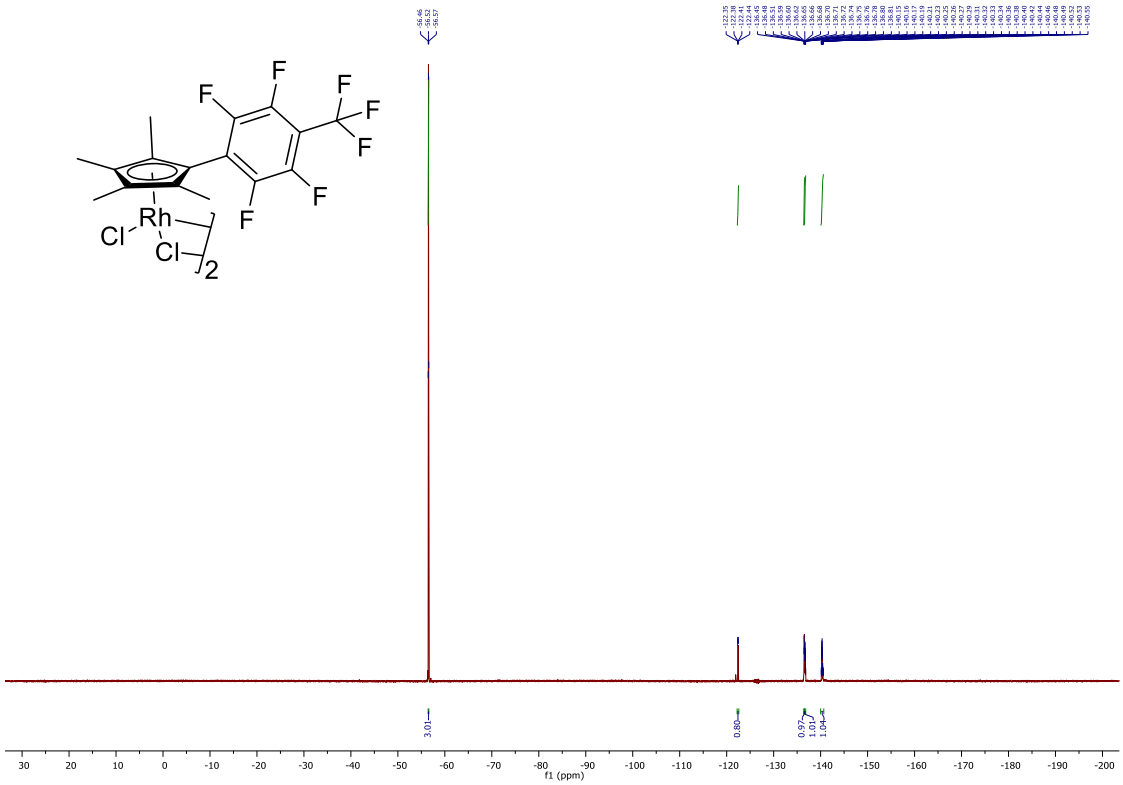

Figure S17. ^{19}F NMR spectrum of **3b** in $CDCl_3$ at 376 MHz.

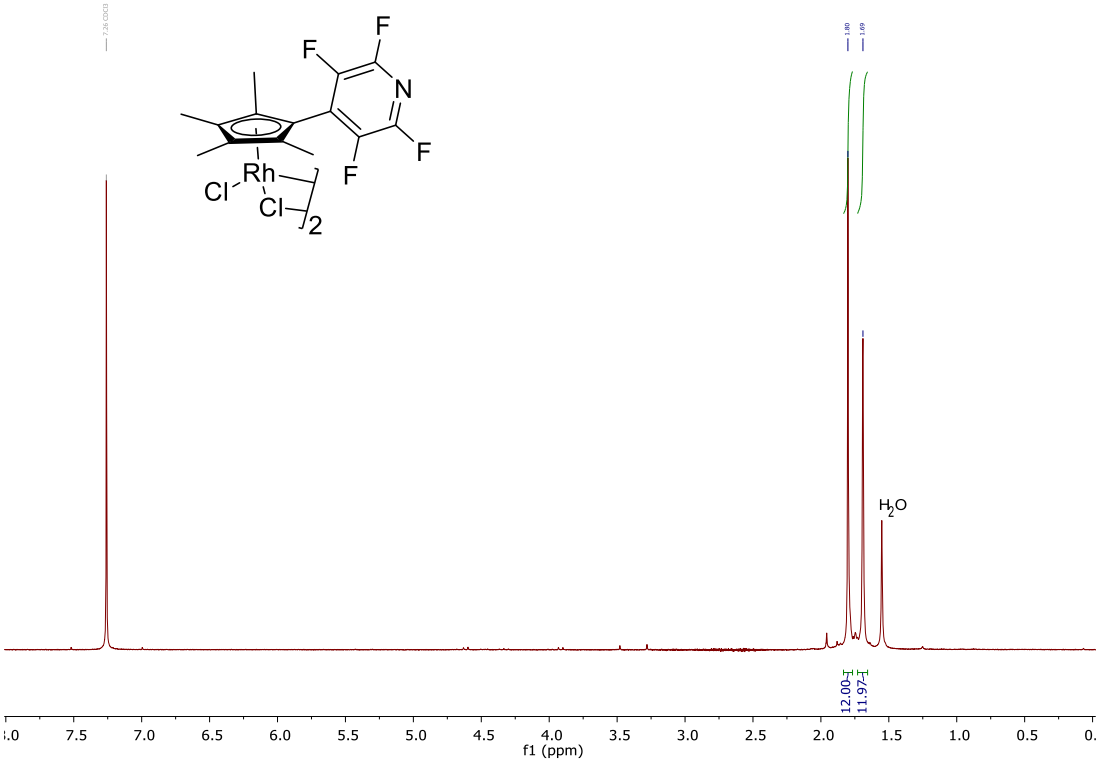

Figure S18. ^{1}H NMR spectrum of **3c** in $CDCl_3$ at 400 MHz.

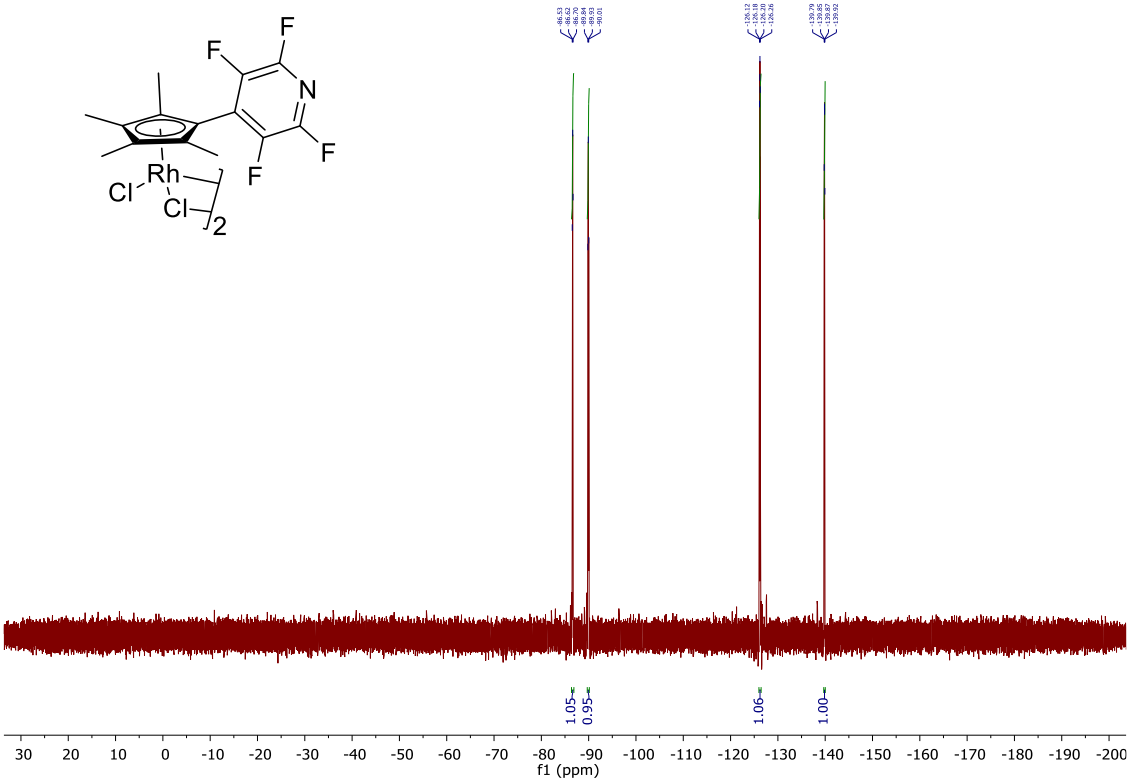

Figure S19. ^{19}F NMR spectrum of **3c** in $CDCl_3$ at 376 MHz.

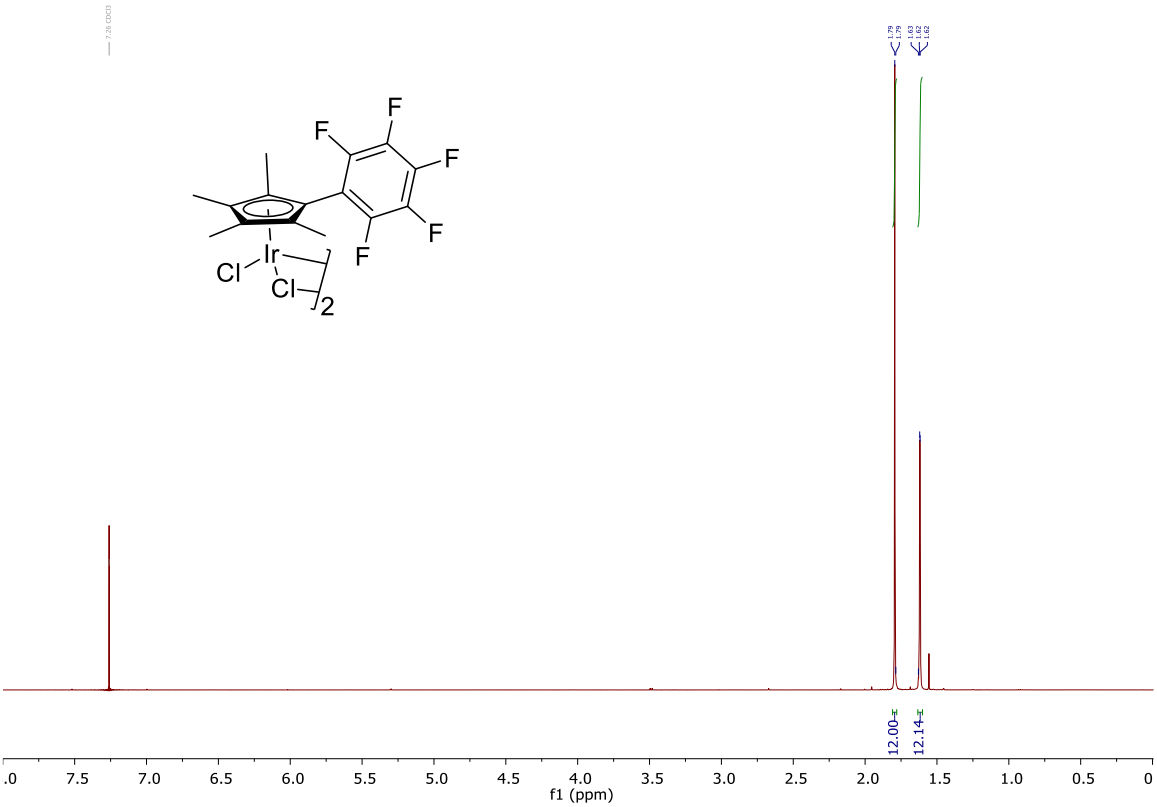

Figure S20. ^{1}H NMR spectrum of **4a** in $CDCl_3$ at 400 MHz.

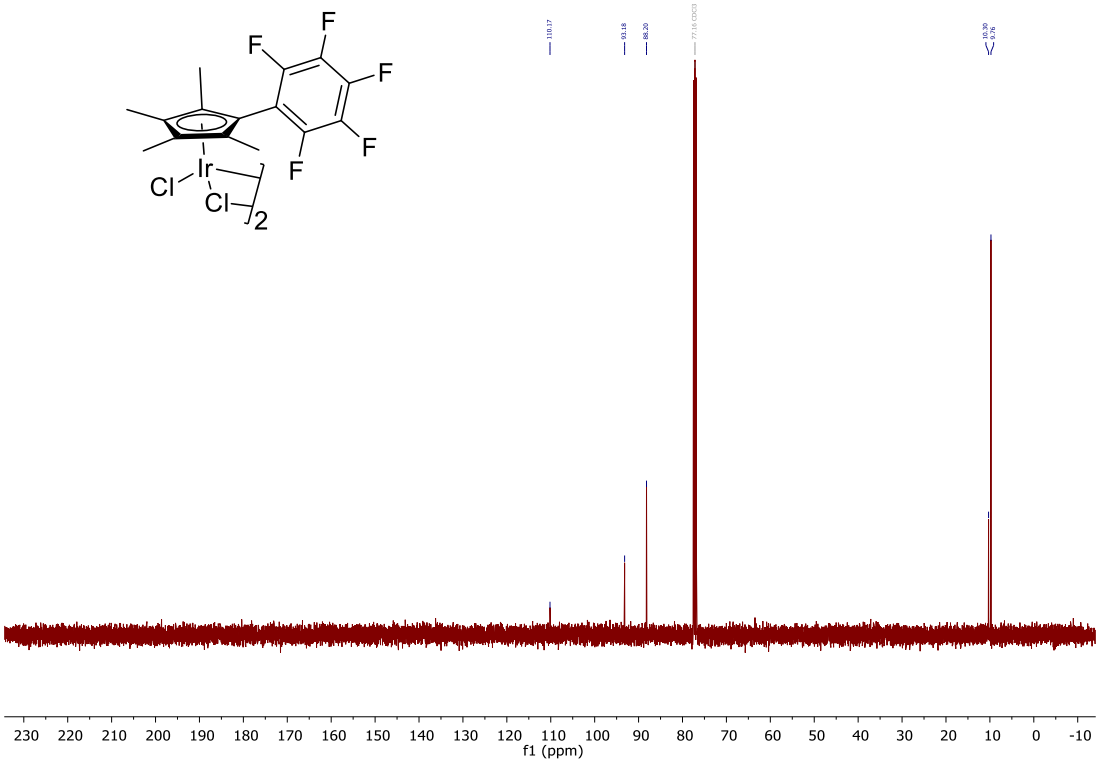

Figure S21. $^{13}C\{^{1}H\}$ NMR spectrum of **4a** in $CDCl_3$ at 101 MHz.

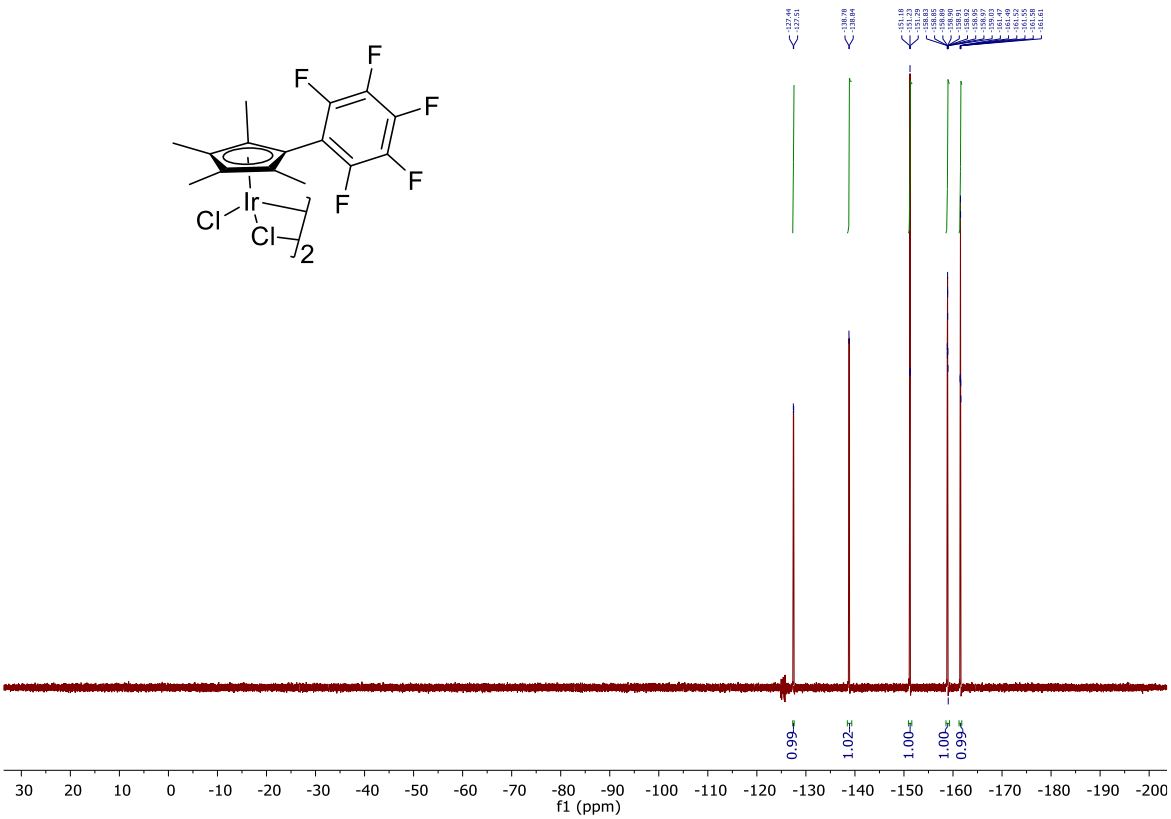

Figure S22. ^{19}F NMR spectrum of **4a** in $CDCl_3$ at 376 MHz.

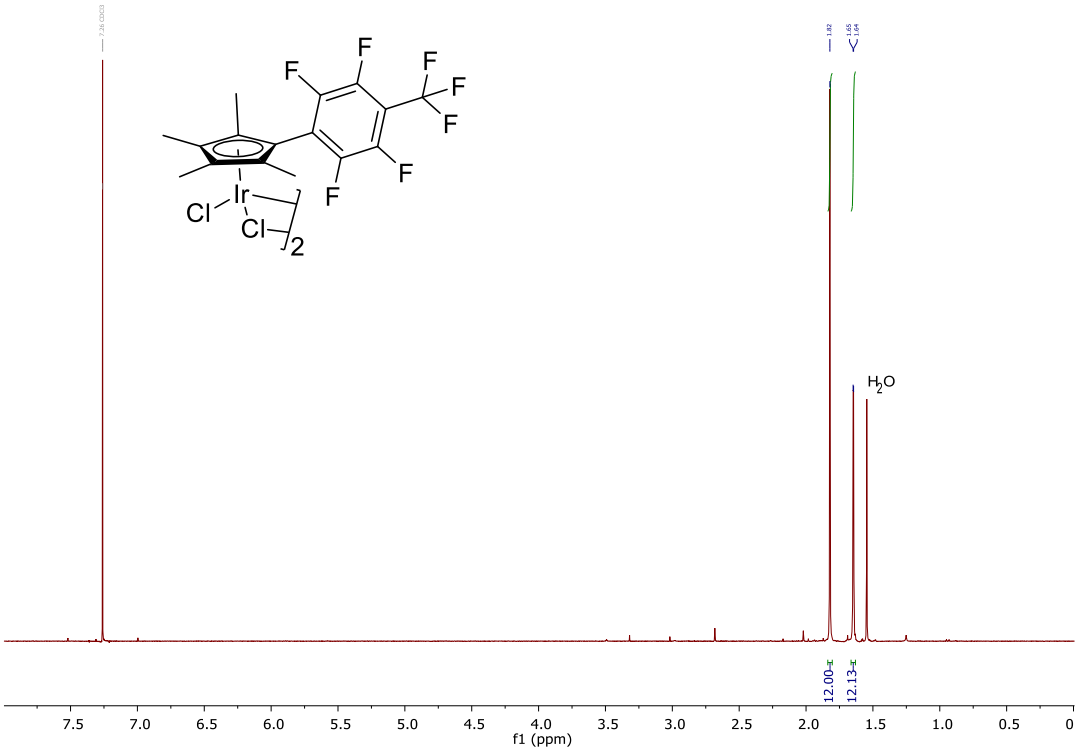

Figure S23. ^{1}H NMR spectrum of **4b** in $CDCl_3$ at 400 MHz.

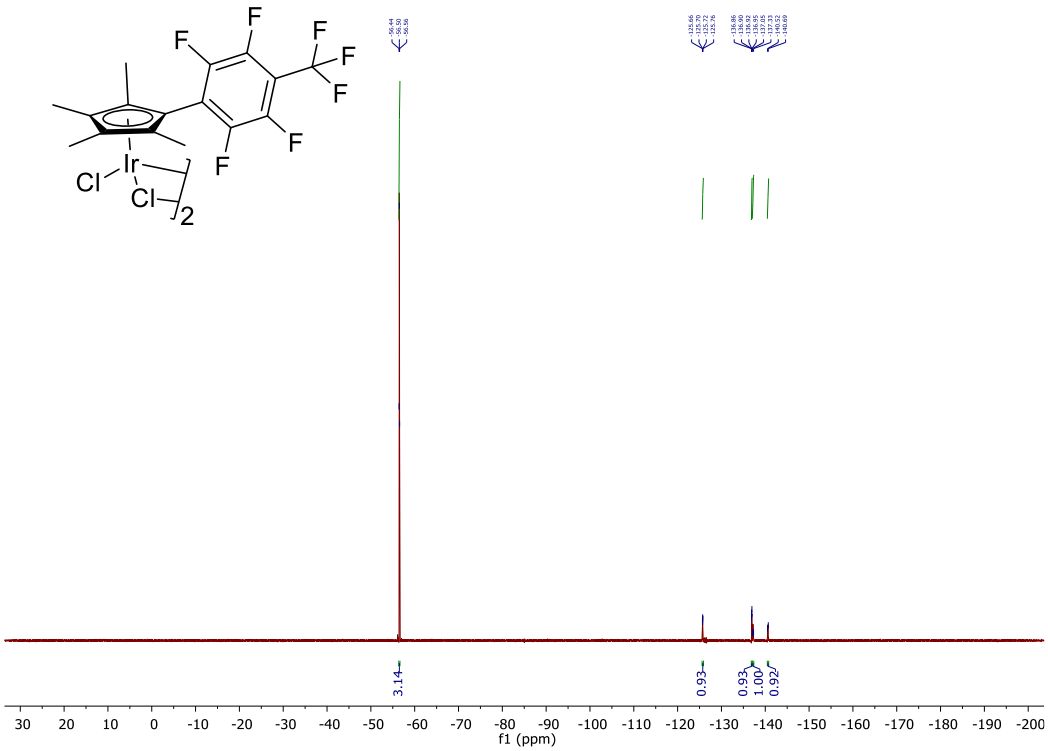

Figure S24. ^{19}F NMR spectrum of **4b** in $CDCl_3$ at 376 MHz.

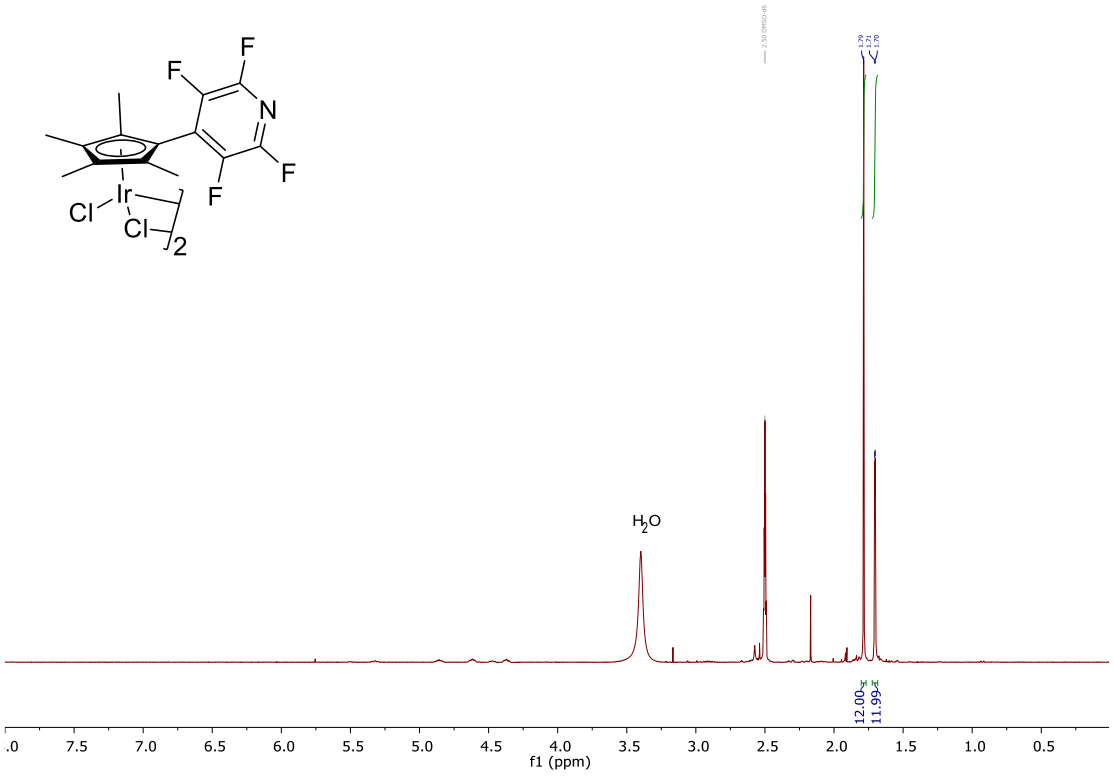

Figure S25. ^{1}H NMR spectrum of **4c** in DMSO at 400 MHz.

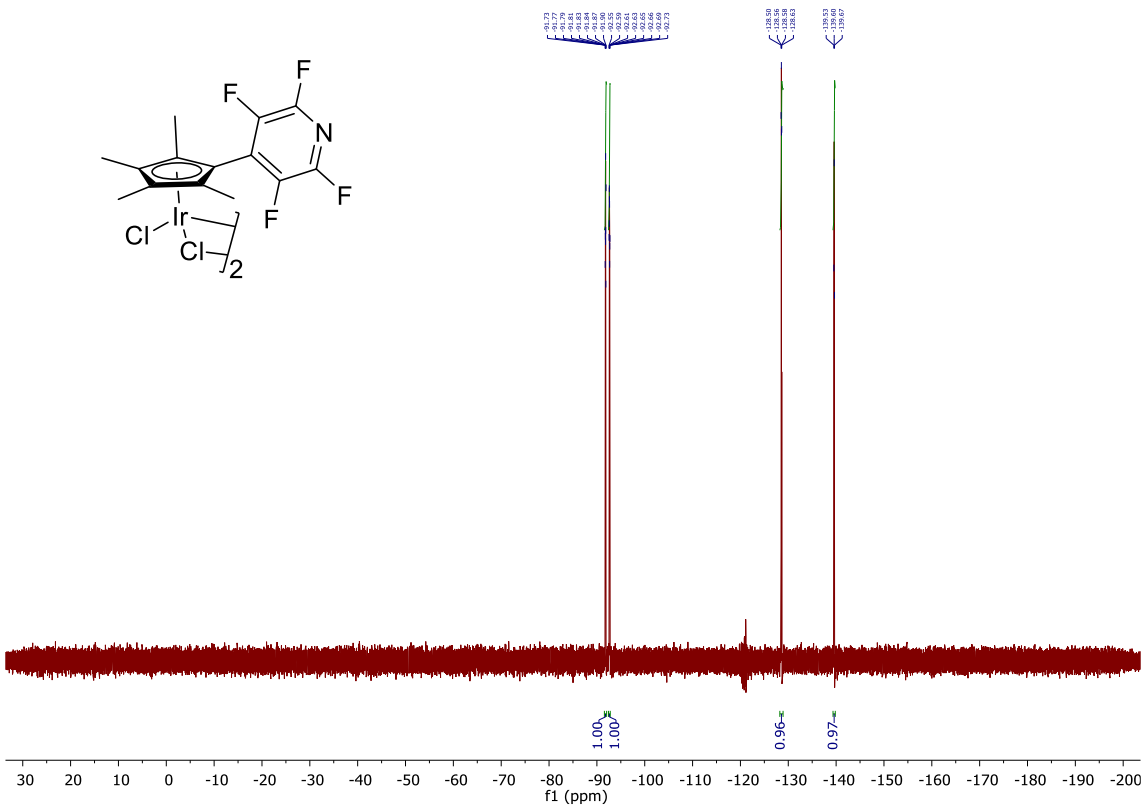

Figure S26. ^{19}F NMR spectrum of **4c** in DMSO at 376 MHz.

Arrhenius Plot

T, deg C	T, K	k (model)	1000/T	ln (k)
−5	268	5	3.73	1.61
15	288	10	3.47	2.30
24	297	30	3.37	3.40
35	308	50	3.25	3.91
45	318	150	3.14	5.01
50	323	300	3.10	5.70

Table S1. Rate data between -5 – 50 ˚C.

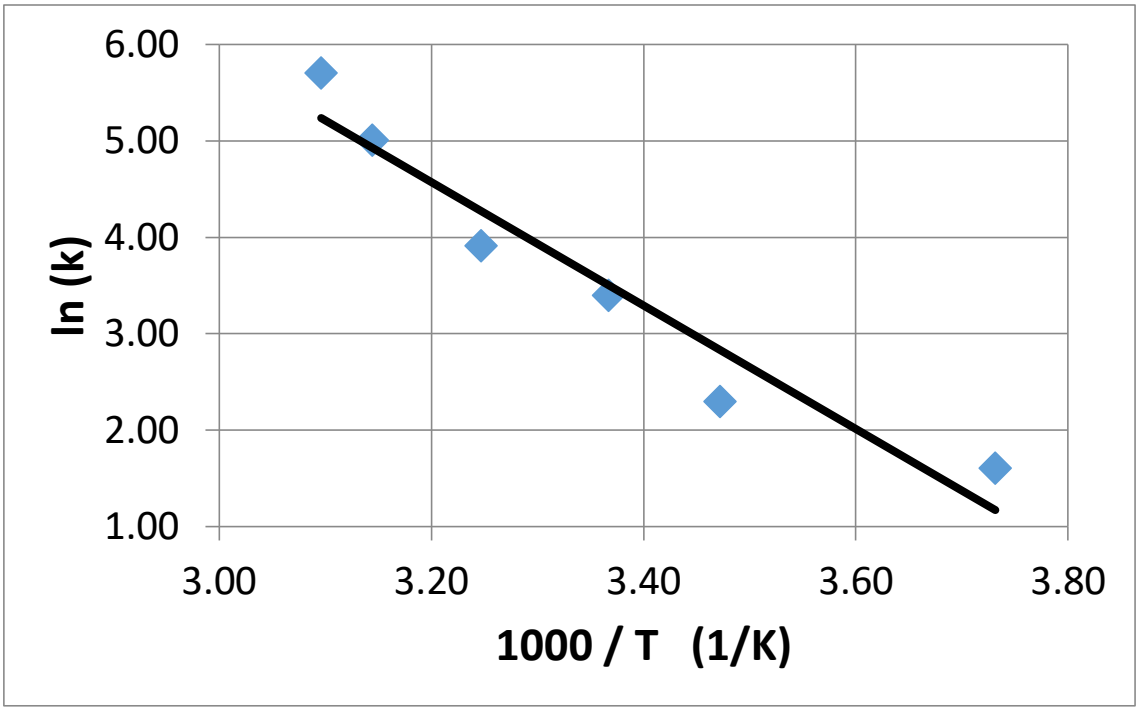

Figure S27. Arrhenius plot to calculate the activation energy (12 kcal/mol) of the rotation about the C_5-C_{ipso}.

Crystal Structures

Table S2. Selected bond lengths (Å) and angles (˚) for diaryl cyclopentadienes.

	2b	**2c**
C1 – C2	1.3501(18)	1.345(2)
C2 – C3	1.4844(19)	1.480(2)
C3 – C4	1.348(2)	1.344(2)
C4 – C5	1.5290(18)	1.527(2)
C5 – C1	1.5271(19)	1.528(2)
C2 – C7	1.4821(19)	1.481(2)
C5 – C15		1.532(2)
C5 – C17	1.5310(19)	
C1 – C2 – C3	110.37(12)	111.01(13)
C2 – C3 – C4	108.66(12)	108.56(13)
C3 – C4 – C5	109.51(12)	109.41(13)
C4 – C5 – C1	102.64(11)	103.00(13)
C5 – C1 – C2	108.38(11)	107.84(13)
C1 – C2 – C7	123.93(12)	126.02(14)
C1 – C5 – C15		110.65(12)
C1 – C5 – C17	111.42(11)	

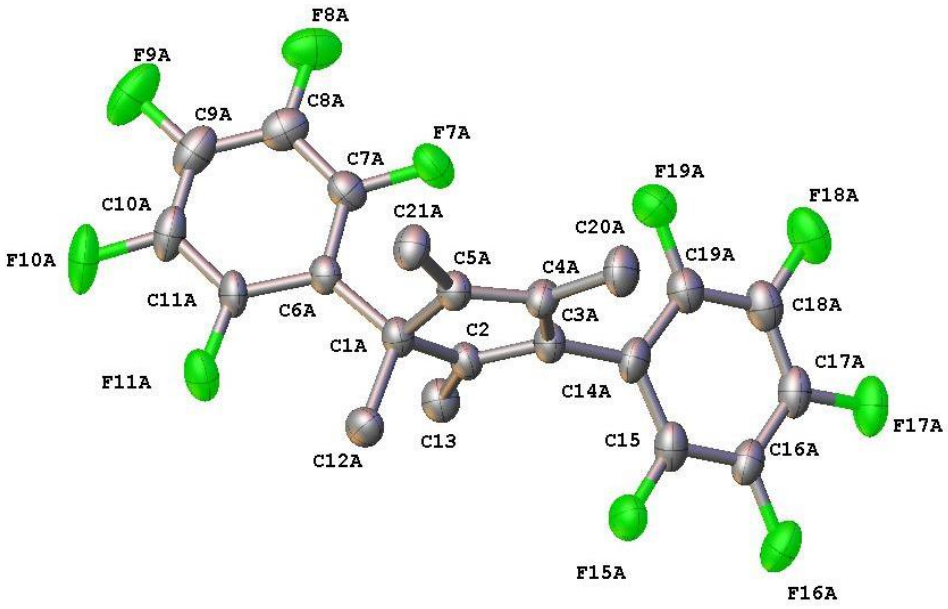

Figure S28. ADP Plot of **2a** (**CSD: 1911804**). Hydrogen atoms omitted for clarity. Ellipsoids shown at 50% probability.

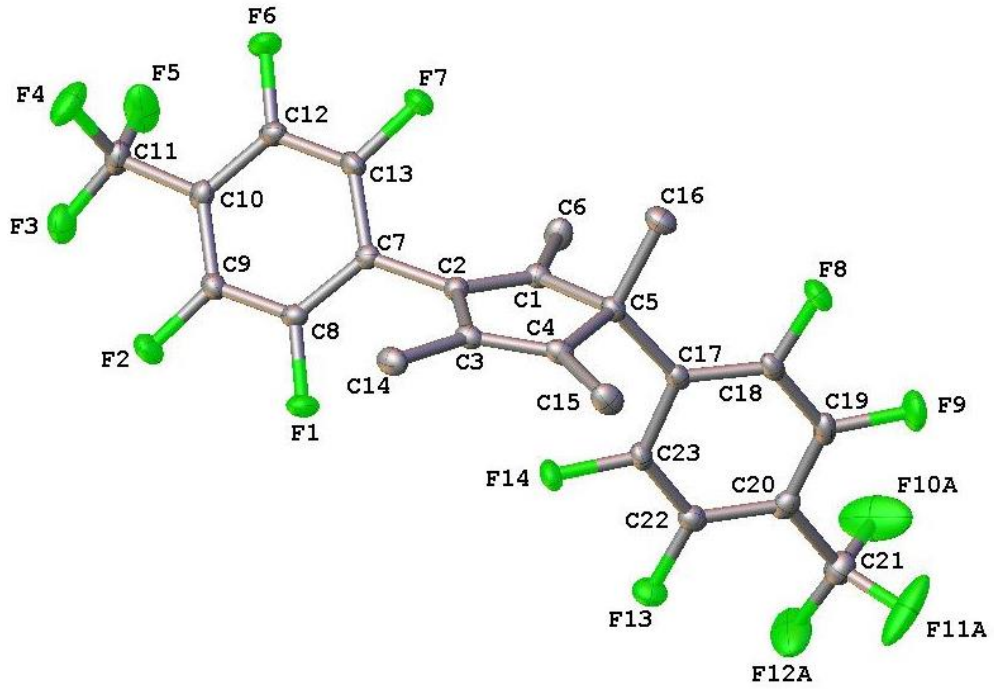

Figure S29. ADP Plot of **2b** (**CSD: 1911800**). Hydrogen atoms omitted for clarity. Ellipsoids shown at 50% probability.

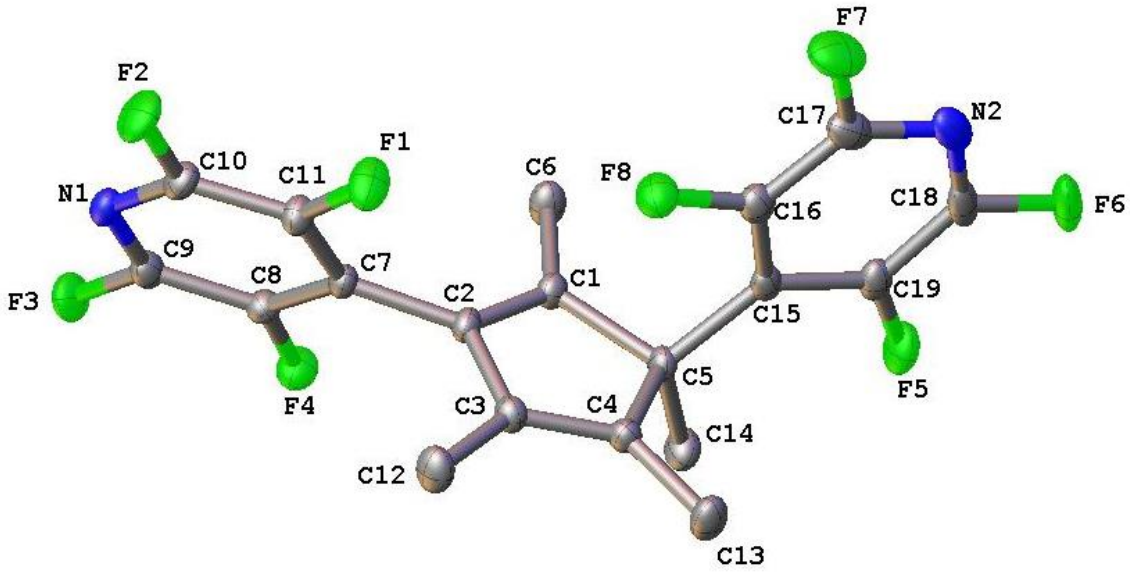

Figure S30. ADP Plot of **2c** (**CSD: 1911805**). Hydrogen atoms omitted for clarity. Ellipsoids shown at 50% probability.

Table S3. Selected bond lengths (Å) and angles (˚) for derivatized rhodium(III) complexes.

	3a	**3b**	**3c**[a]
Rh-C(η^5-ring)	2.1726(14)	2.155(3)	2.1583(19)
	2.1649(15)	2.168(3)	2.169(2)
	2.1412(15)	2.149(3)	2.139(2)
	2.1434(15)	2.139(3)	2.148(2)
	2.1372(14)	2.125(3)	2.1207(19)
Rh-C(centroid)	1.7666(8)	1.7615(16)	1.7622(11)
Rh-X_1	2.4559(4)	2.4458(8)	2.4565(5)
Rh-X_2	2.4494(4)	2.4261(8)	2.4445(5)
Rh-Cl	2.3873(4)	2.3784(8)	2.3852(5)
Rh-Rh	3.7122(6)	3.6668(5)	3.7083(4)
X_1-Rh-X_2	81.643(12)	82.36(3)	81.665(17)
X_1-Rh-Cl	90.379(13)	89.68(3)	90.715(19)
X_2-Rh-Cl	91.536(13)	89.99(3)	90.928(19)
Rh-Cl-Rh	98.359(12)	97.64(3)	98.335(17)

[a] DCM present in the crystal lattice. [b] X_1 = first bridging Cl and X_2 = second bridging Cl

Table S4. Selected bond lengths (Å) and angles (˚) for derivatized iridium(III) complexes.

	4a	**4b**	**4c**
Ir-C(η^5-ring)	2.149(3)	2.142(4)	2.145(3)
	2.147(3)	2.144(4)	2.162(3)
	2.162(3)	2.162(4)	2.137(3)
	2.151(3)	2.145(4)	2.153(3)
	2.123(3)	2.126(4)	2.119(3)
Ir-C(centroid)	1.7591(18)	1.758(2)	1.7552(15)
Ir-X_1	2.4298(7)	2.4268(8)	2.4214(7)
Ir-X_2	2.4408(7)	2.4429(9)	2.4356(7)
Ir-Cl	2.3675(8)	2.3715(8)	2.3630(7)
Ir-Ir	3.7803(4)	3.7197(4)	3.6867(5)
X_1-Ir-X_2	80.54(3)	80.39(3)	81.24(2)
X_1-Ir-Cl	87.87(3)	87.52(3)	87.48(3)
X_2-Ir-Cl	88.07(3)	87.81(3)	87.76(3)
Ir-Cl-Ir	99.46(3)	99.61(3)	98.76(2)

[a] X_1 = first bridging Cl and X_2 = second bridging Cl

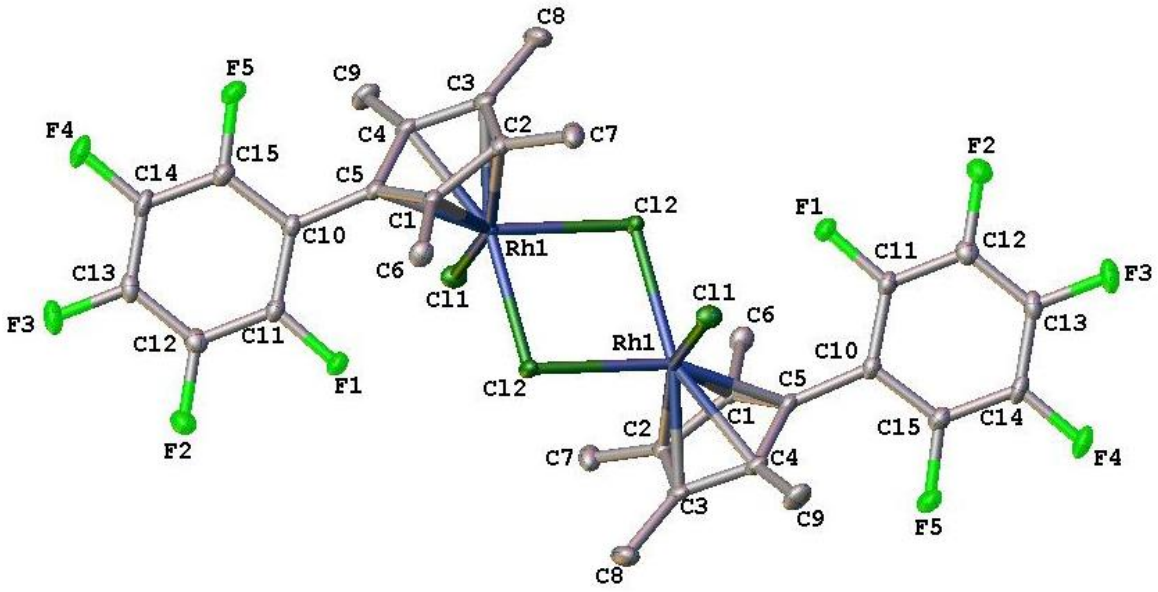

Figure S31. ADP Plot of **3a** (**CSD: 1911803**). Hydrogen atoms omitted for clarity. Ellipsoids shown at 50% probability. Bond lengths and angles are similar to those found in the structure by Piou *et al.*[2]

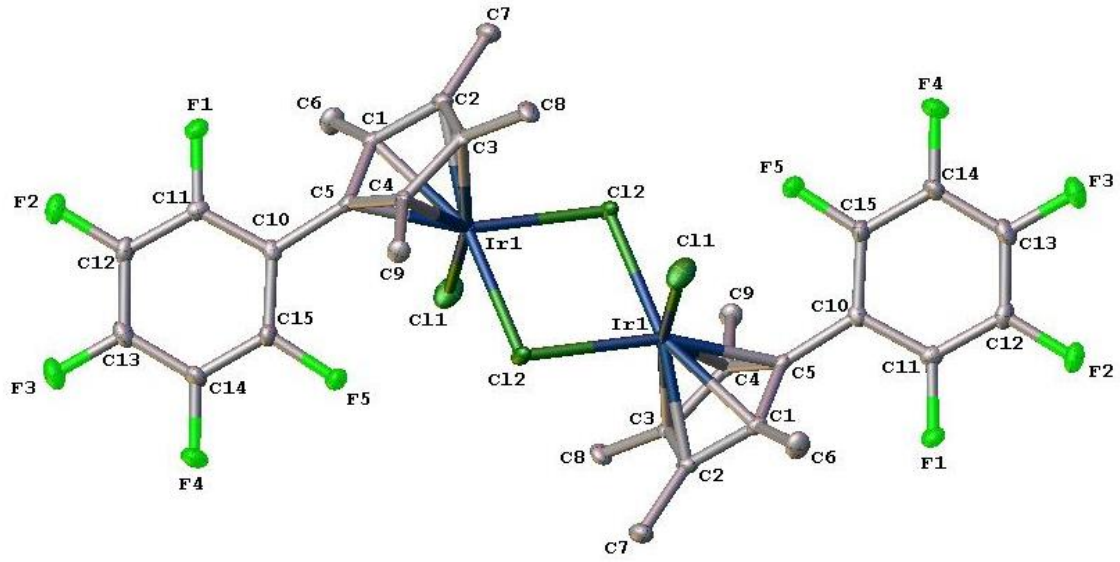

Figure S32. ADP Plot of **4a** (**CSD: 1911798**). Hydrogen atoms omitted for clarity. Ellipsoids shown at 50% probability.

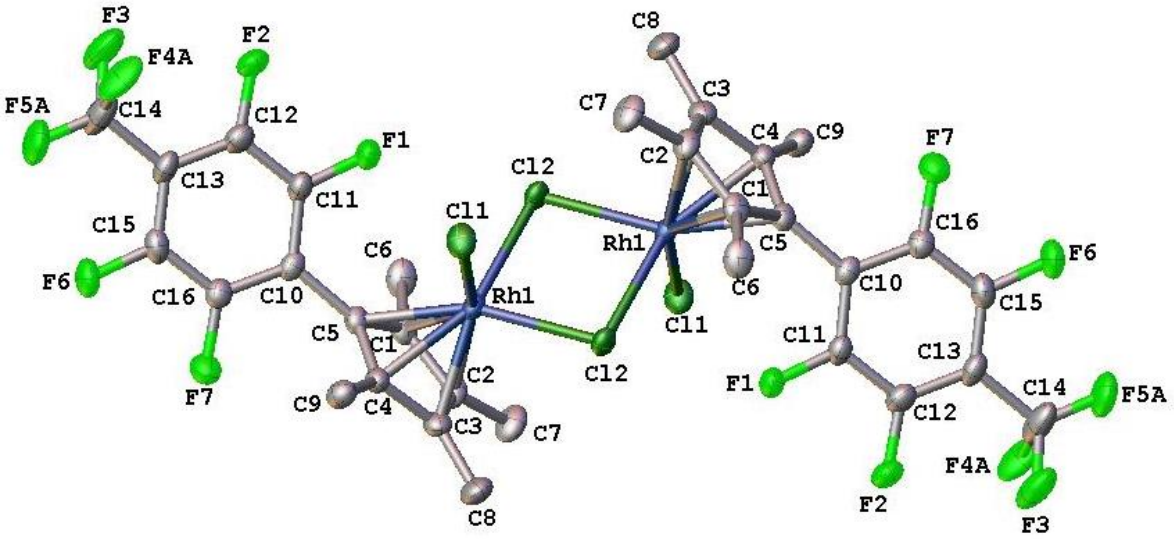

Figure S33. ADP Plot of **3b** (**CSD: 1911802**). Hydrogen atoms omitted for clarity. Ellipsoids shown at 50% probability.

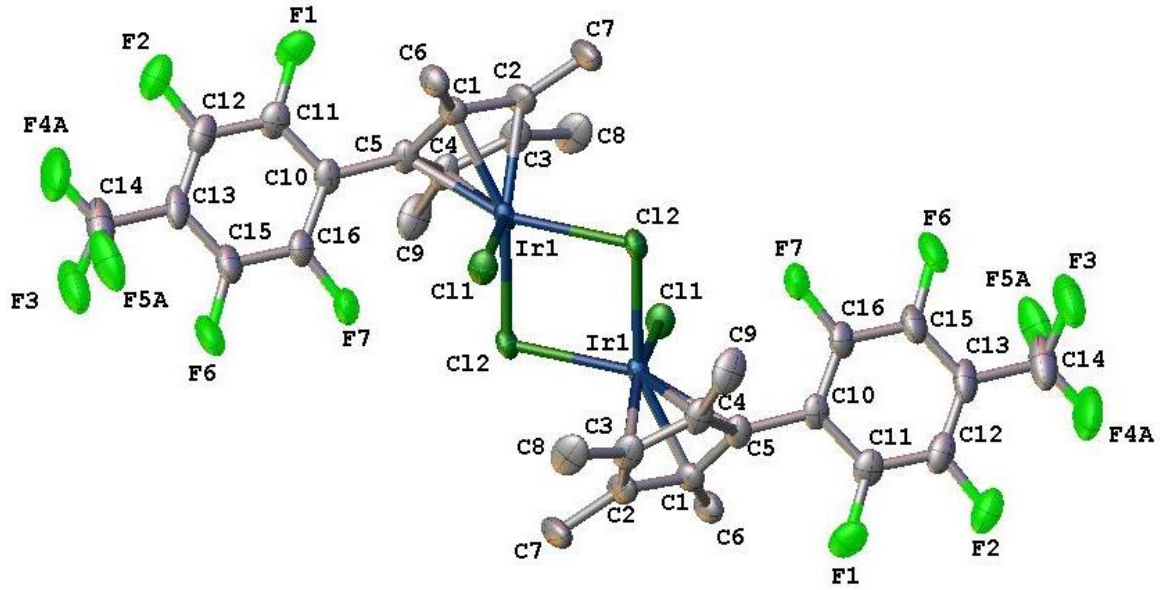

Figure S34. ADP Plot of **4b** (**CSD: 1911799**). Hydrogen atoms omitted for clarity. Ellipsoids shown at 50% probability.

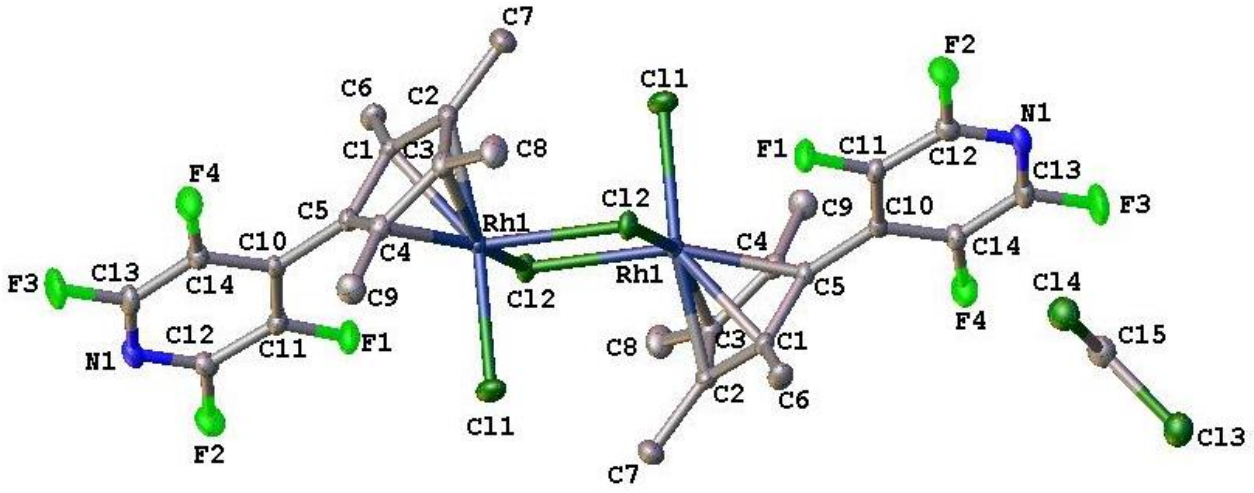

Figure S35. ADP Plot of **3c** (**CSD: 1911806**). Hydrogen atoms omitted for clarity. Ellipsoids shown at 50% probability.

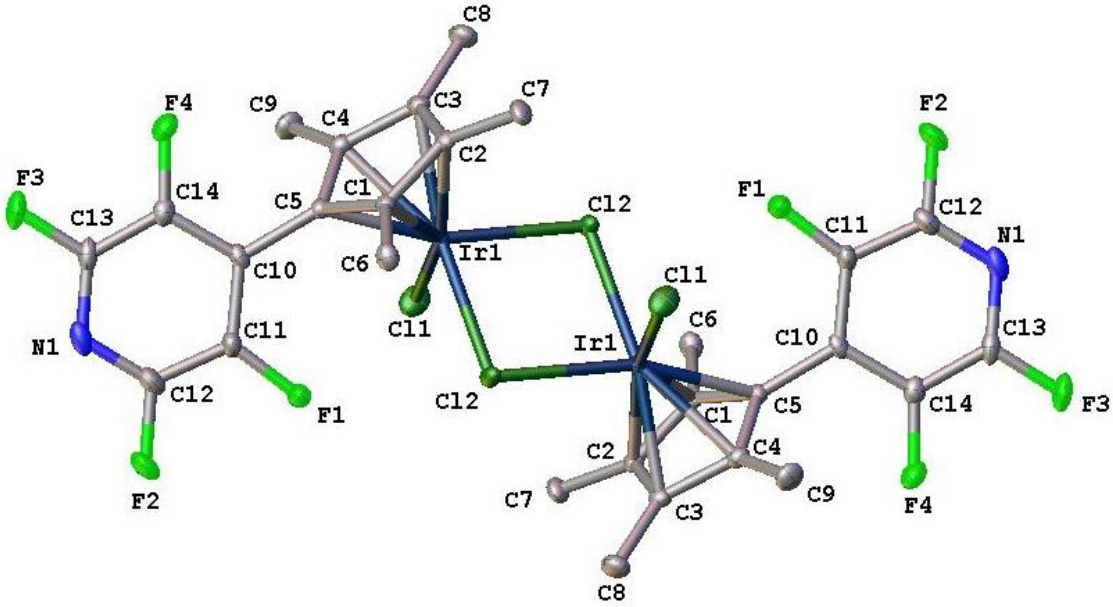

Figure S36. ADP Plot of **4c** (**CSD: 1911801**). Hydrogen atoms omitted for clarity. Ellipsoids shown at 50% probability.

References

(1) Tönnemann, J.; Risse, J.; Grote, Z.; Scopelliti, R.; Severin, K. *Eur. J. Inorg. Chem.* **2013**, *2013* (26), 4558–4562.

(2) Piou, T.; Romanov-Michailidis, F.; Romanova-Michaelides, M.; Jackson, K. E.; Semakul, N.; Taggart, T. D.; Newell, B. S.; Rithner, C. D.; Paton, R. S.; Rovis, T. *J. Am. Chem. Soc.* **2017**, *139* (3), 1296–1310.